LASER ELECTROSPRAY MASS SPECTROMETRY FOR STRUCTURAL ANALYSIS OF BIOMOLECULES

A Dissertation
Submitted
To the Temple University Graduate Board

In Partial Fulfillment
Of the Requirements for the Degree
Doctor OF Philosophy
(College Of Science and Technology)

---

by
Santosh Karki
May 2017

Examining Committee Members:

Robert J. Levis, Advisor, Department of Chemistry, Temple University
Ann M. Valentine, Department of Chemistry, Temple University
Michael J. Zdilla, Department of Chemistry, Temple University
Charles N. McEwen, External Member, Department of Chemistry, University of Sciences

ABSTRACT

This dissertation elucidates a greater understanding of protein folding and unfolding processes during the lifetimes of electrospray and nano-spray droplets in laser electrospray mass spectrometry (LEMS) and nano-laser electrospray mass spectrometry (nano-LEMS) measurements, respectively. The similarity in mass spectral features obtained from conventional electrospray measurements for supercharged proteins with those of LEMS measurements suggested that supercharging phenomena occurs in the electrospray droplets during the droplet desolvation process. It was observed that the laser vaporization of protein from condensed phase into the electrospray droplets containing denaturing electrospray solution and a supercharging reagent resulted in the increase in ion abundance of higher charge states in comparison with electrospray measurements. Conversely, the addition of solution additives with varying gas phase basicity in the electrospray solvent resulted in charge reduction for unfolded protein upon laser vaporization from condensed phase into the charged electrospray droplets. The extent of charge reduction and the fraction of folded protein within the electrospray droplets was found to be dependent upon both the extent of protein denaturation in the solution prior to laser vaporization and the gas phase basicity of solution additives.

The ability of the LEMS technique to analyze molecules from solution with high matrix effects was established by the successful detection of protein molecules from solution with high salt concentration. Experiments with LEMS enabled the detection of a protonated protein feature as the dominating peak in the mass spectra for up to 250 mM sodium chloride while conventional electrospray resulted in predominantly salt-adducted

features, with suppression of the protonated protein ions for the salt concentration of 5 mM. This dissertation also expanded upon the use of a reaction system to measure the lifetimes of laser vaporized liquid droplets coupled with electrospray and nano-spray postionization mass spectrometry. Electrospray and nanospray droplet lifetimes were measured to be 4.5±0.6 ms and 1.4±0.3 ms using LEMS and nano-LEMS measurements, respectively. Time dependent protein folding measurements using LEMS revealed intermediate states during protein folding processes which are often limited in conventional electrospray measurements where bulk solution in manipulated (change in pH) to achieve protein folding.

ACKNOWLEDGMENTS

First of all, I would like to deeply thank my advisor Dr. Robert Levis for all his guidance and support during my graduate career here at Temple University. Dr. Levis has helped me explore my scientific endeavor in countless ways and it would be worth mentioning the help I received during manuscript preparations. I am thankful to all of my group members past and present, especially John Brady, Paul Flanigan, Johnny Perez, Jieutonne Archer, Fengjian Shi, Habiballah Sistani and Rachel Parise. Without their support, assistance, thoughtful discussion, I would not have been able to finish this thesis. I would like to thank Dr. Ann Valentine, Dr. Michael Zdilla, and Dr. Charles McEwen for serving as my dissertation committee members. Finally, I would like to thank my wife Rupa for all her love and support.

For my family, who offered unconditional love and encouragement throughout my graduate studies and the time abroad.

TABLE OF CONTENTS

Page

LIST OF TABLES

LIST OF FIGURES

Figure Page

CHAPTER 1

DEVELOPMENT OF ATMOSPHERIC PRESSURE MASS SPECTROMETRY

1.1 Introduction

The development of the first mass spectrometer by Sir Joseph J. Thompson dates back to 1912, which was then used in the analysis of small molecules such as O_2, N_2, CO, CO_2 and $COCl_2$(1). After decades of continuous improvements, mass spectrometry became feasible in the discovery of isotopes and determination of accurate atomic weights and their relative abundances. By the 1960s, mass spectrometry became a valuable analytical tool in the analysis of organic compounds. However, the limitation in the analysis of macromolecules (>1 kDa) initially restricted the growth of mass spectrometry.

Several ionization methods have been developed in an effort to analyze macromolecules such as secondary ion mass spectrometry (SIMS)(2), plasma desorption (PD)(3), laser desorption (LD)(4) and fast atom bombardment (FAB)(5). SIMS utilizes a focused primary ion beam (e.g. Ar^+, Ga^+, In^+) to desorb the molecules adsorbed onto the substrate. The primary ion induces a collision cascade with atoms and molecules on the surface producing secondary ions, which are then released into the gas phase when their kinetic energy exceeds the binding energy to the substrate. The mass range of ~ 1000 (mass-to-charge, *m/z*) can only be analyzed using SIMS due to extensive surface fragmentation(6). Similar to SIMS, the energy carriers in PD are either ions or neutral

atoms that impinge the sample adsorbed onto the surface resulting in desorption of neutrals and ions. This technique has allowed the analysis of ions >10,000 Da(7). Unlike SIMS and PD, laser desorption uses a pulsed laser to produce gaseous ions. Laser pulses with intensity ranging from 10^6 to 10^{10} W cm^{-2} are focused onto the substrate surface (~10^{-3} to 10^{-4} cm^2) resulting in the vaporization and ionization of the desired analyte. The probability of ionization depends on the physical properties of the analyte such as photoabsorption, and volatility. A nanosecond (ns) laser results in rapid heating (108 to 1013 K/s) of the metallic substrate, which leads to thermal desorption and fragmentation of the analytes(4). Although mass analysis of large molecules became possible with the introduction of these techniques, yet high energy ions, atoms, and photons resulted in extensive fragmentation, thus hindering the analysis of intact molecular ion.

The fragmentation of a molecular ion could be limited by using a suitable matrix in conjunction with the analyte to be investigated. Fast atom bombardment, also known as liquid secondary ion mass spectrometry (LSIMS)(8), uses a beam of high energy neutral atoms/molecules or ions to create ions from the desired sample. In this case, the addition of a matrix to the analyte results in softer ionization. The matrix minimizes sample degradation as it absorbs the high energy from impinging atoms/ions and transfers the suitable energy to the analyte enabling detection of intact molecular ion. Despite the formation of molecular ion, this method suffers from high chemical background and low sensitivity.

The major obstacle for the application of mass spectrometry to biological fields was the inability to transform large biomolecules intact from bulk solution phase into the gas phase with adequate signal intensity. In 1985, Hillenkamp and Karas discovered that the addition of tryptophan (amino acid that absorbs 266 nm laser light) into alanine solution (amino acid that does not absorb 266 nm laser light) resulted in an increase in detection of alanine at a significantly lower irradiance in comparison with alanine without the addition of tryptophan. In this case, tryptophan is an absorbing matrix that transfers energy to the amino acid (alanine) facilitating desorption and ionization(9). The matrix therefore plays an important role in the absorption of laser energy allowing the analyte to be vaporized. The matrix can serve both as proton donor and receptor allowing the ionization of the given analyte in both positive and negative ion modes. This technique was coined as matrix assisted laser desorption ionization (MALDI). In 1987, Tanaka *et al* were the first to report the successful detection of intact protein and polymers >100,000 *m/z* ratio using a matrix that consisted of cobalt powder and glycerol(10). The detection of intact biomolecular ions using MALDI resulted in a Nobel Prize for Tanaka in 2002, and opened the door for numerous opportunities in the field of biological science. The development of MALDI enabled researchers to analyze compounds of interest directly from tissue sample without homogenization and/or extraction.

In recent years, MALDI has been extensively used as an analytical tool for mass spectrometry imaging (MSI)(11-15). The combination of mapping spatial coordinates to obtain molecular information from the given tissue sample makes MSI a valuable asset in bio-medical research. The detection of potential biomarkers, change in chemical

composition as function of disease types, and the ability to measure drug distributions in tissue sample have made MSI a promising tool in bridging biology and chemistry for applications such as clinical biomarker discovery, disease diagnosis, and drug development. The selection of a suitable matrix that resonantly absorbs the laser pulse is an essential step in performing MALDI experiments. Since, MALDI measurements are performed under vacuum conditions, exposing biological samples to non-native conditions often results in the loss of chemical information that could be preserved only under natural environments.

In 1988, John Fenn developed another soft ionization technique known as electrospray ionization mass spectrometry (ESI-MS) that can be operated at atmospheric pressure. Protein analysis using ESI was presented by John Fenn at the ASMS conference in San Francisco (1888) followed by the publication in a later date(16). The electrospray analysis involves dissolving the given analyte in a suitable solvent (usually a mixture of water and methanol or acetonitrile) often with the addition of acid to facilitate ion formation followed by pumping that solution through a hypodermic needle at a flow rate ranging from 1- 10 $\mu L min^{-1}$ (both higher and lower flow rates are common). A potential difference of typically 3-6 kV is applied to initiate the electrospray process. The applied electric field between the electrospray emitter and the counter-electrode (MS inlet) usually separated by 0.3 to 1.5 cm induces a charge accumulation at the tip of the electrospray needle resulting in a formation of a Taylor cone. When the forces from applied electric field exceeds the surface tension of the liquid, the Taylor cone breaks apart emitting a fine mist of charged droplets. These microdroplets are then desolvated

using a counter flow of drying gas (often nitrogen, 180-200 ^{o}C). As the solvent evaporates, the charge density on the electrospray droplet surface increases to a point where the Coulomb repulsion is greater than the surface tension of the liquid resulting in droplet fissioning events of larger droplets to produce smaller daughter droplets(17).

Electrospray ionization has been widely used in the analysis of protein and protein-complexes because of its ability to generate multiply charged $[M + zH]^{z+}$ gas phase ions, where M represents the intact molecule, zH represents the number of protons attached to the molecule, and z+ represents the overall charge on the molecule. ESI-MS measurements of proteins reveal multiply charged gas phase ions with a characteristic charge state distribution (CSD) correlating to the extent of denaturation(18-21). Protein in the native configuration is typically folded (e.g. protein present in ammonium acetate solution). This allows for the protection of basic amino acids in the interior from charging and hence a narrow distribution at lower charge states is observed. Once the protein unfolds (e.g. protein present in acidic solution), additional basic amino acids are exposed to the solvent environment and can acquire more charge. Denatured protein exhibits a much broader charge state distribution at higher charge states. Several reagents have been reported to increase protein charge states such as *m*-nitrobenzyl alcohol (*m*-NBA)(22, 23), sulfolane(24, 25), and ethylene carbonate(26). These reagents are effective in enhancing protein charge states when used in conjunction with an acidic (acetic/formic acid) solution. Enhanced charging of large biomolecules has shown to be valuable for performing high mass accuracy (sub-ppm) measurements(27, 28). In addition, enhanced charging of protein and protein-complexes also improves the efficiency of electron-based

tandem mass spectrometry (MS/MS) techniques for molecular sequencing experiments(29, 30).

Although ESI-MS has been extensively used in mass analysis of a wide range of molecules, the mechanism by which gas phase ions are formed is still an active area of research. The current consensus is that the small analytes in electrospray ionization are charged via the ion evaporation model (IEM)(31, 32). This model suggests that electrospray droplets shrink to a size of about 20 nm in diameter upon solvent evaporation resulting in the increase in electric field strength at the surface of the ES droplet which causes solvent ions to be expelled from the droplet(33). Conversely, large macromolecules (usually globular species) such as folded proteins are believed to be ionized via charge residue model (CRM)(34). This model suggests that a Taylor cone is formed during solvent evaporation at the highest surface curvature of the droplet from which smaller droplets are released. These processes occur until a droplet contains only one analyte molecule. Finally, the residual charge on the droplet surface is transferred to the analyte when solvent evaporates to dryness. It has been proposed that the unfolded proteins and disordered polymers, which are charged above the Rayleigh limit in ESI-MS, are ionized via a chain ejection model (CEM)(35). This model suggests that as the protein unfolds, it exposes non-polar residues to the solvent molecules and therefore partitions to the droplet surface (repelled by water molecules present in the droplet interior). These chains are then expelled in a sequential fashion and the protein will be separated from the droplet. During the chain ejection process, it is believed that the charge migration and charge equilibration between the droplet and the departing droplet

is responsible for the ionization of the protein molecule, which has been supported by molecular dynamics simulation studies(31, 36, 37).

ESI-MS is a useful technique in the analysis of wide range of analytes, however, sample preparation (homogenization and extraction) and lack of spatial information of the samples analyzed makes it challenging for research application involving tissue imaging. The development of techniques that operate at atmospheric pressure with minimal sample preparation and can provide spatial information of a sample is deemed necessary. Atmospheric pressure ionization techniques closely related to laser electrospray mass spectrometry are discussed in this dissertation.

1.2 Atmospheric Pressure Matrix-assisted Laser Desorption/Ionization Mass Spectrometry (AP-MALDI)

Nearly 10 years after the development of ESI and MALDI, atmospheric pressure matrix assisted laser desorption/ionization mass spectrometry was introduced by Burlingame *et al.*(38, 39). AP-MALDI combines the features of atmospheric pressure (AP) ionization and matrix-assisted laser desorption/ionization (MALDI). The common features of AP-MALDI with that of vacuum MALDI includes the nature of the matrix, procedure for sample preparation such as matrix to analyte ratio, energy of the laser beam etc. It has been proposed that the initial processes of laser absorption and desorption of gaseous plume containing analyte for AP-MALDI is similar to that of the vacuum MALDI, however in the case of AP-MALDI, atmospheric pressure processes such as

thermal equilibrium of the excited ions, and ion-ion/molecule reactions could exist for a longer timescales(38).

The transfer of ions generated at atmospheric pressure to the high vacuum region is pneumatically assisted (PA) by using a stream of nitrogen gas, and hence the acronym PA-AP MALDI is used. The ability of PA-AP MALDI to produce molecular ions with minimal fragmentation is of importance for the biological sample analysis. The analysis of peptides such as angiotensin and bombesin mixed with α-cyano-4-hydroxycinnamic (matrix) at a 1:1 ratio resulted in intact molecular ions in contrast to vacuum MALDI. This is attributed to rapid thermalization of ions upon collision with the ambient gas (collisional cooling) before fragmentation can occur, whereas excited ions in vacuum MALDI can dissociate in much lower pressure as the energy is conserved within the rapidly expanding 'plume' resulting in fragment ions(38).

The AP-MALDI measurements that utilize an infrared (IR) laser (AP-IR-MALDI) can analyze water-rich samples without matrix application as the laser couples to the O-H stretch of water(40, 41). The major limitation of AP-MALDI in the past was the sensitivity of the technique due to ion losses during transfer from atmospheric pressure to the vacuum interface.

1.3 Desorption Electrospray Ionization (DESI)

A new atmospheric pressure ionization technique was developed by Z. Takats *et al.* in 2004(42) to overcome some of the limitations of ESI-MS and MALDI. Briefly, ESI lacks spatial information and requires homogenization and dissolution in appropriate

solvents while MALDI requires the addition of a suitable matrix and placement of the sample under vacuum. The development of DESI enabled direct analysis of a sample (tissue) under atmospheric pressure without sample preparation. In DESI, an ionized stream of solvent (produced by ESI source) is directed towards the sample surface rather than centered and parallel with respect to the mass spectrometer inlet. The pneumatically assisted electrospray droplets splash onto the sample surface producing a thin layer of solvent film that dissolves the analyte. The splash of subsequent electrospray droplets releases the analyte dissolved in film into the gas phase by a 'droplet pick-up' mechanism for mass analysis. DESI has been used to analyze a wide range of analytes such as proteins(42, 43), peptides(42, 43), pharmaceuticals(42, 44), explosives(44, 45), plants(46), and tissues(47). The unique ability to analyze sample at atmospheric pressure while obtaining spatial information has made DESI a promising tool in mass spectral imaging research(48-51). The diameter of the electrospray plume that interacts with sample determines the spatial resolution of the technique. The use of nano-ESI has also been investigated to improve the spatial resolution of the technique. In this case, the decrease in electrospray plume diameter improves the spatial resolution. However, spectral imaging in DESI is limited to the sample's surface and therefore, topological information is limited (lack of depth profiling).

DESI has also been used to perform time resolved measurements of the given reaction systems. Reactive DESI was used to detect short-lived intermediates formed in the secondary microdroplets on the millisecond timescale by adding reactant in the spray solution that interacts with a compound adsorbed on a surface(52). Reaction times in

DESI measurements were later calculated by the reaction between oxidized 2, 6-dichloroindophenol (DCIP) and L-ascorbic acid (L-AA)(53).

1.4 Time Resolved Mass Spectrometry (TRMS)

Absorption and fluorescence spectroscopy are commonly used to monitor reaction kinetics on timescales as short as femtoseconds,(54-56) however these methods require endogenous chromophores or labelling of the reactant species. The ability to detect short-lived reaction intermediates with high chemical specificity has made mass spectrometry a suitable tool for studies of chemical and/or biochemical reactions such as formation of organometallic compounds, protein folding/unfolding and enzyme-catalyzed processes(57-60). However, the characterization of chemical/biochemical processes with 'high temporal resolution' is still a challenge. The time resolved information of the given reaction system in mass spectrometry is often limited by the mixing time. For instance, in conventional ESI-MS, reagents are mixed in the bulk solution phase prior to electrospraying and thus the analysis time is usually greater than a minute. In early studies, a flow-through photoreaction cell interfaced with ESI was used to detect intermediates of photochemical reactions of transition-metal complexes with a lifetime of a few minutes(61). Previous investigations have utilized a small-size reactor to minimize the time required for diffusion-dependent mixing(62-64). Further improvements on time resolved measurements were achieved with careful modification of the electrospray experimental set up and the development of new ionization techniques such as desorption electrospray ionization (DESI)(65), extractive electrospray ionization (EESI)(52),

microdroplet fusion mass spectrometry(66), and theta spray ionization mass spectrometry(67). In the section below, an early experimental setup used to perform time resolved mass spectral analysis and a newly developed ionization technique that uses a reaction system similar to the reaction system used in our experiment are discussed.

1.4.1 Stopped and Continuous-flow Electrospray Ionization Mass Spectrometry

Time resolved mass spectrometry was first introduced in late 90's where stopped-flow and continuous flow mixing devices were coupled with mass spectrometry to monitor the reaction kinetics of a reaction system with a time resolution from seconds to milliseconds(68, 69). In stopped-flow method(68), a two-step approach is used where reactant species are first flushed at relatively higher flow rates (~ 4.0 mL/s) through a mixer and a reaction tube via two syringe pumps clearing the contents from previous experiment. A third syringe pump is utilized to pump the reaction mixture along the reaction tube at a lower flow rate (~ 1.7 μL/s) prior to detection using a mass spectrometer. The length of the 'reaction capillary' determines the timescale of the kinetic measurements and the time resolution of 2.5 to 36 s could be achieved using this experimental set-up.

A continuous flow method has higher temporal resolution in comparison with the stopped-flow methods(69). The method consists of two syringe pumps that simultaneously pump solutions containing desired analytes such that the mixing of solutions occurs in a mixing tee. The mixing tee is connected to the third 'reaction capillary' that is connected to an electrospray emitter. The length of the 'reaction

capillary' controls the reaction time of the given reaction system. Time resolution of 81 ± 6 ms was previously achieved using continuous flow method with a dead volume of 3 nL corresponding to ~5 ms(69).

1.4.2 Theta-glass Capillaries for Rapid Mixing and Short Droplet Lifetimes

The development of a 'theta-shaped' borosilicate capillary, which consists of a nano-electrospray emitter with two separate channels, allows extremely small 'mixing volume' on the order of femtoliters(70). The interaction of reactants in this technique occurs partially in the ES tip and the Taylor cone while majority of reactions occur in the droplets during the desolvation process. Hence, this technique is suitable for short time-scale interactions. Protein folding and unfolding processes within the lifetime of the electrospray droplets have been investigated using this method(59, 67, 71).

The droplet lifetime in theta spray ionization was calculated by the reaction between oxidized DCIP (pH 3) and reduced L-AA (pH 3) loaded into the two opposite barrels of the theta-glass capillaries(67). On the basis of the forward rate constant of the reaction between DCIP and L-AA in the bulk solution phase, an average reaction time of 274±60 μs was calculated(67) which corresponds to the lifetime of electrospray droplets generated using theta-spray ionization. However, the surface to volume ratio, concentration of reagents, and the pH are expected to increase during solvent evaporation(72, 73). These factors can therefore escalate the rate of product formation by ~1-3 orders of magnitude in a rapidly desolvating ES droplet in comparison with the bulk solution phase(74-76). Considering the increased rates of product formation in droplets

over the bulk solution phase, the lifetime of ES droplet in the case of theta-spray ionization was estimated to be 10 and 1000 times less than the average reaction times i.e. between 27 μs and 270 ns(67).

1.5 Laser-electrospray Hybrid Techniques for Ambient Mass Analysis

The benefits of direct sample analysis under ambient conditions with minimal to no sample preparation has led to the invention of a wide range of novel ionization methods with application in numerous fields such as forensics, material science, and biomedical research etc. The common goal of the numerous laser vaporization/desorption techniques is to increase sensitivity while maintaining minimal sample preparation for mass analysis. It has been reported that the post-ionization of laser desorbed neutral molecules improves the sensitivity of the system by several orders of magnitude(77, 78). There are several methods that combine desorption and ionization steps together for ambient mass analysis; three of them will be discussed in this dissertation.

1.5.1 Electrospray-assisted Laser Desorption (ELDI)

The development of ELDI in 2005 by Shiea *et al.* considerably expanded the analysis of solid materials under ambient conditions, particularly the study of proteins without the addition of matrix and sample preparation(79). ELDI uses a nitrogen laser with wavelength of 337 nm and pulse duration of 4 ns. The laser (operating at 10 Hz) interacts with the sample at an incidence angle of 45^0 resulting in desorption of the analyte from the surface followed by capture and ionization in the electrospray plume. ELDI is the first laser based technique that enabled the detection of intact protein without

matrix application. However, the requirement for this analysis was that the protein needed to be dried before analysis, which could perturb protein's three dimensional structures. Protein analysis from solution requires the addition of carbon powder(80) or a MALDI matrix(81) for the observation of ion signal. A matrix that resonantly absorbs the laser radiation transfers energy to the solvent molecules surrounding the analytes resulting in desorption of the analyte, which is then captured and ionized by the electrospray plume. Resonant transition occurs when the energy spacing between two energy levels (ground and excited) is equal to the energy of η number of photons, $\eta\hbar\omega$, where $\hbar$ is Planck's constant divided by 2π, and ω is the angular frequency of the photon.

Analysis of an aqueous myoglobin sample using ELDI requires the addition of an appropriate inert particles/matrix. The particles/matrix should absorb laser radiation to facilitate protein desorption into the electrospray plume for ionization and at same time, and should not denature protein upon interaction. For instance, the addition of gold nanoparticles (Au NPs) into the myoglobin solution resulted in entirely denatured protein, which is possibly due to the presence of citric acid in the Au NP solution that was used for synthesis(80). In the case of matrix application, UV-absorbing organic matrixes such as sinnapinic acid (SA) and α-cyano-4-hydroxycinnamic acid (α-CHC) absorbed the UV laser radiation' however, the energy transfer to desorb the protein molecules from the solution was not efficient as indicated by the decrease in signal intensity of the protein ions. In addition, these matrices are acidic in nature, thus obstructing the native analysis of protein molecules. Mass spectra representing the native myoglobin ions were reported

for the carbon powder at concentrations ranging from 0.2 to 0.8 mg/ml. However, the presence of carbon powder in a small volume of protein sample could result in direct energy transfer to protein molecules adsorbed onto the surface of these carbon powders resulting in protein denaturation and fragmentation during desorption.

1.5.2 Matrix-assisted Laser Desorption Electrospray Ionization (MALDESI)

In the case where information obtained from MALDI measurement is not sufficient for unambiguous protein identification, nano-electrospray and/or electrospray ionization tandem mass spectrometry (ESI-MS/MS) analysis is usually performed. However, the analysis of samples in the presence of contaminants, such as salt and detergents, is problematic when using ESI MS because of the increased salt adduction and ion suppression effects(82). Matrix assisted laser desorption electrospray ionization, developed by Muddiman *et al.* in 2006, uses a 337 nm pulsed nitrogen laser to ablate anlaytes mixed with matrix into the electrospray plume for capture and ionization(83). Protein and peptide analysis using MALDESI involves dissolving the analyte in a sinnapinic acid matrix and laser vaporizing from a stainless steel substrate using 4 nanosecond (ns), 120 μJ laser pulses centered at 337 nm into the electrospray plume for capture and ionization. The multiple charging of B-type natriuretic peptide (BNP-32) and ubiquitin protein molecules observed in MALDESI experiments suggests that the gaseous ions in MALDESI experiments are formed in a manner similar to ESI (multiply charged) rather than MALDI where singly charged ions are often observed(84).

Similar to ELDI, MALDESI has also been used to analyze liquid samples of proteins and peptides dissolved in an organic matrix (this technique was coined as liq-MALDESI)(85). Typically, liq-MALDESI measurements are performed by depositing liquid sample (melittin) mixed with an organic matrix (2,5-dihydroxybenzoic acid, DHB) onto a sample target followed by laser ablation into the electrospray plume for ionization. However, when the sample target was biased to a higher voltage (3.0 kV in comparison with 500 V, normally used for solid state MALDESI analysis) ion signal was observed for melittin without the use of electrospray for post-ionization. In this case, the desorbed droplet acted as the electrospray droplet generating multiply charged ions. IR-MALDESI has also been used for mass analysis of bovine milk and egg yolk, which showed more mass spectral features in comparison with UV-MALDESI. This is due to water molecules acting as a matrix for the 2.94 μm laser light similar to laser assisted electrospray ionization (LAESI) mass spectrometry, which will be discussed next. Since, MALDESI combines the benefits of both AP-MALDI and ESI, this technique has serval advantages than either alone such as, enhanced quantitative analysis, spatially resolved analysis and shot-to-shot reproducibility.

1.5.3 Laser Ablation Electrospray Ionization (LAESI)

Laser ablation electrospray ionization developed by Vertes *et al.* in 2007 uses a mid-infrared laser to generate gas phase particles from the given sample which are then post-ionized using an electrospray ionization source(86). The analysis of tissue samples and biological fluids using IR lasers is possible because the laser energy is coupled into

the sample through absorption due to O-H vibrations (OH stretch at ~2.9 μm). The use of water as a matrix for desorption of the desired analytes reduces sample preparation enabling rapid analysis of biological samples at atmospheric pressure without perturbing the structural conformations of biomolecules. Analysis of vitamin B_{12} and peptides using LAESI revealed intact molecular ions similar to ESI whereas fragments were observed in the case of UV-MALDI measurements suggesting that LAESI is a soft ionization technique(87).

The laser desorbed plume in AP-IR-MALDI has shown to contain a sufficient portion of ionic components that enabled mass analysis. However, the detected ion signal decreased rapidly when the sampling distance was increased to ~4 mm from the ablated surface. This effect is attributed to the ion recombination with decreasing plume expansion in the presence of background gas. Conversely, in LAESI experiments, the laser vaporized plume captured by charged electrospray droplets enabled the maximum ion signal at a distance of ~15 mm between the spray axis to the ablated surface indicating a completely different ion formation mechanism compared to AP IR-MALDI(88).

Biological tissue imaging using a mid-IR laser is feasible due to the presence of water, which acts as a matrix to absorb the laser light facilitating the desorption of analytes for electrospray post-ionization. Initial LAESI experiments were carried out with a lateral resolution of 350 μm(88). However with the use of an etched tip GeO_2-based glass fiber, Mid-IR laser pulses were focused down to the spot sizes of 30-40 μm enabling the analysis of individual eggs of *L. pictus* that are 90 to 100 μm in

diameter(89). Due to the higher penetration depth for IR in comparison with UV laser, LAESI has also been used to obtain chemical information from tissue samples with a depth resolution of ~30-40 μm(90).

1.5.4 Laser Electrospray Mass Spectrometry (LEMS)

In 2009, Brady *et al.* used an ultrafast femtosecond (fs) laser pulse centered at 800 nm wavelength to desorb analyte from condensed phase into the gas phase followed by capture and ionization using an electrospray ion source and was mass analyzed using a homebuilt mass spectrometer(91). This technique was named laser electrospray mass spectrometry (LEMS), the experimental setup of which is shown in Figure 1.1. LEMS couples nonresonant femtosecond (fs) laser vaporization with an electrospray ionization source to perform universal mass analysis at atmospheric pressure. The main advantage of using a femtosecond laser pulse over picosecond and nanosecond laser pulses used for desorption/ionization processes is the timescale at which the energy is being deposited into the target analyte. A femtosecond laser pulse (~50-fs) deposits energy to the target analyte on a timescale much shorter than the molecular rearrangement time(92), which results in the parent molecular ion dominating the mass spectra. The increase in ion abundance of a parent molecular ion for fs laser is attributed to a 'ladder climbing' mechanism. Conversely, nanosecond pulses deposit energy into the molecular system for a longer period of time resulting in fragmentation of a parent molecular ion (due to thermal heating), which is attributed to the 'ladder-switching' mechanism(93-95).

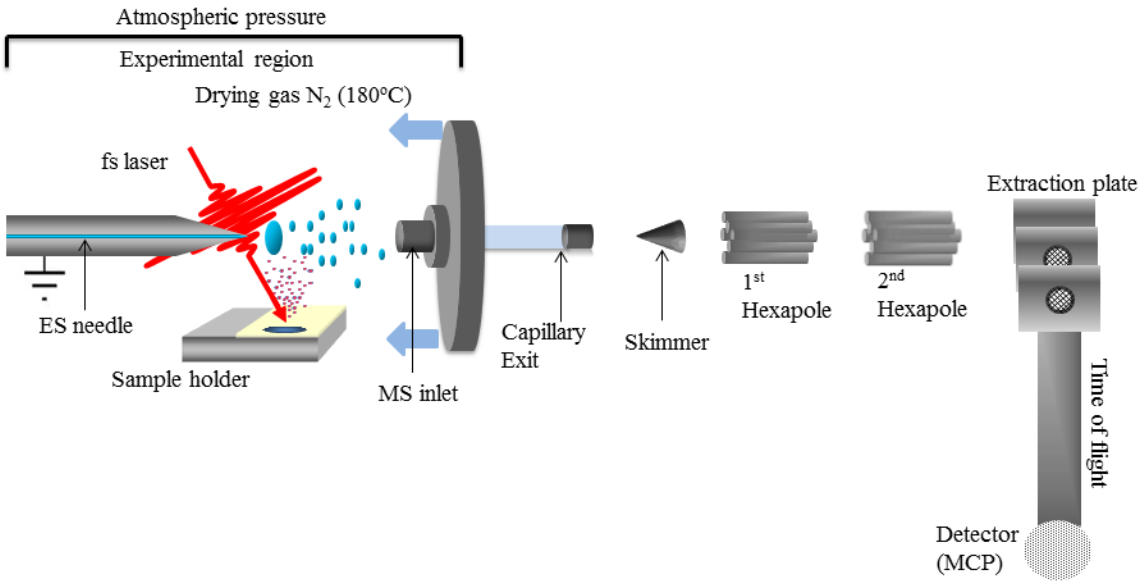

Figure 1.1. Schematic of the instrumental setup for laser electrospray mass spectrometry (LEMS) experiments.

The fs laser pulses couple directly into the target analyte through multiphoton, nonresonant absorption(93-95). Nonresonant absorption occurs when the energy of an incident photon is not equal to the energy required to excite a molecule from its ground state to some excited states. Laser intensities of ~$10^{13\text{-}14}$ W cm^{-2} are required to drive nonresonant multiphoton absorption processes and therefore short (~70 fs) laser pulses are usually required. At similar laser intensities (~$10^{13\text{-}14}$ W cm^{-2}), nanosecond laser pulses induce increased fragmentation.

Since the invention of LEMS in 2009, a wide variety of samples have been successfully analyzed without the need of matrix application at atmospheric pressure. These include small analytes(96), pharmaceuticals(97), lipids(98), proteins(22, 91, 99, 100), explosives(101-103), thermometer ions(104, 105), manganese cubane cluster,(106) and plant and animal tissue(107, 108). Recently, LEMS has also been used to perform high resolution mass spectral imagining using a commercial Bruker Micro-QTOF mass spectrometer with a lateral resolution of ~60 μm(109). The intensity of the fs laser used in our experiments is ~1 x 10^{13} W cm^{-2}, where one anticipates considerable fragmentation of the excited molecule. However, investigations of lysozyme and cytochrome c revealed that the condensed phase structure was preserved during the transfer to ES droplets when an intense fs laser was employed for vaporization(110). The folded protein conformation was observed when native protein was laser vaporized into the ES solvent containing neutral pH. This suggests that the timescale of fs laser vaporization is much shorter than the protein unfolding timescale and hence the native structure and function of protein and protein-complexes can be investigated using this technique.

The interaction time of laser vaporized droplets with that of electrospray generated charged droplets dictates the diffusion of laser vaporized analytes into the electrospray droplet. Considering a simple diffusion process, the mixing time, t, of two analytes depends upon their diffusion coefficient (D) and the distance separating the diffusing solutes (d), where $t=d^2/6D$. A short interaction time should therefore result in nonequilibrium partitioning of laser vaporized analytes into the ES droplet surface where excess charge resides as the available time is not enough for complete diffusion into the electrospray droplet. This effect has been shown to facilitate the quantitative analysis of small molecule mixtures(96), multi-component protein mixtures(100), enhanced charging of protein and protein complexes(22), and detection of protein molecules from high salt concentration(111).

The internal energy distribution of laser vaporized molecules was calculated for para-substituted benzylpyridinium ions (p-Cl, p-Me, p-MeO, p-CN and p-NO_2), commonly called thermometer ions, using a survival yield (ratio of the parent molecular ion to the sum of the parent molecular ion and its fragments) method for comparison with electrospray ionization. The measurement revealed that LEMS deposits more energy into the analytes using a dried droplet method in comparison with conventional ESI-MS. However, the energy deposition into the liquid sample is comparable to conventional ESI-MS suggesting that nonresonant laser vaporization does not impart additional energy to the desorbed analytes and hence is suitable for investigation of protein, protein-complexes, and tissue analysis.

1.6 Scope of this Dissertation

The role of supercharging reagents on gas phase protein structure along with the possibility of using LEMS for Top-down protein sequencing experiments has been discussed in Chapter 2. The use of LEMS enables the decoupling of bulk solution phase processes from processes occurring in the electrospray droplet to investigate supercharging mechanisms. In addition, the effect of adding supercharging reagent into a denaturing electrospray solvent containing trifluoroacetic acid, acetic acid, and formic acid for increasing ion abundance of higher charge states is discussed in Chapter 2. The comparisons between LEMS and ESI-MS for optimal charging of protein and protein complexes have been presented.

Chapter 3 includes the investigation of the hypothesis that laser vaporized acid-denatured protein could fold during the electrospray droplet lifetime upon interacting with the electrospray solvent containing suitable solution additives. The mechanism of protein folding and unfolding during the electrospray process is presented in Chapter 3 by separating the processes that occur in the electrospray droplet from those that occur in the capillary and Taylor cone. This is achieved by laser vaporizing either folded or unfolded protein directly into the electrospray droplets. Solution additives with varying gas phase basicities were investigated to study the correlation between gas phase basicity of the charge reducing additives and protein structure/charge state reduction.

The analysis of salt-rich biological samples usually requires separation steps prior to mass spectral analysis. The possibility of using LEMS for the direct analysis of protein

and protein mixtures from solutions containing high salt concentrations is presented in Chapter 4. It is reported that LEMS displays approximately two orders of magnitude higher salt tolerance in comparison with conventional ESI-MS with a higher protonated feature and lower sodium adduction. The mechanism based on non-equilibrium partitioning of laser vaporized analytes into the electrospray droplets for high salt tolerance in LEMS measurement has been discussed in Chapter 4.

Time resolved mass spectrometry is important in the study of short-lived reaction intermediates, protein folding, and unfolding kinetics etc. The measurements performed using conventional electrospray lacks the temporal information of the reaction systems as the reagents are mixed in the bulk solution phase prior to analysis. Measurements of the lifetime for laser vaporized liquid droplets coupled with electrospray and nano-spray post-ionization mass spectrometry as the possibility of studying reaction intermediates is presented in Chapter 5. The effect of distance between the spray (electrospray and nanospray) emitter and the capillary inlet, and the distance between the spray emitter and the laser vaporized spot on the droplet lifetime has been investigated for both LEMS and nano-LEMS measurements. In addition, the effect of droplet lifetimes on the fraction of folded protein for acid-denatured cytochrome c and myoglobin has been discussed in Chapter 5 using LEMS and nano-LEMS measurements.

1.7 References

1. Thomson, J. Rays of Positive Electricity and their Application to Chemical Analysis. **1913.**

2. Liebl, H. Ion microprobe mass analyzer. *J. Appl. Phys.* **1967,** (38), 5277-5283.

3. Macfarlane, R.; Torgerson, D. Californium-252 plasma desorption mass spectroscopy. *Science.* **1976,** (191), 920-925.

4. Posthumus, M.; Kistemaker, P.; Meuzelaar, H.; Ten Noever de Brauw, M. Laser desorption-mass spectrometry of polar nonvolatile bio-organic molecules. *Anal. Chem.* **1978,** (50), 985-991.

5. Barber, M.; Bordoli, R. S.; Sedgwick, R. D.; Tyler, A. N. Fast atom bombardment of solids (FAB): A new ion source for mass spectrometry. *Journal of the Chemical Society, Chem. Commun.* **1981,** 325-327.

6. Vickerman, J. C.; Briggs, D., ToF-SIMS: surface analysis by mass spectrometry, IM, **2001.**

7. McNeal, C. J.; Macfarlane, R. D. Observation of a fully protected oligonucleotide dimer at m/z 12637 by californium-252 plasma desorption mass spectrometry. *J. Am. Chem. Soc.* **1981,** (103), 1609-1610.

8. Aberth, W.; Straub, K. M.; Burlingame, A. Secondary ion mass spectrometry with cesium ion primary beam and liquid target matrix for analysis of bioorganic compounds. *Anal. Chem.* **1982,** (54), 2029-2034.

9. Karas, M.; Bachmann, D.; Hillenkamp, F. Influence of the wavelength in high-irradiance ultraviolet laser desorption mass spectrometry of organic molecules. *Anal. Chem.* **1985,** (57), 2935-2939.

10. Tanaka, K.; Waki, H.; Ido, Y.; Akita, S.; Yoshida, Y.; Yoshida, T.; Matsuo, T. Protein and polymer analyses up to m/z 100 000 by laser ionization time-of-flight mass spectrometry. *Rapid Commun. Mass Spectrom.* **1988,** (2), 151-153.

11. Grey, A. C.; Chaurand, P.; Caprioli, R. M.; Schey, K. L. MALDI imaging mass spectrometry of integral membrane proteins from ocular lens and retinal tissue. *J. Proteome Res.* **2009,** (8), 3278-3283.

12. Hinsch, A.; Buchholz, M.; Odinga, S.; Borkowski, C.; Koop, C.; Izbicki, J. R.; Wurlitzer, M.; Krech, T.; Wilczak, W.; Steurer, S. MALDI imaging mass

spectrometry reveals multiple clinically relevant masses in colorectal cancer using large-scale tissue microarrays. *J. Mass Spectrom.* **2017,** (52), 165-173.

13. Prentice, B. M.; Chumbley, C. W.; Caprioli, R. M. Absolute quantification of rifampicin by MALDI Imaging mass spectrometry using multiple TOF/TOF events in a single laser shot. *J. Am. Soc. Mass Spectrom.* **2017,** (28), 136-144.

14. Puolitaival, S. M.; Burnum, K. E.; Cornett, D. S.; Caprioli, R. M. Solvent-free matrix dry-coating for MALDI imaging of phospholipids. *J. Am. Soc. Mass Spectrom.* **2008,** (19), 882-886.

15. Xu, B. J.; Caprioli, R. M.; Sanders, M. E.; Jensen, R. A. Direct analysis of laser capture microdissected cells by MALDI mass spectrometry. *J. Am. Soc. Mass Spectrom.* **2002,** (13), 1292-1297.

16. Fenn J. B, M. M., Meng C. K, Wong S. F, Whitehouse C. M. Electrospray ionization for mass spectrometry of large biomolecules *Science.* **1989,** (246), 64-71.

17. Cech, N. B.; Enke, C. G. Practical implications of some recent studies in electrospray ionization fundamentals. *Mass Spectrom. Rev.* **2001,** (20), 362-387.

18. Kharlamova, A.; DeMuth, J. C.; McLuckey, S. A. Vapor treatment of electrospray droplets: evidence for the folding of initially denatured proteins on the sub-millisecond time-scale. *J. Am. Soc. Mass Spectrom.* **2012,** (23), 88-101.

19. Konermann, L.; Douglas, D. Acid-induced unfolding of cytochrome c at different methanol concentrations: electrospray ionization mass spectrometry specifically monitors changes in the tertiary structure. *Biochemistry.* **1997,** (36), 12296-12302.

20. Liu, J.; Konermann, L. Irreversible thermal denaturation of cytochrome C studied by electrospray mass spectrometry. *J. Am. Soc. Mass Spectrom.* **2009,** (20), 819-828.

21. Loo, J. A.; Loo, R. R. O.; Udseth, H. R.; Edmonds, C. G.; Smith, R. D. Solvent-induced conformational changes of polypeptides probed by electrospray-ionization mass spectrometry. *Rapid Commun. Mass Spectrom.* **1991,** (5), 101-105.

22. Karki, S.; Flanigan, P. M.; Perez, J. J.; Archer, J. J.; Levis, R. J. Increasing protein charge state when using laser electrospray mass spectrometry. *J. Am. Soc. Mass Spectrom.* **2015,** (26), 706-715.

23. Sterling, H. J.; Williams, E. R. Origin of supercharging in electrospray ionization of noncovalent complexes from aqueous solution. *J. Am. Soc. Mass Spectrom.* **2009,** (20), 1933-1943.

24. Douglass, K. A.; Venter, A. R. Investigating the role of adducts in protein supercharging with sulfolane. *J. Am. Soc. Mass Spectrom.* **2012,** (23), 489-497.

25. Miladinović, S. a. M.; Fornelli, L.; Lu, Y.; Piech, K. M.; Girault, H. H.; Tsybin, Y. O. In-spray supercharging of peptides and proteins in electrospray ionization mass spectrometry. *Anal. Chem.* **2012,** (84), 4647-4651.

26. Teo, C. A.; Donald, W. A. Solution additives for supercharging proteins beyond the theoretical maximum proton-transfer limit in electrospray ionization mass spectrometry. *Anal. Chem.* **2014,** (86), 4455-4462.

27. Good, D. M.; Wirtala, M.; McAlister, G. C.; Coon, J. J. Performance characteristics of electron transfer dissociation mass spectrometry. *Mol. Cell. Proteomics.* **2007,** (6), 1942-1951.

28. Perry, R. H.; Cooks, R. G.; Noll, R. J. Orbitrap mass spectrometry: instrumentation, ion motion and applications. *Mass Spectrom. Rev.* **2008,** (27), 661-699.

29. Horn, D. M.; Breuker, K.; Frank, A. J.; McLafferty, F. W. Kinetic intermediates in the folding of gaseous protein ions characterized by electron capture dissociation mass spectrometry. *J. Am. Chem. Soc.* **2001,** (123), 9792-9799.

30. Tsybin, Y. O.; Fornelli, L.; Stoermer, C.; Luebeck, M.; Parra, J.; Nallet, S.; Wurm, F. M.; Hartmer, R. Structural analysis of intact monoclonal antibodies by electron transfer dissociation mass spectrometry. *Anal. Chem.* **2011,** (83), 8919-8927.

31. Konermann, L.; Ahadi, E.; Rodriguez, A. D.; Vahidi, S. Unraveling the mechanism of electrospray ionization. *Anal. Chem.* **2012**, 85, 2-9.

32. Loo, R. R. O.; Lakshmanan, R.; Loo, J. A. What protein charging (and supercharging) reveal about the mechanism of electrospray ionization. *J. Am. Soc. Mass Spectrom.* **2014,** (25), 1675-1693.

33. Hogan Jr, C. J.; Carroll, J. A.; Rohrs, H. W.; Biswas, P.; Gross, M. L. Combined charged residue-field emission model of macromolecular electrospray ionization. *Anal. Chem.* **2008,** (81), 369-377.

34. De La Mora, J. F. Electrospray ionization of large multiply charged species proceeds via Dole's charged residue mechanism. *Anal. Chim. Acta.* **2000,** (406), 93-104.

35. Konermann, L.; Rodriguez, A. D.; Liu, J. On the formation of highly charged gaseous ions from unfolded proteins by electrospray ionization. *Anal. Chem.* **2012,** (84), 6798-6804.

36. Metwally, H.; McAllister, R. G.; Konermann, L. Exploring the mechanism of salt-induced signal suppression in protein electrospray mass spectrometry using experiments and molecular dynamics simulations. *Anal. Chem.* **2015,** (87), 2434-2442.

37. Popa, V.; Trecroce, D. A.; McAllister, R. G.; Konermann, L. Collision-induced dissociation of electrosprayed protein complexes: An all-atom molecular dynamics model with mobile protons. *The Journal of Physical Chemistry B.* **2016,** (120), 5114-5124.

38. Laiko, V. V.; Baldwin, M. A.; Burlingame, A. L. Atmospheric pressure matrix-assisted laser desorption/ionization mass spectrometry. *Anal. Chem.* **2000,** (72), 652-657.

39. Wolfender, J. L.; Chu, F.; Ball, H.; Wolfender, F.; Fainzilber, M.; Baldwin, M. A.; Burlingame, A. L. Identification of tyrosine sulfation in Conus pennaceus conotoxins α-PnIA and α-PnIB: further investigation of labile sulfo-and phosphopeptides by electrospray, matrix-assisted laser desorption/ionization (MALDI) and atmospheric pressure MALDI mass spectrometry. *J. Mass Spectrom.* **1999,** (34), 447-454.

40. Li, Y.; Shrestha, B.; Vertes, A. Atmospheric pressure molecular imaging by infrared MALDI mass spectrometry. *Anal. Chem.* **2007,** (79), 523-532.

41. Li, Y.; Shrestha, B.; Vertes, A. Atmospheric pressure infrared MALDI imaging mass spectrometry for plant metabolomics. *Anal. Chem.* **2008,** (80), 407-420.

42. Takats, Z.; Wiseman, J. M.; Gologan, B.; Cooks, R. G. Mass spectrometry sampling under ambient conditions with desorption electrospray ionization. *Science.* **2004,** (306), 471-473.

43. Takats, Z.; Wiseman, J. M.; Cooks, R. G. Ambient mass spectrometry using desorption electrospray ionization (DESI): instrumentation, mechanisms and applications in forensics, chemistry, and biology. *J. Mass Spectrom.* **2005,** (40), 1261-1275.

44. Chen, H.; Talaty, N. N.; Takáts, Z.; Cooks, R. G. Desorption electrospray ionization mass spectrometry for high-throughput analysis of pharmaceutical samples in the ambient environment. *Anal. Chem.* **2005,** (77), 6915-6927.

45. Cotte-Rodríguez, I.; Takáts, Z.; Talaty, N.; Chen, H.; Cooks, R. G. Desorption electrospray ionization of explosives on surfaces: sensitivity and selectivity enhancement by reactive desorption electrospray ionization. *Anal. Chem.* **2005,** (77), 6755-6764.

46. Talaty, N.; Takáts, Z.; Cooks, R. G. Rapid in situ detection of alkaloids in plant tissue under ambient conditions using desorption electrospray ionization. *Analyst.* **2005,** (130), 1624-1633.

47. Wiseman, J. M.; Ifa, D. R.; Song, Q.; Cooks, R. G. Tissue imaging at atmospheric pressure using desorption electrospray ionization (DESI) mass spectrometry. *Angew.Chem. Int. Edit.* **2006,** (45), 7188-7192.

48. Dill, A. L.; Eberlin, L. S.; Zheng, C.; Costa, A. B.; Ifa, D. R.; Cheng, L.; Masterson, T. A.; Koch, M. O.; Vitek, O.; Cooks, R. G. Multivariate statistical differentiation of renal cell carcinomas based on lipidomic analysis by ambient ionization imaging mass spectrometry. *Analytical and bioanalytical chemistry.* **2010,** (398), 2969-2978.

49. Eberlin, L. S.; Dill, A. L.; Costa, A. B.; Ifa, D. R.; Cheng, L.; Masterson, T.; Koch, M.; Ratliff, T. L.; Cooks, R. G. Cholesterol sulfate imaging in human prostate cancer tissue by desorption electrospray ionization mass spectrometry. *Anal. Chem.* **2010,** (82), 3430-3434.

50. Girod, M.; Shi, Y.; Cheng, J.-X.; Cooks, R. G. Desorption electrospray ionization imaging mass spectrometry of lipids in rat spinal cord. *J. Am. Soc. Mass Spectrom.* **2010,** (21), 1177-1189.

51. Ifa, D. R.; Wiseman, J. M.; Song, Q.; Cooks, R. G. Development of capabilities for imaging mass spectrometry under ambient conditions with desorption electrospray ionization (DESI). *International Journal of Mass Spectrometry.* **2007,** (259), 8-15.

52. Marquez, C. A.; Wang, H.; Fabbretti, F.; Metzger, J. r. O. Electron-transfer-catalyzed dimerization of trans-anethole: Detection of the distonic tetramethylene radical cation intermediate by extractive electrospray ionization mass spectrometry. *J. Am. Chem. Soc.* **2008,** (130), 17208-17209.

53. Miao, Z.; Chen, H.; Liu, P.; Liu, Y. Development of submillisecond time-resolved mass spectrometry using desorption electrospray ionization. *Anal. Chem.* **2011,** (83), 3994-3997.

54. Kandori, H.; Sasabe, H.; Mimuro, M. Direct Determination of a Lifetime of the S2 State of. beta.-Carotene by Femtosecond Time-Resolved Fluorescence Spectroscopy. *J. Am. Chem. Soc.* **1994,** (116), 2671-2672.

55. Lian, T.; Bromberg, S. E.; Asplund, M. C.; Yang, H.; Harris, C. Femtosecond infrared studies of the dissociation and dynamics of transition metal carbonyls in solution. *The Journal of Physical Chemistry.* **1996,** (100), 11994-12001.

56. Riekert, L. Chemical Kinetics and Transport. von PC Jordan. Plenum Press, New York 1979. XVI, 368 S., geb. $25.80. *Angewandte Chemie.* **1979,** (91), 947-948.

57. Bergt, M.; Brixner, T.; Dietl, C.; Kiefer, B.; Gerber, G. Time-resolved organometallic photochemistry: Femtosecond fragmentation and adaptive control of CpFe (CO) 2X (X= Cl, Br, I). *J. Organomet. Chem.* **2002,** (661), 199-209.

58. Cheng, S.; Wu, Q.; Xiao, H.; Chen, H. Online Monitoring of Enzymatic Reactions Using Time-Resolved Desorption Electrospray Ionization Mass Spectrometry. *Anal. Chem.* **2017,** (89), 2338-2344.

59. Mortensen, D. N.; Williams, E. R. Ultrafast (1 μs) mixing and fast protein folding in nanodrops monitored by mass spectrometry. *J. Am. Chem. Soc.* **2016,** (138), 3453-3460.

60. Sogbein, O. O.; Simmons, D. A.; Konermann, L. Effects of pH on the kinetic reaction mechanism of myoglobin unfolding studied by time-resolved electrospray ionization mass spectrometry. *J. Am. Soc. Mass Spectrom.* **2000,** (11), 312-319.

61. Arakawa, R.; Tachiashiki, S.; Matsuo, T.; Detection of Reaction Intermediates: Photosubstitution of (Polypyridine) ruthenium (II) Complexes Using On-Line Electrospray Mass Spectrometry. *Anal. Chem.* **1995,** 67, 4133-4138.

62. Bringer, M. R.; Gerdts, C. J.; Song, H.; Tice, J. D.; Ismagilov, R. F. Microfluidic systems for chemical kinetics that rely on chaotic mixing in droplets. *Philosophical Transactions of the Royal Society of London A: Mathematical, Physical and Engineering Sciences.* **2004,** (362), 1087-1104.

63. Fidalgo, L. M.; Abell, C.; Huck, W. T. Surface-induced droplet fusion in microfluidic devices. *Lab on a Chip.* **2007,** (7), 984-986.

64. Yu, L.; Nassar, R.; Fang, J.; Kuila, D.; Varahramyan, K. Investigation of a novel microreactor for enhancing mixing and conversion. *Chemical Engineering Communications.* **2008,** (195), 745-757.

65. Perry, R. H.; Splendore, M.; Chien, A.; Davis, N. K.; Zare, R. N. Detecting reaction intermediates in liquids on the millisecond time scale using desorption electrospray ionization. *Angewandte Chemie.* **2011,** (123), 264-268.

66. Lee, J. K.; Kim, S.; Nam, H. G.; Zare, R. N. Microdroplet fusion mass spectrometry for fast reaction kinetics. *Proceedings of the National Academy of Sciences.* **2015,** (112), 3898-3903.

67. Mortensen, D. N.; Williams, E. R. Theta-glass capillaries in electrospray ionization: rapid mixing and short droplet lifetimes. *Anal. Chem.* **2014,** (86), 9315-9321.

68. Kolakowski, B. M.; Simmons, D. A.; Konermann, L. Stopped-flow electrospray ionization mass spectrometry: a new method for studying chemical reaction kinetics in solution. *Rapid Commun. Mass Spectrom.* **2000,** (14), 772-776.

69. Konermann, L.; Collings, B.; Douglas, D. Cytochrome c folding kinetics studied by time-resolved electrospray ionization mass spectrometry. *Biochemistry.* **1997,** (36), 5554-5559.

70. Mark, L.; Gill, M.; Mahut, M.; Derrick, P. Dual nano-electrospray for probing solution interactions and fast reactions of complex biomolecules. *European Journal of Mass Spectrometry.* **2012,** (18), 439.

71. Fisher, C. M.; Kharlamova, A.; McLuckey, S. A. Affecting protein charge state distributions in nano-electrospray ionization via in-spray solution mixing using Theta capillaries. *Anal. Chem.* **2014,** (86), 4581-4588.

72. Gatlin, C. L.; Turecek, F. Acidity determination in droplets formed by electrospraying methanol-water solutions. *Anal. Chem.* **1994,** (66), 712-718.

73. Girod, M.; Dagany, X.; Antoine, R.; Dugourd, P. Relation between charge state distributions of peptide anions and pH changes in the electrospray plume. A mass spectrometry and optical spectroscopy investigation. *International Journal of Mass Spectrometry.* **2011,** (308), 41-48.

74. Badu-Tawiah, A. K.; Campbell, D. I.; Cooks, R. G. Accelerated C–N bond formation in dropcast thin films on ambient surfaces. *J. Am. Soc. Mass Spectrom.* **2012,** (23), 1461-1468.

75. Badu-Tawiah, A. K.; Li, A.; Jjunju, F. P.; Cooks, R. G. Peptide cross-linking at ambient surfaces by reactions of nanosprayed molecular cations. *Angewandte Chemie International Edition.* **2012,** (51), 9417-9421.

76. Girod, M.; Moyano, E.; Campbell, D. I.; Cooks, R. G. Accelerated bimolecular reactions in microdroplets studied by desorption electrospray ionization mass spectrometry. *Chemical Science.* **2011,** (2), 501-510.

77. Coon, J. J.; Harrison, W. Laser desorption-atmospheric pressure chemical ionization mass spectrometry for the analysis of peptides from aqueous solutions. *Anal. Chem.* **2002,** (74), 5600-5605.

78. Coon, J. J.; McHale, K. J.; Harrison, W. Atmospheric pressure laser desorption/chemical ionization mass spectrometry: a new ionization method based on existing themes. *Rapid Commun. Mass Spectrom.* **2002,** (16), 681-685.

79. Shiea, J.; Huang, M. Z.; HSu, H. J.; Lee, C. Y.; Yuan, C. H.; Beech, I.; Sunner, J. Electrospray-assisted laser desorption/ionization mass spectrometry for direct ambient analysis of solids. *Rapid Commun. Mass Spectrom.* **2005,** (19), 3701-3704.

80. Shiea, J.; Yuan, C.-H.; Huang, M.-Z.; Cheng, S.-C.; Ma, Y.-L.; Tseng, W.-L.; Chang, H.-C.; Hung, W.-C. Detection of native protein ions in aqueous solution under ambient conditions by electrospray laser desorption/ionization mass spectrometry. *Anal. Chem.* **2008,** (80), 4845-4852.

81. Peng, I. X.; Shiea, J.; Loo, R. R. O.; Loo, J. A. Electrospray-assisted laser desorption/ionization and tandem mass spectrometry of peptides and proteins. *Rapid Commun. Mass Spectrom.* **2007,** (21), 2541-2546.

82. Mandal, M. K.; Chen, L. C.; Hashimoto, Y.; Yu, Z.; Hiraoka, K. Detection of biomolecules from solutions with high concentration of salts using probe electrospray and nano-electrospray ionization mass spectrometry. *Analytical Methods.* **2010,** (2), 1905-1912.

83. Sampson, J. S.; Hawkridge, A. M.; Muddiman, D. C. Generation and detection of multiply-charged peptides and proteins by matrix-assisted laser desorption electrospray ionization (MALDESI) Fourier transform ion cyclotron resonance mass spectrometry. *J. Am. Soc. Mass Spectrom.* **2006,** (17), 1712-1716.

84. Dixon, R. B.; Sampson, J. S.; Hawkridge, A. M.; Muddiman, D. C. Ambient aerodynamic ionization source for remote analyte sampling and mass spectrometric analysis. *Anal. Chem.* **2008,** (80), 5266-5271.

85. Sampson, J. S.; Hawkridge, A. M.; Muddiman, D. C. Development and characterization of an ionization technique for analysis of biological macromolecules: liquid matrix-assisted laser desorption electrospray ionization. *Anal.Chem.* **2008,** (80), 6773-6778.

86. Nemes, P.; Vertes, A. Laser ablation electrospray ionization for atmospheric pressure, in vivo, and imaging mass spectrometry. *Anal. Chem.* **2007,** (79), 8098-8106.

87. Nemes, P.; Huang, H.; Vertes, A. Internal energy deposition and ion fragmentation in atmospheric-pressure mid-infrared laser ablation electrospray ionization. *Phys. Chem. Chem. Phys.* **2012,** (14), 2501-2507.

88. Vertes, A.; Nemes, P.; Shrestha, B.; Barton, A. A.; Chen, Z.; Li, Y. Molecular imaging by Mid-IR laser ablation mass spectrometry. *Applied Physics A.* **2008,** (93), 885-891.

89. Shrestha, B.; Vertes, A. In situ metabolic profiling of single cells by laser ablation electrospray ionization mass spectrometry. *Anal. Chem.* **2009,** (81), 8265-8271.

90. Nemes, P.; Barton, A. A.; Li, Y.; Vertes, A. Ambient molecular imaging and depth profiling of live tissue by infrared laser ablation electrospray ionization mass spectrometry. *Anal. Chem.* **2008,** (80), 4575-4582.

91. Brady, J. J.; Judge, E. J.; Levis, R. J. Mass spectrometry of intact neutral macromolecules using intense non-resonant femtosecond laser vaporization with electrospray post-ionization. *Rapid Commun. Mass Spectrom.* **2009,** (23), 3151-3157.

92. Gobeli, D.; El-Sayed, M. Change in the mechanism of laser multiphoton ionization-dissociation in benzaldehyde by changing the laser pulse width. *J. Phys. Chem.* **1985,** (89), 3426-3429.

93. DeWitt, M. J.; Levis, R. J. Near-infrared femtosecond photoionization/dissociation of cyclic aromatic hydrocarbons. *J. Chem. Phys.* **1995,** (102), 8670-8673.

94. DeWitt, M. J.; Peters, D. W.; Levis, R. J. Photoionization/dissociation of alkyl substituted benzene molecules using intense near-infrared radiation. *Chem. Phys.* **1997,** (218), 211-223.

95. Levis, R. J.; DeWitt, M. J. Photoexcitation, ionization, and dissociation of molecules using intense near-infrared radiation of femtosecond duration. *J. Phys. Chem. A.* **1999,** (103), 6493-6507.

96. Flanigan IV, P. M.; Perez, J. J.; Karki, S.; Levis, R. J. Quantitative measurements of small molecule mixtures using laser electrospray mass spectrometry. *Anal. Chem.* **2013,** (85), 3629-3637.

97. Judge, E. J.; Brady, J. J.; Dalton, D.; Levis, R. J. Analysis of pharmaceutical compounds from glass, fabric, steel, and wood surfaces at atmospheric pressure using spatially resolved, nonresonant femtosecond laser vaporization electrospray mass spectrometry. *Anal. Chem.* **2010,** (82), 3231-3238.

98. Brady, J. J.; Judge, E. J.; Levis, R. J. Analysis of amphiphilic lipids and hydrophobic proteins using nonresonant femtosecond laser vaporization with electrospray post-ionization. *J. Am. Soc. Mass Spectrom.* **2011,** (22), 762-772.

99. Karki, S.; Sistani, H.; Archer, J. J.; Shi, F.; Levis, R. J. Isolating Protein Charge State Reduction in Electrospray Droplets Using Femtosecond Laser Vaporization. *J. Am. Soc. Mass Spectrom.* **2017,** (28), 470-478.

100. Perez, J. J.; Flanigan IV, P. M.; Karki, S.; Levis, R. J. Laser electrospray mass spectrometry minimizes ion suppression facilitating quantitative mass spectral response for multicomponent mixtures of proteins. *Anal. Chem.* **2013,** (85), 6667-6673.

101. Brady, J. J.; Judge, E. J.; Levis, R. J. Identification of explosives and explosive formulations using laser electrospray mass spectrometry. *Rapid Commun. Mass Spectrom.* **2010,** (24), 1659-1664.

102. Flanigan IV, P. M.; Brady, J. J.; Judge, E. J.; Levis, R. J. Determination of inorganic improvised explosive device signatures using laser electrospray mass spectrometry detection with offline classification. *Anal. Chem.* **2011,** (83), 7115-7122.

103. Perez, J. J.; Flanigan IV, P. M.; Brady, J. J.; Levis, R. J. Classification of smokeless powders using laser electrospray mass spectrometry and offline multivariate statistical analysis. *Anal. Chem.* **2012,** (85), 296-302.

104. Flanigan, P. M.; Shi, F.; Archer, J. J.; Levis, R. J. Internal energy deposition for low energy, femtosecond laser vaporization and nanospray post-ionization mass spectrometry using thermometer ions. *J. Am. Soc. Mass Spectrom.* **2015,** (26), 716-724.

105. Flanigan, P. M.; Shi, F.; Perez, J. J.; Karki, S.; Pfeiffer, C.; Schafmeister, C.; Levis, R. J. Determination of internal energy distributions of laser electrospray mass spectrometry using thermometer ions and other biomolecules. *J. Am. Soc. Mass Spectrom.* **2014,** (25), 1572-1582.

106. Vaddypally, S.; Kondaveeti, S. K.; Karki, S.; Van Vliet, M. M.; Levis, R. J.; Zdilla, M. J. Reactive Pendant Mn□ O in a Synthetic Structural Model of a Proposed S4 State in the Photosynthetic Oxygen Evolving Complex. *J. Am. Chem. Soc.* **2017,**

107. Flanigan IV, P. M.; Radell, L. L.; Brady, J. J.; Levis, R. J. Differentiation of eight phenotypes and discovery of potential biomarkers for a single plant organ class using laser electrospray mass spectrometry and multivariate statistical analysis. *Anal. Chem.* **2012,** (84), 6225-6232.

108. Shi, F.; Flanigan IV, P. M.; Archer, J. J.; Levis, R. J. Ambient Molecular Analysis of Biological Tissue Using Low-Energy, Femtosecond Laser Vaporization and Nanospray Postionization Mass Spectrometry. *J. Am. Soc. Mass Spectrom.* **2016,** (27), 542-551.

109. Shi, F.; Archer, J. J.; Levis, R. J. Nonresonant, femtosecond laser vaporization and electrospray post-ionization mass spectrometry as a tool for biological tissue imaging. *Methods.* **2016,** (104), 79-85.

110. Brady, J. J.; Judge, E. J.; Levis, R. J. Nonresonant femtosecond laser vaporization of aqueous protein preserves folded structure. *Pro. Natl. Acad. Sci.* **2011,** (108), 12217-12222.

111. Karki, S.; Shi, F.; Archer, J. J.; Sistani, H.; Levis, R. J. Direct analysis of proteins from solutions with high salt concentration using laser electrospray mass spectrometry. *Submitted to Analytical Chemistry.* **2017.**

CHAPTER 2

INCREASING PROTEIN CHARGE STATE WHEN USING LASER ELETCROPSRAY MASS SPECTROMETRY

2.1 Overview

This chapter details the possibility of using laser electrospray mass spectrometry (LEMS) for top-down protein sequencing experiments. The supercharging mechanism for protein and protein complexes is discussed based upon the mass spectral measurements that revealed similar charge state distributions (CSDs) for LEMS when compared to conventional electrospray ionization mass spectrometry (ESI-MS). A marked increase in ion abundance of higher charge states was observed for LEMS in comparison with conventional electrospray for cytochrome c (ranging from 19+ to 21+ vs. 13+ to 16+) and myoglobin (ranging from 19+ to 26+ vs. 18+ to 21+) using an ES solution containing *m*-nitro benzyl alcohol (*m*-NBA) and trifluoroacetic acid (TFA). The likely reason for an increase in both the average charge states and charge state with maximum intensity for acid-sensitive proteins (cytochrome c, and myoglobin) when using LEMS measurements in comparison with ESI-MS under equivalent solvent conditions has been discussed. The measure of protein CSD as a function of electrospray flow rate for cytochrome c and myoglobin is presented.

2.2 Introduction

Electrospray ionization of proteins generates multiply charged gas phase ions with

a charge state distribution (CSD) characteristic of the extent of denaturation(1). One of the factors that affects the CSD is the configuration of the protein in the solution phase prior to transfer to the gas phase(1, 2). A protein in its native configuration displays a narrow range of lower charge states because the amino acid side chains in the folded protein are protected from the solvent environment and lack the ability to pick up additional charge. A higher range of charge states typically results from an extended (unfolded) protein conformation where the amino acid side chains are exposed to the solvent and thus can accommodate more charge. In addition to protein conformation, other factors affect the CSD including: gas phase basicity of the analyte and solvent(3-5), presence of supercharging reagents(6-9), instrument settings and desolvation processes(10).

Increasing the number of charges on a given protein can be achieved either by adding protein to an acidic solution prior to electrospraying(2) or by exposing electrospray (ES) droplets containing protein molecules to acid vapors in the region between the spray tip and the MS inlet(11, 12). During the desolvation process, the ES droplets are enriched with acid content due to the faster evaporation rate of electrospray solvents such as water and methanol in comparison with an acid (*e.g.* acetic acid). An increase in the acid concentration lowers the droplet pH and provides a favorable condition for denaturation and increase in protein charging. In addition to increasing ion charge, interaction of protein molecules with acid vapors also helps to improve the ES signal response and to prevent the dissociation of noncovalent complexes resulting from a denaturing ES solvent prior to mass analysis(12). A reduction in the average charge state,

Z_{avg}, can be accomplished using basic vapors and has been reported using extractive electrospray ionization (EESI)(13) and electrosonic spray ionization (ESSI)(14). For example, in EESI, the basic reagent nebulized by the nitrogen gas interacts with the ES stream containing multiply charged protein ions, allowing ion/molecule reactions to reduce Z_{avg}.

Supercharging reagents, such as *m*-nitro benzyl alcohol (*m*-NBA), can also be employed to enhance charging of proteins. The low vapor pressure of *m*-NBA compared to conventional electrospray solvents results in an increased concentration of supercharging reagent in the droplet at the end of the desolvation process. This will change the properties of the droplet, which may result in chemical and/or thermal denaturation, although this has been the subject of debate (15-18). The change in protein conformation during the supercharging event is likely to be protein dependent(19). An investigation of the σ^{54} activator protein complex revealed a decrease in relative abundance of high-order complexes (heptamer, tetramer, trimer, and dimer) with a simultaneous increase in monomer abundance with increasing *m*-NBA concentration, suggesting a change in the structure due to partial dissociation of the complex(18). Conversely, using a supercharging reagent resulted in an increase in the average charge of phosphorylase b dimer (195 kDa) without the disruption of dimer complex suggesting that supercharging occurs without significant structural modification(16).

There are several merits associated with obtaining higher charge states. Enhanced charging of large biomolecules has been shown to be of value for performing high mass

accuracy (sub-ppm) measurements(20, 21) and for improving the efficiency of electron-based tandem mass spectrometry (MS/MS) techniques for molecular sequencing experiments(22-25). Increasing the protein ion charge state is important for performing top-down proteomics because the greater the charge state, the more rapid the dissociation during the MS/MS experiments giving rise to more useful information on the molecular sequence and structure of macromolecules(26).

The interaction of laser-desorbed proteins with the ES droplets containing a supercharging reagent can increase protein charge states, as shown by electrospray-assisted laser desorption/ionization (ELDI) measurements(27). The ELDI process, employing a UV laser for desorption of dried proteins into ES droplets containing *m*-NBA, was utilized for the online supercharging of human insulin and bovine carbonic anhydrase, resulting in an increase in the average charge state from 4.0 to 4.8 and from 27.7 to 30.0, respectively. Besides ELDI, several other laser based ionization techniques, such as laser ablation electrospray ionization (LAESI)(28), infrared laser-assisted desorption electrospray ionization (IR LADESI)(29), infrared laser desorption electrospray ionization (IR-LDESI)(30), matrix assisted laser desorption spray post-ionization mass spectrometry (LDSPI-MS)(31), and matrix-assisted laser desorption electrospray ionization (MALDESI)(32) have been developed. All these ambient ionization methods utilize a laser to desorb or ablate either liquid or solid samples followed by electrospray post-ionization. A detailed review of ambient laser mass spectrometry techniques has recently been published(33).

A recently developed atmospheric pressure ionization technique, (LEMS)(34) has enabled rapid analysis of large biomolecules and complex mixtures without pre-processing steps such as deposition of matrix, extraction from a homogenized sample, or placement into vacuum. LEMS couples nonresonant femtosecond (fs) laser vaporization with ES ionization to perform ambient pressure mass analysis on a wide variety of samples including pharmaceuticals(35), lipids(36), narcotics(37), dipeptides(34), explosives(38-40), and plant tissues(41, 42) for phenotype classification(41). Most importantly, investigations of lysozyme and cytochrome c revealed that the solution phase conformation was preserved during transfer to ES droplets when an intense, nonresonant ultrafast laser was employed for vaporization(43). Previous LEMS investigations suggested that the reduced interaction time of the laser vaporized analytes with the ES droplets limits partitioning into the interior of the droplet(43-45). This would allow vaporized analytes to preferentially interact with the surface of the ES droplet where charges reside. This nonequilibrium partitioning of laser vaporized proteins could facilitate a larger yield of higher charge states when subjected to highly acidic solvent conditions combined with a supercharging reagent, creating optimal conditions for performing electron-based tandem mass spectrometry (MS/MS) for top-down sequencing.

Here, we investigate nonresonant fs laser vaporization of proteins into ES solvents containing either a supercharging reagent (*m*-NBA) or the mixture of *m*-NBA and denaturing ES solvents, which consisted of either trifluoroacetic acid (TFA), acetic acid (AA), or formic acid (FA). We report the mass spectral charge state distributions for

cytochrome c, myoglobin, lysozyme and ubiquitin as a function of acid concentration in ES solution. The CSDs are compared for laser vaporization ES post-ionization and conventional ESI analyses. Charge state distributions were also measured as a function of electrospray solvent flow rate.

2.3 Experimental Section

2.3.1 Sample Preparation

Solid samples of ammonium acetate, cytochrome c and myoglobin from horse heart, ubiquitin from bovine erythrocytes and liquid samples of *m*-nitro benzyl alcohol (*m*-NBA) and trifluoroacetic acid were purchased from Sigma Aldrich (St. Louis, MO). Propylene carbonate, ethylene carbonate, and diethyl carbonate were also purchased from Sigma Aldrich (St. Louis, MO). Solid hen egg lysozyme was purchased from USB Corporation (Cleveland, OH). Liquid samples of acetic acid and formic acid were purchased from J.T. Baker (Phillipsburg, NJ). All analytes and reagents were used without further purification. A 1 x 10^{-3} M stock solution of cytochrome c, myoglobin, lysozyme and ubiquitin was prepared in HPLC grade water (Fisher Scientific, Pittsburgh, PA). For conventional ESI-MS, an aliquot of the stock solution was then diluted into 5 mM ammonium acetate prepared in 1:1 (v:v) water:methanol to yield a final protein concentration of 1 x 10^{-5} M. For native state analysis of cytochrome c using ESI, an aliquot of the stock solution was diluted into 5 mM aqueous ammonium acetate to yield the final protein concentration of 1 x 10^{-5} M. Five 1:1 (v:v) water:methanol ESI solutions containing 5 mM ammonium acetate were utilized in this study. These ESI solutions

included 0.4% *m*-NBA, 1% acetic acid, 0.4% *m*-NBA with either 0.1% trifluoroacetic acid, 0.1% acetic acid, or 0.1% formic acid. For LEMS analysis, 10 μL of the stock protein solution spotted on a stainless steel plate was vaporized from solution into the same ES solvents used for conventional ESI-MS but without any protein.

2.3.2 Laser Vaporization and Ionization Apparatus

A Ti:sapphire laser oscillator (KM Laboratories, Inc., Boulder, CO) seeded a regenerative amplifier (Coherent, Inc., Santa Clara, CA) for the creation of 75 fs, 2.0 mJ laser pulses centered at 800 nm. The laser, operated at 10 Hz to couple with the ES ion source, was focused to a spot size of ~350 μm in diameter with an incident angle of 45^{o} respect to the sample using a 16.9 cm focal length lens, with an approximate intensity of 2 x 10^{13} W/cm^{2}. The steel sample plate was biased to -2.0 kV to compensate for the distortion of electric field between the capillary and the needle caused by the sample stage. The area sampled was 6.4 mm below and approximately 1 mm in front of the ES needle. Aqueous protein sample (10 μL) deposited on the steel substrate was vaporized by the intense pulses allowing for capture and ionization by an ES plume travelling perpendicular to the vaporized material. The flow rate for ES solvent was typically set at 3 μL/min by a syringe pump (Harvard Apparatus, Holliston, MA), except for the flow rate study. The charged droplets containing captured analytes were dried by counter propagating nitrogen gas at 180 ^{o}C during transit to the MS inlet.

2.3.3 Mass Spectrometry and Data Analysis

The mass spectrometer used in this experiment has been previously described(34). The system combines an intense nonresonant femtosecond laser pulse that enables transference of the analytes into the gas phase for capture and ionization in an ES plume at atmospheric pressure. The ES ionization source (Analytica of Branford, Inc., Brandford, CT) operated in a configuration to generate positive ions consists of an ES needle, dielectric capillary, skimmer and hexapole. The ES needle was maintained at ground while the inlet capillary was biased to -4.5 kV to operate in positive ion mode. The ESI needle was 6.4 mm above and parallel to, the sample stage and was approximately 6.4 mm in front of the capillary entrance. The hexapole was operated in the trapping mode, where the positive ions were collected at 10 Hz. After exiting the ESI source, the ions were transferred to the extraction region by a second hexapole where they were injected orthogonally into the linear time-of-flight analyzer and extracted via two high voltage pulsers (Directed Energy Inc., Fort Collins, CO, and Quantum Technology Inc., Lake Mary, FL) that were triggered 210 μs after the ions exit the first hexapole. The positive ions were then detected, and the resulting mass spectra were averaged for 5 seconds for ESI and (50 laser shots) LEMS analysis.

The raw mass spectral data files were imported into the Cutter program (46) for integration of the protein features. Baseline subtraction and spectral realignment were performed before integration to ensure consistent integration. The average charge state (Z_{avg}) was calculated using equation 1,

$$Z_{avg} = \frac{\sum_{i}^{N} q_i w_i}{\sum_{i}^{N} w_i} \qquad (1)$$

where q_i is the net charge, W_i is the sum of signal intensity of the i^{th} charge state, and N is the number of charge states present in the mass spectra. The charge state with maximum intensity (Z_{mode}) was determined from the average of seven mass spectra.

2.3.4 Safety Considerations

Appropriate laser eye protection was worn by all lab personnel.

2.4 Results and Discussion

2.4.1 Analysis of Acid Sensitive Proteins

2.4.1.1 Cytochrome c

Cytochrome c is a small globular protein that contains a covalently bound heme group. The ESI-MS charge state distribution (CSD) of cytochrome c has been shown to correlate with solution phase conformation(2). The native configuration of the protein results in a narrow range of charge states (mostly 8+ and 7+) at high *m/z* ratio as shown by nano-ESI-MS experiments(47), while the broad range of charge states centered around 12+ is indicative of the unfolded configuration(47, 48).

To investigate whether supercharging occurs during the desolvation process in the ES droplet, nonresonant laser vaporization was employed to transfer aqueous proteins

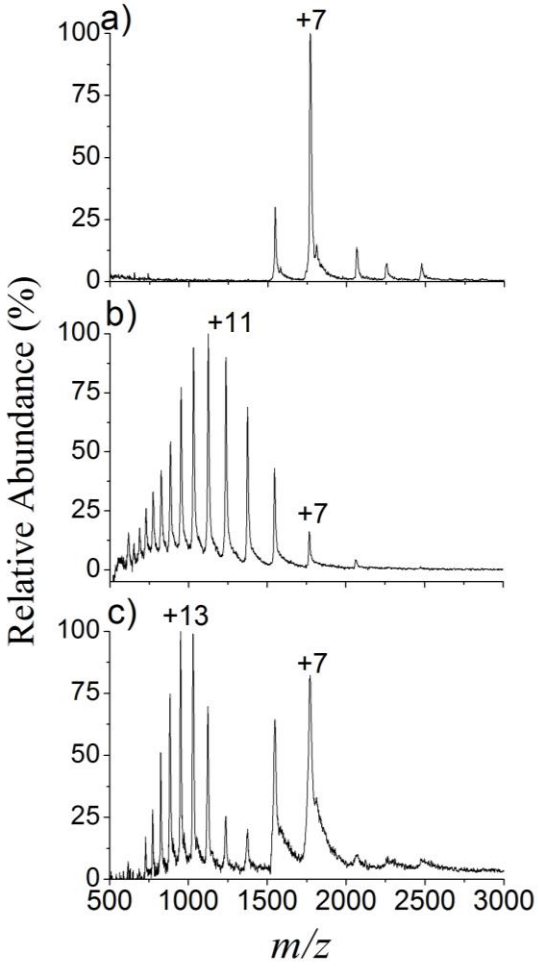

Figure 2.1. LEMS mass spectra of cytochrome c in ES solvent of a) ammonium acetate, and b) 0.4% *m*-NBA in ammonium acetate. Panel c represents LEMS mass spectra of cytochrome c with 1% AA in ES of ammonium acetate. Note: 5 mM ammonium acetate was prepared in 1:1 (v:v) water: methanol.

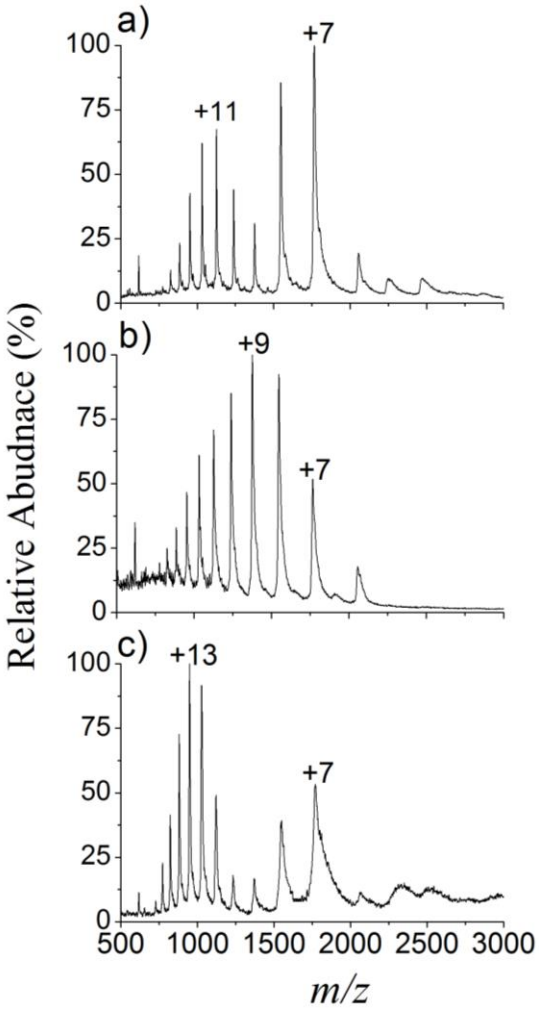

Figure 2.2. ESI mass spectra of cytochrome c prepared in a) ammonium acetate, b) 0.4% *m*-NBA in ammonium acetate, and c) 1% AA in ammonium acetate solution.

directly into the electrospray plume. Previous investigations suggest that condensed phase native structure is preserved to a large degree upon femtosecond laser vaporization into the gas phase(43, 49). The ESI solution consisted of water:methanol solvent with additives including ammonium acetate, and *m*-NBA. The LEMS mass spectra obtained from vaporizing cytochrome c into the electrospray solvent consisting of ammonium acetate displayed a narrow range of charge states centered at 7+ with average charge state (Z_{avg}) of 7.4 (Figure 2.1 a). Upon laser vaporization of cytochrome c into the solvent containing a supercharging reagent (0.4% *m*-NBA in ammonium acetate solution), the CSD shifts towards the higher charge state, peaked at 11+ (Z_{avg} = 11.9), as seen in Figure 2.1 b. Conventional electrospray of cytochrome c using the same electrospray solvents (Figure 2.2 a and b) revealed that the Z_{avg} of native and supercharged cytochrome c was 8.6 and 9.9, respectively. The mass spectral features obtained from conventional ESI-MS for supercharged cytochrome c are similar to those obtained with the LEMS measurements, suggesting that supercharging occurs after the transfer from the Taylor cone into the droplet during the desolvation process. This is in agreement with previous ELDI measurements(27).

The much greater shift in the CSD measured for LEMS (~60%) vs. that for ESI (~15%) is attributed in part to the fact that the Z_{avg} = 7.4 of cytochrome c in buffered solution is lower for LEMS than for ESI-MS Z_{avg} = 8.6, presumably because of the decreased interaction time of laser vaporized cytochrome c in the denaturing electrospray electrospray solution inducing some unfolding of the cytochrome c in conventional

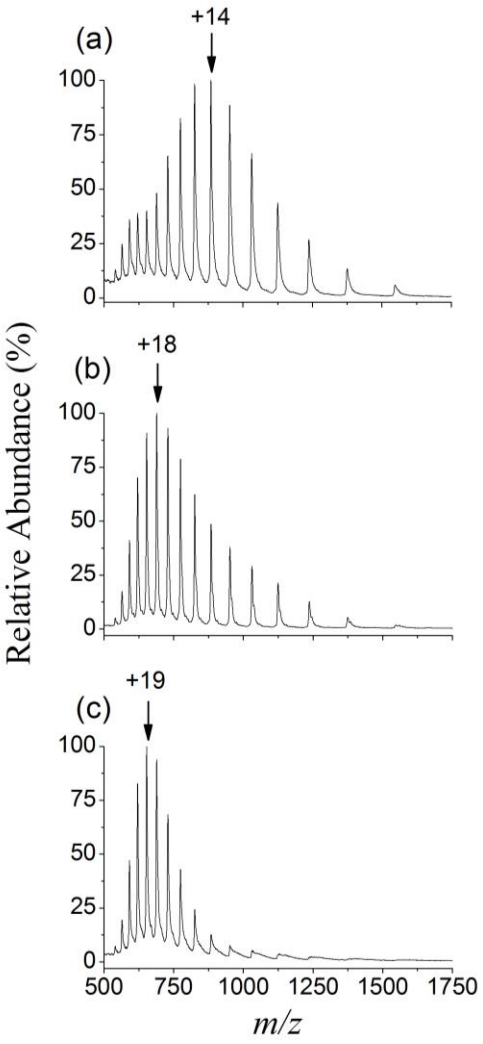

Figure 2.3. ESI mass spectra of cytochrome c prepared in ammonium acetate with 0.4% *m*-NBA and 0.1% (a) TFA, (b) AA, and (c) FA. The pH of the solution was measured to be 2.2 with TFA, 2.9 with AA, and 2.5 with FA.

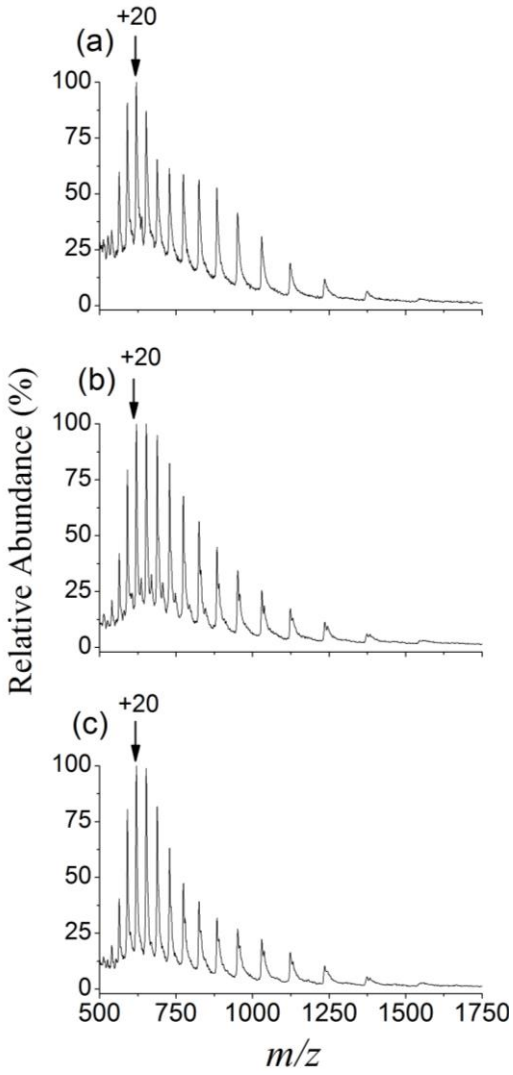

Figure 2.4. LEMS mass spectra of cytochrome c in ES solvent of ammonium acetate with 0.4% *m*-NBA and 0.1% a) TFA, b) AA, and c) FA.

ESI- MS analyses. Evidence for the unfolding is seen in the bimodal charge distribution in Figure 2.2 a. In addition, supercharging with LEMS results in a highest charge state (Z_{max} = 20) and average charge states (Z_{avg} = 11.9) that are greater than conventional ESI-MS (Z_{max} = 18, Z_{avg} = 9.9). The reduced interaction time of cytochrome c with electrospray droplets could allow interaction only with the surface where the charge resides, rather than partitioning into the interior of the droplet. Such nonequilibrium surface interaction would promote enhanced charging of cytochrome c for LEMS measurements as compared to the conventional electrospray process where equilibrium partitioning occurs(45).

The conventional ESI mass spectra of cytochrome c measured in solvent containing a mixture of *m*-NBA with either TFA, AA, or FA are shown in Figure 2.3 a, b and c, respectively. The measurements reveal monomodal CSDs with most abundant charge states (Z_{mode}) of 14+, 18+, and 19+ for TFA, AA, and FA, respectively. An increase in protein charge was achieved using a solvent containing either an acid or *m*-NBA in comparison with buffered water:methanol (Figure 2.1), but the solvents combining both an acid and *m*-NBA (Figure 2.3 and Figure 2.4) resulted in larger increase in ion intensities of the higher charge states than either alone. The Z_{max} observed in the mass spectra was 23+ for all three electrospray solvents, while the lowest charge state (Z_{min}) observed was 8+ for TFA and AA with *m*-NBA, and 10+ for FA with *m*-NBA. The broad range and increased abundance of higher charge states indicate that the

Protein	Acid	pH	Average charge state (Z_{avg})		Average Charge state with maximum intensity (Z_{mode})	
			ESI	**LEMS**	**ESI**	**LEMS**
Cytochrome	TFA	2.2	14.5 ± 0.1	16.3 ± 0.3	14.2 ± 0.4	20.0 ± 0.6
	AA	2.9	16.2 ± 0.1	16.5 ± 0.5	17.9 ± 0.4	18.8 ± 0.9
	FA	2.5	17.8 ± 0.1	16.8 ± 0.3	18.2 ± 0.5	19.8 ± 0.4
Myoglobin	TFA	2.2	18.6 ± 0.1	20.0 ± 0.4	17.4 ± 1.9	20.0 ± 3.4
	AA	2.9	20.5 ± 0.1	21.5 ± 0.5	22.5 ± 0.5	23.8 ± 0.5
	FA	2.5	21.3 ± 0.1	22.1 ± 0.4	23.4 ± 0.5	24.7 ± 0.5
Lysozyme	TFA	2.2	11.3 ± 0.1	11.9 ± 0.3	11.2 ± 0.9	12.6 ± 0.5
	AA	2.9	11.5 ± 0.0	11.4 ± 0.3	11.4 ± 0.5	11.3 ± 0.9
	FA	2.5	12.2 ± 0.0	11.9 ± 0.1	13.0 ± 0.0	11.7 ± 0.6
Ubquitin	TFA	2.2	10.5 ± 0.1	10.8 ± 0.3	12.0 ± 0.0	12.0 ± 0.4
	AA	2.9	11.5 ± 0.0	10.3 ± 0.3	12.0 ± 0.0	11.8 ± 0.4
	FA	2.5	11.2 ± 0.1	10.4 ± 0.2	12.0 ± 0.0	11.7 ± 0.5

Table 2.1. Summary of the mean of charge state distribution (Z_{avg}) and the charge state with maximum intensity (Z_{mode}) for cytochrome c, myoglobin, lysozyme and ubiquitin obtained from both ESI and LEMS measurements.

Table 2.2. Physiochemical properties[a] of different electrospray solvents

Solvent	Vapor pressure at 20° C	Boiling point (^{o}C)	Surface tension (dyn/cm) at 20^{0}C
Water	17.5	100	72
Methanol	97.66	64.6	22.50
Trifluoroacetic acid	97.5	73	13.63 (at 24^{o}C)[b]
Acetic acid	11.7	117.9	27
Formic acid	44.8	101	37.67
m-NBA	1.9 (at 80^{o}C)[c]	405[d]	50

[a]Data are taken from Ref.(50) , except as noted

[b]Data taken from Ref.(51)

[c] Data taken from Ref.(11)

[d] Data taken from Ref.(52)

cytochrome c unfolds as the result of the denaturing solvent containing acid and *m*-NBA. The mean of the CSD (Z_{avg}) and the charge states with maximum intensity (Z_{mode}) resulting from the analysis of the four proteins with different electrospray solvents are shown in Table 2.1. The variation in protein charge states (Z_{avg} and Z_{mode}) presumably arise from the pK_a, boiling point and/or the surface tension of the acids (Table 2.2). A correlation between the CSD shift of cytochrome c with the strength of the acid was previously reported by studying the effect of acid vapors leaked into the ESI interface(12). However, neither Z_{avg} nor Z_{mode} correlated to acid strength in this study. Trifluoroacetic acid is the strongest acid, followed by formic acid and acetic acid (pKa values of 0.52, 3.75, and 4.76, respectively). FA, followed by AA, provided the highest Z_{avg} and a larger increase in ion intensity of higher charge states when compared to TFA. The discrepancy in the Z_{avg} as a function of pK_a might be due to the difference in other physiochemical properties of the acids, such as boiling point, ion pairing ability and the surface tension. Trifluoroacetic acid has a lower boiling point than water and will evaporate during desolvation resulting in an increase in droplet pH compared to that of the starting solution, lowering the proton concentration at the droplet surface. Acetic acid has a higher boiling point than water, and during solvent evaporation, the ES droplets likely become enriched with acetic acid, increasing the proton concentration. In addition to the proton density, the nature of the anionic species present in the solution may also affect the distribution of protein charge states. Anions can pair with positively charged basic amino acids of the protein in the solution phase and reduce the total number of charges on a protein molecule(53). The stability of the adduct ($R\text{-}NH_2\cdots H^+\cdots A^-$) formed

depends on the gas-phase basicity of the amino group and the attaching anion(54). The limited resolution of the mass spectrometer does not enable the identification of adducts in this experiment. The CF_3COO^- anion (TFA) has a greater propensity to form an ion pair in comparison with CH_3COO^- anion (AA), which results in greater ion suppression effects. The increase in Z_{avg} for cytochrome c for *m*-NBA and FA in comparison with *m*-NBA and AA is most likely due to the pKa and/or the surface tension values of these acids.

Laser vaporization of aqueous cytochrome c into electrospray solutions consisting of 1:1 (v:v) water:methanol with *m*-NBA and TFA, AA, or FA was performed to investigate the nonequilibrium partitioning effect on Z_{avg} or the relative abundance of the higher charge states. The LEMS measurements for cytochrome c with *m*-NBA and TFA (Figure 2.4 a), AA (Figure 2.4 b), and FA (Figure 2.4 c) displayed monomodal CSDs with Z_{mode} values of 20+. The Z_{max} and Z_{min} observed in the mass spectra were 24+ and 8+, respectively, for all three electrospray solvent conditions. Investigations of cytochrome c, laser vaporized into a buffered water:methanol ESI solution, showed a Z_{mode} of 7+ (Figure 2.1 a). The high charge states observed from the interaction of laser vaporized folded cytochrome c with the denaturing electrospray solvents in this study suggests a conformational change in the protein. The Z_{avg} for the LEMS measurements in comparison with the ESI-MS measurements were: 16.3 ± 0.3 vs. 14.5 ± 0.1 for TFA, 16.5 ± 0.5 vs. 16.2 ± 0.1 for AA, and 16.8 ± 0.3 vs. 17.8 ± 0.1 for FA, as seen in Table 2.1. The fact that the Z_{avg} values for LEMS measurements were approximately the same suggests that the solution phase processes within the droplet are not important for laser vaporized protein. A droplet mixing experiment performed by colliding a 370 nL droplet

of a basic solution containing phenophthalein into an acoustically levitated 4 μL droplet of an acid showed that the basic solution remained on the surface for more than 2 seconds(55). This time scale is larger than the ~100 ms(43) time scale that the protein spends with the ES droplet during the transit to the capillary inlet in LEMS measurements. The Z_{avg} for cytochrome c laser vaporized into TFA and *m*-NBA is ~13% higher than for ESI. The increase in Z_{avg} is presumably due to the laser vaporization process allowing cytochrome c to interact exclusively with the ES droplet surface where the charge is located, eliminating interactions with the TFA anion, CF_3COO^-. The increase in Z_{avg} for LEMS measurement may also be due to the reduced protein concentration in electrospray plume. The capture efficiency of proteins is ~1% for LEMS measurements(35) which results in a higher charge availability for the given concentration of protein, resulting in a higher Z_{avg} compared to ESI. Previous CSD measurements for electrospray reveal a decrease in average charge state with increasing analyte concentration due to the decrease in excess charge with increasing protein concentration(56). Conversely, LEMS measurements of cytochrome c and myoglobin did not show the same trend as a function of increasing protein concentration suggesting minimal ion suppression compared to conventional electrospray(45). The adducts observed in the mass spectra are likely due to a reduction in desolvation of protein molecules during LEMS analysis. In the LEMS experiment, proteins are laser vaporized from pure water which presumably encapsulates the analyte thereby increasing the water concentration in the droplets. In ESI, proteins are dissolved in 1:1 (v:v) water:methanol for electrospray measurements. The increase in Z_{avg} for ESI measurements using FA with *m*-NBA is probably due to the

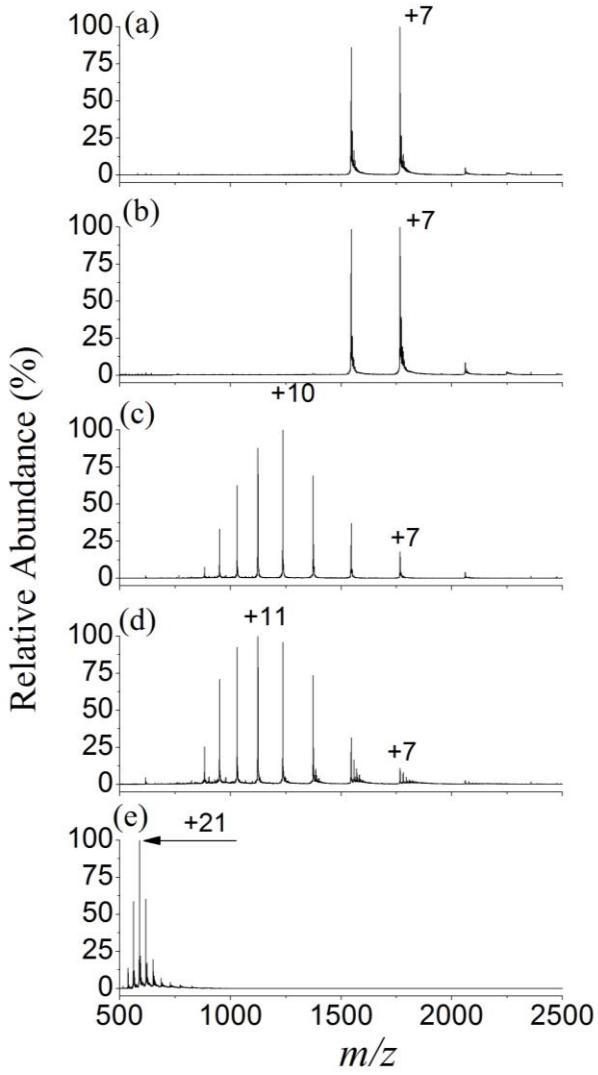

Figure 2.5. ESI mass spectra of cytochrome c prepared in 5 mM aqueous ammonium acetate and a) without the addition of supercharging reagent, b) 4.3% DEC, c) 3% PC, d) 2.4% EC. Different concentrations of supercharging reagents were added to the native protein solution to yield a final reagent concentration of 350 mM. Panel e represents ESI mass spectra of cytochrome c prepared in aqueous ES solution with 1% FA and 15% PC.

enhanced denaturation (cytochrome c is present in the denaturing ES for a longer time in ESI-MS) that is not present in the nonequilibrium mixing of the laser vaporized protein droplets. However, the role of *m*-NBA in the supercharging process and its effect on protein's structure has been debated(16, 18).

Alternative solution additives were also investigated as the means to increase protein CSD using a high resolution micrOTOF-Q II mass spectrometer. These reagents include diethyl carbonate (DEC), propylene carbonate (PC), and ethylene carbonate (EC). The effectiveness of these reagents in increasing protein charge states were tested for both native (ammonium acetate) and denaturing (acidic solution) electrospray solvent conditions. The ESI mass spectra of cytochrome c prepared in 5 mM aqueous ammonium acetate with DEC, PC, and EC are shown in Figure 2.5 b, c, and d, respectively. The measurements reveal CSDs with Z_{mode} of 7+, 10+, and 11+ for DEC, PC, and EC, respectively. The use of PC, and EC resulted in CSDs ranging from 5+ to 14+, and peaked at 10+ and 11+, respectively. However, a remarkable shift in protein CSD was observed when using PC in the denaturing ES (solution containing 1% FA) solvent conditions. In this case, the CSD ranged from 14+ to 23+ with a Z_{mode} of 21+. The effectiveness of these reagents in denaturing ES solvent conditions is currently under investigations using LEMS and nano-laser electrospray mass spectrometry (nano-LEMS) measurements.

2.4.1.2 Myoglobin

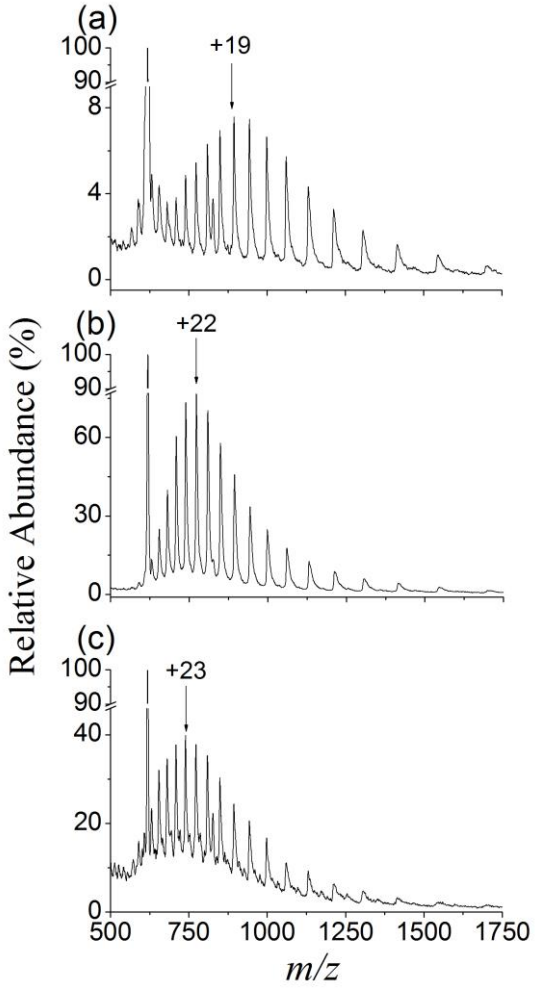

Figure 2.6. ESI mass spectra of myoglobin prepared in ammonium acetate with 0.4% *m*-NBA and 0.1% (a) TFA, (b) AA, and (c) FA.

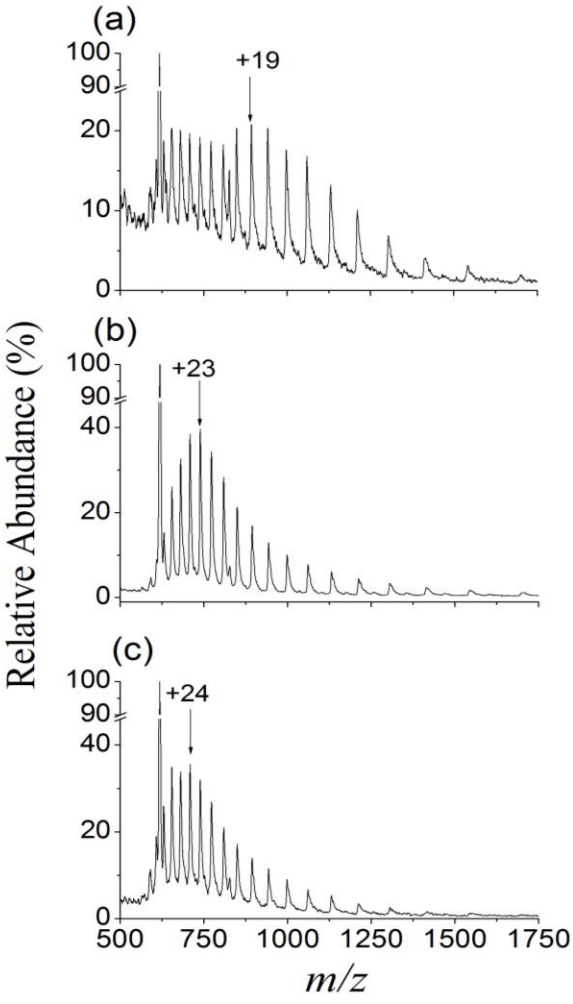

Figure 2.7. LEMS mass spectra of myoglobin in ES solvent conatining ammonium acetate with 0.4% *m*-NBA and 0.1% a) TFA, b) AA, and c) FA.

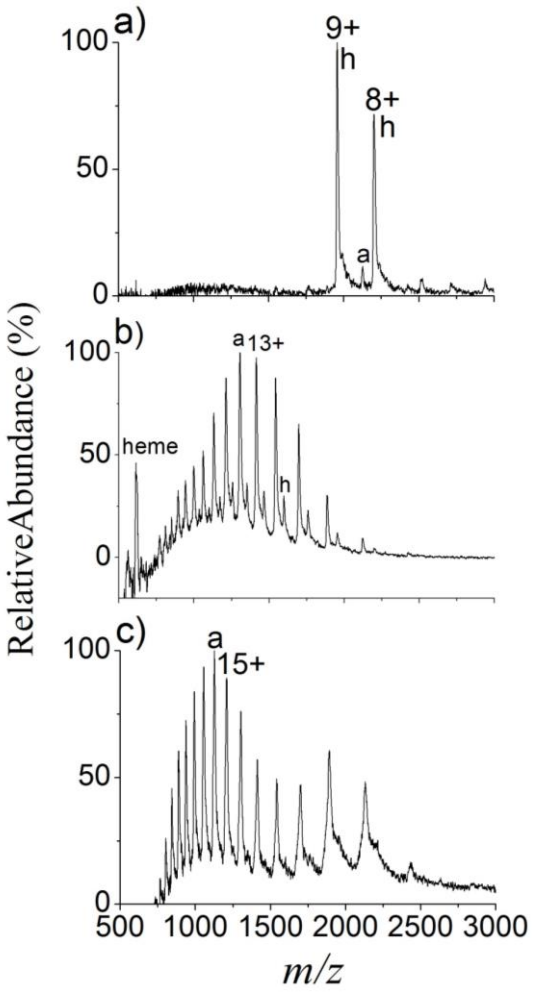

Figure 2.8. LEMS mass spectra of myoglobin in ES of a) ammonium acetate, and b) 0.4% *m*-NBA in ammonium acetate. Panel c represents LEMS mass spectra of myoglobin with 1% AA in ES of ammonium acetate (‘a’ represents apo-myoglobin and ‘h’ represents holomyoglobin).

Myoglobin is a globular protein that binds heme in its hydrophobic pocket by van der Waals forces. The folded conformation with the heme group located in the interior of the protein is called holomyoglobin. The heme is released in conditions of extreme pH and/or high temperatures, and in the presence of organic solvents to produce apo-myoglobin(57). Myoglobin prepared in 1:1 (v:v) water:methanol with TFA, AA, or FA in combination with *m*-NBA was analyzed using ESI and the mass spectra are shown in Figure 2.6 (a, b and c, respectively). The ESI CSD measurements are monomodal with Z_{mode} values of 19+, 22+, and 23+ for TFA, AA, and FA, respectively. The Z_{max} observed in the mass spectra was 28+ for all three electrospray solvents. The calculated Z_{mode} and Z_{avg} values for myoglobin in the solution of *m*-NBA with TFA, AA, and FA also do not correlate with the strength of the acid, as shown in Table 2.1. The presence of apomyoglobin features observed for all three electrospray solvents indicate a conformational change in the protein. The release of the heme cofactor is possibly due to the weakening of heme-protein interactions in the low pH ($\leq$ 3.5) solution(2) and the increasing concentration of *m*-NBA during the solvent evaporation which could further destabilizes the protein structure.

Myoglobin was laser vaporized into an electrospray solvent consisting of 1:1 (v:v) water:methanol with *m*-NBA and the various acids. The LEMS mass spectra resulting from the interaction of laser vaporized native myoglobin (holomyoglobin) with different electrospray solvents are shown in Figure 2.7 (a, b and c). A bimodal distribution was observed with charge states centered at 19+ and 26+ for the solution of *m*-NBA with TFA, whereas monomodal distributions centered at 23+ and 24+ were observed for the

solutions of *m*-NBA with AA and FA, respectively. The Z_{max} and Z_{min} observed in the mass spectra were 28+ and 10+, respectively, for all three electrospray solvents. The ion intensity of higher charge states increases significantly for myoglobin with LEMS in comparison to ESI. The relative abundance of charge states from 19+ to 26+ for the solution of TFA and 24+ to 26+ for the solution of FA was higher for LEMS measurements compared to conventional electrospray measurements. The charge states in the mass spectra represent apo-myoglobin features that resulted from the interaction of holomyoglobin with the denaturing electrospray solvent. Laser vaporization of myoglobin into ES droplets containing buffered water:methanol solution displayed only holomyoglobin features (Figure 2.8 a). The release of the heme cofactor indicates a conformational change of myoglobin after the laser vaporized protein droplets interact with the denaturing ES droplets. Z_{avg} is higher for LEMS measurements than for ESI-MS, 20.0 ± 0.4 vs. 18.6 ± 0.1 for TFA, 21.5 ± 0.5 vs. 20.5 ± 0.1 for AA, and 22.1 ± 0.4 vs. 21.3 ± 0.1 for FA. The increased Z_{avg} of myoglobin in LEMS measurements is similar to the observations made for cytochrome c, again suggesting that the laser vaporized protein acquires additional charge from the droplet surface where the excess charge resides.

2.4.2 Analysis of Acid Stable Proteins

2.4.2.1 Lysozyme

Lysozyme contains four disulfide bonds that stabilize the protein structure resulting in less denaturation when compared to myoglobin and cytochrome c. The native form of this protein is indicated by a narrow range of charge states (mostly centered at 9+ and 8+)

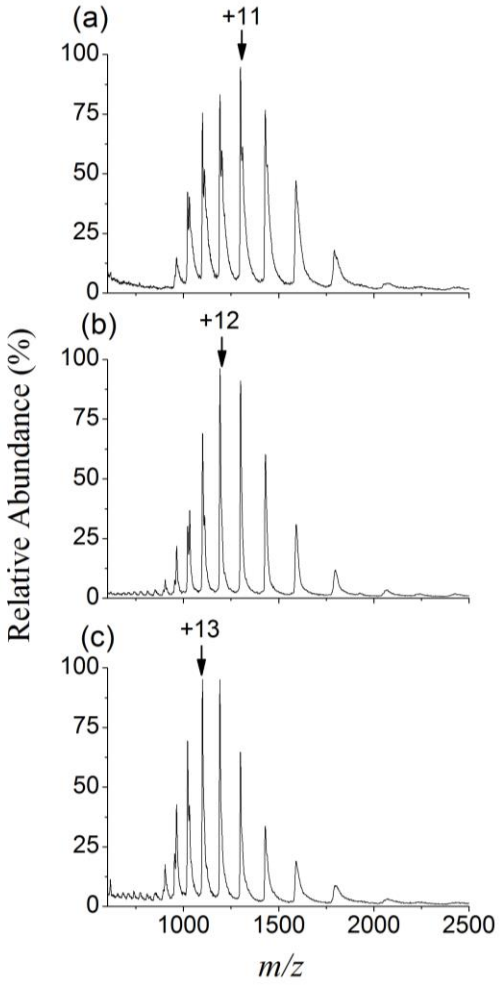

Figure 2.9. ESI mass spectra of lysozyme prepared in ammonium acetate with 0.4% *m*-NBA and 0.1% (a) TFA, (b) AA, and (c) FA.

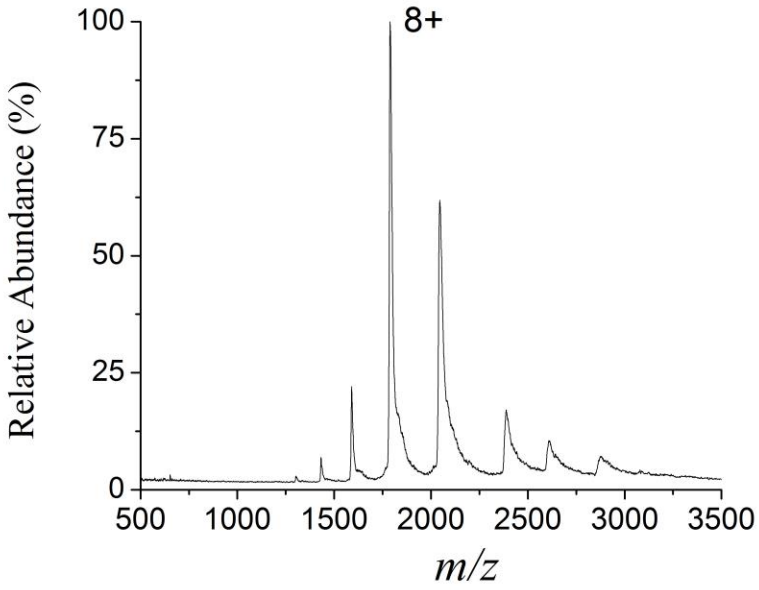

Figure 2.10. ESI mass spectra of lysozyme prepared in ammonium acetate.

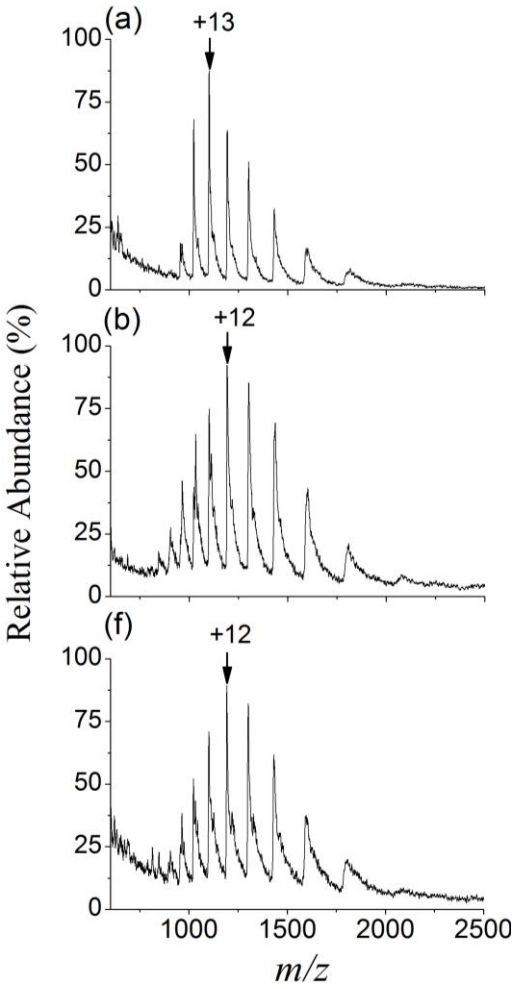

Figure 2.11. LEMS mass spectra of lysozyme in ES solvent of ammonium acetate with 0.4% *m*-NBA and a) 0.1% TFA, b) AA, and c) FA.

whereas unfolded conformation displays a much broader bell-shaped distribution at higher charge states(58). The ESI mass spectra obtained for lysozyme using the combinations of *m*-NBA and different acids are shown in Figure 2.9 (a, b and c). Monomodal CSDs with Z_{mode} at 11+, 12+, and 13+ were observed for *m*-NBA solutions with TFA, AA, and FA, respectively. The Z_{min} observed in the mass spectra was 8+ for all three solvent conditions, while the Z_{max} was 16+ for AA and FA, and 15+ for TFA solutions. The broad range of charge states ranging from 8+ to 16+ indicate an unfolded configuration of lysozyme that results from the solvents employed. The ESI mass spectra of native lysozyme prepared in buffered water:methanol solutions showed a narrow range of lower charge states with a Z_{mode} of 8+ (Figure 2.10). The Z_{avg} values (Table 2.1) measured for TFA is lower compared to AA and FA, similar to the ESI measurements of cytochrome c and myoglobin. Aqueous lysozyme was laser vaporized into various electrospray solutions consisting of an acidic solvent and *m*-NBA to determine whether disulfide linkages stabilize the protein structure in the presence of denaturing electrospray solvents. The LEMS mass spectra of lyoszyme with *m*-NBA and TFA (Figure 2.11 a), AA (Figure 2.11 b), and FA (Figure 2.11 c) displayed monomodal CSDs. The Z_{mode} in these measurements was 13+ for the solution of TFA, and 12+ for the solutions of AA and FA (combined with *m*-NBA). The Z_{min} observed in the mass spectra was 8+ for all solvent conditions, while Z_{max} was 16+ for AA and FA, and 15+ for TFA solutions. The broad range of CSDs in lysozyme for all three solvent conditions indicates at least a partial change in protein structure, which occurs after the laser vaporized protein, interacts with the denaturing ES solvents containing different acids and *m*-NBA. Laser

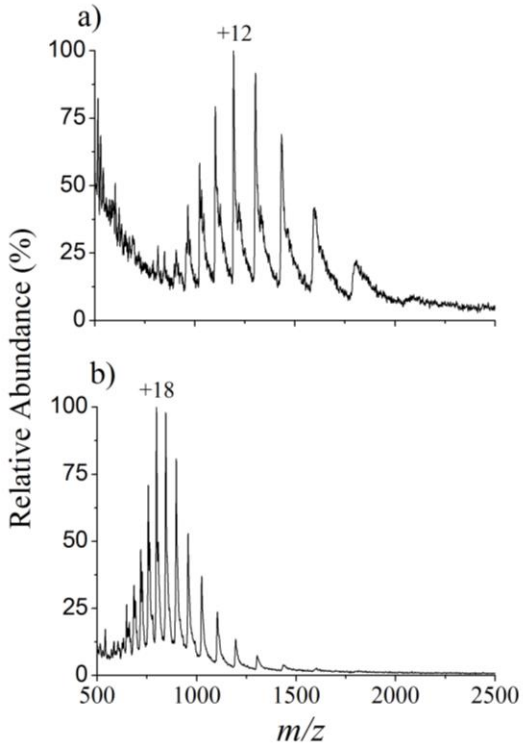

Figure 2.12. LEMS mass spectra of a) disulfide intact and b) disulfide reduced lysozyme in ES solvent cantaining ammonium acetate with 0.4% *m*-NBA and 0.1% FA.

vaporization into a buffered electrospray solution containing water:methanol showed a Z_{mode} of 8+ corresponding to the folded lysozyme, similar to the corresponding ESI measurement. Unlike cytochrome c and myoglobin, the calculated Z_{avg} for LEMS measurements was slightly lower in comparison to ESI-MS measurements for FA (11.9 ± 0.1 vs. 12.2) and within the standard deviation for AA (11.4 ± 0.3 vs. 11.5), as seen in Table 2.1. LEMS measurements using TFA and *m*-NBA resulted in an increase Z_{avg} and Z_{mode} in comparison to ESI measurements. The slight decrease in Z_{avg} for laser vaporized lysozyme into *m*-NBA and either FA or AA indicates a non-equilibrium interaction of the protein with the denaturing electrospray solvent. As the result of such a short interaction time with the denaturing solvent, acid-stable proteins may not denature to the same extent as the protein subjected to conventional electrospray where the protein spends a longer time in the denaturing solvent.

Lysozyme with reduced disulfide bonds was laser vaporized into the denaturing ES containing *m*-NBA to investigate the effect of protein structure prior to mixing with the ES droplets. The LEMS mass spectra of disulfide-reduced lysozyme using the ESI solution of FA and *m*-NBA resulted in a monomodal CSD centered around 18+ (Figure 2.12 b). The Z_{max} and Z_{min} observed in the disulfide-reduced mass spectrum were 25+ and 9+, respectively. The increase in overall ion charge of the protein upon disulfide bond reduction is due to unfolding of the protein, which increases the solvent accessible surface area, improving the protein ionization efficiency(59). The increase in ion charge above the number of basic amino acids (18) is presumably due to the protonation of amino acids such as proline (Pro), tryptophan (Trp), and glutamine (Gln)(12, 60).

2.4.2.2 Ubiquitin

Ubiquitin is a small globular protein with 76 amino-acid residues(61). ESI measurements of the native configuration of this protein result in lower charge states (with Z_{mode} of 6+) while higher charge states (~11+) indicate an unfolded conformation(62). The ESI mass spectra of ubiquitin obtained from the mixtures of *m*-NBA with the acids investigated displayed monomodal CSDs with Z_{mode} values of 12+, as observed in Figure 2.13 (a, b and c). The higher charge states resulting from the interaction of ubiquitin with the denaturing electrospray solutions are indicative of the unfolded conformation while the lower charge states (6+ and 7+) probably represent a folded or partially folded conformation. Although there is no fluctuation in Z_{mode} (12+) for any of the solvents, the calculated Z_{avg} values vary for the different electrospray solvents and do not follow the expected trend of acid strength (10.5 ± 0.1 (TFA), 11.5 ± 0.03 (AA), and 11.2 ± 0.1 (FA)). This again suggests that the nature of the protein also plays an important role in determining the Z_{avg} in addition to the acid added to the electrospray solution. The conformational flexibility and the number of ionizable groups (basic residues for positive ion mode) in a protein molecule are some of the important parameters for the observed CSD. The Z_{avg} values (Table 2.1) measured for myoglobin (21.3) and cytochrome c (17.8) were higher than lysozyme (12.2) and ubiquitin (11.2) for similar solvent conditions suggesting that the increased number of basic residues in cytochrome c and myoglobin favors the shift in CSD to higher charge states.

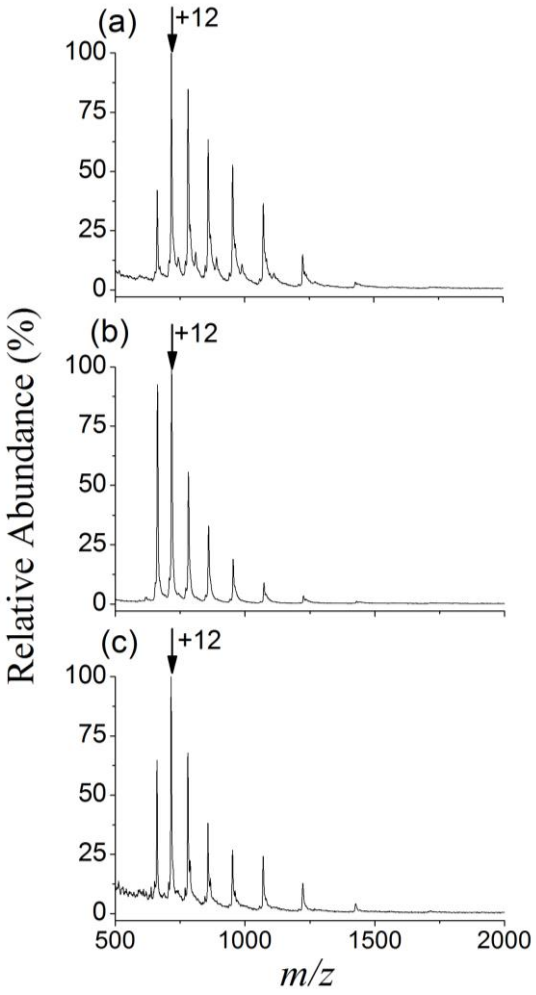

Figure 2.13. ESI mass spectra of ubiquitin prepared in ammonium acetate with 0.4% *m*-NBA and 0.1% (a) TFA, (b) AA, and (c) FA.

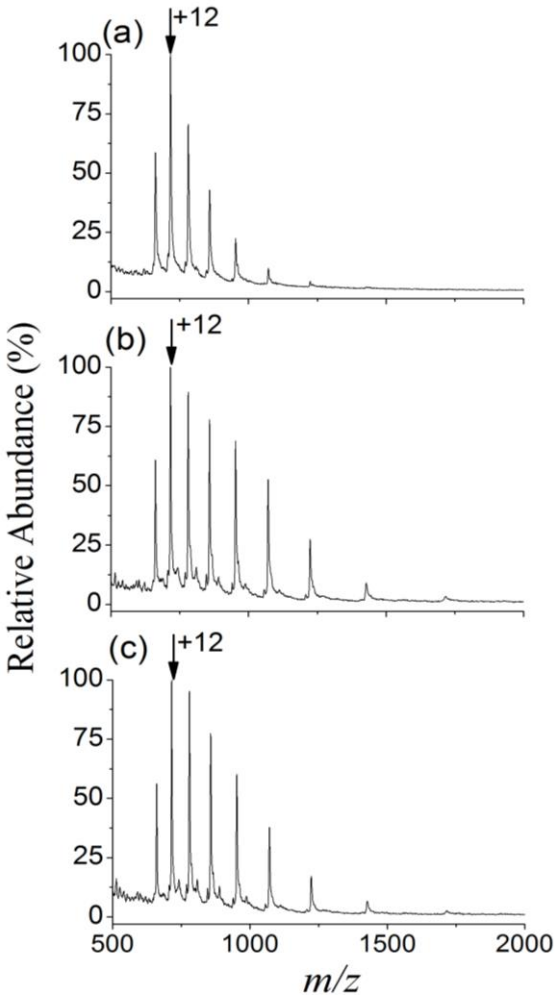

Figure 2.14. LEMS mass spectra of ubiquitin prepared in ammonium acetate with 0.4% *m*-NBA and 0.1% (a) TFA, (b) AA, and (c) FA.

Laser vaporization of ubiquitin resulted in monomodal CSDs with Z_{mode} at 12+ for all the solvent conditions, Figure 2.14 (a, b and c). The mass spectra revealed a broad range of high charge states indicating a possible denaturation of ubiquitin after the interaction of native protein with the denaturing ES solvents. The calculated Z_{avg} for LEMS was lower than ESI-MS for *m*-NBA with AA (10.3 ± 0.3 vs. 11.5 ± 0.03) and FA (10.4 ± 0.2 vs. 11.2 ± 0.1), but not for TFA (10.8 ± 0.3 vs. 10.5 ± 0.1), as seen in Table 2.1. The decrease in Z_{avg} is possibly due to the reduced interaction time between protein and the electrospray solvent in the laser vaporization experiment in comparison with conventional electrospray where the protein spends several minutes in the solvent. Acid-stable proteins like ubiquitin may not undergo significant denaturation during the short time (100 ms) that the protein is present in the ESI droplet after laser vaporization.

2.4.3 Effect of Flow Rates on Average Charge State Distribution of Cytochrome c and Myoglobin

We investigated the influence of flow rate on the charge state distributions of cytochrome c and myoglobin given that the charge density on the droplet surface increases for lower flow rates(63). The protein solutions were prepared in water:methanol with *m*-NBA and either TFA or FA. The flow rate of the ES solvent was varied from 3 µL/min to 600 nL/min and the CSD was measured. The electrospray measurements of cytochrome c and myoglobin revealed that Z_{avg} increases as the electrospray flow rate decreases, as shown in Figure 2.15. The Z_{avg} values for cytochrome c and myoglobin increased linearly in the solutions of *m*-NBA and TFA as the flow rate was reduced from 3 µL/min to 1 µL/min but decreased as the flow rate was further reduced to 600 nL/min.

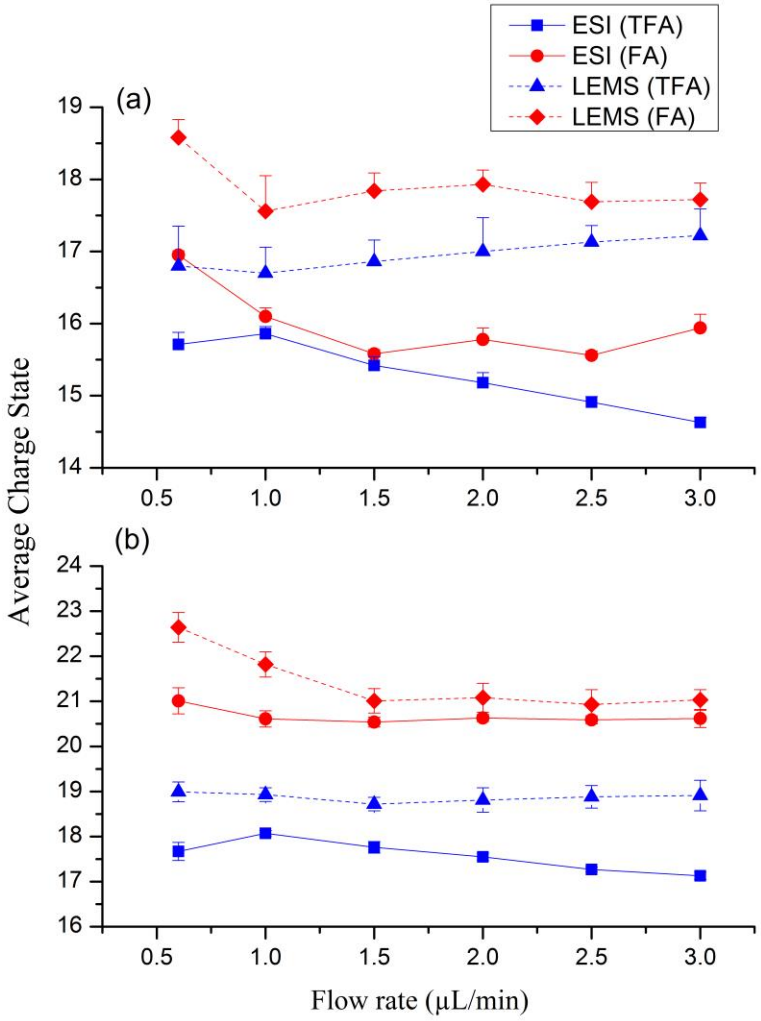

Figure 2.15. Plot of the average charge state of a) cytochrome c, and b) myoglobin as a function of electrospray flow rate for solvents consisting of *m*-NBA and either TFA (blue lines) and FA (red lines) for measurements using ESI-MS (solid lines) and LEMS (dashed lines).

Conversely, the Z_{avg} of these proteins in the solutions of *m*-NBA and FA remained almost constant until the flow rate of 1.5 µL/min and started increasing as the flow rate decreased to 600 nL/min. The increase in Z_{avg} of the protein with decreasing flow rate is presumably due to the production of smaller electrospray droplets(64), that undergo rapid solvent evaporation, requiring fewer Coulombic fission events to generate gas phase ions(10). This was proposed to result in an increase in surface charge density per volume of the daughter droplets compared to larger droplets generated at higher flow rates, thus improving the ionization efficiency(63). In addition to the increase in ionization efficiency, the rate of solvent evaporation also affects the time that the protein remains in the regime of high/low surface charge density(65). For smaller droplets, rapid solvent evaporation in the early stages of the electrospray process increases the time that protein spends in the regime of high surface charge density, contributing to the increase in high charge states in comparison with the low charge states.

To investigate whether the charge density on the droplet surface affected the Z_{avg} for the LEMS measurements, cytochrome c and myoglobin were laser vaporized into the electrospray plume and the flow rate of the electrospray solvent was varied. The plot of Z_{avg} vs. the flow rate of the electrospray solvent is shown in Figure 2.15. The Z_{avg} of both proteins showed little deviation as the flow rate was reduced from 3 µL/min to 1.5 µL/min and started increasing at 1 µL/min for cytochrome c, and at 1.5 µL/min for myoglobin for the LEMS measurements using an ES solution of *m*-NBA with FA. However, when using the solution of *m*-NBA with TFA, the Z_{avg} remained approximately constant for myoglobin and slightly decreased for cytochrome c as the flow rate

decreased. The decrease in Z_{avg} upon lowering the flow rate could be due to the decrease in the proton concentration on the droplet surface due to the lower boiling point of TFA in comparison with water. In this scenario, rapid evaporation of TFA for smaller droplets reduces the charge density on the droplet surface, thus decreasing the Z_{avg}.

2.5 Conclusions

The extent of the shift to higher charge states for proteins in the presence of denaturing solutions containing an acid and a supercharging reagent depended upon the nature of the protein, the acid, and the mass spectral technique (LEMS or ESI). The Z_{avg} values for cytochrome c and myoglobin were greater for LEMS measurements in comparison with ESI-MS. This is attributed to the nonequilibrium interaction of proteins with the surface of the ES droplets where the excess charge is located. The decrease in Z_{avg} with the similar solvent conditions for proteins like lysozyme and ubiquitin for LEMS measurements was attributed to their structural rigidity preventing extensive denaturation in the acidic solution on the 100 ms timescale. The reduced interaction time of the vaporized protein with the ES plume can either enhance or limit the protein unfolding, depending on the nature of the protein and electrospray solvent. The general increase in Z_{avg} of cytochrome c and myoglobin with decreasing flow rate (3 μL/min to 600 nL/min) was attributed to the production of smaller droplets compared to higher flow rates experiments. The more rapid solvent evaporation for smaller droplets in the early stages of the electrospray process increases the time protein spends in the regime of high

surface charge density, contributing to the increase in ion abundance of high charge states.

The combination of *m*-NBA and formic acid resulted in the highest average charge states for proteins in both ESI-MS and LEMS measurements. This is presumably due to the increase in proton density on the droplet surface, which improves the ionization efficiency of the proteins. Further, increase in both the Z_{avg} and the Z_{mode} values for LEMS measurements compared to conventional electrospray for acid-sensitive proteins like cytochrome c and myoglobin suggest that LEMS could be utilized to create higher charge states for performing top-down, tandem mass spectrometry on proteins. The ability to vaporize and ionize multiple components irrespective of chemical functionality from complex mixtures without the addition of matrix illustrates the potential of LEMS for various applications such as imaging mass spectrometry, quantitative measurements of biological samples, forensic analysis, etc. With the advances in laser technology, the measurements can now be performed using a commercial fiber laser, which is turnkey and affordable.

2.6 References

1. Konermann, L.; Douglas, D. Acid-induced unfolding of cytochrome c at different methanol concentrations: electrospray ionization mass spectrometry specifically monitors changes in the tertiary structure. *Biochemistry.* **1997,** (36), 12296-12302.

2. Chowdhury, S. K.; Katta, V.; Chait, B. T. Probing conformational changes in proteins by mass spectrometry. *J. Am. Chem. Soc.* **1990,** (112), 9012-9013.

3. Iavarone, A. T.; Jurchen, J. C.; Williams, E. R. Effects of solvent on the maximum charge state and charge state distribution of protein ions produced by electrospray ionization. *J. Am. Soc. Mass Spectrom.* **2000,** (11), 976-985.

4. Loo, R. R. O.; Smith, R. D. Proton transfer reactions of multiply charged peptide and protein cations and anions. *J. Mass Spectrom.* **1995,** (30), 339-347.

5. Williams, E. R. Proton transfer reactivity of large multiply charged ions. *JMS.* **1996,** (31), 831.

6. Flick, T. G.; Williams, E. R. Supercharging with trivalent metal ions in native mass spectrometry. *J. Am. Soc. Mass Spectrom.* **2012,** (23), 1885-1895.

7. Iavarone, A. T.; Jurchen, J. C.; Williams, E. R. Supercharged protein and peptide ions formed by electrospray ionization. *Anal. Chem.* **2001,** (73), 1455-1460.

8. Lomeli, S. H.; Peng, I. X.; Yin, S.; Ogorzalek Loo, R. R.; Loo, J. A. New reagents for increasing ESI multiple charging of proteins and protein complexes. *J. Am. Soc. Mass Spectrom.* **2010,** (21), 127-131.

9. Sterling, H. J.; Prell, J. S.; Cassou, C. A.; Williams, E. R. Protein conformation and supercharging with DMSO from aqueous solution. *J. Am. Soc. Mass Spectrom.* **2011,** (22), 1178-1186.

10. Page, J. S.; Kelly, R. T.; Tang, K.; Smith, R. D. Ionization and transmission efficiency in an electrospray ionization–mass spectrometry interface. *J. Am. Soc. Mass Spectrom.* **2007,** (18), 1582-1590.

11. Banerjee, S. Induction of protein conformational change inside the charged electrospray droplet. *J. Mass Spectrom.* **2013,** (48), 193-204.

12. Kharlamova, A.; Prentice, B. M.; Huang, T.-Y.; McLuckey, S. A. Electrospray droplet exposure to gaseous acids for the manipulation of protein charge state distributions. *Anal. Chem.* **2010,** (82), 7422-7429.

13. Chen, H.; Touboul, D.; Jecklin, M. C.; Zheng, J.; Luo, M.; Zenobi, R. Manipulation of charge states of biopolymer ions by atmospheric pressure ion/molecule reactions implemented in an extractive electrospray ionization source. *Eur. J. Mass.* **2007,** (13), 273.

14. Touboul, D.; Jecklin, M. C.; Zenobi, R. Investigation of deprotonation reactions on globular and denatured proteins at atmospheric pressure by ESSI-MS. *J. Am. Soc. Mass Spectrom.* **2008,** (19), 455-466.

15. Hogan Jr, C. J.; Loo, R. R. O.; Loo, J. A.; de la Mora, J. F. Ion mobility–mass spectrometry of phosphorylase B ions generated with supercharging reagents but in charge-reducing buffer. *Phys. Chem. Chem. Phys.* **2010,** (12), 13476-13483.

16. Lomeli, S. H.; Yin, S.; Ogorzalek Loo, R. R.; Loo, J. A. Increasing charge while preserving noncovalent protein complexes for ESI-MS. *J. Am. Soc. Mass Spectrom.* **2009,** (20), 593-596.

17. Sterling, H. J.; Cassou, C. A.; Trnka, M. J.; Burlingame, A.; Krantz, B. A.; Williams, E. R. The role of conformational flexibility on protein supercharging in native electrospray ionization. *Phys. Chem. Chem. Phys.* **2011,** (13), 18288-18296.

18. Sterling, H. J.; Williams, E. R. Origin of supercharging in electrospray ionization of noncovalent complexes from aqueous solution. *J. Am. Soc. Mass. Spectrom.* **2009,** (20), 1933-1943.

19. Hall, Z.; Robinson, C. V. Do charge state signatures guarantee protein conformations? *J. Am. Soc. Mass Spectrom.* **2012,** (23), 1161-1168.

20. Marshall, A. G. Fourier transform ion cyclotron resonance mass spectrometry. *Acc. Chem. Res.* **1985,** (18), 316-322.

21. Perry, R. H.; Cooks, R. G.; Noll, R. J. Orbitrap mass spectrometry: instrumentation, ion motion and applications. *Mass Spectrom. Rev.* **2008,** (27), 661-699.

22. Good, D. M.; Wirtala, M.; McAlister, G. C.; Coon, J. J. Performance characteristics of electron transfer dissociation mass spectrometry. *Mol. Cell. Proteomics.* **2007,** (6), 1942-1951.

23. Horn, D. M.; Breuker, K.; Frank, A. J.; McLafferty, F. W. Kinetic intermediates in the folding of gaseous protein ions characterized by electron capture dissociation mass spectrometry. *J. Am. Chem. Soc.* **2001,** (123), 9792-9799.

24. Tsybin, Y. O.; Fornelli, L.; Stoermer, C.; Luebeck, M.; Parra, J.; Nallet, S.; Wurm, F. M.; Hartmer, R. Structural analysis of intact monoclonal antibodies by electron transfer dissociation mass spectrometry. *Anal. Chem.* **2011,** (83), 8919-8927.

25. Zubarev, R. A.; Kelleher, N. L.; McLafferty, F. W. Electron capture dissociation of multiply charged protein cations. A nonergodic process. *J. Am. Chem. Soc.* **1998,** (120), 3265-3266.

26. Zubarev, R. A.; Horn, D. M.; Fridriksson, E. K.; Kelleher, N. L.; Kruger, N. A.; Lewis, M. A.; Carpenter, B. K.; McLafferty, F. W. Electron capture dissociation for structural characterization of multiply charged protein cations. *Anal. Chem.* **2000,** (72), 563-573.

27. Peng, I. X.; Ogorzalek Loo, R. R.; Shiea, J.; Loo, J. A. Reactive-electrospray-assisted laser desorption/ionization for characterization of peptides and proteins. *Anal. Chem.* **2008,** (80), 6995-7003.

28. Nemes, P.; Vertes, A. Laser ablation electrospray ionization f or atmospheric pressure, in vivo, and imaging mass spectrometry. *Anal. Chem.* **2007,** (79), 8098-8106.

29. Rezenom, Y. H.; Dong, J.; Murray, K. K. Infrared laser-assisted desorption electrospray ionization mass spectrometry. *Analyst.* **2008,** (133), 226-232.

30. Sampson, J. S.; Muddiman, D. C. Atmospheric pressure infrared (10.6 μm) laser desorption electrospray ionization (IR-LDESI) coupled to a LTQ Fourier transform ion cyclotron resonance mass spectrometer. *Rapid Commun. Mass Spectrom.* **2009,** (23), 1989-1992.

31. Liu, J.; Qiu, B.; Luo, H. Fingerprinting of yogurt products by laser desorption spray post-ionization mass spectrometry. *Rapid Commun. Mass Spectrom.* **2010,** (24), 1365-1370.

32. Sampson, J. S.; Hawkridge, A. M.; Muddiman, D. C. Construction of a versatile high precision ambient ionization source for direct analysis and imaging. *J. Am. Soc. Mass Spectrom.* **2008,** (19), 1527-1534.

33. Flanigan, P.; Levis, R. Ambient Femtosecond LaserVaporization and Nanosecond Laser Desorption Electrospray Ionization Mass Spectrometry. *Ann. Rev. Anal. Chem.* **2014,** (7), 229-256.

34. Brady, J. J.; Judge, E. J.; Levis, R. J. Mass spectrometry of intact neutral macromolecules using intense non-resonant femtosecond laser vaporization with electrospray post-ionization. *Rapid Commun. Mass Spectrom.* **2009,** (23), 3151-3157.

35. Judge, E. J.; Brady, J. J.; Dalton, D.; Levis, R. J. Analysis of pharmaceutical compounds from glass, fabric, steel, and wood surfaces at atmospheric pressure using spatially resolved, nonresonant femtosecond laser vaporization electrospray mass spectrometry. *Anal. Chem.* **2010,** (82), 3231-3238.

36. Brady, J. J.; Judge, E. J.; Levis, R. J. Analysis of amphiphilic lipids and hydrophobic proteins using nonresonant femtosecond laser vaporization with electrospray post-ionization. *J. Am. Soc. Mass Spectrom.* **2011,** (22), 762-772.

37. Brady J. J.; Judge, E. J.; Levis, R. J. *Presented in part at Proc. SPIE 7568, Imaging, Manipulation, and Analysis of Biomolecules, Cells, and Tissues VIII* **2010.**

38. Brady, J. J.; Judge, E. J.; Levis, R. J. Identification of explosives and explosive formulations using laser electrospray mass spectrometry. *Rapid Commun. Mass Spectrom.* **2010,** (24), 1659-1664.

39. Flanigan IV, P. M.; Brady, J. J.; Judge, E. J.; Levis, R. J. Determination of Inorganic Improvised Explosive Device Signatures Using Laser Electrospray Mass Spectrometry Detection with Offline Classification. *Anal. Chem.* **2011,** (83), 7115-7122.

40. Perez, J. J.; Flanigan IV, P. M.; Brady, J. J.; Levis, R. J. Classification of smokeless powders using laser electrospray mass spectrometry and offline multivariate statistical analysis. *Anal. Chem.* **2012,** (85), 296-302.

41. Flanigan IV, P. M.; Radell, L. L.; Brady, J. J.; Levis, R. J. Differentiation of Eight Phenotypes and Discovery of Potential Biomarkers for a Single Plant Organ Class Using Laser Electrospray Mass Spectrometry and Multivariate Statistical Analysis. *Anal. Chem.* **2012,** (84), 6225-6232.

42. Judge, E. J.; Brady, J. J.; Barbano, P. E.; Levis, R. J. Nonresonant femtosecond laser vaporization with electrospray postionization for ex vivo plant tissue typing using compressive linear classification. *Anal. Chem.* **2011,** (83), 2145-2151.

43. Brady, J. J.; Judge, E. J.; Levis, R. J. Nonresonant femtosecond laser vaporization of aqueous protein preserves folded structure. *Pro. Natl. Acad. Sci.*. **2011,** (108), 12217-12222.

44. Flanigan IV, P. M.; Perez, J. J.; Karki, S.; Levis, R. J. Quantitative Measurements of Small Molecule Mixtures Using Laser Electrospray Mass Spectrometry. *Anal. Chem.* **2013,** (85), 3629-3637.

45. Perez, J. J.; Flanigan, P. M.; Karki, S.; Levis, R. J. Laser Electrospray Mass Spectrometry Minimizes Ion Suppression Facilitating Quantitative Mass Spectral Response for Multi-Component Mixtures of Proteins. *Anal. Chem.* **2013,**

46. Shackman, J. G.; Watson, C. J.; Kennedy, R. T. High-throughput automated post-processing of separation data. *J. Chromatogr. A.* **2004,** (1040), 273-282.

47. Fligge, T. A.; Kast, J.; Bruns, K.; Przybylski, M. Direct monitoring of protein–chemical reactions utilising nanoelectrospray mass spectrometry. *J. Am. Soc. Mass Spectrom.* **1999,** (10), 112-118.

48. Valentine, S. J.; Clemmer, D. E. H/D exchange levels of shape-resolved cytochrome c conformers in the gas phase. *J. Am. Chem. Soc.* **1997,** (119), 3558-3566.

49. Judge, E. J.; Brady, J. J.; Levis, R. J. Mass analysis of biological macromolecules at atmospheric pressure using nonresonant femtosecond laser vaporization and electrospray ionization. *Anal. Chem.* **2010,** (82), 10203-10207.

50. Frederikse, H.; Lide, D. CRC handbook of chemistry and physics. *CRC, Boca Raton.* **1996.**

51. Jasper, J. J.; Wedlick, H. L. Effect of Temperature on the Surface Tension and Density of Trifluoroacetic Acid. *J. Chem. Eng. Data.* **1964,** (9), 446-447.

52. Goodman, J. M.; Kirby, P. D.; Haustedt, L. O. Some calculations for organic chemists: boiling point variation, Boltzmann factors and the Eyring equation. *Tetrahedron Lett.* **2000,** (41), 9879-9882.

53. Mirza, U. A.; Chait, B. T. Effects of anions on the positive ion electrospray ionization mass spectra of peptides and proteins. *Anal. Chem.* **1994,** (66), 2898-2904.

54. Liu, X.; Cole, R. B. A new model for multiply charged adduct formation between peptides and anions in electrospray mass spectrometry. *J. Am. Soc. Mass Spectrom.* **2011,** (22), 2125-2136.

55. Chainani, E. T.; Choi, W.-H.; Ngo, K. T.; Scheeline, A. Mixing in Colliding, Ultrasonically Levitated Drops. *Anal. Chem.* **2014,** (86), 2229-2237.

56. Wang, G.; Cole, R. B. Mechanistic interpretation of the dependence of charge state distributions on analyte concentrations in electrospray ionization mass spectrometry. *Anal. Chem.* **1995,** (67), 2892-2900.

57. Creighton, T. E., Proteins: structures and molecular properties, Macmillan, (1993).

58. Gross, D. S.; Schnier, P. D.; Rodriguez-Cruz, S. E.; Fagerquist, C. K.; Williams, E. R. Conformations and folding of lysozyme ions in vacuo. *Pro. Natl. Acad. Sci.* **1996,** (93), 3143-3148.

59. Testa, L.; Brocca, S.; Grandori, R. Charge-surface correlation in electrospray ionization of folded and unfolded proteins. *Anal. Chem.* **2011,** (83), 6459-6463.

60. Schnier, P. D.; Gross, D. S.; Williams, E. R. On the maximum charge state and proton transfer reactivity of peptide and protein ions formed by electrospray ionization. *J. Am. Soc. Mass Spectrom.* **1995,** (6), 1086-1097.

61. Vijay-Kumar, S.; Bugg, C. E.; Cook, W. J. Structure of ubiquitin refined at 1.8 Åresolution. *J. Mol. Biol.* **1987,** (194), 531-544.

62. Konermann, L.; Douglas, D. Unfolding of proteins monitored by electrospray ionization mass spectrometry: a comparison of positive and negative ion modes. *J. Am. Soc. Mass Spectrom.* **1998,** (9), 1248-1254.

63. Schmidt, A.; Karas, M.; Dülcks, T. Effect of different solution flow rates on analyte ion signals in nano-ESI MS, or: when does ESI turn into nano-ESI? *J. Am. Soc. Mass Spectrom.* **2003,** (14), 492-500.

64. Ganan-Calvo, A.; Davila, J.; Barrero, A. Current and droplet size in the electrospraying of liquids. Scaling laws. *J. Aerosol Sci.* **1997,** (28), 249-275.

65. Fenn, J. B. Ion formation from charged droplets: roles of geometry, energy, and time. *J. Am. Soc. Mass Spectrom.* **1993,** (4), 524-535.

CHAPTER 3

ISOLATING PROTEIN CHARGE STATE REDUCTION IN ELECTROSPRAY DROPLETS USING FEMTOSECOND LASER VAPORIZATION

3.1 Overview

This chapter details protein folding, unfolding, and charge state reduction in electrospray (ES) droplets when using solution additives with varying gas phase basicities. Charge state distributions measured using mass spectrometry for both native and acid-denatured cytochrome c and myoglobin after laser vaporization from the solution phase into an ES plume consisting of a series of solution additives differing in gas phase basicity are reported. It was observed that the charge distribution depends on both the pH of the protein in bulk solution prior to laser vaporization, as well as the gas phase basicity of the solution additive employed in the ES solvent. The trend in average charge state distribution (Z_{avg}) and the fraction of folded protein obtained from the mreasurement of cytochrome c and myoglobin (prepared in solutions with pH of 7.0, 2.6, and 2.3) in different ES solvents are discussed. The possibility of protein folding during the ES droplet lifetime after laser vaporized, acid-denatured protein interacts with the ES solvent containing ammonium formate, ammonium acetate, triethyl ammonium formate, and triethyl ammonium acetate has been discussed.

3.2 Introduction

Electrospray ionization mass spectrometry (ESI-MS) has been widely used to study the conformation of proteins in various solvent conditions(1). Electrospray

ionization of proteins reveal a characteristic charge state distribution (CSD) correlating to the extent of denaturation(2). Protein in the native configuration is typically folded, which protects the basic amino acids in the interior from charging and hence produces a narrow distribution at lower charge states in comparison to denatured protein. Denatured protein exhibits a much broader CSD at higher charge states because additional basic amino acids are exposed to the solvent environment and therefore can acquire more charge. Investigations of solvent-induced conformational change(1), acid and thermal denaturation(2, 3), and refolding of initially denatured proteins(4) suggest a strong correlation between the observed CSD and protein conformation. The role of protein structure in determining the CSD has also been investigated using ion mobility mass spectrometry (IM-MS) measurements. The collision cross section (CCS) of cytochrome c(5) and ubiquitin(6) measured as a function of charge state showed higher CCSs for unfolded protein ions. The consensus from these studies is that lower charge states correlate to more folded, native-like structure and higher charge states correlate to a more unfolded structure.

Protein conformational change may occur during the electrospray process. Exposing ES droplets containing protein molecules to either acidic or basic vapors in the region between the spray tip and the MS inlet can either induce unfolding(7, 8) or refolding(4) of proteins. For instance, exposing ES droplets containing native proteins to acidic vapors results in a lower droplet pH, a favorable condition for protein denaturation(8). Exposing acid-denatured proteins to basic vapor results in a bimodal CSD, indicating charge state reduction in at least a fraction of protein population,

presumably folding as a result of an increase pH of the ES droplet(4). Without some degree of folding, a simple monotonic shift of the CSD to lower charge is expected, not the formation of a second, narrowly peaked distribution.

In the electrospray process, the gas phase basicity of a solvent is related to the ability to promote proton transfer from an analyte, thus reducing the overall charge. Gas phase basicity is defined as the change in free energy when a proton attaches to an anion or neutral molecule. A solution additive with high gas phase basicity has been found to charge reduce and stabilize non-covalent protein complexes(9). In that study, the native state of myoglobin (holomyoglobin) was preserved during ESI and subsequent collision-induced dissociation (CID) measurements revealed higher energy thresholds for dissociation of heme/myoglobin complex using triethyl ammonium bicarbonate (dissociation threshold = 144V) in comparison with ammonium bicarbonate (dissociation threshold = 84V)(9). The higher gas phase basicity results in enhanced charge reduction for the protein, decreasing Columbic repulsion among the charged residues and making protein denaturation more difficult. Charge reducing buffers have also been used to stabilize membrane protein complexes after release from detergent micelles in the gas phase(10). The CCS value obtained from IM-MS measurement for charge reduced states of trimeric outer membrane protein (OmpF) is lower than the value generated from X-ray crystal structure of the protein, and is in close agreement with the CCS value generated from molecular dynamics simulations for native-like compact structure. This suggests that the lower charge states of OmpF resemble more compact, folded-like states of proteins. The development of laser electrospray mass spectrometry (LEMS) has enabled

the rapid analysis of complex mixtures at atmospheric pressure without sample pre-processing. LEMS analysis has been performed on variety of samples including proteins(11, 12), pharmaceuticals(13), explosives(14, 15), plant tissue(16), thermometer ions(17), and small analytes(18). Femtosecond laser vaporization can be employed to deliver either native or denatured protein into the electrospray plume with various solvent conditions(11, 19). This enables the delivery of native or denatured protein directly into the charged electrospray droplets, avoiding any structural changes and/or oxidation/reduction processes that might occur in the Taylor cone of the electrospray source. The gas phase protein ions are presumably formed after the laser vaporized liquid aerosols containing protein molecule interacts with the charged ES droplets containing solution additives of interest.

In the present study, we investigate the role of solution additives with varying gas phase basicities on the CSD of folded and unfolded cytochrome c and myoglobin. We separate the droplet processes from processes occurring in the solution flowing through the capillary and the Taylor cone on the capillary emitting the charged droplets, by laser vaporizing protein directly into the spray containing the solution additive of interest. Considering the solution, intermediate, and gas phase regimes of electrospray ionization process(20), our measurements emulates the intermediate regime, from which gas phase ions are released. We also determine whether interaction of the laser vaporized acid-denatured protein with the electrospray droplets containing additives with high gas phase basicity induces charge reduction and protein folding within the approximately 100 ms(11) timescale of the LEMS process. The shift in average charge states (Z_{avg}) and the

respective contribution of folded and unfolded protein to the charge state distribution are calculated to determine the charge reduction and protein folding processes in LEMS measurements as a function of solution additives.

3.3 Experimental Section

3.3.1 Sample Preparation

Solid samples of cytochrome c, myoglobin, ammonium acetate, ammonium formate, and ammonium bicarbonate and aqueous samples of triethyl ammonium acetate, triethyl ammonium formate, and triethyl ammonium bicarbonate were purchased from Sigma Aldrich (St. Louis, MO). Aqueous formic acid was purchased from J.T. Baker (Phillipsburg, NJ). from For LEMS measurements, a 10^{-3} M stock solution of cytochrome c and myoglobin was prepared in HPLC grade water (Fisher Scientific, Pittsburgh, PA). An aliquot of the stock solution was diluted into water to yield a final protein concentration of 2 x 10^{-4} M for native proteins. For denatured proteins, an aliquot of stock solution was diluted into water with addition of formic acid to yield a protein concentration of 2 x 10^{-4} M with a pH of either 2.6 or 2.3. Seven ESI aqueous solutions with or without the addition of charge reducing additives were utilized in this study. The electrospray solvent consisted of 5 x 10^{-3} M concentration of ammonium acetate, ammonium formate, ammonium bicarbonate, triethyl ammonium acetate, triethyl ammonium formate or triethyl ammonium bicarbonate solution. A 10 μL aliquot of the diluted protein either native or denatured was spotted on a stainless steel plate and then subjected to laser vaporization into the ES solvents.

3.3.2 Laser Vaporization and Ionization Apparatus

A Ti:sapphire laser oscillator (KM Laboratories, Inc., Boulder, CO) seeded a regenerative amplifier (Coherent, Inc., Santa Clara, CA) for the creation of 75 fs, 0.6 mJ laser pulses centered at 800 nm. The laser, operated at 10 Hz to couple with the ES ion source, was focused to a spot size of ~250 μm in diameter with an incident angle of 45^{o} respect to the sample using a 16.9 cm focal length lens, with an approximate intensity of 1.6×10^{13} W/cm^2. The steel sample plate was biased to -2.0 kV to compensate for the distortion of electric field between the capillary and the needle caused by the sample stage. The area sampled was 6.4 mm below and approximately 1 mm in front of the ES needle. Aqueous protein sample (10 μL) deposited on the steel substrate was vaporized by the intense pulses allowing for capture and ionization by an ES plume travelling perpendicular to the vaporized material. The flow rate for ES solvent was set at 2 μL/min by a syringe pump (Harvard Apparatus, Holliston, MA).

3.3.3 Mass Spectrometry and Data Analysis

The mass spectrometer used in this experiment has been previously described(21). The ES needle was maintained at ground while the inlet capillary was biased to -4.5 kV to operate in positive ion mode. The postionized analytes were dried before entering the inlet capillary by countercurrent nitrogen gas at 180°C flowed at 3 L/min and were mass analyzed using microTOF-Q II mass spectrometer (Bruker Daltonics, Billerica, MA). The average charge state (Z_{avg}) was calculated using equation 1,

$$Z_{avg} = \frac{\sum_{i}^{N} q_i w_i}{\sum_{i}^{N} w_i} \quad (1)$$

where q_i is the net charge, W_i is the sum of signal intensity of the i^{th} charge state, and N is the number of charge states present in the mass spectra.

3.3.4 Safety Considerations

Appropriate eye protection were worn by all lab professional.

3.4 Results and Discussion

3.4.1 Analysis of Cytochrome c in Conventional Versus Charge Reducing Solution Additives

3.4.1.1 Conventional Electrospray Solvents

To determine the charge state distribution as a function of acid concentration, solutions of cytochrome c with pH of 7.0, 2.6 and 2.3, were laser vaporized into aqueous ES droplets and the resulting CSDs were measured. The LEMS measurement of cytochrome c prepared in solution with pH 7.0 in aqueous ES reveals a CSD ranging from 5+ to 12+ and is peaked at 9+ (Figure 3.1 a), with an average charge state distribution (Z_{avg}) of 8.5±0.2, as listed in Table 3.1. As the pH of solution containing cytochrome c is decreased, a bimodal CSD is observed, peaked at 9+ and 17+ for pH 2.6 and 2.3, (Figure 3.1 b and c). The Z_{avg} values obtained for cytochrome c at pH 2.6, and 2.3 are 12.7±0.1, and 14.1±0.1, respectively (Table 3.1). The lower charge states ranging from 7+ to 10+ contains 45±4% and 24±2% of the cytochrome c ion intensity for solution

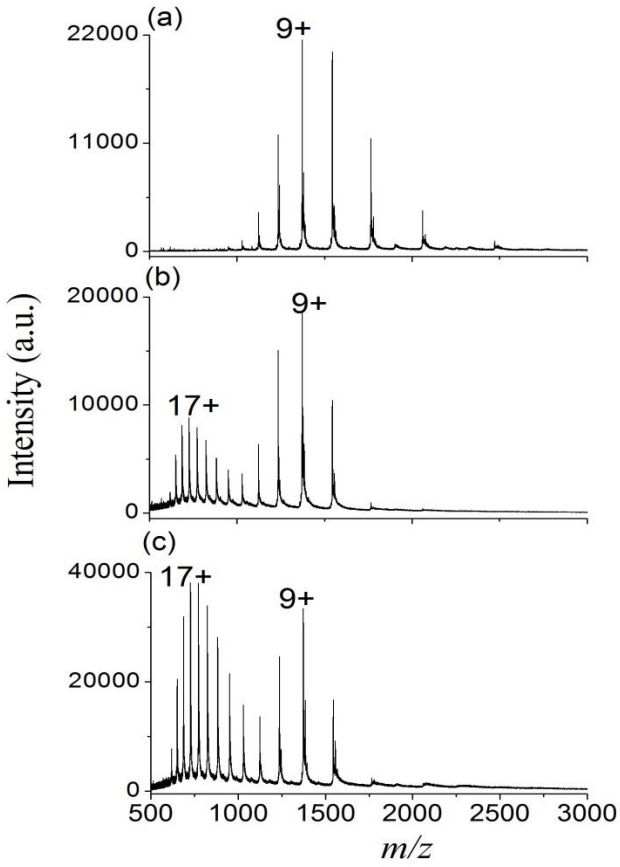

Figure 3.1. Representative LEMS mass spectra resulting from laser induced vaporization of cytochrome c at solution pH of a) 7, b) 2.6, and c) 2.3 into aqueous ES solvent.

Protein	pH	Average charge state (Fraction folded protein)						
		Water	**AF**	**AA**	**AB**	**TEAF**	**TEAA**	**TEAB**
Cytochrome c	7.0	8.5±0.2	7.0±0.1	6.9±0.1	7.7±0.4	4.9±0.0	5.2±0.1	4.7±0.2
	2.6	12.7±0.1 (45±4%)	9.7±0.2 (56±3%)	9.6±0.2 (54±4%)	12.7±0.2 (15±2%)	7.4±0.2 (41±3%)	6.7±0.2 (46±4%)	7.0±0.3 (37±4%)
	2.3	14.1±0.1 (24±2%)	11.6±0.3 (28±1%)	11.5±0.3 (27±2%)	13.1±0.1 (10±1%)	7.9±0.3 (28±2%)	6.5±0.1 (47±5%)	7.1±0.1 (29±6%)
Myoglobin	7.0	11.8±0.3	8.2±0.1	8.0±0.1	8.2±0.3	5.7±0.0	5.9±0.0	5.5±0.1
	2.6	20.0±0.1 (3±2%)	14.5±0.3 (20±4%)	14.2±0.4 (19±6%)	16.6±0.1 (8±2%)	9.6±0.3 (22±4%)	9.0±0.1 (27±1%)	9.8±0.2 (12±2%)
	2.3	20.5±0.1 (2±1%)	16.4±0.1 (6±4%)	16.2±0.1 (9±3%)	18.6±0.1 (5±1%)	9.8±0.2 (19±3%)	8.8±0.3 (26±2%)	10.0±0.2 (9±3%)

Table 3.1. Summary of average charge state distribution (Z_{avg}) of cytochrome c, and myoglobin in electrospray solvent consisting of either water, ammonium formate (AF), ammonium acetate (AA), ammonium bicarbonate (AB), triethyl ammonium formate (TEAF), triethyl ammonium acetate (TEAA) or triethyl ammonium bicarbonate (TEAB). The values reported in the parenthesis are the folded protein fractions.

with pH 2.6, and 2.3, respectively (Table 3.1). The decrease of the low charge state ion intensity and the increase in Z_{avg} with decreasing pH suggests that the protein unfolds at lower solution pH.

Ammonium formate and ammonium acetate are volatile additives that are routinely used in ESI-MS to maintain the native structure of protein and protein complexes. The effect of ammonium acetate solution on CSD of cytochrome c was measured by adjusting the pH of the protein solution vaporized. The LEMS measurement of cytochrome c prepared in a solution with pH 7.0 vaporized into ES droplets containing ammonium formate (solution pH of 6.2) reveals mainly 7+ charge state (Figure 3.2 a), indicating charge reduction of the folded state of the protein in comparison with aqueous ES solvent. As the pH of the cytochrome c solution is decreased, laser vaporization into the ammonium formate ES solution reveals a bimodal CSD, peaked at 7+ and 14+ for pH 2.6 (Figure 3.2 b), and 7+ and 15+ for pH 2.3 (Figure 3.2 c). The bimodal distributions indicate the presence of at least two conformations of the protein. The lower charge states ranging from 6+ to 9+ contain 56±3% at pH 2.6, and 28±1% at pH 2.3, of the cytochrome c ion intensity (Table 3.1), indicating folded states of the protein while the higher charge states ranging from 10+ to 20+ indicate unfolded protein. The ~20% enhancement in the folded distribution between the aqueous (~45%) and ammonium formate (~56%) ES solutions suggest that some of the protein population folds in the electrospray droplets containing ammonium formate. The contribution of unfolded protein to the charge state

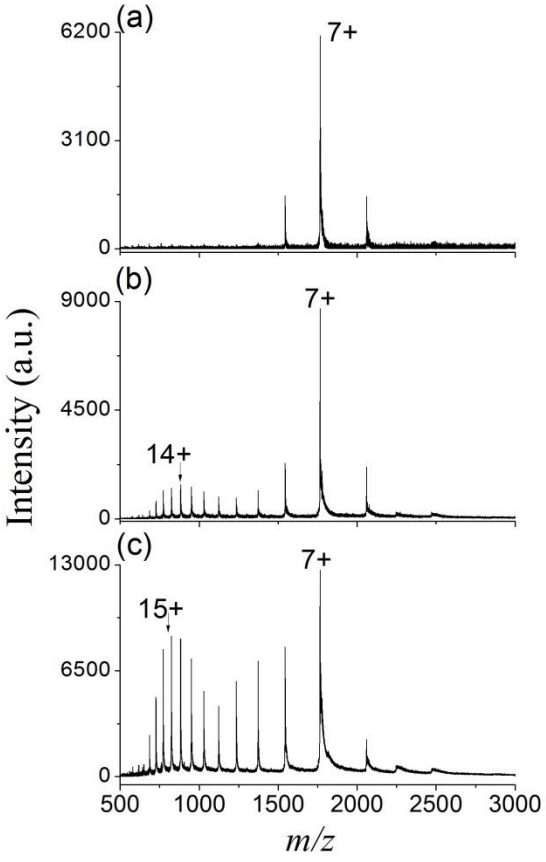

Figure 3.2. Representative LEMS mass spectra resulting from laser induced vaporization of cytochrome c at solution pH of a) 7, b) 2.6, and c) 2.3 into the ES solvent consisting of aqueous ammonium formate.

distribution increased when the protein was laser vaporized from solution pH of 2.3 in comparison with 2.6. In this case, the Z_{avg} increased to 11.6±0.3 for cytochrome c as the pH was decreased, see Table 3.1. This indicates that the extent of protein unfolding prior to laser vaporization affects the observed protein CSD in a buffered ES solvent.

ESI-MS measurements were also performed as a control experiment in which acid-denatured cytochrome c was pre-mixed with similar solution additive (e.g. ammonium formate, ammonium bicarbonate, and triethyl ammonium formate) utilized in the LEMS measurement at 1:1 ratio. The mass spectra, average charge state, and the fractions of folded protein obtained from these measurements are reported in Figure 3.3, Figure 3.4, Figure 3.5, and Table 3.2. The ESI mass spectra obtained from mixing cytochrome c (solution pH of 2.6) with 5 mM aqueous ammonium formate at 1:1 ratio reveals a bimodal CSD, peaked at 7+ and 14+ (Figure 3.3 b). Note that the pH of this solution was 3.5, so direct comparison to LEMS is problematic. Similar to the LEMS measurement, the contribution of unfolded protein to the CSD increased when the pH of the cytochrome c solution was decreased to 2.3 (prior to mixing with the ammonium formate solution). Note that the final pH of this solution was 2.5, making comparison to LEMS measurement at pH 2.6 more reasonable. LEMS had approximately twice the folded state distribution in comparison with ESI suggesting that the change in pH of the laser vaporized acidic solution after the interaction with ES droplets (containing ammonium formate) provides favorable condition for protein folding. Z_{avg} increased from 8.8±0.04 to 12.5±0.1 and the ion intensity of lower charge states ranging from 5+ to 9+

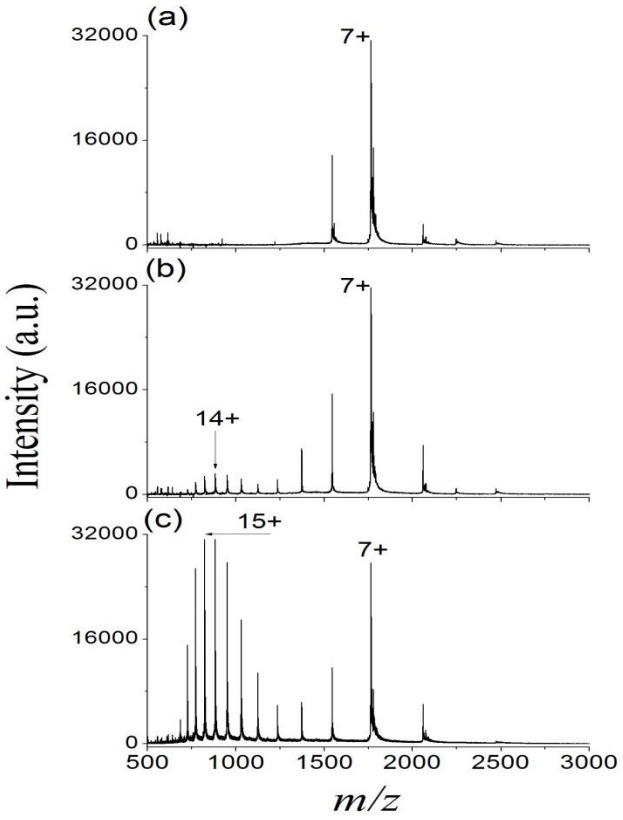

Figure 3.3. Representative ESI mass spectra of native cytochrome c prepared in a) aqueous AF. Panel b and c represent acid-denatured cytchorme c (panel b, pH 2.6 and panel c, pH 2.3) mixed with aqueous AF at 1:1 ratio. The pH of the final solution after mixing cytochrome c at pH 2.6 (pH 2.3) with 5 mM AF at 1:1 ratio is 3.5 (2.5).

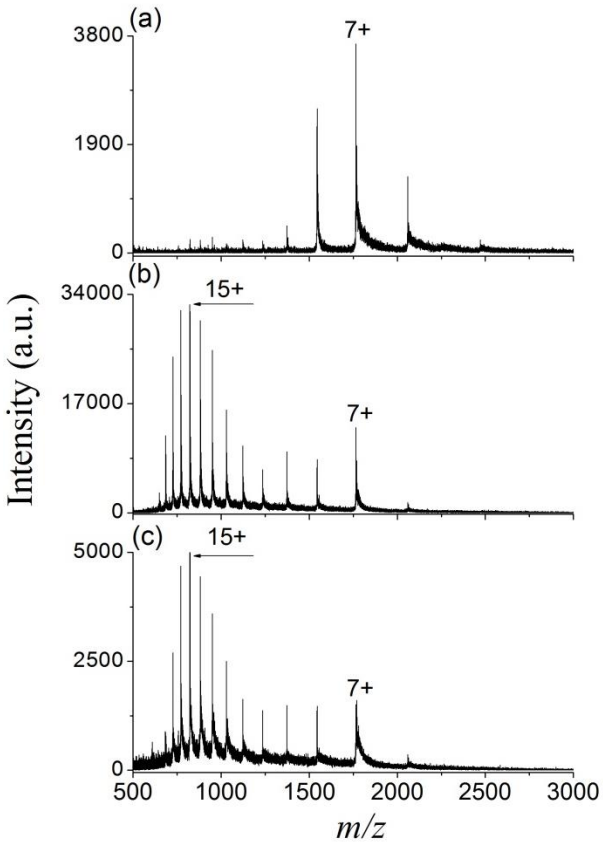

Figure 3.4. Representative ESI mass spectra of native cytochrome c prepared in a) aqueous AB. Panel b and c represent acid-denatured cytchorme c (panel b, pH 2.6 and panel c, pH 2.3) mixed with aqueous AB at 1:1 ratio. The pH of the final solution after mixing cytochrome c at pH 2.6 (pH 2.3) with 5 mM AB at 1:1 ratio is 3.7 (2.7).

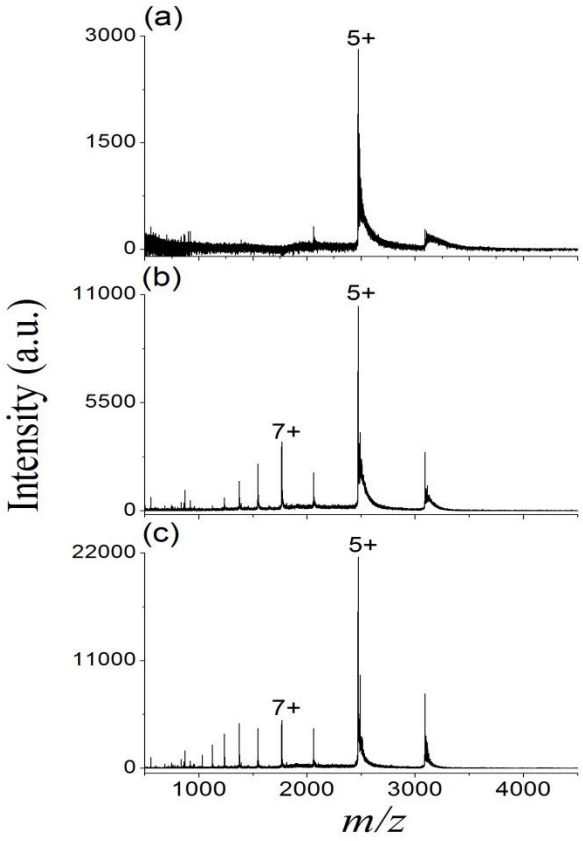

Figure 3.5. Representative ESI mass spectra of native cytochrome c prepared in a) aqueous TEAF. Panel b and c represent acid-denatured cytchorme c (panel b, pH 2.6 and panel c, pH 2.3) mixed with aqueous TEAF at 1:1 ratio. The pH of the final solution after mixing cytochrome c at pH 2.6 (pH 2.3) with 5 mM TEAF at 1:1 ratio is 3.3 (2.6).

Protein	pH	Average charge state (Fraction folded protein)			
		Water	**AF**	**AB**	**TEAF**
Cytochrome c	7.0	8.9±0.1	7.2±0.02	7.5±0.1	5.0±0.0
	2.6	13.8±0.02 (24±3%)	8.8±0.04 (72±2%)	13.6±0.1 (15±1%)	6.0±0.03 (64±1%)
	2.3	14.7±0.1 (11±3%)	12.5±0.1 (23±3%)	13.2±0.2 (15±3%)	6.5±0.2 (59±1%)
Myoglobin	7.0	11.2±0.1	8.3±0.1	-	5.9±0.01
	2.6	18.9±0.2 (7±2%)	15.1±0.2 (13±2%)	-	11.9±0.05 (8±1%)
	2.3	19.8±0.1 (4±1%)	17.4±0.03 (3±1%)	-	12.4±0.1 (5±2%)

Table 3.2. Summary of average charge state distribution (Z_{avg}) of cytochrome c, and myoglobin measured using ESI with electrospray solvent consisting of either water, AF, AB or TEAF. The values reported in the parenthesis are the folded protein fractions of cytochrome c and myoglobin.

decreased from 72±2% to 23± 3% for cytochrome c as the pH was decreased in the control ESI measurements (Table 3.2).

The LEMS measurement of cytochrome c prepared in a solution with pH 7.0 in ammonium acetate (solution pH of 6.5) reveals mainly the 7+ charge state (Figure 3.6 a), with a Z_{avg} value of 6.9±0.1, indicating charge reduction of the folded state of the protein. As the pH of the cytochrome c solution is decreased, bimodal CSDs are observed, peaked at 7+ and 13+ for pH 2.6 (Figure 3.6 b), and 7+ and 15+ for pH 2.3 (Figure 3.6 c), with a Z_{avg} value of 9.6±0.2, and 11.5±0.3, respectively. The lower charge states ranging from 6+ to 9+ contain 54±4% at pH 2.6, and 27±2% at pH 2.3, of the cytochrome c ion intensity. Again, the bimodal CSDs indicate the presence of at least two conformations of the protein. These measurements suggest that the addition of solution additive like ammonium acetate to an electrospray solvent can promote protein folding in the electrospray droplet and promote some degree of charge reduction.

Assessment of protein conformation was made by assuming that the CSD is a reliable indicator of either folded or unfolded structure. This assumption is in agreement with measurements revealing a folded protein distribution for acid denatured protein upon interaction with basic vapors(4), and aqueous buffer system(22, 23). The underlying assumption that there is a correlation between CSD and structure has been tested in many previous investigations(1-3, 24). The use of CSD to assess solution phase structure in the LEMS experiment further assumes that the structure in solution is preserved during laser vaporization. This has been tested through direct comparison of ESI and LEMS measurements for cytochrome c as a function of both sample pH before vaporization and

ESI pH into which the sample is transferred(11). Both the CSD and collision induced dissociation (CID) measurements support this assumption. The major limitation of using CSD as a probe of protein structure is the insensitivity of the method with regard to differentiating native and near native structures. Multiple structures may contribute to a particular charge state as has been demonstrated by ion mobility measurements(25, 26).

Ammonium bicarbonate is often used to maintain the near-neutral pH of the bulk solution to preserve the native structure of the protein. LEMS measurement of cytochrome c prepared in a solution with pH 7 vaporized into ES droplets containing ammonium bicarbonate (solution pH of 8.2) reveals mainly 7+ and 8+ charge states (Figure 3.7 a) and a small distribution ranging from 10+ to 14+ containing 13±4% of the cytochrome c ion intensity, corresponding to unfolded states of the protein, as seen in the inset of Figure 3.7 a. The Z_{avg} calculated for cytochrome c in ES consisting of ammonium bicarbonate (Z_{avg} of 7.7±0.4) was slightly higher in comparison with ammonium formate (Z_{avg} of 7.0±0.1), and ammonium acetate (Z_{avg} of 6.9±0.1). As the pH of solution containing cytochrome c is lowered, a trimodal CSD peaked at 7+, 9+, and 15+ for pH 2.6 (Figure 3.7 b), and a much broader CSD is observed, peaked at 15+ for pH 2.3 (Figure 3.7 c). The ammonium bicarbonate spray did not show a large fraction of folded cytochrome c at solution pH of 2.6 despite the expected higher pH (solution pH of 8.2). The calculated Z_{avg} for pH 2.6 (Z_{avg} of 12.7±0.2), and pH 2.3 (Z_{avg} of 13.1±0.1) were higher with the ammonium bicarbonate solution in comparison with the ammonium formate and ammonium acetate solutions. The increase in Z_{avg} for ammonium bicarbonate is possibly due to foaming of the electrospray solvent (ammonium

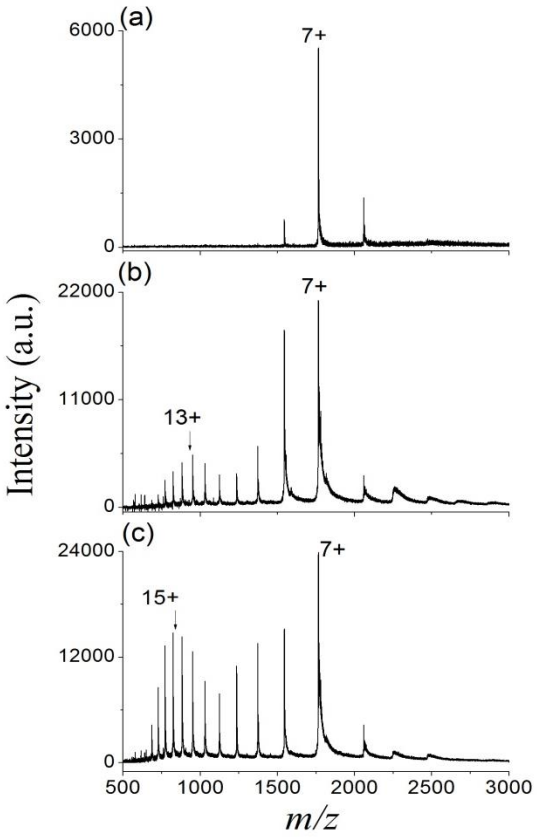

Figure 3.6. Representative LEMS mass spectra resulting from laser induced vaporization of cytochrome c at solution pH of a) 7, b) 2.6, and c) 2.3 into the ES solvent consisting of aqueous ammonium acetate.

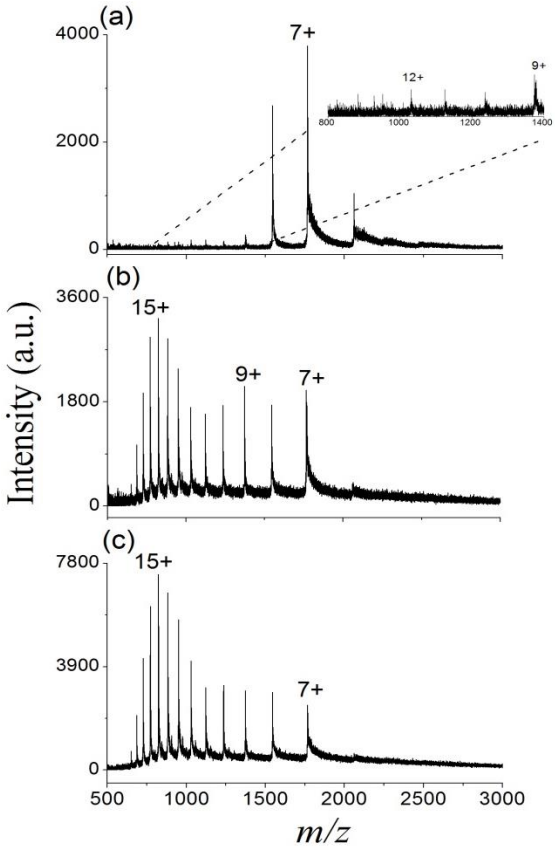

Figure 3.7. Representative LEMS mass spectra resulting from laser induced vaporization of cytochrome c at solution pH of a) 7, b) 2.6, and c) 2.3 into the ES solvent consisting of aqueous ammonium bicarbonate.

bicarbonate) caused by $CO_{2(g)}$ outgassing during the desolvation process via the reaction $HCOOH + NH_4^+HCO_3^- \rightarrow NH_4^+HCOO^- + H_2O + CO_{2\ (g)}$(27). In this reaction, the counter ion (HCO_3^-) decomposes to CO_2 and H_2O in the presence of acid, creating bubbles which facilitate protein unfolding. We note that in the case of electrothermal supercharging experiment, bubble formation due to buffer decomposition was found not to be the primary reason for protein unfolding(28). We note, however, that no acid was present in that study to induce the decomposition to H_2O and CO_2. The presence of both an acid and $CO_{2\ (g)}$ outgassing in our measurements contribute to the formation of relatively higher charge states in ES consisting of ammonium bicarbonate in comparison with ammonium formate, and ammonium acetate solution.

3.4.1.2 Solution Additives with High Gas Phase Basicity

Previous studies have shown that the use of charge reducing solution additives results in a shift in protein CSD to lower charge states(9, 29). The electrospray measurements of globular and denatured lysozyme showed a decrease in net charging of the protein with increasing gas phase basicity with the appearance of monomodal CSD(29, 30). In conventional electrospray containing a solution additive with high gas phase basicity there is the question of whether the additive assists in folding the denatured protein in solution to provide lower charge states or whether charge reduction simply occurs in the gas phase upon ionization at the end of the desolvation process(29, 31). The charge reduction observed in a conventional ESI measurement using an additive with high gas phase basicity is consistent with either hypothesis. The ionization of globular macromolecules in ESI-MS is believed to occur via charge residue model

(CRM), where residual charge on the droplet surface is transferred to the macromolecules upon solvent evaporation(32-34). LEMS is used here to decouple the solution phase effects from processes occurring in the ES droplet during desolvation.

To investigate whether charge reduction occurs in the electrospray droplet, laser vaporization is used to transfer either folded or denatured proteins into the electrospray plume containing solution additives with high gas phase basicities. Cytochrome c is prepared in three solutions having a pH of 7.0, 2.6 and 2.3 and was laser vaporized into the ES droplets containing either triethyl ammonium formate (TEAF), triethyl ammonium acetate (TEAA) or triethyl ammonium bicarbonate (TEAB). The LEMS measurement of cytochrome c prepared in a solution with pH 7 vaporized into ES droplets containing TEAF (solution pH of 6.1) reveals mainly 5+ charge state (Figure 3.8 a) with a Z_{avg} value of 4.9, indicating enhanced charge reduction of the folded states of the protein in comparison with ammonium formate (Z_{avg} of 7.0±0.1), acetate (Z_{avg} of 6.9±0.1), and bicarbonate (Z_{avg} of 7.7±0.4), as well as the aqueous (Z_{avg} of 8.5±0.2) ES solvent. As the pH of laser vaporized cytochrome c solution is decreased to 2.6 and 2.3, bimodal CSDs are observed, peaked at 5+ and 8+ (Figure 3.8 b and c). The fact that there are two distributions and not just a shifted distribution for TEAF suggests that there are both folded and unfolded states in the electrospray droplets. The lower charge states peaked at 5+ indicate significant charge reduction of the folded states, in comparison with both aqueous (peaked at 9+) and ammonium formate ES solvent (peaked at 7+). The distribution peaked at 8+ likely corresponds to the charge reduction of unfolded states of

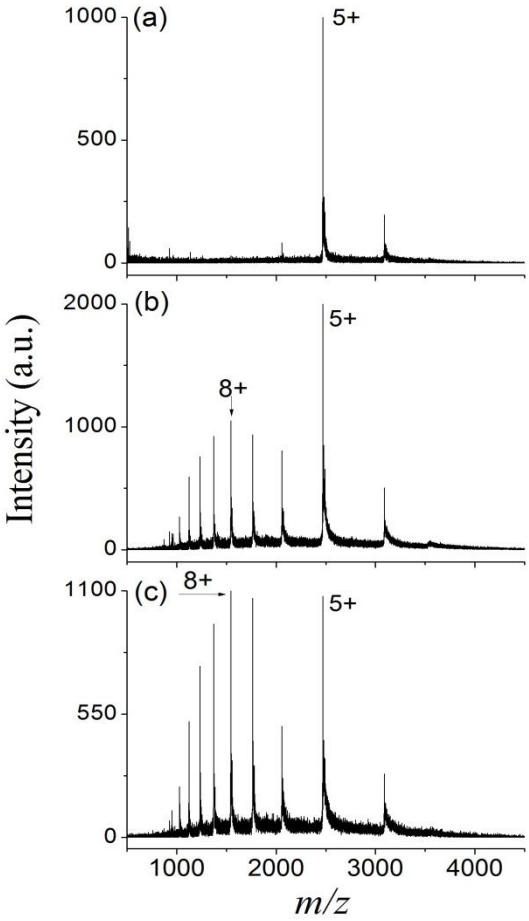

Figure 3.8. Representative LEMS mass spectra resulting from laser induced vaporization of cytochrome c at solution pH of a) 7, b) 2.6, and c) 2.3 into the ES solvent consisting of aqueous triethyl ammonium formate.

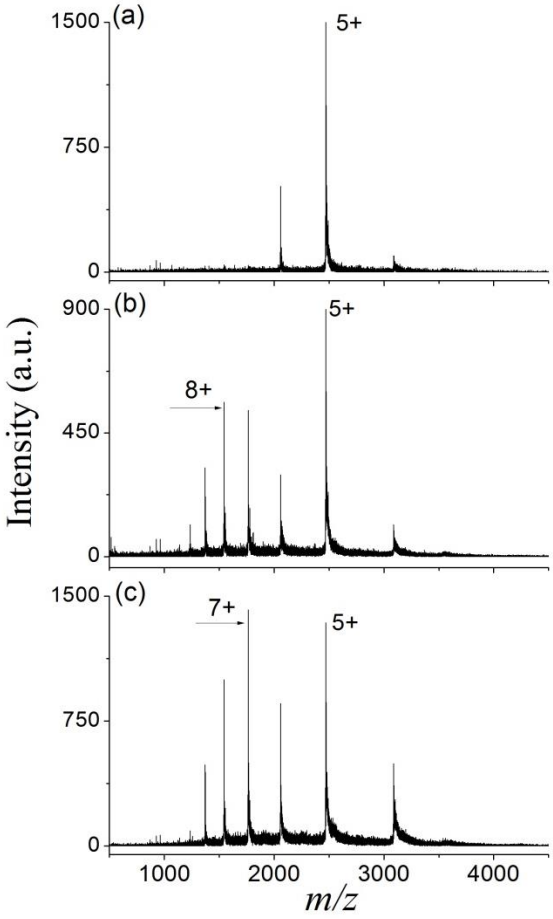

Figure 3.9. Representative LEMS mass spectra resulting from laser induced vaporization of cytochrome c at solution pH of a) 7, b) 2.6, and c) 2.3 into the ES solvent consisting of aqueous triethyl ammonium acetate.

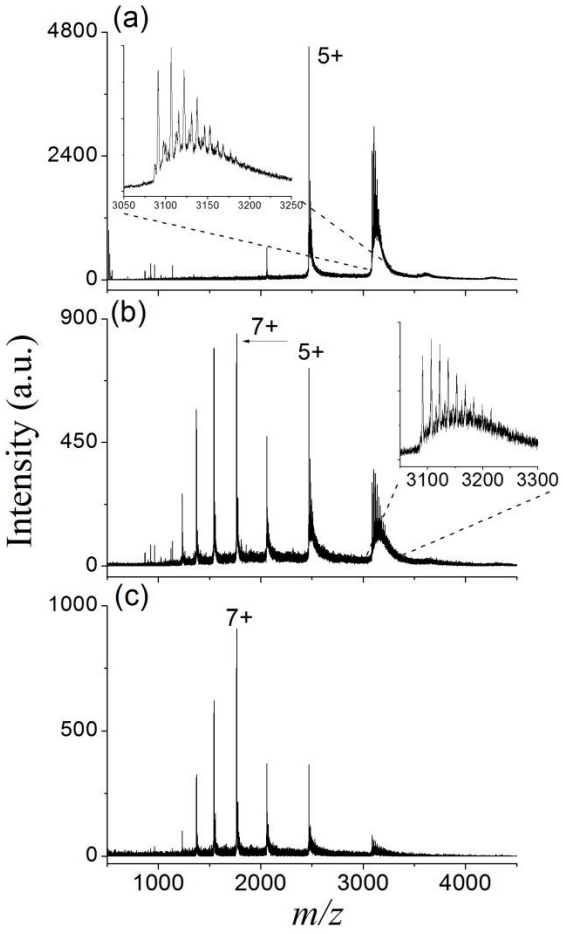

Figure 3.10. Representative LEMS mass spectra resulting from laser induced vaporization of cytochrome c at solution pH of a) 7, b) 2.6, and c) 2.3 into the ES solvent consisting of aqueous triethyl ammonium bicarbonate.

the protein. The low charge states ranging from 4+ to 6+ contain 41±3% at pH 2.6, and 28±2% at pH 2.3 of the cytochrome c ion intensity (Table 3.1). The fraction of folded state of cytochrome c (solution pH of 2.6) for TEAF (41±3%) is within the standard deviation in comparison with aqueous ES (45±4%), and ~20% lower in comparison with ammonium formate (56±3%), and ammonium acetate (54±4%) ES solutions. This suggests that the use of solution additive with high gas phase basicity does not enhance protein folding in the ES droplets like the commonly used solvent systems. However, a significant reduction in Z_{avg} was observed for cytochrome c (pH of 2.3) in the presence of TEAF (Z_{avg} of 7.9±0.3) in comparison with aqueous (Z_{avg} of 14.1±0.1), ammonium acetate (Z_{avg} of 11.5±0.3), and ammonium formate (Z_{avg} of 11.6±0.3) ES solution.

The LEMS measurement of cytochrome c prepared in solutions with pH of 7.0, 2.6 and 2.3 vaporized into ES droplets containing TEAA (Figure 3.9 a, b and c) are very similar to the measurements made using TEAF (Figure 3.8 a, b and c). TEAA displays, however, enhanced charge reduction for the unfolded distribution in comparison with TEAF in the case of cytochrome c.

Cytochrome c solutions with pH of 7.0, 2.6, and 2.3 were laser vaporized into ES droplets containing TEAB to measure the subsequent charge reduction and protein folding as a function of pH. LEMS measurement of cytochrome c prepared in a solution with pH of 7 in ES consisting of TEAB revealed mainly 5+ and 4+ charge states (Figure 3.10 a), with a Z_{avg} value of 4.7±0.2, indicating enhanced charge reduction in comparison with ammonium formate (Z_{avg} of 7.0±0.1), ammonium acetate (Z_{avg} of 6.9±0.1), ammonium bicarbonate (Z_{avg} of 7.7±0.4), and aqueous (Z_{avg} of 8.5±0.2) ES solvent. As

the pH of solution containing cytochrome c is decreased to 2.6, a bimodal CSD is observed, peaked at 5+ and 7+ (Figure 3.10 b), indicating the presence of at least two conformation of the protein. The low charge states ranging from 4+ to 6+ contain 37± 4% of the cytochrome c ion intensity. The LEMS measurement of cytochrome c prepared in a solution with pH of 2.3 revealed a monomodal CSD distribution peaked at 7+ (Figure 3.10 c) indicating substantial unfolding of the protein. The reduction in Z_{avg} observed for cytochrome c (pH of 2.3) in the presence of triethyl ammonium bicarbonate (Z_{avg} of 7.1±0.1) in comparison with ammonium bicarbonate (Z_{avg} of 13.1±0.1) and aqueous ES solution (Z_{avg} of 14.1±0.1) is consistent with the notion that the charge reduction scales with the gas phase basicity of their neutral conjugates, i.e. the gas phase basicity of triethyl amine is 221 Kcal mol^{-1}, ammonia is 193 Kcal mol^{-1}, and water is 167 Kcal mol^{-1}.

3.4.2 Analysis of Myoglobin in Conventional Versus Charge Reducing Solution Additives

3.4.2.1 Conventional Electrospray Solvents

Holomyoglobin in the native state contains a heme group in the interior of the protein. The heme is released in conditions of extreme pH, high temperatures, and in the presence of organic solvents to produce apomyoglobin(35). Here we seek to investigate whether the solution phase conformation (holomyoglobin) is preserved upon the transfer into the gas phase, and whether the acid-denatured myoglobin can refold in the charged electrospray droplets with heme reincorporation into its hydrophobic pocket. Laser vaporization is used to transfer both the native (holomyoglobin) and acid-denatured

myoglobin (apo-myoglobin) and heme into electrospray droplets containing various solution additives.

To determine the charge state distribution as a function of acid concentration, solutions of myoglobin with pH of 7.0, 2.6, and 2.3, were laser vaporized into aqueous ES droplets and the resulting CSDs were measured. The LEMS measurement of myoglobin prepared in solution with pH 7.0 in aqueous ES reveals a broad CSD ranging from 7+ to 15+ and is peaked at 12+ with both holo (~86%) and apo (~14%) myoglobin features (Figure 3.11 a). The Z_{avg} values calculated for these measurements are 11.8±0.3 and 11.2±0.2 for holomyoglobin and apomyoglobin, respectively, as listed in Table 3.1. Acid-denatured myoglobin was laser vaporized and the LEMS measurements reveal exclusively apomyoglobin features with broad, monomodal CSDs peaked at 22+ and 23+ for solution pH of 2.6 and 2.3, respectively (Figure 3.11 b and c). The apomyoglobin features observed at higher charge states indicate the presence of unfolded states of the protein. The lower charge states ranging from 10+ to 13+ contains 3±2% and 2±1% of the apomyoglobin ion intensity for solution with pH 2.6, and 2.3, respectively (Table 3.1).

The effect of ES solution containing ammonium formate on the CSD of myoglobin in the folded or unfolded state was measured by adjusting the pH of the solution vaporized. The LEMS measurement of myoglobin prepared in a solution with pH 7.0 vaporized into ES droplets containing ammonium formate (pH 6.2) reveals mainly 8+ and 9+ charge states corresponding to predominately holomyoglobin features, (Figure 3.12 a) with a Z_{avg} value of 8.2±0.1, indicating both charge reduction of the folded state

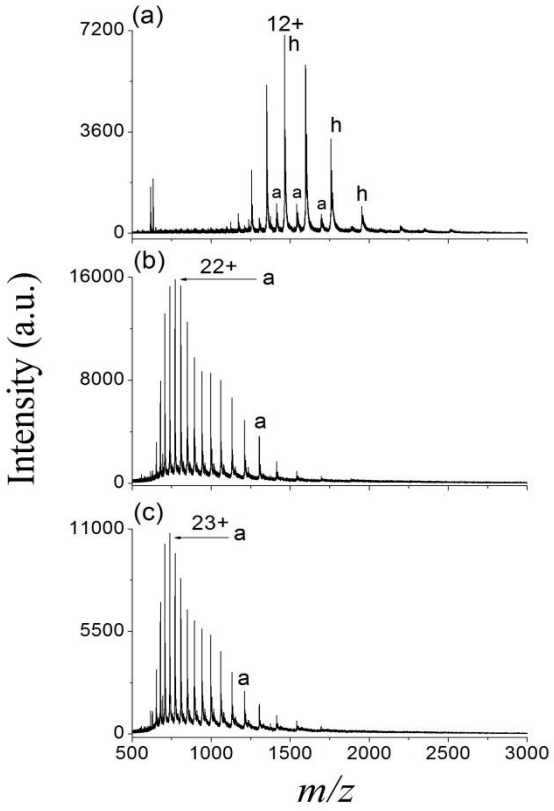

Figure 3.11. Representative LEMS mass spectra resulting from laser induced vaporization of myoglobin at solution pH of a) 7, b) 2.6, and c) 2.3 into aqueous ES solvent.

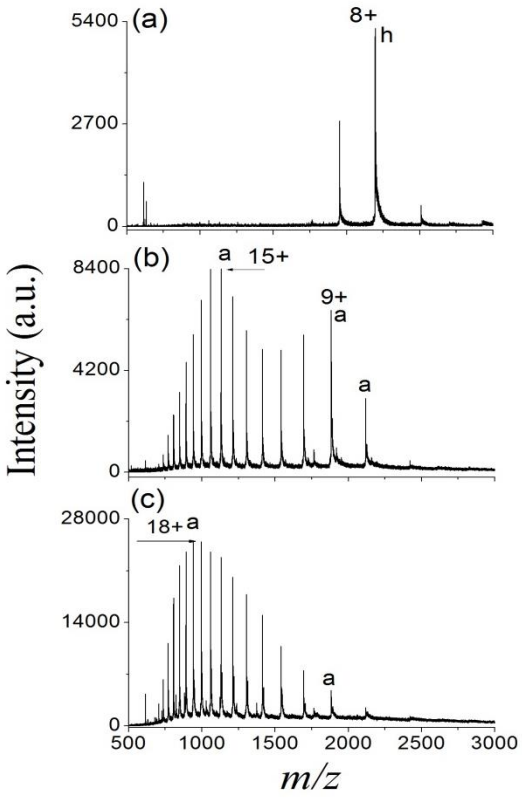

Figure 3.12. Representative LEMS mass spectra resulting from laser induced vaporization of myoglobin at solution pH of a) 7, b) 2.6, and c) 2.3 into aqueous ammonium formate solution.

of the protein in comparison with aqueous (Z_{avg} of 11.8±0.3) ES solvent and that the ammonium formate maintains the heme co-factor in the hydrophobic pocket in comparison with aqueous ES solvent where ~15% of the protein is found in apomyoglobin form. This measurement suggests that the formation of apomyoglobin in the case of vaporization of myoglobin (solution pH of 7.0) into the aqueous ES solution occurs after the laser vaporized protein interacts with the aqueous ES droplets. An alternative explanation is that apomyoglobin is vaporized but incorporates heme in the spray containing ammonium formate.

Myoglobin in a solution with pH 2.6 was vaporized into ES droplets containing ammonium formate to determine whether apomyoglobin can convert to holomyoglobin within the electrospray process. The mass spectrum revealed ~100% apomyoglobin features with bimodal CSDs, peaked at 9+ and 15+, ranging from 7+ to 24+ (Figure 3.12 b). This indicates that the time required for heme reincorporation into the hydrophobic pocket, upon the interaction with ammonium formate ES solvent, is longer than the LEMS measurement time transiting from the vaporization region into the vacuum of the mass spectrometer. A previous study suggested that the refolding of apomyoglobin to the globular holomyoglobin (with heme reincorporation into the hydrophobic pocket) takes hundreds of milliseconds to seconds(36). The time available during the LEMS analysis is estimated to be 100 ms(11), suggesting that there is insufficient time for heme reincorporation. The bimodal CSDs peaked at 9+ and 15+ suggest at least a fraction of apomyoglobin (charge states ranging from 7+ to 10+ containing 20±4% of the

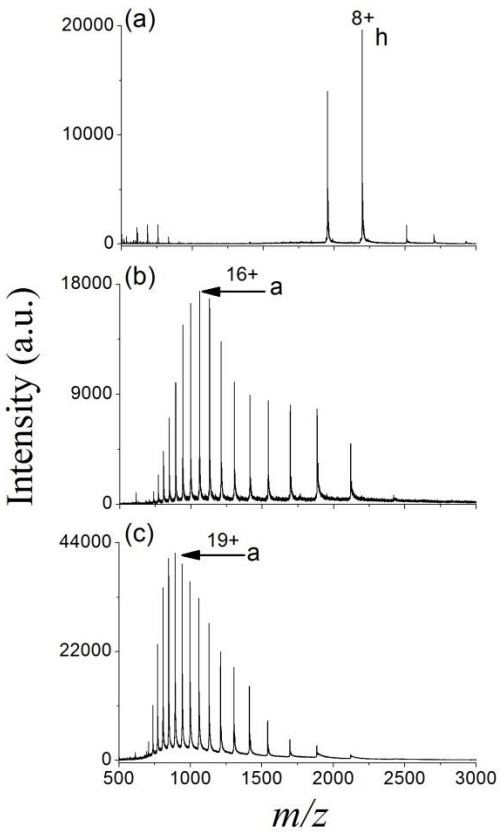

Figure 3.13. Representative ESI mass spectra of native myoglobin prepared in a) aqueous AF. Panel b and c represent acid-denatured myoglobin (panel b, pH 2.6 and panel c, pH 2.3) mixed with aqueous AF at 1:1 ratio. The pH of the final solution after mixing cytochrome c at pH 2.6 (pH 2.3) with 5 mM AF at 1:1 ratio is 3.5 (2.5).

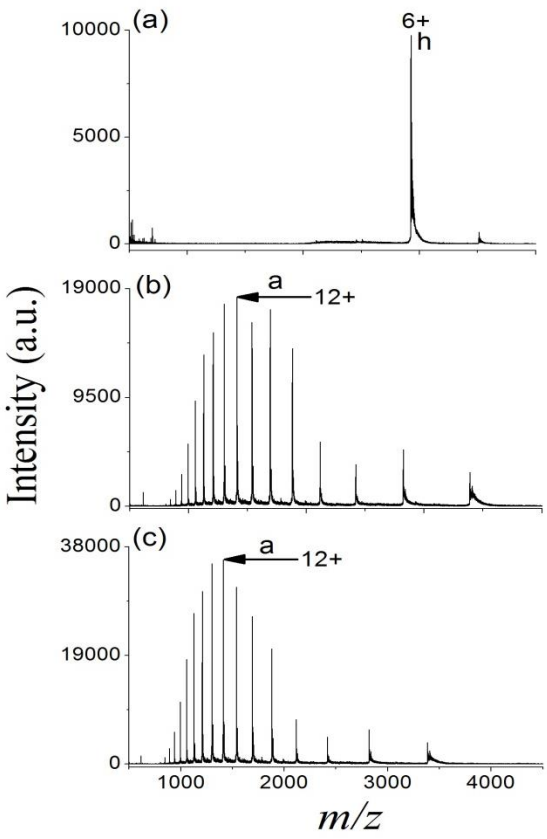

Figure 3.14. Representative ESI mass spectra of native myoglobin prepared in a) aqueous AF. Panel b and c represent acid-denatured myoglobin (panel b, pH 2.6 and panel c, pH 2.3) mixed with aqueous AF at 1:1 ratio. The pH of the final solution after mixing cytochrome c at pH 2.6 (pH 2.3) with 5 mM TEAF at 1:1 ratio is 3.3 (2.6).

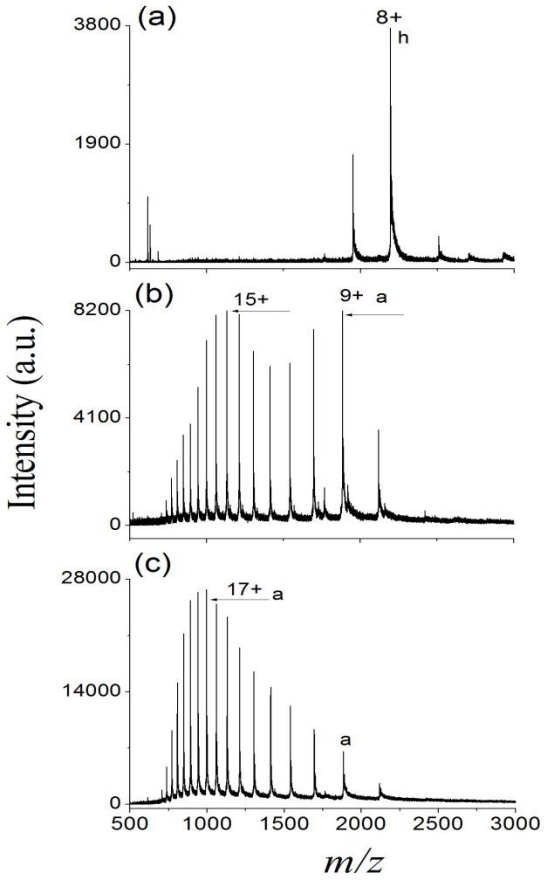

Figure 3.15. Representative LEMS mass spectra resulting from laser induced vaporization of myoglobin at solution pH of a) 7, b) 2.6, and c) 2.3 into aqueous ammonium acetate solution.

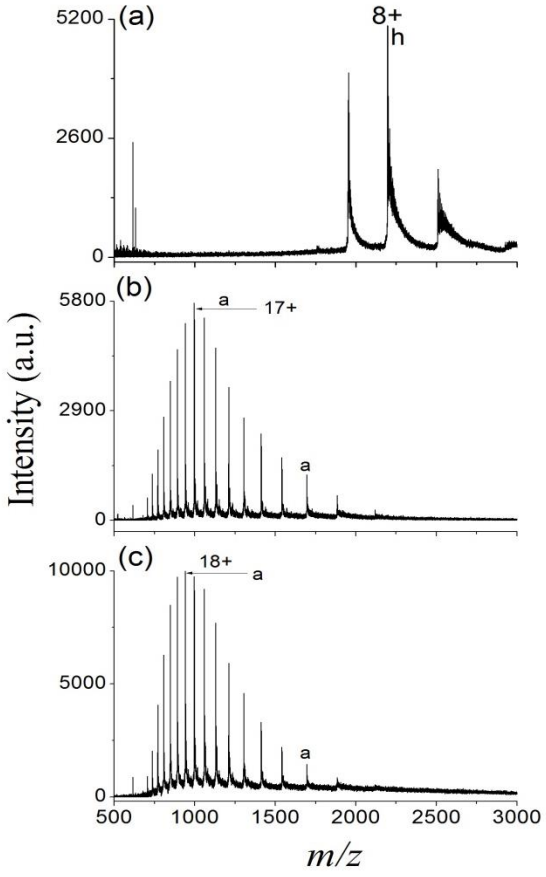

Figure 3.16. Representative LEMS mass spectra resulting from laser induced vaporization of myoglobin at solution pH of a) 7, b) 2.6, and c) 2.3 into aqueous ammonium bicarbonate solution.

apo-myoglobin ion intensity) folds into a globular apo-myoglobin conformer in the presence of the ammonium formate ES solvent. This is supported by the fact that vaporization of pH 2.6 protein solution into water only contained 3±2% folded distribution. The time scale for refolding of apo-myoglobin into globular apo-myoglobin conformation is reported to be in the order of few microseconds(37), which is short compared to the 100 ms that the complex spends in the ES droplet. This experiment confirms that the formation of apo-myoglobin occurs in the aqueous droplet for the pH 7.0 measurement and not during the vaporization process. The LEMS measurement of myoglobin prepared in a solution with pH 2.3 vaporized into ES droplets containing ammonium formate revealed a monomodal CSD ranging from 7+ to 24+, peaked at 18+ (Figure 3.12 c). The charge states ranging from 7+ to 10+ contain 6±4% of the apo-myoglobin ion intensity while the majority of apo-myoglobin features are observed at higher charge states ranging from 11+ to 24+, indicating unfolded states of the protein. The monomodal distribution suggests that the extent of charge reduction and the appearance of folded states depend either on the extent of protein unfolding prior to laser vaporization or on the pH of the ES droplet after mixing with the vaporized acidic protein solution. Similar to cytochrome c, ESI-MS measurements were performed as a control experiment for complete mixing of acid-denatured myoglobin with similar solution additives (e.g. ammonium formate, and triethyl ammonium formate) utilized in the LEMS measurement at 1:1 ratio. The mass spectra, average charge state, and the fraction folded protein obtained from these measurements are reported in Figure 3.13 and Figure 3.14 and Table 3.2.

The LEMS measurement of myoglobin prepared in solutions with pH of 7.0, 2.6 and 2.3 vaporized into ES droplets containing ammonium acetate (Figure 3.15 a, b and c) are very similar to the measurements made using ammonium formate (Figure 3.12 a, b and c). Similar to the measurements for cytochrome c, the LEMS measurements of myoglobin at lower solution pH (pH of 2.6, and 2.3) in ES solution containing ammonium bicarbonate did not result in charge reduction when compared to ammonium formate, and ammonium acetate despite the higher solution pH (Figure 3.16 b and c), which is probably due to the decomposition of HCO_3^- (counter ions) to CO_2 and H_2O in the presence of acid, creating bubbles which facilitate protein unfolding.

3.4.2.2 Solution Additives with High Gas Phase Basicity

Myoglobin prepared in solutions with pH of 7.0, 2.6, and 2.3 were laser vaporized into solution additives with gas phase basicity to measure the subsequent charge reduction and protein folding in ES droplets. The LEMS measurement of myoglobin prepared in a solution with pH of 7.0 vaporized into ES droplets containing TEAF (solution pH of 6.1) reveals mainly 6+ and 5+ charge states (holomyoglobin features, Figure 3.17 a) with a Z_{avg} value of 5.7±0.0, indicating enhanced charge reduction of the folded state of the protein in comparison with ammonium formate (Z_{avg} of 8.2±0.1), ammonium acetate (Z_{avg} of 8.0±0.1), ammonium bicarbonate (Z_{avg} of 8.2±0.3), and aqueous (Z_{avg} of 11.8±0.3) ES solvent. Laser vaporization of myoglobin prepared in solutions with pH of 2.6 and 2.3 into the same ES solvent revealed bimodal CSDs with most probable charge states at 6+ and 10+ with exclusively apo-myoglobin features, as

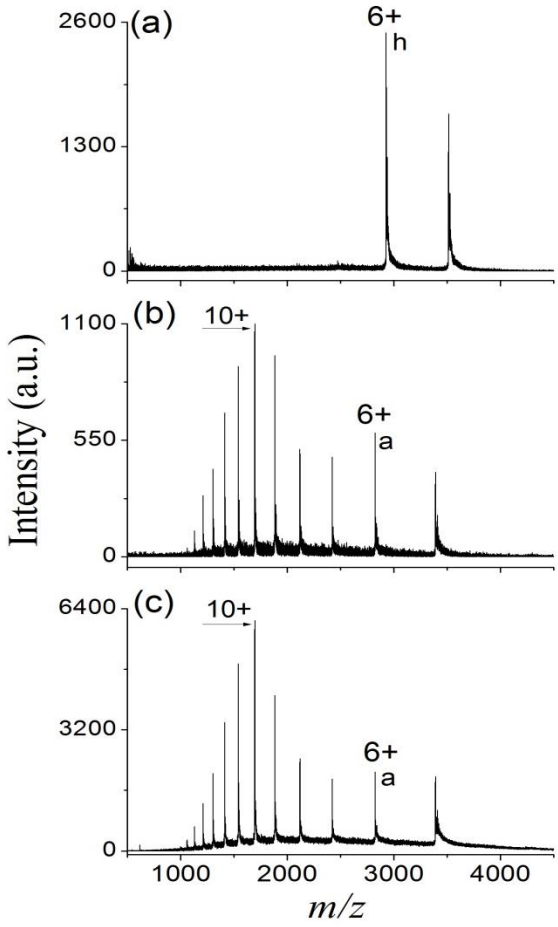

Figure 3.17. Representative LEMS mass spectra resulting from laser induced vaporization of myoglobin at solution pH of a) 7, b) 2.6, and c) 2.3 into the ES solvent consisting of aqueous triethyl ammonium formate.

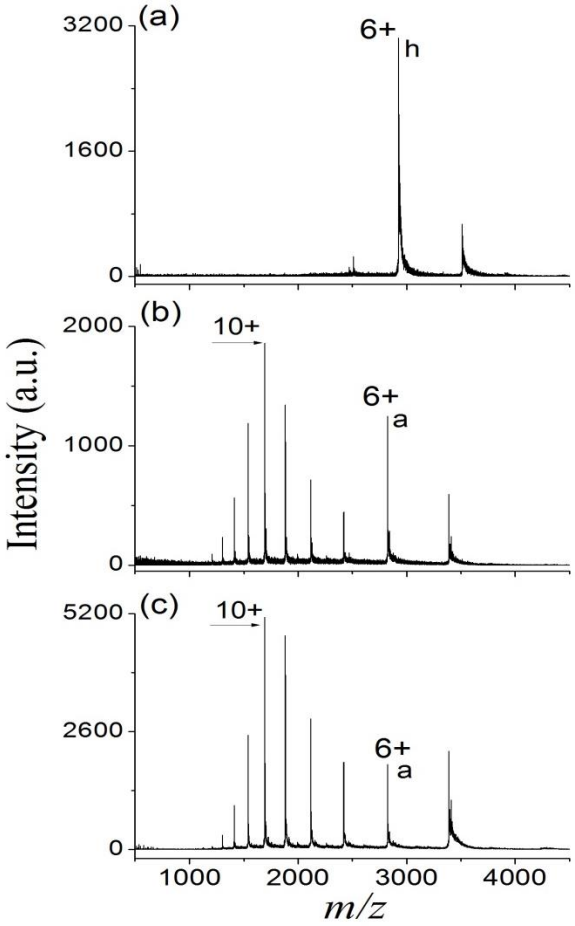

Figure 3.18. Representative LEMS mass spectra resulting from laser induced vaporization of myoglobin at solution pH of a) 7, b) 2.6, and c) 2.3 into the ES solvent consisting of aqueous triethyl ammonium acetate.

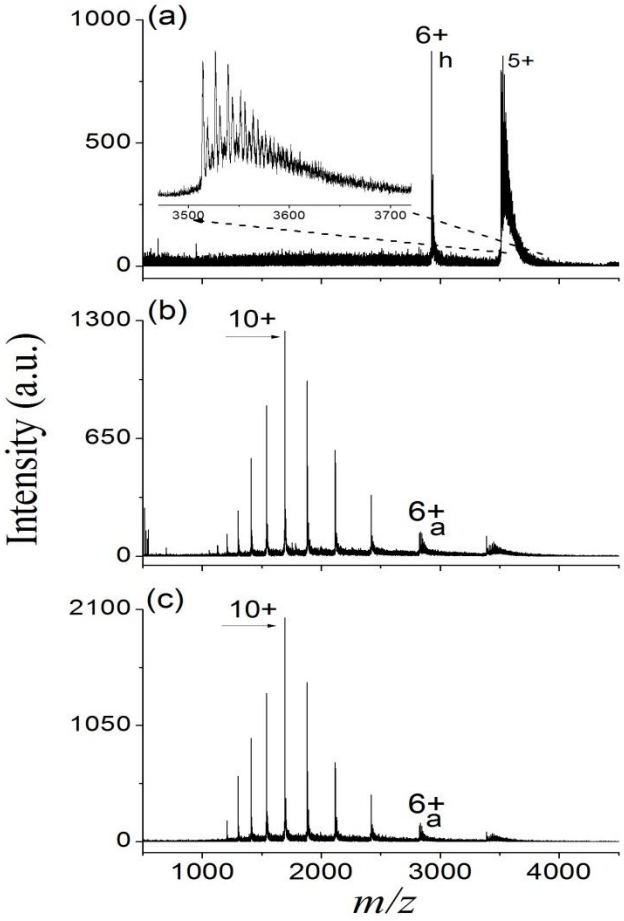

Figure 3.19. Representative LEMS mass spectra resulting from laser induced vaporization of myoglobin at solution pH of a) 7, b) 2.6, and c) 2.3 into the ES solvent consisting of aqueous triethyl ammonium bicarbonate.

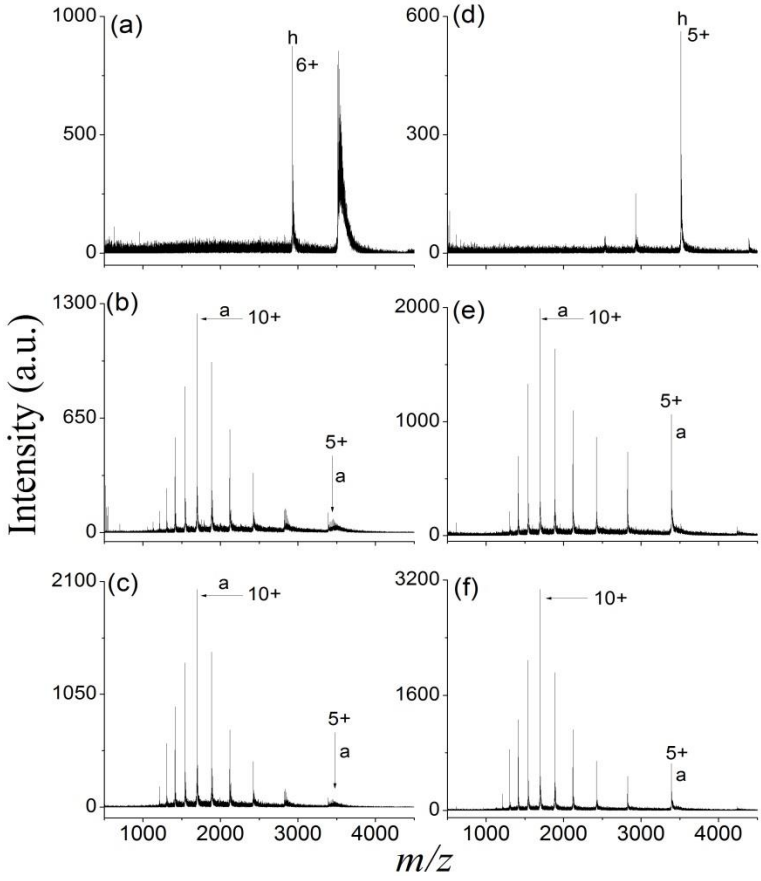

Figure 3.20. Representative LEMS mass spectra resulting from laser induced vaporization of myoglobin at pH 7 (panel a, and d), myoglobin at pH 2.6 (panel b, and e), and myoglobin at pH 2.3 (panel c, and f) into the electrospray solvent consisting of aqueous triethyl ammonium bicarbonate (5mM) at two different CID potentials. The measurements shown in figure a-c, and d-f are taken at 10 and 35 eV respectively.

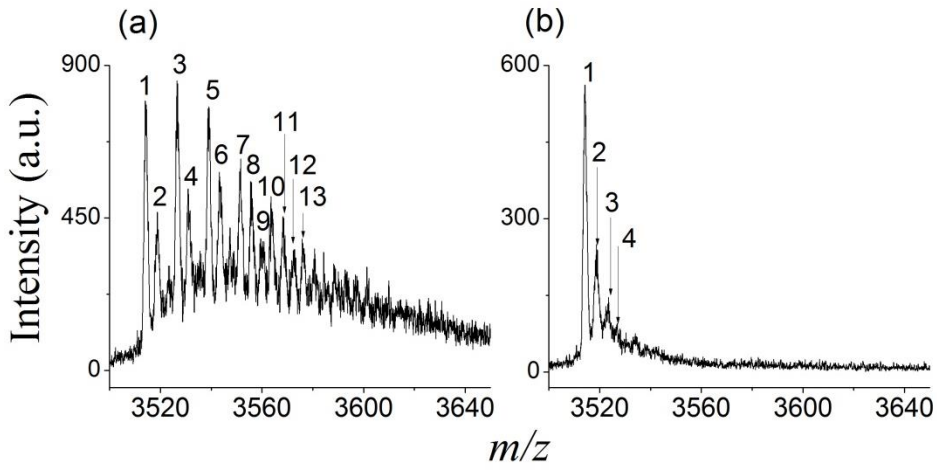

Figure 3.21. High resolution LEMS mass spectra resulting from laser induced vaporization of myoglobin at pH 7 into the electrospray solvent consisting of 5 mM triethyl ammonium bicarbonate at the collision potential of a) 10 eV and b) 35 eV. Deconvoluted mass difference of 23 between peak 1 and 2 in panel a suggests that peak 2 is the sodiated protein feature while deconvoluted mass difference of 61 between peak 1 and 3 suggests that peak 3 is the protein feature with counter ion (HCO_3^-) from triethyl ammonium bicarbonate. Peak 4 represents $[M+5H^++Na^++HCO_3^-]^{5+}$, peak 5 represents $[M+7H^++2HCO_3^-]^{5+}$, peak 6, 7, 8, 9, 10, 11, 12, 13 are the repeating unit of either HCO_3^- or $Na^+HCO_3^-$. Deconvoluted mass difference of 23 between peak 1 and 2 in panel b suggests that peak 1 represents the sodiated protein feature. Peak 2, 3, 4 represent the repeating unit of sodiated protein features.

shown in Figure 3.17 b and c. The charge states ranging from 5+ to 7+ contain 22±4% and 19±3% of the apo-myoglobin ion intensity for solutions with pH of 2.6, and 2.3, respectively. The lower charge states peaked at 6+ indicate charge reduction, presumably of the globular conformer of apo-myoglobin. The distribution peaked at 10+ likely corresponds to the charge reduction of unfolded states of the protein. The fraction of globular apo-myoglobin, calculated for myoglobin prepared in a solution with pH of 2.6, using TEAF (22±4%) is greater in comparison with aqueous ES (3±1%), and is within the standard deviation in comparison with ammonium acetate (19±6%), and ammonium formate (20±4%) ES solutions.This again suggests that the use of solution additive with high gas phase basicity promotes charge reduction, and presumably results in some degree of protein folding within the ES droplets. The reduction in Z_{avg} observed for myoglobin (pH of 2.3) in the presence of TEAF (Z_{avg} of 9.8±0.2) in comparison with ammonium formate solution (Z_{avg} of 16.4±0.1) is consistent with the hypothesis that the solution additives with high gas phase basicity can significantly reduce the protein CSD in the gas phase. The lack of heme inclusion to the protein again suggests that a refolding of apo-myoglobin to holomyoglobin is limited by the time available for protein folding in LEMS measurement.

The LEMS measurement of myoglobin prepared in solutions with pH 7.0, 2.6 and 2.3 vaporized into ES droplets containing TEAA (Figure 3.18 a, b and c) are similar to the measurements made using TEAF (Figure 3.17 a, b and c). TEAA displays enhanced charge reduction for the myoglobin prepared in solution pH of 2.6 and 2.3 in comparison with TEAF.

Laser vaporization of myoglobin prepared in a solution with pH 7.0 into the ES droplets containing TEAB revealed mainly 6+ and 5+ charge states corresponding to holomyoglobin features, (Figure 3.19 a) as compared to 8+ and 9+ for ammonium bicarbonate solution, indicating enhanced charge reduction of the folded states of the protein. The LEMS measurement of myoglobin prepared in solutions with pH of 2.6 and 2.3 vaporized into the ES droplets containing TEAB revealed monomodal CSDs peaked at 10+ (apo-myoglobin features, Figure 3.19 b and c) with Z_{avg} values of 9.8±0.2 and 10.2±0.2, respectively. The monomodal CSD suggests substantial unfolding of the protein. A reduction in Z_{avg} was observed for myoglobin prepared in solution with pH of 2.3 in the presence of TEAB (Z_{avg} of 10.0±0.2) when compared to ammonium bicarbonate (Z_{avg} of 18.6±0.1) and aqueous ES (Z_{avg} of 20.5±0.1). This is again consistent with the ordering of the gas phase basicities.

In addition to the shift in protein CSD, adduction of Na^+ and HCO_3^- ions to the protein ion was also observed for lower charge states (mainly 6+ and 5+), as seen in the inset of Figure 3.19 a-c. The enhanced adduction is due to the lower collision energy with background gas at lower charge state in comparison with higher charge states. The peak broadening due to adduct formation was significantly reduced upon increasing the collision energy to 35 eV as compared to 10 eV, suggesting the loss of an anion (HCO_3^-) and neutral ($NaHCO_3$) molecule from protein ion (Figure 3.20 d-f, and Figure 3.21 b).

3.5 Conclusions

The charge state distributions for both native and acid-denatured proteins were measured as a function of solution additives with varying gas phase basicities using laser electrospray mass spectrometry. The observation of charge-reduced ion states for acid-denatured protein upon the interaction with the charge reducing solution additives suggests at least a part of the protein population folds to some degree within the electrospray droplets. We determined that the myoglobin (holo-myoglobin, solution pH of 7.0) was laser vaporized without the loss of heme into the electrospray droplets, and that acid-denatured protein refolds in the electrospray droplets to some degree without heme reincorporation into its hydrophobic pocket. Evidence was provided for the formation of apo-myoglobin in aqueous electrospray droplets. Comparison to conventional electrospray measurements for both proteins reveals a greater fraction of low charge state distribution, suggesting that ESI enhances the unfolding of protein either in solution or in the Taylor cone of the emitter.

The use of solution additives with high gas phase basicities resulted in greater shift in the protein CSD to the lower charge states for native and acid-denatured proteins in comparison with both aqueous and conventional solvent system. This suggests that the charge reduction, which is expected to occur in the gas phase, is dominated by proton transfer processes from multiply charged protein ions to neutral amines. We note that in addition to the charge state distribution, coupling LEMS with hydrogen/deuterium exchange, ion mobility measurement, and/or electron capture dissociation would provide alternative means of investigating the gas phase protein conformation. We have investigated the reduction of 2,6-dichloroindophenol by L-ascorbic acid in a manner

similar to previous studies(22, 38), to determine the droplet lifetime in LEMS measurement. We find that the droplet lifetime is ~5 milliseconds(39) suggesting that LEMS could be used to decouple proteins and various solvent systems, prior to mixing in the electrospray droplets, to study protein folding on the millisecond timescale.

3.6 References

1. Loo, J. A.; Loo, R. R. O.; Udseth, H. R.; Edmonds, C. G.; Smith, R. D. Solvent-induced conformational changes of polypeptides probed by electrospray-ionization mass spectrometry. *Rapid Commun. Mass Spectrom.* **1991,** (5), 101-105.

2. Konermann, L.; Douglas, D. Acid-induced unfolding of cytochrome c at different methanol concentrations: electrospray ionization mass spectrometry specifically monitors changes in the tertiary structure. *Biochemistry.* **1997,** (36), 12296-12302.

3. Liu, J.; Konermann, L. Irreversible thermal denaturation of cytochrome C studied by electrospray mass spectrometry. *J. Am. Soc. Mass Spectrom.* **2009,** (20), 819-828.

4. Kharlamova, A.; DeMuth, J. C.; McLuckey, S. A. Vapor treatment of electrospray droplets: evidence for the folding of initially denatured proteins on the sub-millisecond time-scale. *J. Am. Soc. Mass Spectrom.* **2012,** (23), 88-101.

5. Shelimov, K. B.; Clemmer, D. E.; Hudgins, R. R.; Jarrold, M. F. Protein structure in vacuo: gas-phase conformations of BPTI and cytochrome c. *J. Am. Chem. Soc.* **1997,** (119), 2240-2248.

6. Wyttenbach, T.; Bowers, M. T. Structural stability from solution to the gas phase: native solution structure of ubiquitin survives analysis in a solvent-free ion mobility–mass spectrometry environment. *J. Phys. Chem. B.* **2011,** (115), 12266-12275.

7. Banerjee, S. Induction of protein conformational change inside the charged electrospray droplet. *J. Mass Spectrom.* **2013,** (48), 193-204.

8. Kharlamova, A.; Prentice, B. M.; Huang, T.-Y.; McLuckey, S. A. Electrospray droplet exposure to gaseous acids for the manipulation of protein charge state distributions. *Anal. Chem.* **2010,** (82), 7422-7429.

9. Lemaire, D.; Marie, G.; Serani, L.; Laprévote, O. Stabilization of gas-phase noncovalent macromolecular complexes in electrospray mass spectrometry using aqueous triethylammonium bicarbonate buffer. *Anal. Chem.* **2001,** (73), 1699-1706.

10. Mehmood, S.; Marcoux, J.; Hopper, J. T.; Allison, T. M.; Liko, I.; Borysik, A. J.; Robinson, C. V. Charge reduction stabilizes intact membrane protein complexes for mass spectrometry. *J. Am. Chem. Soc.* **2014,** (136), 17010-17012.

11. Brady, J. J.; Judge, E. J.; Levis, R. J. Nonresonant femtosecond laser vaporization of aqueous protein preserves folded structure. *Proc. Natl. Acad. Sci.* **2011,** (108), 12217-12222.

12. Perez, J. J.; Flanigan IV, P. M.; Karki, S.; Levis, R. J. Laser electrospray mass spectrometry minimizes ion suppression facilitating quantitative mass spectral response for multicomponent mixtures of proteins. *Anal. Chem.* **2013,** (85), 6667-6673.

13. Judge, E. J.; Brady, J. J.; Dalton, D.; Levis, R. J. Analysis of pharmaceutical compounds from glass, fabric, steel, and wood surfaces at atmospheric pressure using spatially resolved, nonresonant femtosecond laser vaporization electrospray mass spectrometry. *Anal. Chem.* **2010,** (82), 3231-3238.

14. Flanigan IV, P. M.; Brady, J. J.; Judge, E. J.; Levis, R. J. Determination of inorganic improvised explosive device signatures using laser electrospray mass spectrometry detection with offline classification. *Anal. Chem.* **2011,** (83), 7115-7122.

15. Perez, J. J.; Flanigan IV, P. M.; Brady, J. J.; Levis, R. J. Classification of smokeless powders using laser electrospray mass spectrometry and offline multivariate statistical analysis. *Anal. Chem.* **2012,** (85), 296-302.

16. Judge, E. J.; Brady, J. J.; Barbano, P. E.; Levis, R. J. Nonresonant femtosecond laser vaporization with electrospray postionization for ex vivo plant tissue typing using compressive linear classification. *Anal. Chem.* **2011,** (83), 2145-2151.

17. Flanigan, P. M.;Shi, F.; Perez, J. J.; Karki, S.; Pfeiffer, C.; Schafmeister, C.; Levis, R. J. Determination of internal energy distributions of laser electrospray mass spectrometry using thermometer ions and other biomolecules. *J. Am. Soc. Mass Spectrom.* **2014,** (25), 1572-1582.

18. Flanigan IV, P. M.; Perez, J. J.; Karki, S.; Levis, R. J. Quantitative measurements of small molecule mixtures using laser electrospray mass spectrometry. *Anal. Chem.* **2013,** (85), 3629-3637.

19. Karki, S.; Flanigan IV, P. M.; Perez, J. J.; Archer, J. J.; Levis, R. J. Increasing Protein Charge State When Using Laser Electrospray Mass Spectrometry. *J. Am. Soc. Mass Spectrom.* **2015,** (26), 706-715.

20. Loo, R. R. O.; Lakshmanan, R.; Loo, J. A. What protein charging (and supercharging) reveal about the mechanism of electrospray ionization. *J. Am. Soc. Mass Spectrom.* **2014,** (25), 1675-1693.

21. Flanigan IV, P. M.; Shi, F.; Archer, J. J.; Levis, R. J. Internal Energy Deposition for Low Energy, Femtosecond Laser Vaporization and Nanospray Post-ionization Mass Spectrometry using Thermometer Ions. *J. Am. Soc. Mass Spectrom.* **2015,** (26), 716-724.

22. Mortensen, D. N.; Williams, E. R. Investigating Protein Folding and Unfolding in Electrospray Nanodrops Upon Rapid Mixing Using Theta-Glass Emitters. *Anal. Chem.* **2014,** (87), 1281-1287.

23. Mortensen, D. N.;Williams, E. R. Ultrafast (1 μs) Mixing and Fast Protein Folding in Nanodrops Monitored by Mass Spectrometry. *J. Am. Chem. Soc.* **2016,** (138), 3453-3460.

24. Konermann, L.; Collings, B.; Douglas, D. Cytochrome c folding kinetics studied by time-resolved electrospray ionization mass spectrometry. *Biochemistry.* **1997,** (36), 5554-5559.

25. Clemmer, D. E.; Hudgins, R. R.; Jarrold, M. F. Naked protein conformations: cytochrome c in the gas phase. *J. Am. Chem. Soc.* **1995,** (117), 10141-10142.

26. Hall, Z.; Robinson, C. V. Do charge state signatures guarantee protein conformations? *J. Am. Soc. Mass Spectrom.* **2012,** (23), 1161-1168.

27. Hedges, J. B.; Vahidi, S.; Yue, X.; Konermann, L. Effects of ammonium bicarbonate on the electrospray mass spectra of proteins: evidence for bubble-induced unfolding. *Anal. Chem.* **2013,** (85), 6469-6476.

28. Cassou, C. A.; Williams, E. R. Anions in electrothermal supercharging of proteins with electrospray ionization follow a reverse Hofmeister series. *Anal. Chem.* **2014,** (86), 1640-1647.

29. Catalina, M. I.; van den Heuvel, R. H.; van Duijn, E.; Heck, A. J. Decharging of globular proteins and protein complexes in electrospray. *Chem-Eur. J.* **2005,** (11), 960-968.

30. Touboul, D.; Jecklin, M. C.; Zenobi, R. Investigation of deprotonation reactions on globular and denatured proteins at atmospheric pressure by ESSI-MS. *J. Am. Soc. Mass Spectrom.* **2008,** (19), 455-466.

31. Hogan Jr, C. J.; Loo, R. R. O.; Loo, J. A.; de la Mora, J. F. Ion mobility–mass spectrometry of phosphorylase B ions generated with supercharging reagents but in charge-reducing buffer. *Phys. Chem. Chem. Phys.* **2010,** (12), 13476-13483.

32. Cole, R. B. Some tenets pertaining to electrospray ionization mass spectrometry. *J. Mass Spectrom.* **2000,** (35), 763-772.

33. Hogan Jr, C. J.; Carroll, J. A.; Rohrs, H. W.; Biswas, P.; Gross, M. L. Combined charged residue-field emission model of macromolecular electrospray ionization. *Anal. Chem.* **2008,** (81), 369-377.

34. Kebarle, P.; Verkerk, U. H. Electrospray: from ions in solution to ions in the gas phase, what we know now. *Mass Spectrom. Rev.* **2009,** (28), 898-917.

35. Creighton, T. E., Proteins: structures and molecular properties, Macmillan, (1993).

36. Simmons, D. A.; Konermann, L. Characterization of transient protein folding intermediates during myoglobin reconstitution by time-resolved electrospray mass spectrometry with on-line isotopic pulse labeling. *Biochemistry.* **2002,** (41), 1906-1914.

37. Ballew, R.; Sabelko, J.; Gruebele, M. Direct observation of fast protein folding: the initial collapse of apomyoglobin. *Proc. Natl. Acad. Sci.* **1996,** (93), 5759-5764.

38. Lee, J. K.; Kim, S.; Nam, H. G.; Zare, R. N. Microdroplet fusion mass spectrometry for fast reaction kinetics. *Proc. Natl. Acad. Sci.* **2015,** (112), 3898-3903.

39. Karki, S.; Levis, R. J. Measurement of lifetime for laser vaporized liquid droplets coupled with electrospray and nano-spray postionization mass spectrometry. *Manuscript in preparation.* **2017.**

CHAPTER 4

DIRECT ANALYSIS OF PROTEINS FROM SOLUTIONS WITH HIGH SALT CONCENTRATION USING LASER ELECTROSPRAY MASS SPECTROMETRY

4.1 Overview

In this chapter, the detection of lysozyme, or a mixture of lysozyme, cytochrome c, and myoglobin, from solutions with varying salt concentration (0.1 mM to 250 mM NaCl) using laser electrospray mass spectrometry (LEMS) and electrospray ionization-mass spectrometry (ESI-MS) is presented. Protonated protein peaks were observed up to a concentration of 250 mM NaCl in the case of LEMS. In the case of ESI-MS, a protein solution with salt concentration >0.5 mM resulted in predominantly salt-adducted features, with suppression of the protonated protein ions. The average sodium adducts ($< n >$) bound to the 7+ charge state of lysozyme for LEMS measurements from salt concentrations of 2.5, 25, 50, and 100 mM NaCl were 1.71, 5.23, 5.26, and 5.11, respectively. The conventional electrospray measurements for lysozyme solution containing salt concentrations of 0.1, 1, 2, and 5 mM NaCl resulted in $< n >$ of 2.65, 6.44, 7.57, and 8.48, respectively. LEMS displayed an approximately two order of magnitude higher salt tolerance in comparison with conventional ESI-MS. A mechanism for high salt tolerance observed for LEMS measurements in comparison with ESI is presented.

4.2 Introduction

The analysis of biomolecules using electrospray ionization-mass spectrometry (ESI-MS) is often hindered by matrix effects due to the presence of phosphate buffers, urea, or inorganic salts(1, 2). ESI-MS measurements of proteins in the presence of sodium chloride (NaCl) reveal extensive sodium ion adduction even for a low millimolar concentration(3). The presence of NaCl also results in a decrease in both the stability of the electrospray and the yield of protonated ions(4). The adduction of sodium ions to protein molecules distributes the signal over multiple mass-to-charge (*m/z*) peaks, reducing the signal-to-noise ratio of each protein feature and broadening the mass spectral peaks, resulting in a decrease in accuracy for mass measurement.

Since salt is ubiquitous in many biological samples, several strategies have been developed to desalt biomolecules prior to ESI-MS analysis including nanoparticle-based micro-extraction(5), microdialysis(6), liquid chromatography(7), and ion exchange chromatography(8, 9). However, removal of salts can affect the structure of protein complexes. For example, a sigma activator protein (NtrC4) from *Aquifex aeolicus* requires millimolar concentrations of Mg^{2+}, BeF^{3-}, and adenosine 5'-diphosphate sodium salt (ADP) to form an active hexamer(10, 11). Desalting processes that require multiple buffer exchange steps will denature the hexamer and may also produce spurious signal in the ESI analysis due to inefficient removal of detergents(12).

Decoupling the sampling and electrospray ionization processes has enabled analysis of analytes from samples containing high salt concentrations. Fused-droplet electrospray ionization mass spectrometry (FD-ESI-MS) involves ultrasonic nebulization of the sample solution to produce a fine aerosol which is then combined with electrospray

generated charged droplets(3). Although this method showed a significantly higher salt tolerance in comparison with conventional electrospray (1.70 M versus 0.17 M NaCl), interaction of protein molecules with electrosprayed methanol droplets containing 1% acetic acid denatures protein and shifts the charge state distribution (CSD) to higher charge in comparison with native state measurements. Probe electrospray ionization (PESI) uses a wire as both the sampling probe and electrospray emitter, and has been used to detect biomolecules from solutions with high-salt concentration.(1) The analysis of myoglobin using PESI displayed a salt tolerance, or ability to detect protein without ion suppression, of up to 250 mM in comparison with nano-electrospray ionization (nano-ESI) which has a salt tolerance of 50 mM. The high salt tolerance for PESI and nano-ESI is likely due to the formation of higher charge states given the fact that sodium ion adduction occurs mostly for low charge states(4, 13, 14). Selective sampling of analytes rather than salt from a solution has been proposed to enhance detection in the PESI experiment in comparison with nano-ESI where the entire solution within the capillary is subjected to the nanospray process resulting in analyte signal suppression given the higher salt concentration(1). The investigation of drug mixtures (cocaine and diacetylmorphine) using desorption electrospray ionization (DESI) showed higher salt tolerance in comparison with ESI(15). The salt tolerance in DESI was investigated by changing the sample substrate such as paper, polytetrafluoroethylene (PTFE), and a variety of coated glasses. The salt tolerance was dependent upon the surface being used and PTFE was the optimal substrate for reducing ion suppression effects at higher salt concentration. A raw urine sample spiked with atrazine and 1,3,5-trinitroperhydro-1,3,5-

triazine (RDX) was successfully examined using extractive electrospray ionization (EESI), eliminating clean-up steps used to remove the matrix effects(16). The stable signal intensity in EESI during salt-rich biological sample analysis was attributed to the difference in surface partitioning of polar and non-polar analytes. The non-polar analytes tend to compete for the surface while the polar analytes and salts are stabilized by increased solvation in the droplet interior.

The use of laser electrospray mass spectrometry (LEMS) has enabled the quantitative analysis of complex mixtures without sample pre-processing at atmospheric pressure(17). LEMS couples nonresonant femtosecond (fs) laser vaporization (10^{13} W/cm^2) with an electrospray ionization source for postionization. LEMS analyses have been performed on a variety of samples including proteins(18-20), pharmaceuticals(21), explosives(22, 23), plant and animal tissues(24-26). The successful detection of 1,2-dihexanoyl-sn-glycero-3-phosphocoline (DHPC) spiked into whole blood sample and the detection of lipids and proteins from reduced-fat milk sample demonstrate that LEMS is capable of detecting anlaytes from complex mixtures with no pre-processing(18). In addition, LEMS measurements on small molecule mixtures(27) and multicomponent proteins mixtures(20) have shown that LEMS enables quantitative measurements up to ~ 2.5 orders of magnitude and over 4 orders of magnitude higher in concentration, respectively, in comparison with conventional electrospray where quantitative measurement of mixtures is not possible. The nonequilibrium partitioning of analyte on the surface of the charged droplet is likely responsible for the quantitative capability(20, 27). This suggests that LEMS may be utilized to significantly reduce ion suppression

effects in comparison with conventional ESI analysis, in particular for biomolecules from solution containing high salt concentration because the salt will partition into the droplet interior while the protein resides on the surface where excess charge resides.

In this study, the mass spectral features of either a single protein (lysozyme) or a mixture of the proteins lysozyme, cytochrome c, and myoglobin as a function of salt concentration are compared using LEMS and ESI-MS. The amount of protonated protein is measured as a function of salt concentration for both LEMS and ESI and the average number of sodium adducts (< n>) bound to the 7+ charge state of lysozyme is calculated. The ability to identify protein components in a mixture using LEMS and ESI is compared as a function of salt concentration. Finally a mechanism is presented for reduced salt adduction in the LEMS measurement in comparison with ESI.

4.3 Experimental Section

4.3.1 Sample Preparation

Lysozyme, cytochrome c, myoglobin, and ammonium acetate (Sigma Aldrich, St. Louis, MO) were prepared in HPLC grade water (Fisher Scientific, Pittsburgh, PA) to yield the final concentration of 1.0 x 10^{-3} M. A 1.0 M stock solution of sodium chloride was prepared in HPLC grade water (Fisher Scientific, Pittsburgh, PA). For ESI measurements, an aliquot of the stock solution (single protein or protein mixtures) was diluted into 10 mM aqueous ammonium acetate to yield a final protein concentration of 1.0 x 10^{-5} M with the salt concentration ranging from 0.1 mM to 5.0 mM. For LEMS measurements, an aliquot of the stock solution (either individual or the protein mixtures)

was diluted into water to yield a final protein concentration of 2.0 x 10^{-4} M with the salt concentration ranging from 2.5 mM to 250 mM. A 10 μL aliquot of the diluted protein solution was spotted onto a stainless steel plate and then subjected to laser vaporization into the electrospray (ES) charged droplet stream consisting of aqueous ammonium acetate.

4.3.2 Laser Vaporization and Ionization Apparatus

A Ti:sapphire laser oscillator (KM Laboratories, Inc., Boulder, CO) seeded a regenerative amplifier (Coherent, Inc., Santa Clara, CA) that delivered 75 fs, 0.6 mJ laser pulses centered at 800 nm. The laser, operated at 10 Hz to couple with the ES ion source, was focused to a spot size of ~250 μm in diameter with an incident angle of 45^{o} with respect to the sample using a 16.9 cm focal length lens, with an approximate intensity of 1 x 10^{13} W/cm^{2}. The steel sample plate was biased to -2.0 kV to compensate for the distortion of electric field between the capillary inlet and the needle caused by the sample stage. Aqueous protein sample (10 μL) deposited onto a steel substrate was vaporized by the laser pulse allowing for capture and ionization by an ES plume travelling perpendicular to the vaporized material.

4.3.3 Mass Spectrometry and data analysis

The laser electrospray mass spectrometer used in this experiment has been described previously(28). The nonresonant femtosecond laser pulse transfers the analyte into the gas phase for capture and ionization in an ES plume at atmospheric pressure. The flow rate for ES solvent was set at 2 μL/min by a syringe pump (Harvard Apparatus,

Holliston, MA). The ESI needle was 6.4 mm above and parallel to the sample stage, and was approximately 6.4 mm in front of the capillary entrance. The ES needle was maintained at ground while the inlet capillary was biased to -4.5 kV to operate in positive ion mode. The postionized analytes were dried before entering the inlet capillary by countercurrent nitrogen gas at 200 °C flowing at 4 L/min. The charged sample was mass analyzed using a microTOF-Q II mass spectrometer (Bruker Daltonics, Billerica, MA).

4.3.4 Safety Considerations

Appropriate laser eye protection was worn by all lab personnel.

4.4 Results and Discussion

4.4.1. Detection of protein/protein mixtures from solutions with varying salt concentration

The LEMS and ESI measurements for lysozyme are shown in Figure 4.1 and Figure 4.2 for salt concentrations ranging from 0 to 100 mM and 0 to 5 mM, respectively. The LEMS measurement for lysozyme vaporized without NaCl, shown in Figure 4.1 a, reveals a narrow range of low charge states ranging from 6+ to 9+. The predominance of the 8+ charge state in Figure 4.1 b-e indicates that the native state of lysozyme was preserved when vaporized from a solution with salt concentration up to 100 mM. Salt adduction to the protein ions for LEMS increases with decreasing charge. The 9+ feature reveals no adduction in any of the spectra, minimal adduction in 8+ and adduction in the 7+ through 4+ species, Figure 4.1 b-e (also shown in Figure 4.3 c-e, measurements taken

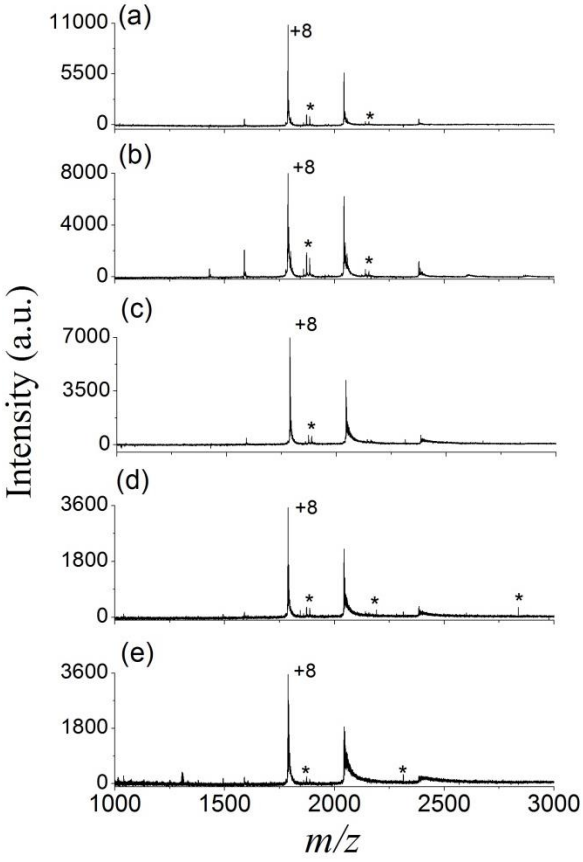

Figure 4.1. Mass spectra representing laser induced vaporization of 200 μM lysozyme with (a), no salt; (b), 2.5 mM NaCl; (c), 25 mM NaCl; (d), 50 mM NaCl; and (e), 100 mM NaCl; into the ES of 10 mM aqueous ammonium acetate. The measurements were performed at collision potential of 15 eV. A feature with an asterisk (*) represents solvent.

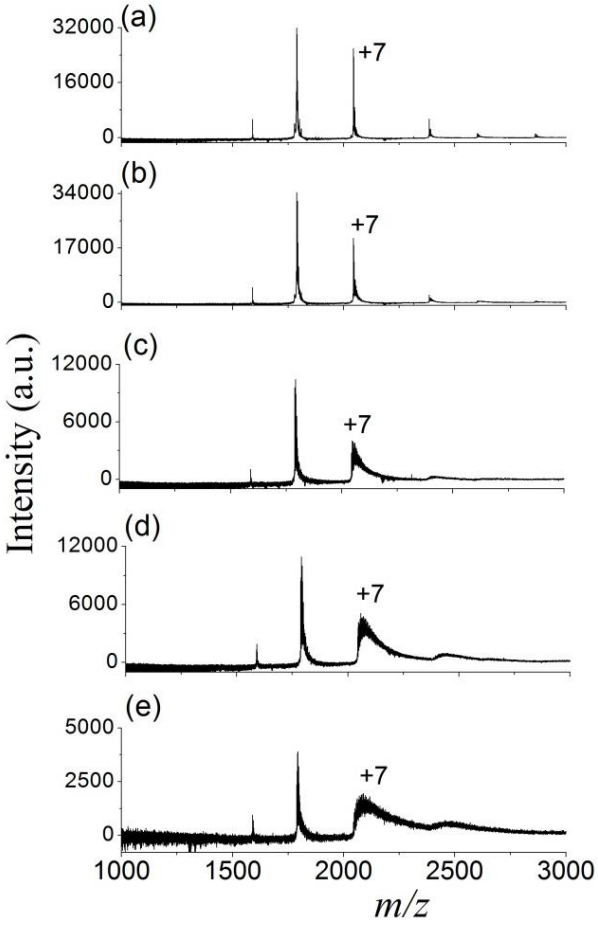

Figure 4.2. Electrospray mass spectra of 10 μM lysozyme prepared in 10 mM aqueous ammonium acetate with (a), no salt; (b), 0.1 mM NaCl; (c), 1 mM NaCl; (d), 2 mM NaCl; and (e) 5 mM NaCl. The measurements were performed at collision potential of 15 eV.

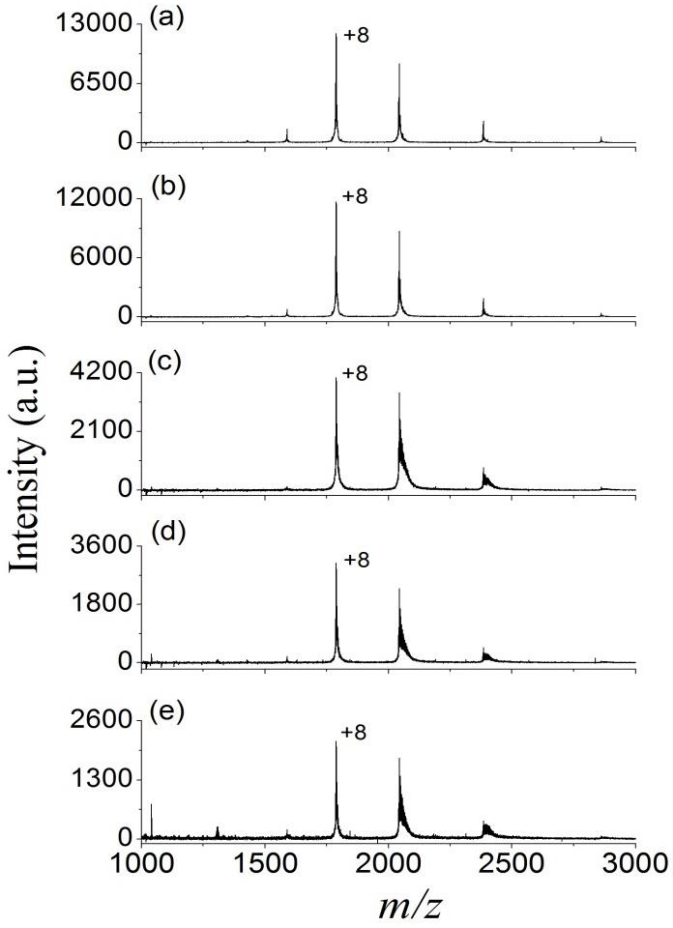

Figure 4.3. Mass spectra representing laser induced vaporization of 200 μM lysozyme with (a), no salt; (b), 2.5 mM NaCl; (c), 25 mM NaCl; (d), 50 mM NaCl; and (e) 100 mM NaCl into the ES of 10 mM aqueous ammonium acetate. The measurements were performed at collision potential of 70 eV.

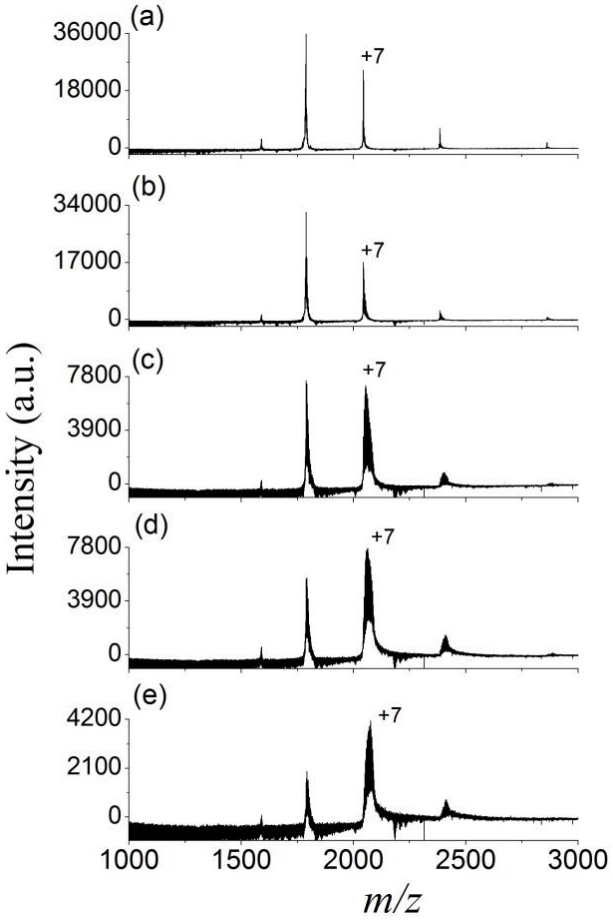

Figure 4.4. Electrospray mass spectra of 10 μM lysozyme prepared in 10 mM aqueous ammonium acetate with (a), no salt; (b), 0.1 mM NaCl; (c), 1 mM NaCl; (d), 2 mM NaCl; and (e) 5 mM NaCl. The measurements were performed at collision potential of 70 eV.

at collision potential of 70 eV). It has been proposed that the salt adduction to lower charge (folded) states is due to the increased salt concentration within the ES droplet during desolvation process in the charge residue mechanism(4). The increasing salt concentration facilitates non-specific pairing of Na^+ and Cl^- with the protein ions. Sodium adducts are evident at higher collision potential (~70 V) while a lower potential of ~5 V results in a series of *n*(Na - H) and *m*(Cl + H) peaks in the mass spectrum. In the case of higher charge states, Konermann has proposed that the unfolded protein resides at the surface of the droplet, enabling charge ejection during the desolvation process when the salt concentration is lower(4). The increase in local kinetic energy for the 8+ charge state in comparison with the 7+ and 6+ charge states (for a given collision potential) can remove salt from protein molecules resulting in the lower Na^+ adduction for 8+ charge state of lysozyme in comparison with 7+ and 6+ charge state.

The ESI-MS measurements for lysozyme in aqueous ammonium acetate solution with NaCl concentrations ranging from 0 to 5 mM are shown in Figure 4.2 a-e. The ESI mass spectrum of lysozyme in ammonium acetate, without NaCl, reveals a narrow range of low charge states ranging from 6+ to 9+ in Figure 4.2 a. The spectra corresponding to ESI measurements in the presence of salt, Figure 4.2 b-e, again shows that increasing salt adduction occurs for the 8+, 7+, and 6+ charge states with decreasing charge. In the ESI measurement, the adduction is significantly enhanced in comparison with LEMS for similar concentrations of salt, e.g. Figure 4.1 b and Figure 4.2 d. Peak broadening due to sodium ion adduction to the 6+ and 7+ charge states for salt concentration of ≥1 mM makes the detection of protonated lysozyme ($[L+7H]^{7+}$ and $[L+6H]^{6+}$) challenging. In

particular, peak broadening limited the detection of 6+ charge state of lysozyme for salt concentration of ≥1 mM.

The LEMS and ESI measurements for an equimolar mixture of lysozyme, cytochrome c, and myoglobin in salt concentration ranging from 0 to 250 mM are shown in Figure 4.5 and Figure 4.6. The LEMS measurement of protein mixtures without NaCl vaporized into an ES solvent consisting of aqueous ammonium acetate, shown in Figure 4.5 a, reveals a narrow range of low charge states ranging from 7+ to 10+ for lysozyme, 6+ and 8+ for cytochrome c, and 7+ to 9+ for myoglobin, respectively. The CSDs of lysozyme, cytochrome c, and myoglobin vaporized from concentrations of NaCl ranging from 75 to 250 mM (Figure 4.5 b-d) are similar to the 0 mM salt solution and correspond to the folded protein charge state distribution. This suggests that the native states of the proteins were preserved when vaporized from solutions with high salt concentration. The majority of salt adduction to the protein mixture occurred for the 6+, 7+ and 8+ charge states of lysozyme, for the 6+, 7+ and 8+ charge states of cytochrome c, and for the 7+, 8+, and 9+ charge states of myoglobin, see Figure 4.5 b-d (also shown in Figure 4.7 b-d). The majority of salt adduction occurred at 6+ and 7+ charge states in the case of lysozyme during single protein analysis, see Figure 4.1 b-e (also shown in Figure 4.3 b-e).

ESI measurements were performed for equimolar mixtures of lysozyme, cytochrome c, and myoglobin (10 μM of each) from aqueous ammonium acetate solution containing NaCl concentrations ranging from 0 to 5 mM, as shown in Figure 4.6 a-d. The

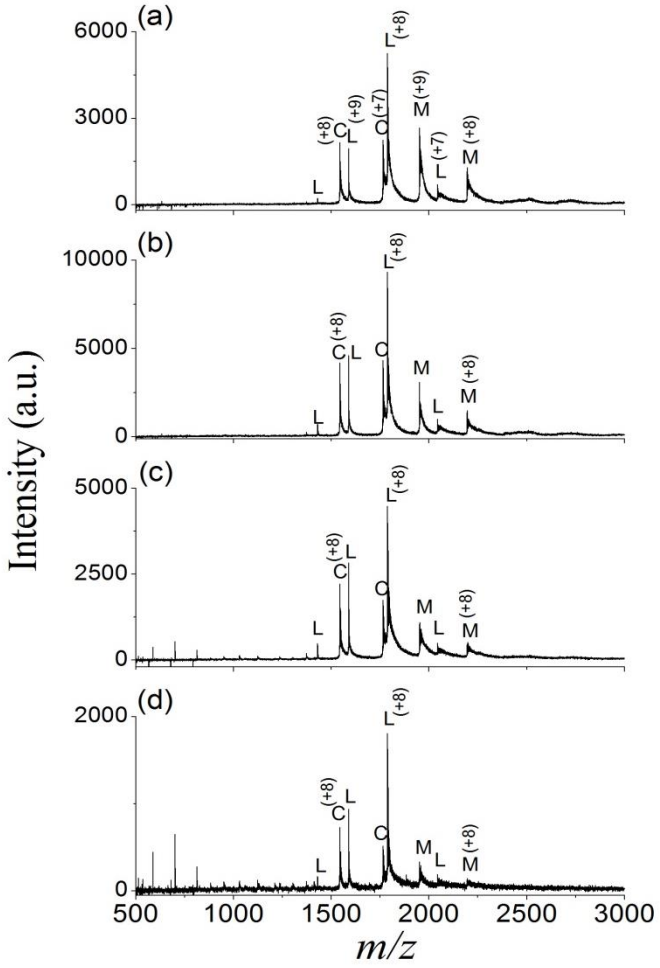

Figure 4.5. Mass spectra representing laser induced vaporization of 200 µM protein mixtures (lysozyme (L), cytochrome c (C), and myoglobin (M)) with (a), no salt; (b), 75 mM; (c), 125 mM; and (d), 250 mM NaCl; into the ES of 10 mM aqueous ammonium acetate. The measurements were performed at collision potential of 15 eV.

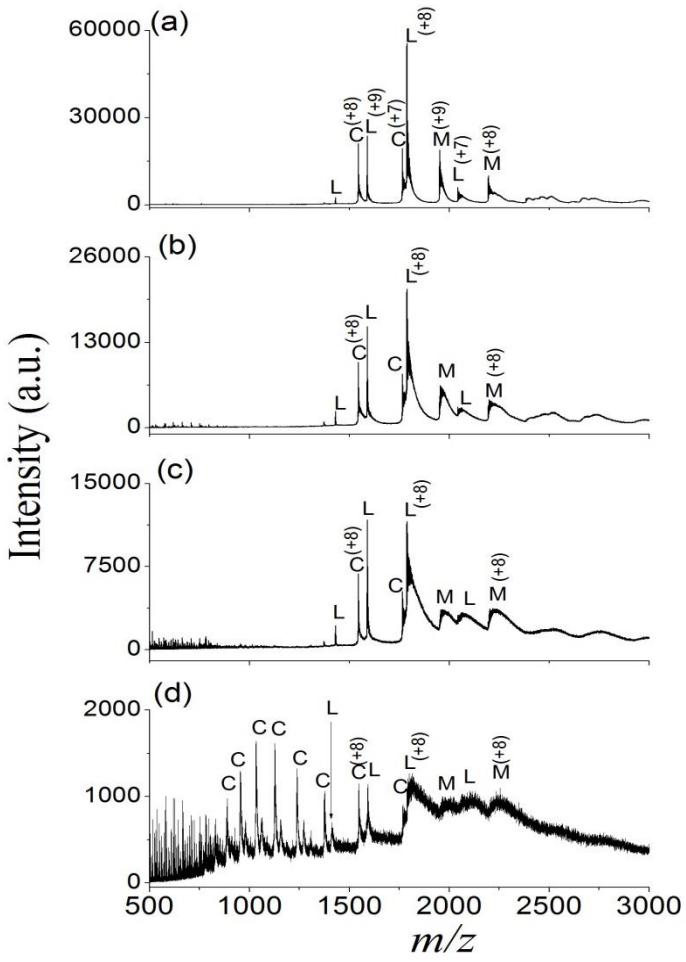

Figure 4.6. Electrospray mass spectra of 10 μM protein mixtures (lysozyme (L), cytochrome c (C), and myoglobin (M)) prepared in 10 mM aqueous ammonium acetate with (a), no salt; (b), 0.5 mM NaCl; (c), 2 mM NaCl; and (d), 5 mM NaCl. The measurements were performed at collision potential of 15 eV.

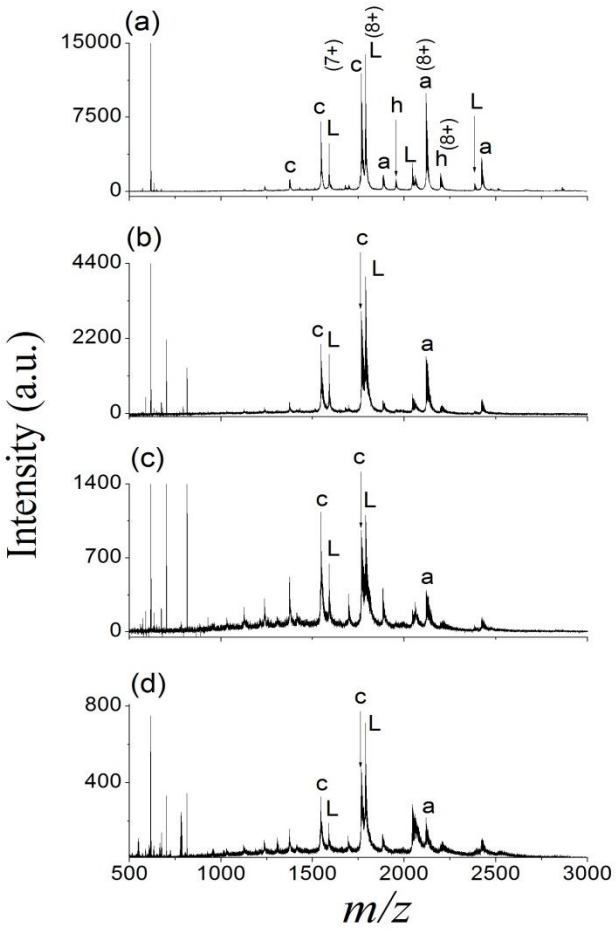

Figure 4.7. Mass spectra representing laser induced vaporization of 200 μM protein mixtures (lysozyme(L), cytochrome c (C), and myoglobin (h represents holomyoglobin, and a represents apomyoglobin)) with (a), no salt; (b), 75 mM NaCl; (c), 125 mM NaCl; and (d) 250 mM NaCl; into the ES of 10 mM aqueous ammonium acetate. The measurements were performed at collision potential of 70 eV.

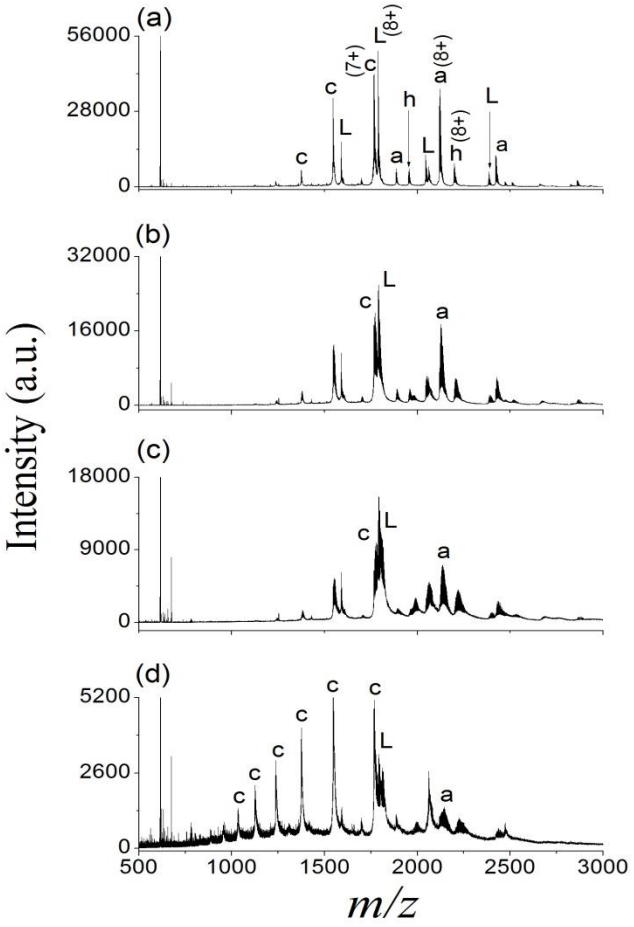

Figure 4.8. Electrospray mass spectra of 10 μM protein mixtures (lysozyme(L), cytochrome c (C), and myoglobin (h represents holomyoglobin, and a represents apomyoglobin)) prepared in 10 mM aqueous ammonium acetate with (a), no salt; (b), 0.5 mM NaCl; (c), 2 mM NaCl; ,and (d) 5 mM NaCl. The measurements were performed at collision potential of 70 eV.

ESI mass spectra of protein mixtures with no added NaCl revealed charge states ranging from 7+ to 10+ for lysozyme, 7+ and 8+ for cytochrome c, and 8+ and 9+ for myoglobin, as shown in Figure 4.6 a. The ESI measurements for salt concentrations of 0.5 and 2 mM NaCl, Figure 4.6 b and 4.6 c, show significant salt adduction for the 7+ and 8+ charge states of lysozyme, the 7+ and 8+ charge states of cytochrome c, and the 8+ and 9+ charge states for myoglobin. The ESI measurement of protein mixtures at salt concentration of 5 mM resulted in charge states ranging from 7+ to 14+ for cytochrome c and suppressed the detection of the lower charge states of myoglobin (8+ and 9+ charge states) and lysozyme (7+ and 8+ charge states) by significant salt adduction, as shown in Figure 4.6 d. The observation of unfolded charge state distribution for cytochrome c is likely due to the increase in electrospray droplet temperature at higher salt concentration due to the non-volatile nature of the salt. The formation of higher charge states were also observed in a previous experiment when the electrospray solvent contained higher salt concentration(1). In that study, the addition of 50 mM NaCl into the 10 μM myoglobin solution resulted in a CSD ranging from 10+ to 22+ (peaked at 12+ and 20+), while the lower salt concentration (5 mM NaCl) resulted in a CSD ranging from 7+ to 18+ (peaked at 11+). Identification of individual proteins from multi-component mixtures is difficult using ESI when salt is present in the sample solution at concentration > 5mM due to ion suppression effects (29) and spectral congestion (30) arising from overlapping features. Direct analysis of protein mixtures using ESI in the presence of inorganic salts is complicated because of the peak broadening effect due to adduction. This is not the case for LEMS where salt concentrations up to 250 mM do not result in protein structural

change or significant adduction and thus, the identification of individual protein from the multi-component mixture is possible.

4.4.2 Salt adduction to proteins: LEMS versus ESI-MS

The adduction of sodium ion to protein was compared for LEMS and ESI-MS measurements to provide insight into the ionization mechanisms of each experiment. Sodium adduction to the protein molecule can be expressed using equation 1(4),

$$[M + zH^+ + n(Na^+ - H^+) + m(Cl^- + H^+)]^{z+} + 70 \text{ eV CID} \rightarrow [M + (z-n)H^+ + nNa^+]^{z+} + m\text{HCl} \quad (1)$$

where M is the protein molecule, z is the number of protons (H^+), n and m are the number of Na^+ and Cl^- adducts, respectively, *z* is the charge state of the protein, and z+ is the overall charge on the protein molecule. At lower collision potential, 15 eV in this measurement resulted in a series of $n(Na^+ - H^+)$ and $m(Cl^- + H^+)$ features that complicate the mass spectra(4). Increasing the collision potential to 70 eV resulted in the complete loss of HCl and Na-adducted protein ions are predominately formed as shown in Figure 4.9 – 4.14. The removal of HCl is mainly attributed to an in-source reaction(31, 32) where protein ions are subjected to collision-induced dissociation (CID). The increase in collision potential also resulted in the loss of H_2O from lysozyme as shown in Figure 4.15.

To compare the Na^+ ion adduction as a function of salt concentration for both LEMS and ESI-MS measurements, we focus on the 7+ charge state of lysozyme as shown in Figure 4.9. LEMS analysis of lysozyme with salt concentration of 25 mM NaCl revealed

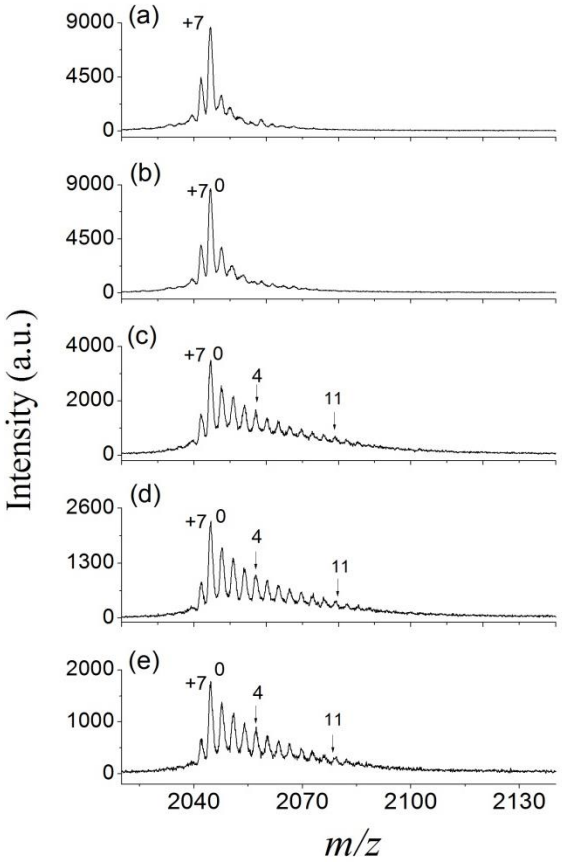

Figure 4.9. High resolution LEMS mass spectra of 200 µM lysozyme $[L+7H]^{7+}$ with (a), no salt; (b), 2.5 mM NaCl; (c), 25 mM NaCl; (d), 50 mM NaCl; and (e), 100 mM NaCl; into the ES of 10 mM aqueous ammonium acetate. The measurements were performed at collision potential of 70 eV. Sodium adducts are indicated as n = 0, 1, 2, etc.

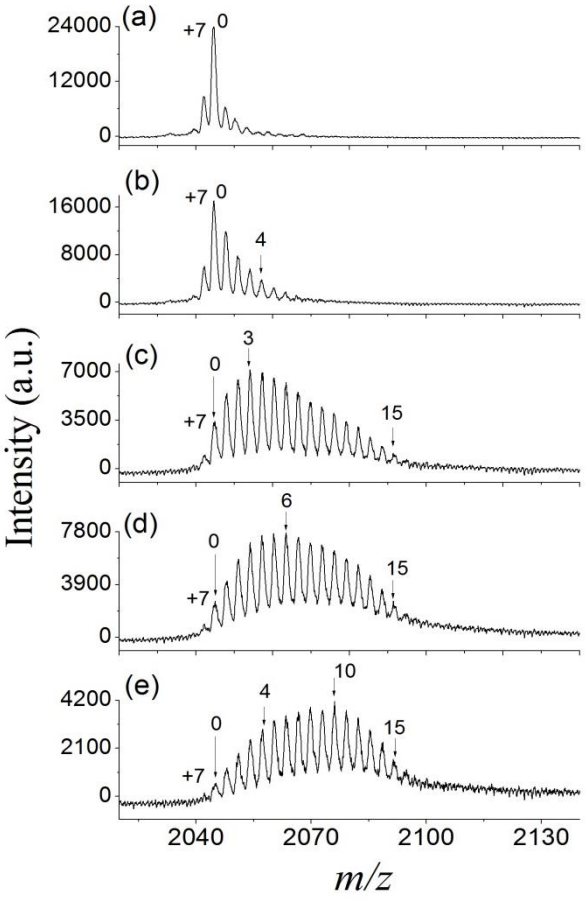

Figure 4.10. High resolution electrospray mass spectra of 10 µM lysozyme $[L+7H^+]^{7+}$ prepared in 10 mM aqueous ammonium acetate with (a), no salt; (b), 0.1 mM NaCl; (c), 1 mM NaCl; (d), 2 mM NaCl; and (e) 5 mM NaCl. The measurements were performed at collision potential of 70 eV. Sodium adducts are indicated as n = 0, 1, 2, etc.

salt adducts ranging from 1 to 13, Figure 4.9 c. The dominant feature in the mass spectra collected with a CID potential of 70 eV is the protonated peak of lysozyme $[L+7H]^{7+}$. Conversely, ESI analysis of lysozyme with 1 mM NaCl resulted in the Na=3 adduct dominating with sodium-adducted protein peaks ranging from 1 to 16, Figure 4.10 c. The sodium adducts resulted in peak broadening for ESI-MS measurements, Figure 4.2 c-e. The average number of sodium ions adducts $< n >$ can be calculated(4) as follows:

$$< n > = \frac{\sum_{n=0}^{N} (n * I_n)}{\sum_{n=0}^{N} I_n} \qquad (2)$$

where I_n is the peak intensity of the Na^+ adducts, and N is the maximum number of Na^+ observed for each charge state. The average number of sodium ions bound to the 7+ charge state of lysozyme ($< n >$) for the LEMS measurement are 1.71, 5.23, 5.26, and 5.11 for the salt concentration of 2.5 mM, 25 mM, 50 mM, and 100 mM NaCl, respectively. The Na^+ adduction did not increase between 25 mM and 100 mM NaCl concentration in the LEMS analysis. The average number of sodium ions bound to the 7+ charge state of lysozyme for the ESI measurement for salt concentrations of 0.1 mM, 1 mM, 2 mM, and 5 mM NaCl are 2.65, 6.44, 7.57, and 8.48, respectively. Conventional electrospray measurements showed increasing salt adduction with increasing salt concentration with a corresponding decrease in intensity for the protonated peak of the protein. The measurements revealed significantly reduced sodium adduction for LEMS measurements in comparison with ESI-MS for all charge states.

For the mass spectral analysis of multicomponent protein mixtures, the collision potential was increased to 70 eV to eliminate HCl to form predominately Na-adducted

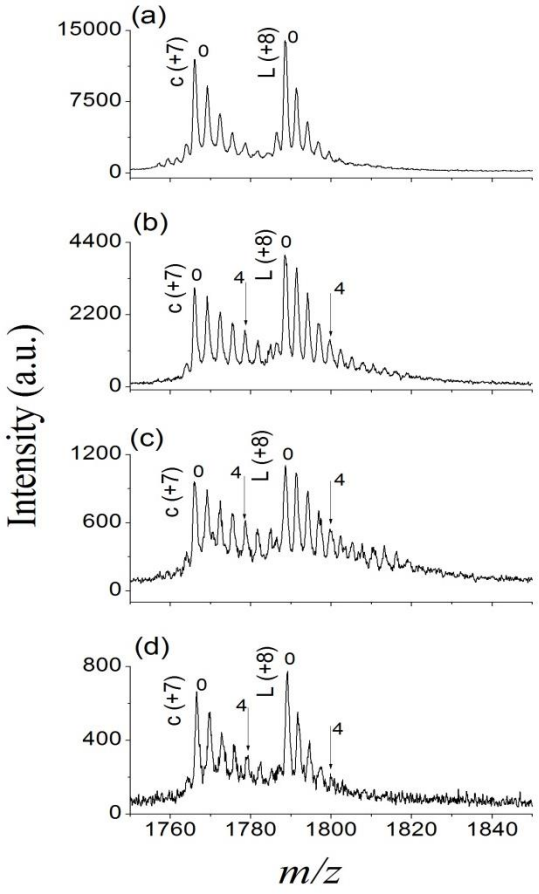

Figure 4.11. High resolution LEMS mass spectra of 200 μM protein mixtures (cytochrome c $[C+7H]^{7+}$, and lysozyme $[L+8H]^{8+}$) with (a), no salt; (b), 75 mM NaCl; (c), 125 mM NaCl; and (d), 250 mM NaCl; into the ES of 10 mM aqueous ammonium acetate. The measurements were performed at collision potential of 70 eV. Sodium adducts are indicated as n=0, 1, 2, etc.

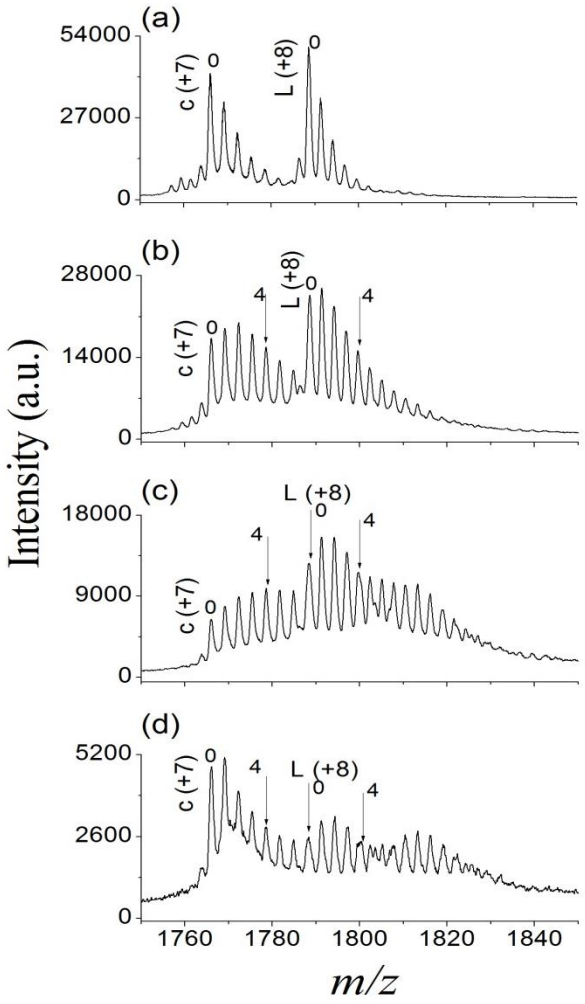

Figure 4.12. High resolution electrospray mass spectra of 10 μM protein mixtures (cytochrome c $[C+7H]^{7+}$, and lysozyme $[L+8H]^{8+}$) prepared in 10 mM aqueous ammonium acetate with (a), no salt; (b), 0.5 mM NaCl; (c), 2 mM NaCl; (d), 5 mM NaCl. The measurements were performed at collision potential of 70 eV. Sodium adducts are indicated as n=0, 1, 2, etc.

protein ions(4). To compare the sodium adduction to the protein molecule for LEMS and ESI-MS measurements, 7+ charge state of cytochrome c (*m/z* 1766.5), 8+ charge state of lysozyme (*m/z* 1789.1), and 8+ charge state of myoglobin (*m/z* 2122.4) were chosen. Salt adduction to the 7+ charge state of cytochrome c overlaps with the protonated ($(L+8H)^{8+}$) lysozyme peak. LEMS measurements revealed well-resolved, protonated features for cytochrome c ($(C+7H)^{7+}$) and lysozyme ($(L+8H)^{8+}$) for salt concentration of 250 mM NaCl, as shown in Figure 4.11 d. This suggests minimal adduction/overlap and limited ion suppression of the protonated protein ions even in the presence of high salt concentration using laser vaporization to transfer sample into the ES droplets. Conversely, in ESI-MS measurements, the mass spectra revealed congested features and suppression of protonated ions ($(C+7H)^{7+}$ and $(L+8H)^{8+}$) for NaCl concentrations ranging from 0.5 to 5 mM, as shown in Figure 4.12 b, c, and d. The ESI measurements for cytochrome c and lysozyme with 0.5 mM NaCl revealed that the Na=2 and Na=1 adducts were the dominant features with sodium adducts ranging from 1 to 6 and 1 to 11, respectively, Figure 4.12 b. At a salt concentration of 5 mM, unresolvable spectral features for both cytochrome c and lysozyme are observed due to excessive salt adduction. Adducted protein features were observed for 0 mM NaCl in both LEMS and ESI measurements of cytochrome c and lysozyme, presumably due to impurities in the solvents, Figure 4.11 a and Figure 4.12 a.

The LEMS measurement for the 8+ charge state of myoglobin revealed salt adducts ranging from 1 to 14 for salt concentration of 75 mM NaCl, Figure 4.13 b. The dominant feature in the mass spectra is the protonated peak of apo-myoglobin $[M+8H]^{8+}$.

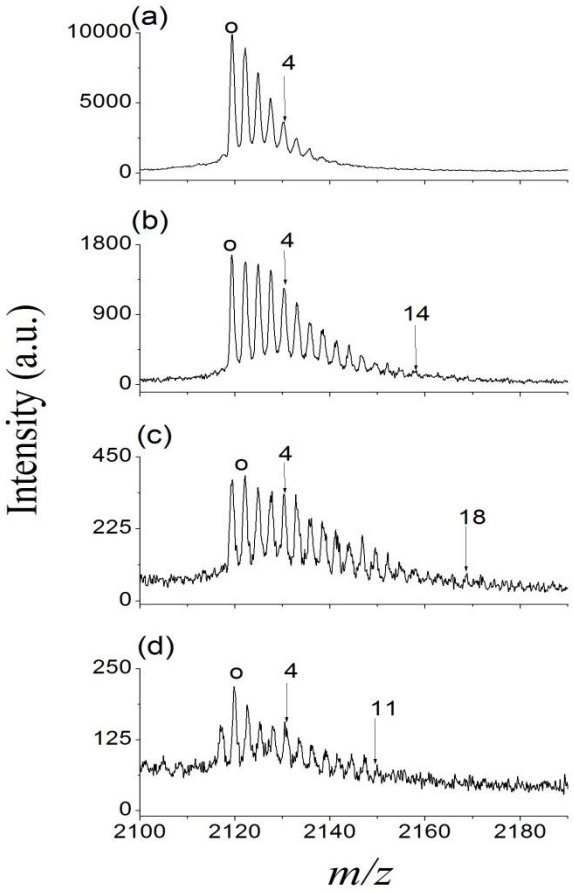

Figure 4.13. High resolution LEMS mass spectra of 200 μM apo-myoglobin $[M+8H]^{8+}$ with (a), no salt; (b), 75 mM NaCl; (c), 125 mM NaCl; and (d), 250 mM NaCl; into the ES of 10 mM aqueous ammonium acetate. The measurements were performed at collision potential of 70 eV. Sodium adducts are indicated as n = 0, 1, 2, etc.

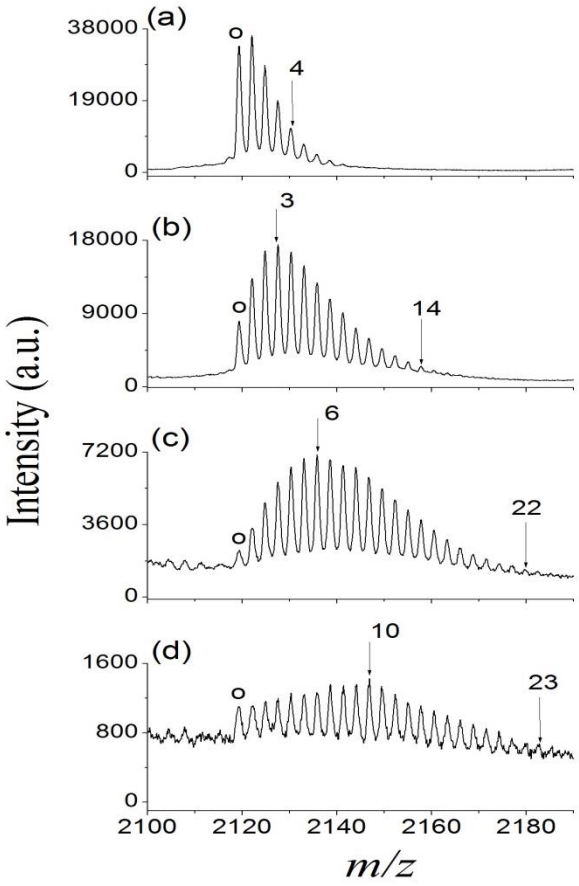

Figure 4.14. High resolution electrospray mass spectra of 10 μM apo-myoglobin $[M+8H]^{8+}$ prepared in 10 mM aqueous ammonium acetate with (a), no salt; (b), 0.5 mM NaCl; (c), 2 mM NaCl; and (d), 5 mM NaCl. The measurements were performed at collision potential of 70 eV. Sodium adducts are indicated as n = 0, 1, 2, etc.

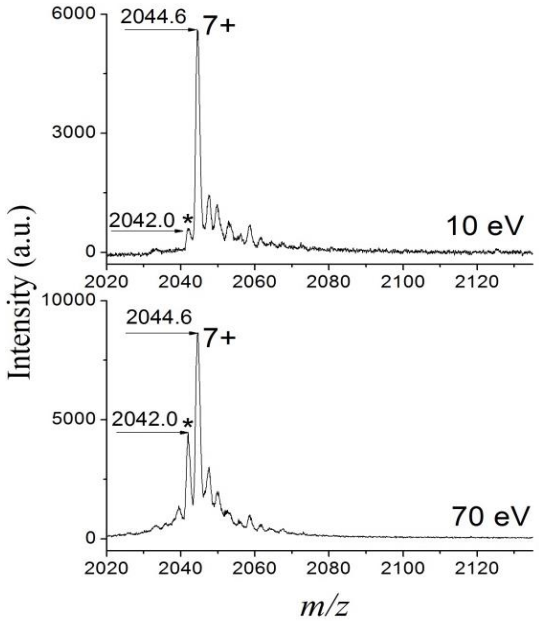

Figure 4.15. High resolution LEMS mass spectra of 200 μM lysozyme $[L+7H]^{7+}$ into the ES of 10 mM aqueous ammonium acetate. Deconvoluted mass difference between *m/z* of 2044.6 and 2042.0 is 18.2 amu, which corresponds to the loss of water molecule due to the increase in collision potential.

The formation of apo-myoglobin is due to collision-induced unfolding of myoglobin upon increasing the collision energy to 70 eV. The ESI analysis of myoglobin with 0.5 mM NaCl resulted in the Na=3 adduct being the largest feature with sodium adduct features ranging from 1 to 15, Figure 4.14 b. Again, the LEMS experiment enabled measurements of protein molecules for samples with higher salt concentration because of reduced adduct formation.

These measurements suggest that in the LEMS experiments, the Na^+ ions are somehow excluded from interacting with the protein molecules. The reduced Na^+ ion adduction in LEMS measurements in comparison with ESI may be due to the non-equilibrium nature of laser vaporized proteins interacting with the ES droplets. We have previously proposed (20, 27, 33) that the partitioning of analytes into the ES droplets is limited by the time that laser vaporized analytes spend on the droplet surface prior to entering into the MS inlet capillary. The time for interaction between the vaporized protein and the charged droplet is estimated to be <100 ms(33) and this time will therefore dictate the partitioning of anlaytes based on their respective sizes and solution enthalpy. Considering a simple diffusion process, the mixing time, t, of two analytes depends upon their diffusion coefficient (D) and the distance separating the diffusing solutes (d), where $t=d^2/6D$. Given the fact that the diffusion coefficient of analytes depend on their size and shape, we anticipate that Na^+ and Cl^- will diffuse into the interior of the droplet much more quickly than the protein in the LEMS process, thus limiting the opportunity for the chemistry described by reaction 2 if the droplet lifetime is short compared to the protein diffusion time. The diffusion constant for Na^+ is 1.3×10^{-7}

m^2/s and assuming d = 1 micron the diffusion time is $(1 \times 10^{-6}\ m)^2 / 6 \times 1.6\ 10^{-9}\ m^2/s$ = 104.2 μs. This time is short compared to the lifetime of the droplet ~10 ms, and thus the salt ions can partition into the interior of the droplet. The diffusion constant for hemoglobin is $6.9 \times 10^{-11}\ m^2/s$ suggesting a 23X longer diffusion time. The proteins are also much more hydrophobic than salt ions and thus will tend to remain on the surface of the charged droplet(34, 35). This results in a lower salt concentration on the surface of the newly formed electrospray droplet from which a gaseous protein ion is released. This also results in a higher concentration of protein on the surface of the electrospray droplet where the charge resides. Thus the nonequilibrium nature of the partitioning of salt and protein between droplet surface and interior will reduce adduction in the LEMS measurement. A previous study investigating the ionization mechanism of proteins in ESI-MS revealed a completely different salt adduction pattern for folded and unfolded proteins(4). The folded protein revealed higher salt adduction, which is in agreement with charge residue model (CRM) where the non-specific interaction between salt and protein increases as the solvent evaporates. The unfolded protein however revealed minimal to no salt adduction which is attributed to the difference in ionization mechanism for folded and unfolded proteins in ESI. Unfolded proteins are likely expelled from the ES droplet via chain ejection model (CEM)(36) prior to the increase in salt concentration within the ES droplets resulting in minimal to no salt adduction for higher charge states. The reduced salt adduction for proteins in LEMS measurement suggests that protein ionization in LEMS likely occurs in a manner similar to the chain ejection model. In the case of LEMS, it is likely that the laser vaporized proteins are ionized and released into

the gas phase upon interaction with the surface of highly charged ES droplets prior to the increased concentration of non-volatile salt within the ES droplets. However, the salt adduction in LEMS is significantly lower than for ESI suggesting that the proteins do not equilibrate into the interior of the droplet. The polar analytes (e.g. salt) equilibrating into the droplet interior due to increased solvation will thus be isolated from proteins resulting in minimal salt adduction in LEMS measurements.

The preferential interaction of laser vaporized protein with the highly charged electrospray droplets in LEMS measurements has been proposed to enhance the detection of protonated protein ions in comparison with conventional ESI measurements.(19) Protein residing in the droplet interior in the ESI-MS measurement has to partition onto the droplet exterior for ionization. This enhances interaction of protein with salt in the case of ESI resulting in an increased salt adduction.

4.5 Conclusions

The analysis of lysozyme, and a mixture of lysozyme, cytochrome c, and myoglobin, in solution with varying salt concentration revealed a significantly higher salt tolerance for LEMS measurements in comparison with conventional electrospray with respect to suppression of the protonated ion signal and the ability to distinguish mixture components. The average sodium adducts bound to the 7+ charge state of lysozyme for LEMS measurements from salt concentrations of 2.5, 25, 50, and 100 mM NaCl are 1.71, 5.23, 5.26, and 5.11, respectively, whereas conventional electrospray measurements for lysozyme from solutions containing salt concentrations of 0.1, 1, 2, and 5 mM NaCl

resulted in $< n >$ of 2.65, 6.44, 7.57, and 8.48, respectively. The reduced salt adduction in the LEMS experiment is likely due to the non-equilibrium nature of partitioning of laser vaporized proteins between the surface and interior of the charged electrospray droplets. The reduced interaction time of the laser vaporized analytes with the ES droplets presumably allows small ions like Na^+ and Cl^- to partition into the droplet interior on the time scale of transit to the capillary leaving the much larger protein on the droplet surface where excess charge resides. This results in a lower salt concentration on the surface of the ES droplets, which leads to the formation of a higher fraction of protonated protein ions in comparison with conventional ESI measurements. Conversely, proteins in electrospray measurements have to partition from the droplet interior to the droplet's surface for ionization which results in an increased interaction of protein with salt in the ES droplet from which an ionized protein is released.

4.6 References

1. Mandal, M. K.; Chen, L. C.; Hashimoto, Y.; Yu, Z.; Hiraoka, K. Detection of biomolecules from solutions with high concentration of salts using probe electrospray and nano-electrospray ionization mass spectrometry. *Anal. Methods.* **2010,** (2), 1905-1912.

2. Flick, T. G.; Cassou, C. A.; Chang, T. M.; Williams, E. R. Solution additives that desalt protein ions in native mass spectrometry. *Anal. Chem.* **2012,** (84), 7511-7517.

3. Chang, D.-Y.; Lee, C.-C.; Shiea, J. Detecting large biomolecules from high-salt solutions by fused-droplet electrospray ionization mass spectrometry. *Anal. Chem.* **2002,** (74), 2465-2469.

4. Yue, X.; Vahidi, S.; Konermann, L. Insights into the mechanism of protein electrospray ionization from salt adduction measurements. *J. Am. Soc. Mass Spectrom.* **2014,** (25), 1322-1331.

5. Shrivas, K.; Wu, H.-F. Modified silver nanoparticle as a hydrophobic affinity probe for analysis of peptides and proteins in biological samples by using liquid-liquid microextraction coupled to AP-MALDI-ion trap and MALDI-TOF mass spectrometry. *Anal. Chem.* **2008,** (80), 2583-2589.

6. Liu, C.; Hofstadler, S. A.; Bresson, J. A.; Udseth, H. R.; Tsukuda, T.; Smith, R. D.; Snyder, A. P. On-line dual microdialysis with ESI-MS for direct analysis of complex biological samples and microorganism lysates. *Anal. Chem.* **1998,** (70), 1797-1801.

7. Bauer, K.-H.; Knepper, T. P.; Maes, A.; Schatz, V.; Voihsel, M. Analysis of polar organic micropollutants in water with ion chromatography–electrospray mass spectrometry. *J. Chromatogr. A.* **1999,** (837), 117-128.

8. Huber, C. G.; Buchmeiser, M. R. On-line cation exchange for suppression of adduct formation in negative-ion electrospray mass spectrometry of nucleic acids. *Anal. Chem.* **1998,** (70), 5288-5295.

9. Jiang, Y.; Hofstadler, S. A. A highly efficient and automated method of purifying and desalting PCR products for analysis by electrospray ionization mass spectrometry. *Anal. Biochem.* **2003,** (316), 50-57.

10. Batchelor, J. D.; Doucleff, M.; Lee, C.-J.; Matsubara, K.; De Carlo, S.; Heideker, J.; Lamers, M. H.; Pelton, J. G.; Wemmer, D. E. Structure and regulatory

mechanism of Aquifex aeolicus NtrC4: variability and evolution in bacterial transcriptional regulation. *J. Mol. Biol.* **2008,** (384), 1058-1075.

11. Batchelor, J. D.; Sterling, H. J.; Hong, E.; Williams, E. R.; Wemmer, D. E. Receiver Domains Control the Active-State Stoichiometry of Aquifex aeolicus σ 54 Activator NtrC4, as Revealed by Electrospray Ionization Mass Spectrometry. *J. Mol. Biol.* **2009,** (393), 634-643.

12. Nagaraj, N.; Lu, A.; Mann, M.; Wiśniewski, J. R. Detergent-based but gel-free method allows identification of several hundred membrane proteins in single LC-MS runs. *J. Proteome Res.* **2008,** (7), 5028-5032.

13. Flick, T. G.; Merenbloom, S. I.; Williams, E. R. Anion effects on sodium ion and acid molecule adduction to protein ions in electrospray ionization mass spectrometry. *J. Am. Soc. Mass Spectrom.* **2011,** (22), 1968-1977.

14. Pan, P.; Gunawardena, H. P.; Xia, Y.; McLuckey, S. A. Nanoelectrospray Ionization of Protein Mixtures: Solution pH and Protein p I. *Anal. Chem.* **2004,** (76), 1165-1174.

15. Jackson, A. U.; Talaty, N.; Cooks, R. G.; Van Berkel, G. J. Salt tolerance of desorption electrospray ionization (DESI). *J. Am. Soc. Mass Spectrom.* **2007,** (18), 2218-2225.

16. Chen, H.; Venter, A.; Cooks, R. G. Extractive electrospray ionization for direct analysis of undiluted urine, milk and other complex mixtures without sample preparation. *Chem. Commun.*. **2006,** (42), 2042-2044.

17. Brady, J. J.; Judge, E. J.; Levis, R. J. Mass spectrometry of intact neutral macromolecules using intense non-resonant femtosecond laser vaporization with electrospray post-ionization. *Rapid Commun. Mass Spectrom.* **2009,** (23), 3151-3157.

18. Brady, J. J.; Judge, E. J.; Levis, R. J. Analysis of amphiphilic lipids and hydrophobic proteins using nonresonant femtosecond laser vaporization with electrospray post-ionization. *J. Am. Soc. Mass Spectrom.* **2011,** (22), 762-772.

19. Karki, S.; Flanigan IV, P. M.; Perez, J. J.; Archer, J. J.; Levis, R. J. Increasing Protein Charge State When Using Laser Electrospray Mass Spectrometry. *J. Am. Soc. Mass Spectrom.* **2015,** (26), 706-715.

20. Perez, J. J.; Flanigan IV, P. M.; Karki, S.; Levis, R. J. Laser electrospray mass spectrometry minimizes ion suppression facilitating quantitative mass spectral

response for multicomponent mixtures of proteins. *Anal. Chem.* **2013,** (85), 6667-6673.

21. Judge, E. J.; Brady, J. J.; Dalton, D.; Levis, R. J. Analysis of pharmaceutical compounds from glass, fabric, steel, and wood surfaces at atmospheric pressure using spatially resolved, nonresonant femtosecond laser vaporization electrospray mass spectrometry. *Anal. Chem.* **2010,** (82), 3231-3238.

22. Flanigan IV, P. M.; Brady, J. J.; Judge, E. J.; Levis, R. J. Determination of inorganic improvised explosive device signatures using laser electrospray mass spectrometry detection with offline classification. *Anal. Chem.* **2011,** (83), 7115-7122.

23. Perez, J. J.; Flanigan IV, P. M.; Brady, J. J.; Levis, R. J. Classification of smokeless powders using laser electrospray mass spectrometry and offline multivariate statistical analysis. *Anal. Chem.* **2012,** (85), 296-302.

24. Flanigan IV, P. M.; Radell, L. L.; Brady, J. J.; Levis, R. J. Differentiation of eight phenotypes and discovery of potential biomarkers for a single plant organ class using laser electrospray mass spectrometry and multivariate statistical analysis. *Anal. Chem.* **2012,** (84), 6225-6232.

25. Judge, E. J.; Brady, J. J.; Barbano, P. E.; Levis, R. J. Nonresonant femtosecond laser vaporization with electrospray postionization for ex vivo plant tissue typing using compressive linear classification. *Anal. Chem.* **2011,** (83), 2145-2151.

26. Shi, F.; Flanigan IV, P. M.; Archer, J. J.; Levis, R. J. Ambient Molecular Analysis of Biological Tissue Using Low-Energy, Femtosecond Laser Vaporization and Nanospray Postionization Mass Spectrometry. *J. Am. Soc. Mass Spectrom.* **2016,** (27), 542-551.

27. Flanigan IV, P. M.; Perez, J. J.; Karki, S.; Levis, R. J. Quantitative measurements of small molecule mixtures using laser electrospray mass spectrometry. *Anal. Chem.* **2013,** (85), 3629-3637.

28. Flanigan IV, P. M.; Shi, F.; Archer, J. J.; Levis, R. J. Internal Energy Deposition for Low Energy, Femtosecond Laser Vaporization and Nanospray Post-ionization Mass Spectrometry using Thermometer Ions. *J. Am. Soc. Mass Spectrom.* **2015,** (26), 716-724.

29. Wang, G.; Cole, R. B. Mechanistic interpretation of the dependence of charge state distributions on analyte concentrations in electrospray ionization mass spectrometry. *Anal. Chem.* **1995,** (67), 2892-2900.

30. Frey, B. L.; Lin, Y.; Westphall, M. S.; Smith, L. M. Controlling gas-phase reactions for efficient charge reduction electrospray mass spectrometry of intact proteins. *J. Am. Soc. Mass Spectrom.* **2005,** (16), 1876-1887.

31. Verkerk, U. H.; Kebarle, P. Ion-ion and ion-molecule reactions at the surface of proteins produced by nanospray. Information on the number of acidic residues and control of the number of ionized acidic and basic residues. *J. Am. Soc. Mass Spectrom.* **2005,** (16), 1325-1341.

32. Liu, J.; Konermann, L. Cation-induced stabilization of protein complexes in the gas phase: mechanistic insights from hemoglobin dissociation studies. *J. Am. Soc. Mass Spectrom.* **2014,** (25), 595-603.

33. Brady, J. J.; Judge, E. J.; Levis, R. J. Nonresonant femtosecond laser vaporization of aqueous protein preserves folded structure. *Proc. Natl Acad. Sci.* **2011,** (108), 12217-12222.

34. Pace, C. N.; Trevino, S.; Prabhakaran, E.; Scholtz, J. M. Protein structure, stability and solubility in water and other solvents. *Philos. Trans. R. Soc. Lond. B.* **2004,** (359), 1225-1235.

35. Pinho, S. P.; Macedo, E. A. Solubility of NaCl, NaBr, and KCl in water, methanol, ethanol, and their mixed solvents. *Journal of Chemical & Engineering Data.* **2005,** (50), 29-32.

36. Konermann, L.; Ahadi, E.; Rodriguez, A. D.; Vahidi, S. Unraveling the mechanism of electrospray ionization. *Anal. Chem.* **2012,** (85), 2-9.

CHAPTER 5

MEASUREMENT OF THE LIFETIME FOR LASER VAPORIZED LIQUID DROPLETS COUPLED WITH ELECTROSPRAY AND NANOSPRAY POST-IONIZATION MASS SPECTROMETRY

5.1 Overview

In this chapter, measurement of the lifetime for laser vaporized liquid droplets coupled with electrospray and nano-spray post-ionization is presented. Electrospray and nano-spray droplet lifetimes were measured to be 4.5±0.5 ms and 1.4±0.3 ms using laser electrospray mass spectrometry (LEMS) and nano-laser electrospray mass spectrometry (nano-LEMS), respectively. The droplet lifetimes were calculated on the basis of forward rate constant of the reaction between 2, 6-dichloroindophenol (oDCIP) and L-ascorbic acid (L-AA) in the bulk solution phase. The measurement of droplet lifetimes by varying both the distance from the spray emitter to laser vaporized spot and the drying gas temperature is also presented. Fractions of folded protein are reported as a function of droplet lifetime for acid-denatured cytochrome c and myoglobin in ammonium acetate solution using LEMS and nano-LEMS measurements.

5.2 Introduction

Absorption and fluorescence spectroscopy are commonly used to monitor reaction kinetics on timescales as short as femtoseconds(1, 2), however these methods require endogenous chromophores or labelling of the reacting species. Quench-flow is another method for obtaining time-resolved information from a reaction system(3), however the

quenched reaction products are required to be stable during off-line analysis. The ability to detect short-lived reaction intermediates with high chemical specificity has made mass spectrometry a suitable tool for studies of chemical and/or biochemical reactions such as formation of organometallic compounds, protein folding/unfolding and enzyme-catalyzed processes(4-8).

Time-resolved mass spectrometry (TRMS) was first introduced in late 90's where stopped-flow and continuous flow mixing devices were coupled with electrospray ionization mass spectrometry (ESI-MS) to monitor the kinetics of the given reaction system with time resolution ranging from seconds to milliseconds(9, 10). The length of the 'reaction' capillaries in these experiments determines the timescale of the kinetic measurements. The diffusion-limited mixing time of the two reactant species in bulk solution phase is a major obstacle for improving temporal resolution of any kinetic system. The mixing time of reactant species can be improved by colliding liquid droplets through inertial mixing(11). The development of new ionization techniques such as desorption electrospray ionization (DESI)(12), extractive electrospray ionization (EESI)(13), microdroplet fusion mass spectrometry(14), and theta spray ionization mass spectrometry(15) has enabled the reaction to be monitored in droplets (few microns in diameter) rather than in the bulk solution phase. Hence, measurements with high temporal resolution can be achieved. Reactive DESI was used to detect short-lived intermediates formed in the secondary microdroplets on millisecond timescale by adding reactant in the spray solution that interacts with a compound adsorbed onto a surface(12). The formation of a radical cation intermediate (expected lifetime to be shorter than 4 ms)

in the dimerization reaction of *trans*-anethole was successfully detected using EESI experimental setup where the reaction occurs within the ES droplets(13). Sub-microsecond time resolution was later achieved using fused droplet and theta spray ionization mass spectrometry(14, 15).

The development of a 'theta-shaped' borosilicate capillary, consisting of a nano-electrospray emitter with two separate channels, allows extremely small 'mixing volume' on the order of femtoliters(16). The interaction of reactants in this technique occurs partially in the ES tip and the Taylor cone while majority of reactions occur in the droplets during the desolvation process and hence the technique is suitable of short timescale measurements. An average reaction time (droplet lifetimes) of 274±60 μs was calculated using theta spray on the basis of forward rate constant of the reaction between DCIP and L-AA in the bulk solution phase(15). The lifetime of the ES droplet depends on the initial droplet size (diameter), which can be varied by changing the solution flow rate and the inner diameters of the spray emitter(17-19). Recently, shorter reaction times (1 to 22 μs) in theta spray measurements were achieved by changing the solution flow rates from 48 pL/s to 2880 pL/s(6). However, the surface to volume ratio, concentration of reagents, and the pH are expected to increase during solvent evaporation(20, 21). These factors can therefore escalate the rate of product formation by ~1-3 orders of magnitude in a rapidly desolvating ES droplet in comparison with the bulk solution phase(22-25). The extent of product formation monitored using nano-ESI for the reaction between piperidine and acrylamide revealed that ~99% of piperidine was converted into product (within 10 minutes) when the drop-casting (thin films deposited on ambient

surfaces) approach was used for synthesis(23). However, only about 5% of piperidine was converted into product when the reagents were mixed in bulk solution phase (for reaction time of 1 hour).

LEMS couples nonresonant femtosecond (fs) laser vaporization with an electrospray ionization source to perform mass analysis without the need for sample pre-processing. LEMS analysis has been performed on a variety of samples including proteins(26-29), pharmaceuticals(30), plant and animal tissue(31, 32). However, the lifetime of laser vaporized liquid droplets that interact with ES generated charged droplets in the LEMS process has not been measured before.

In this study, we investigated a reacting system to calculate the reaction time based on the extent of product (reduced DCIP) formed when the laser vaporized oDCIP interacts with electrospray droplets containing reduced L-AA. The use of nanospray emitters with a smaller inner diameter and a lower flow rates in comparison with the electrospray emitter has been investigated to determine the temporal resolution of our experiment. In addition, we also investigated the temporal resolution for both LEMS and nano-LEMS measurements by systematically varying the experimental parameters such as distance between the spray (electrospray or nanospray) emitter to MS inlet, spray emitter to laser vaporized spot, and temperature of drying gas (nitrogen). Protein charge state distributions were also measured a function of droplet lifetime for acid-denatured cytochrome c and myoglobin in ammonium acetate solution to investigate the time dependence protein folding within the ES droplets.

5.3 Experimental Section

5.3.1 Sample Preparation

Cytochrome c, myoglobin, ammonium acetate, 2, 6- dichloroindophenol sodium salt (DCIP), L-ascorbic acid (L-AA), (Sigma Aldrich, St. Louis, MO) were prepared in HPLC grade water (Fisher Scientific, Pittsburgh, PA) to yield the protein concentration of 1.0×10^{-3} M, ammonium acetate concentration of 2.0×10^{-2} M, DCIP concentration of 2.0×10^{-4} M, and L-AA concentration of 1.0×10^{-2} M. For the droplet lifetime measurements using LEMS and nano-LEMS, a 10 μL aliquot of 2.0×10^{-4} M DCIP (pH 3) was spotted onto a stainless steel plate and was laser vaporized into electrospray and/or nano-spray droplets containing 1.0×10^{-3} M and 5×10^{-3} M L-AA (pH 3), respectively. For the protein folding experiments using LEMS and nano-LEMS measurements, a 10 μL aliquot of 2.0×10^{-4} M protein was spotted onto a stainless steel plate and then subjected to laser vaporization into the electrospray (ES) charged droplet stream consisting of 10 mM aqueous ammonium acetate.

5.3.2 Laser Vaporization and Ionization Apparatus

A Ti:sapphire laser oscillator (KM Laboratories, Inc., Boulder, CO) seeded a regenerative amplifier (Coherent, Inc., Santa Clara, CA) that delivered 75 fs, 1 mJ laser pulses centered at 800 nm. The laser, operated at 10 Hz to couple with the ESI ion source, was focused to a spot size of ~250 μm in diameter with an incident angle of 45^{o} with respect to the sample using a 16.9 cm focal length lens, with an approximate intensity of 4×10^{13} W/cm^2. The steel sample plate was biased to -2.0 kV to compensate for the

distortion of electric field between the capillary inlet and the needle caused by the sample stage. Aqueous protein sample (6 μL) and oxidized DCIP (6 μL) deposited onto a steel substrate was vaporized by the laser pulse allowing for capture and ionization by an ES plume travelling perpendicular to the vaporized material.

5.3.3 Mass Spectrometry and Data Analysis

The spectrometer used in this experiment has been described previously(33). The flow rate for ES solvent was set at 2 μL/min by a syringe pump (Harvard Apparatus, Holliston, MA). The ESI and nano-ESI needle was 6.4 mm above and parallel to the sample stage, and was adjusted to be 3.4 mm to 12.8 mm from the front of the capillary entrance for this study. The ES needle was maintained at ground while the inlet capillary was biased and adjusted from -3.5 to -6 kV to achieve a stable electrospray signal. For the nano-LEMS measurements, flow rate of the ES solvent was set at 400 nL/min, the needle was maintained at ground and the MS inlet was biased and adjusted from -2.0 to 3.5 kV. The postionized analytes were desolvated before entering the inlet capillary by countercurrent nitrogen gas ranging from 140 °C to 350 °C flowing at 4 L/min. The charged sample was mass analyzed using a microTOF-Q II mass spectrometer (Bruker Daltonics, Billerica, Germany). The average charge state (Z_{avg}) was calculated using equation 1,

$$Z_{avg} = \frac{\sum_{i}^{N} q_i w_i}{\sum_{i}^{N} w_i} \qquad (1)$$

where q_i is the net charge, W_i is the sum of signal intensity of the i^{th} charge state, and N is the number of charge states present in the mass spectra.

5.3.4 Safety Considerations

Appropriate laser eye protection was worn by all lab personnel

5.4 Results and Discussion

5.4.1 Measurement of Droplet Lifetimes in LEMS and nano-LEMS Experiments

LEMS can be used to decouple two reactants in separate bulk solution phase until they interact in the ES droplets. This allows the reaction to be monitored to determine the lifetime of the ES droplet. To calculate the lifetime of laser vaporized liquid droplets coupled with electrospray and nano-spray postionization, oxidized DCIP (pH 3) was laser vaporized into electrospray and/or nanospray droplets containing reduced L-AA (pH 3) and the rate of product (reduced DCIP) formation was monitored using mass spectrometry. The calculated reaction time obtained from the measurement can be correlated to the lifetime of the laser vaporized liquid droplet assuming that the reaction between oDCIP and reduced L-AA stops when the laser vaporized liquid droplet undergoes complete desolvation (losing the liquid media where reaction takes place). The LEMS measurement of oxidized DCIP in ES solvent containing reduced L-AA revealed both oxidized and reduced forms of DCIP as shown in Figure 5.1. Similar to the previous DESI measurement(34), the peak at mass-to-charge (*m/z*) ratio of 268 corresponds to the oxidized form (reactant) of DCIP while peaks at *m/z* of 270, and 272 correspond to the combination of both the reduced (product) form of DCIP as well as an isotope of the oxidized (reactant) form of DCIP (isotopic distribution of two chlorines present on oxidized DCIP results in the peak at *m/z* of 270 and 272). Since, the resolution of the mass spectrometer used in this study is not sufficient to resolve the oxidized and

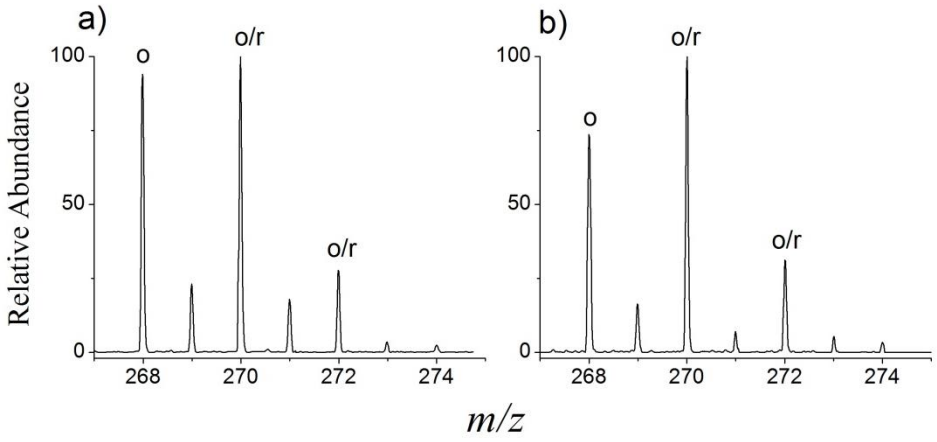

Figure 5.1. Representative mass spectra resulting from laser induced vaporization of 200 µM DCIP into a) electrospray and b) nanospray droplets containing 1 and 5 mM L-ascorbic acid, respectively. The peak at *m/z* of 268 represented as 'o' indicates the relative abundance of oxidized DCIP whereas peaks at *m/z* of 270 and 272 represented as "o/r' indicates both the oxidized and reduced form of DCIP.

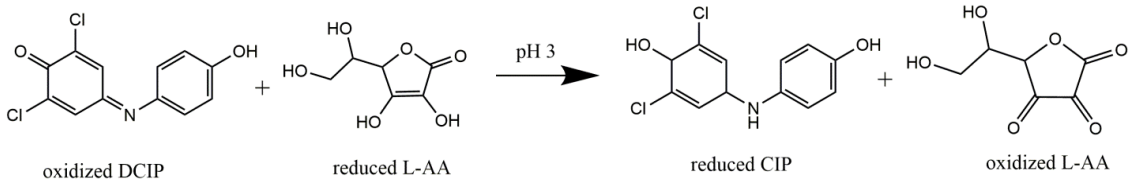

Scheme 5.1. Reduction of 2,6-Dichloroindophenol by L-Ascorbic Acid

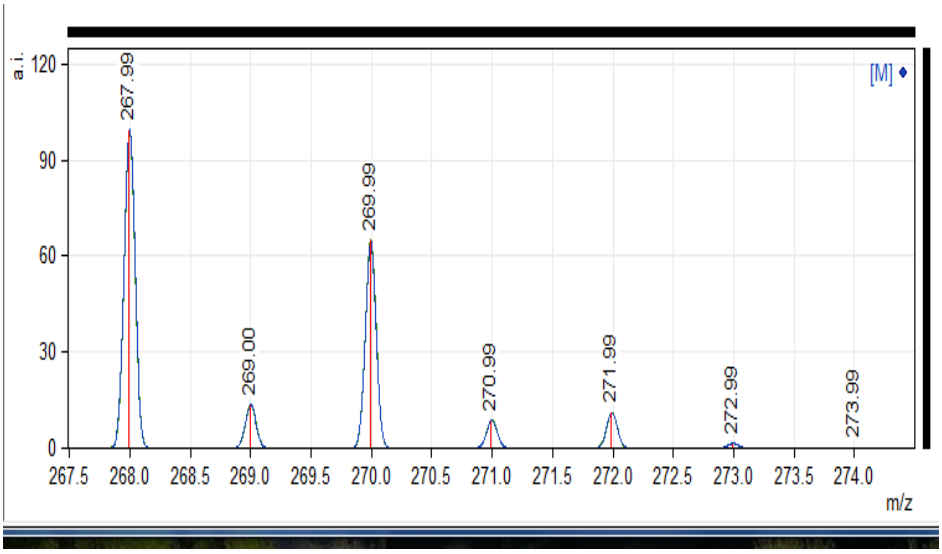

Figure 5.2. Theoretical mass spectra as obtained from n-mass software (an open source mass spectrometry tool) showing the isotopic distribution of oxidized form of DCIP.

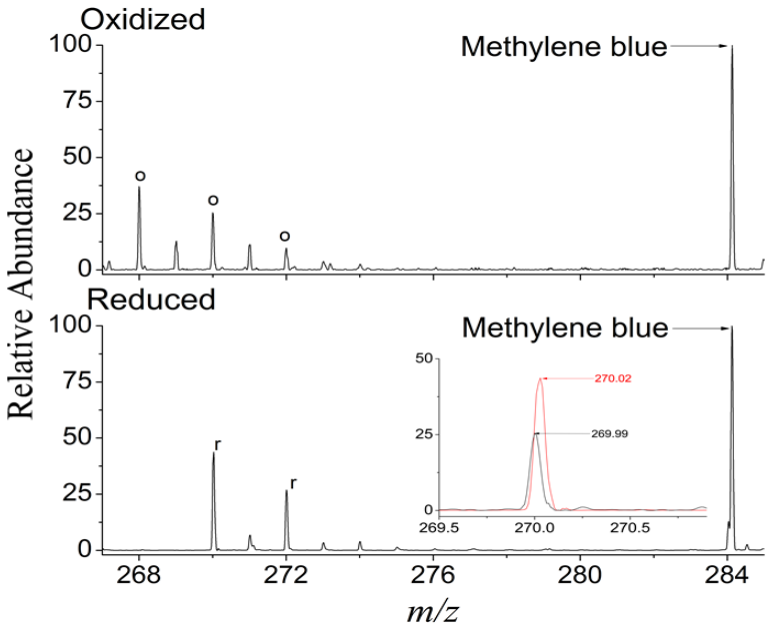

Figure 5.3. Representative mass spectra resulting from laser induced vaporization of a) 200 µM oxidized DCIP, and b) 200 µM reduced DCIP mixed with 10 µM Methylene blue solution (both pH 3) into ES droplets containing oxalic acid (pH 3). The inset shows the overlapping features from oxidized and reduced form of DCIP.

reduced forms of DCIP, the relative contributions of oxidized and reduced forms of DCIP in the mass spectra were obtained based on the isotopic (theoretical) abundance of oxidized form of DCIP using n-mass software (Figure 5.2).

The initial concentration of L-AA in electrospray (1 mM) and nano-spray (5 mM) solvents is large compared to laser vaporized DCIP (~3.5% of laser vaporized oxidized DCIP, 200 µM, is captured by the ES plume), the reaction can be modeled using pseudo-first-order reaction kinetics(15). The droplet lifetimes in LEMS and nano-LEMS experiments were calculated on the basis of the rate constant of the reaction in the bulk solution phase as follows:

$$t = \frac{ln\left(\frac{(A_{oDCIP} + i_{DCIP}A_{rDCIP})}{A_{oDCIP}}\right)}{\mathrm{K_f}[\mathrm{L-AA}]_0} \qquad (2)$$

where t is the reaction time, A_{oDCIP} and A_{rDCIP} are the oxidized and reduced form of DCIP, i_{DCIP} is the relative ionization efficiency of the oxidized to the reduced form of DCIP, K_f is the forward rate constant and $[L\text{-}AA]_o$ is the initial concentration of ascorbic acid. The forward rate constant of the reaction between oxidized DCIP and L-AA (shown in Scheme 5.1) in the bulk solution phase is 5.6 X 10^4 L mol^{-1} s^{-1} at pH of 3(35). To calculate the ionization efficiency of oxidized form of DCIP relative to the reduced form, 200 µM oxidized DCIP and 200 µM reduced DCIP were prepared in solutions containing 10 µM of methylene blue. Two LEMS measurements were performed, first a 6 µL solution of oxidized DCIP (mixed with methylene blue) was laser vaporized into aqueous

ES solvent (pH 3). Second, the same volume of solution containing reduced DCIP (mixed with methylene blue) was laser vaporized into aqueous ES solvent (pH 3). The dominant peak in the LEMS mass spectra for both solutions is methylene blue as shown in Figure 5.3, which was used as an internal standard. The relative abundances of $[_{o}DCIP + H]^{+}$ and $[_{r}DCIP + H]^{+}$ were 73.3±6.9 and 70.7±5.4, respectively. The ionization efficiency of oxidized form of DCIP relative to the reduced form of DCIP was calculated to be 1.03±0.07. The calculated droplet lifetimes for LEMS and nano-LEMS measurements using equation 2 for the (usual) distance of 6.4 mm between the spray emitter to MS inlet were 4.54±0.55 ms and 1.39±0.34 ms, respectively.

The rate of reaction within a rapidly desolvating droplet is reported to increase between 1 to 3 orders of magnitude in comparison with bulk solution phase(22-25), which suggests that the lifetime of laser vaporized liquid droplets coupled with electrospray and nanospray post-ionization is between 10 to 1000 times less than the calculated values obtained on the basis of the rate constant of bulk solution phase. Therefore, the lifetime of laser vaporized liquid droplets coupled with electrospray and nano-spray postionization may be as short as 4.5 μs, and 1.3 μs, respectively for the spray emitter to MS inlet distance of 6.4 mm and the drying gas temperature of 220 ^{o}C.

5.4.2 Effect of Distance between Spray Emitter and MS Inlet on Droplet Lifetime

Parameters such as distance from spray emitter to inlet capillary and drying gas temperature should influence the droplet lifetime. An increase in ambient temperature around the ES droplets results in an increase in solvent evaporation which could result in

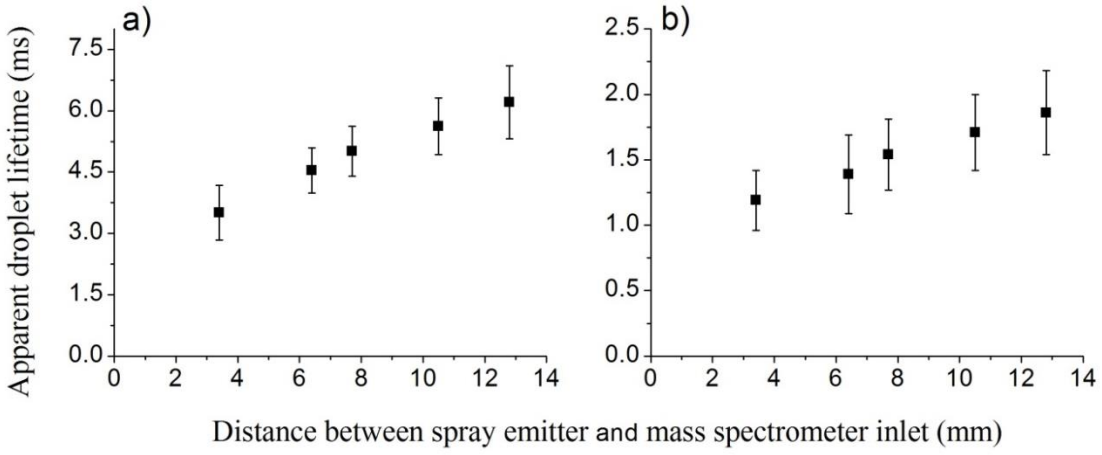

Figure 5.4. Plot of apparent droplet lifetime versus the distance between a) electrospray, and b) nano-spray emitter and the MS inlet (calculated using equation 2). The distance between the spray emitter and MS inlet was varied from 3.4 to 12.8 mm.

Distance between the spray emitter and MS inlet (mm)	Droplet lifetime for LEMS (ms)	Droplet lifetime for nano-LEMS (ms)
3.4	3.5±0.7	1.2±0.23
6.4	4.5±0.5	1.4±0.3
7.7	5.1±0.6	1.5±0.3
10.5	5.6±0.7	1.7±0.3
12.8	6.2±0.9	1.9±0.3
Distance between the spray emitter to laser vaporized spot (mm)		
1	6.4±0.6	1.9±0.2
2.5	5.8±0.6	1.7±0.2
4	3.4±0.6	1.2±0.2
5.5	2.2±0.5	0.9±0.2
7	1.8±0.4	--
Drying gas temperature (^{o}C)		
140	8.3±0.9	2.9±0.4
180	7.6±0.8	2.4±0.4
220	4.8±0.6	1.3±0.2
260	3.5±0.6	0.8±0.2
300	2.4±0.5	0.4±0.1
350	1.3±0.3	0.2±0.04

Table 5.1 Summary of droplet lifetime for LEMS, and nano-LEMS measurements for different experimental parameters

decrease in the droplet lifetime. The temperature of the drying gas is expected to decrease with increasing distance between the spray emitter and the MS inlet resulting in delayed desolvation at a lower temperature. The distance between the spray emitter and MS inlet was varied from 3.4 to 12.8 mm. To monitor the effect of distance between spray emitter and MS inlet on droplet lifetime for LEMS and nano-LEMS measurements, the DCIP solution was laser vaporized ~1 mm away from the spray emitter tip for all measurements. The mass spectra obtained by laser vaporizing oxidized DCIP into ES droplets containing 1 mM L-AA resulted in peaks at *m/z* 268, 270, and 272. As the distance between the ES emitter and MS inlet increases, the relative abundance of reduced DCIP (peaks at *m/z* of 270, and 272) increases suggesting a longer droplet lifetime for increased distance. Similar to the calculation for droplet lifetime in LEMS and nano-LEMS measurement for the distance of 6.4 mm between the spray emitter to the MS inlet, the contribution of reduced DCIP in these measurements was also obtained using the isotopic abundance of the oxidized and reduced forms of DCIP. The plot of droplet lifetime versus the distance between the spray emitter to MS inlet is shown in Figure 5.4 and the calculated values for all the experimental parameters investigated in this study are reported in Table 5.1. The droplet lifetime approximately doubles when the distance is increased from 3.4 to 12.8 mm. The increase in droplet lifetime is likely due to the decrease in effective temperature of the drying gas for longer distances which decreases the desolvation of the droplets.

Similar experiments were performed using nano-LEMS, where oxidized DCIP was laser vaporized into the nanospray droplets containing 5 mM L-AA and the distance

between the spray emitter and the MS inlet was varied. An increase in distance between the ES emitter and the MS inlet resulted in an increase in the relative abundance of oxidized/reduced peaks at *m/z* ratios of 270, and 272 corresponding to a longer droplet lifetime. The plot of droplet lifetime versus the distance between the nano-spray emitter to the MS inlet is shown in Figure 5.4 b. The lifetime again increases with distance. The reason for increase in droplet lifetime for longer distance in nano-LEMS measurements is again likely to due to lower drying gas temperature with longer distance between the nano-spray emitter and capillary inlet.

5.4.3 Effect of Distance between the Spray Emitter and Laser Vaporized Spot on Droplet Lifetime

During the electrospray process, solvent evaporation and droplet fissioning events result in a decrease in the size of ES droplets during transit from the spray emitter towards the MS inlet. The size of the electrospray and nano-spray droplets should therefore be smaller further away from the spray emitter and finally releasing gaseous ions for mass analysis. The distance between the spray emitter and the laser vaporized spot was varied to test whether the decrease in initial size of electrospray/nanospray generated charged droplets interacting with laser vaporized liquid droplets affects the droplet lifetime. The distance between the spray emitter and the MS inlet was kept constant at 12.8 mm while the vaporization position was varied from 1 to 7 mm. In principle, the laser vaporized analytes should interact with ES droplets with decreasing size for increasing distance. The plot of droplet lifetime versus the distance from the

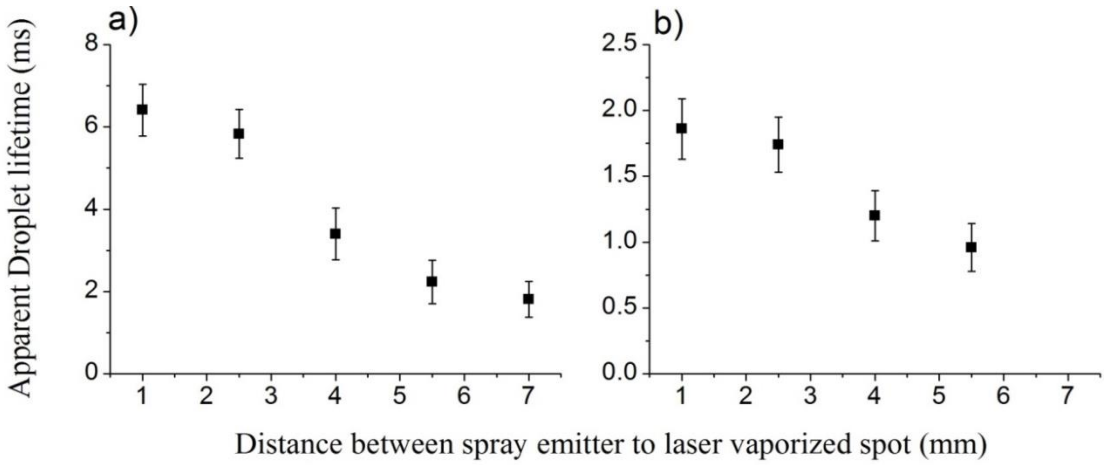

Figure 5.5. Plot of apparent droplet lifetime versus the distance between a) electrospray, and b) nanospray emitter and the laser vaporized spot (calculated using equation 2). The distance between the spray emitter and MS inlet was kept constant at 12.8 mm.

spray emitter to laser vaporized spot is shown in Figure 5.5. The droplet lifetime decreased from 6.41 ms to 1.81 ms when the distance from electrospray emitter to the laser vaporized spot was increased from 1 to 7 mm. As the distance between the electrospray emitter and the laser vaporized spot increased, the relative abundance of reduced DCIP (peaks at *m/z* of 270, and 272) decreased, corresponding to a shorter droplet lifetime. Similar observations were made when using nano-LEMS measurements suggesting that the interaction of laser vaporized droplets with smaller electrospray droplets results in a shorter droplet lifetime. The droplet lifetime in this case decreased from 1.86 ms to 0.96 ms when the distance between the nano-spray emitter to the laser vaporized spot was increased from 1 to 5.5 mm. In addition to decreasing droplet size, the temperature of the drying gas increases as the vaporization region approaches the capillary inlet. Thus increasing droplet temperature can also play a role.

5.4.4 Effect of Drying Gas Temperature on Droplet Lifetime

The rate of solvent evaporation should dependent upon the temperature of air surrounding the droplet. An increase in temperature should therefore result in the decrease in droplet lifetime because of the efficient solvent evaporation at higher temperatures. To investigate the effect of drying gas (nitrogen) temperature on droplet lifetime, the relative abundance of oxidized and reduced form of DCIP was monitored by changing the temperature of the drying gas from 140 to 350 ^{o}C for both LEMS and nano-LEMS measurement. The distance between the spray emitter and MS inlet in this experiment was kept at 6.4 mm. The plot of the droplet lifetime as a function of drying

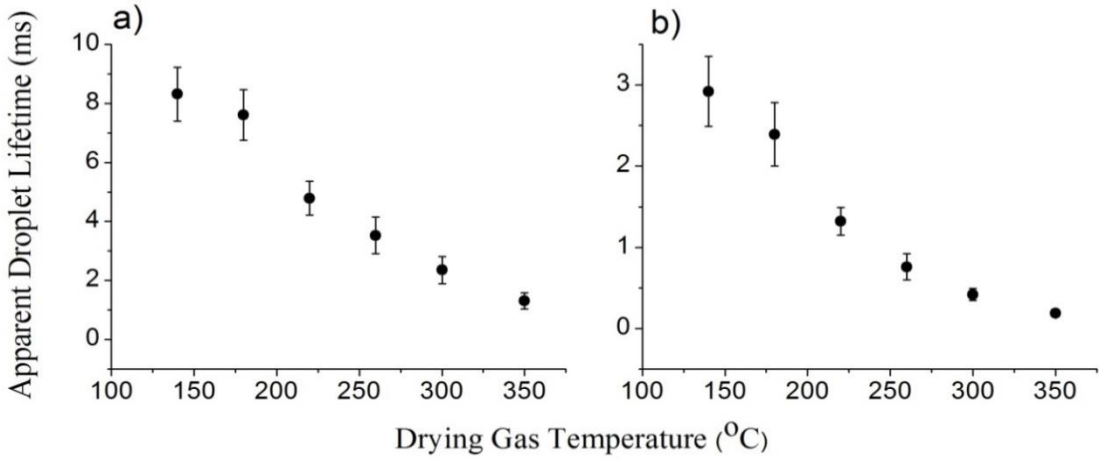

Figure 5.6. Plot of apparent droplet lifetime (ms) versus the drying gas (nitrogen) temperature (^{o}C) for a) LEMS, and b) nano-LEMS measurement (calculated using equation 2).

gas temperature is shown in Figure 5.6 for both LEMS and nano-LEMS experiment. The contribution of reduced form of DCIP (peak at m/z of 270 and 272) decreased as the function of drying gas temperature. The droplet lifetime decreases with increasing drying gas temperature and this is likely due to the efficient desolvation of the electrospray solvent (liquid medium where reaction between oxidized DCIP and reduced L-AA occurs) from the ES droplets. Assuming that the reaction in rapidly desolvating electrospray droplets increases by approximately 1 to 3 orders of magnitude in comparison with the bulk solution phase, the shortest droplet lifetime obtained in these measurements is for nano-LEMS experiment with a drying gas temperature of 350 ^{o}C at the spray emitter and capillary inlet distance of 6.4 mm. In this case, the droplet lifetime is likely in between 19 μs and 190 ns.

5.4.5 Protein Folding as a Function of Droplet Lifetime

5.4.5.1 Analysis of Cytochrome c

The ability of LEMS to decouple the processes that occur within ES droplet from processes that occur in the bulk solution phase allows time-dependent protein folding measurements on the microsecond to millisecond time scale, and perhaps, the possibility of detecting short lived intermediate states. To investigate protein folding as a function of droplet lifetime, acid-denatured cytochrome c and myoglobin were laser vaporized into electrospray and nano-spray droplets containing ammonium acetate solution. Ammonium acetate is an additive known to promote protein folding. The droplet lifetime was varied by changing the distance between the spray emitter and the MS inlet, and also by controlling the temperature of the drying gas temperature. The LEMS measurement of

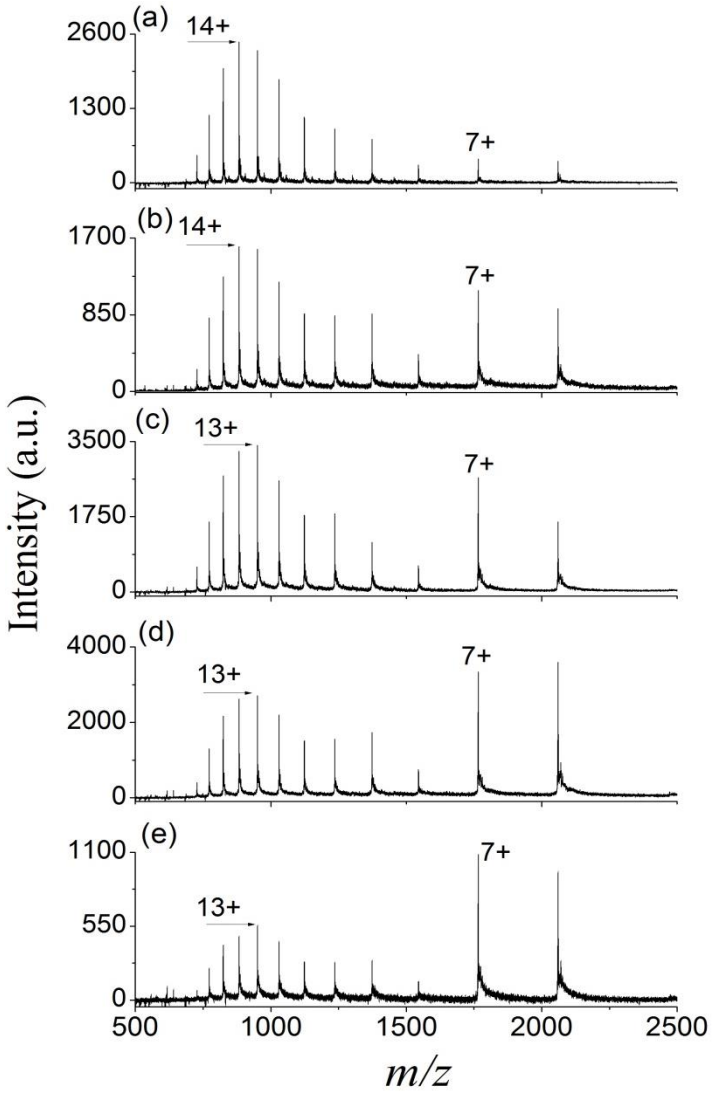

Figure 5.7. Representative LEMS mass spectra resulting from laser induced vaporization of cytochrome c at pH 2.2 into the ES solvent consisting of 10 mM ammonium acetate. Protein was laser vaporized a) 2.4, b) 5.4, c) 6.7, d) 9.5, and e) 11.8 mm away from the MS inlet. The distance between the ES emitter and MS inlet (d1 to d5) was varied from 3.4 to 12.8 mm.

Protein		Average charge state (Fraction folded protein)				
		d1	**d2**	**d3**	**d4**	**d5**
Cytochrome c pH 2.2	LEMS	12.2±0.1 (12±3%)	10.6±0.1 (33±2%)	10.8±0.2 (31±4%)	9.8±0.2 (42±3%)	9.6±0.3 (46±4%)
	nano-LEMS	14.6±0.3 --	13.4±0.1 (8±2%)	13.2±0.2 (9±4%)	12.9±0.1 (9±2%)	12.4±0.2 (17±3%)
Myoglobin pH 2.2	LEMS	15.9±0.2 (5±2%)	14.8±013 (9±4%)	14.4±0.3 (12±2%)	14.1±0.2 (12±4%)	13.9±0.3 (16±3%)
	nano-LEMS	21.8±0.4 --	16.9±0.2 (2±1%)	16.6±0.1 (3±2%)	15.7±0.1 (3±1%)	15.8±0.2 (5±2%)

Table 5.2. Summary of average charge state distribution (Z_{avg}) of cytochrome c, and myoglobin obtained from LEMS and nano-LEMS measurements for the spray to MS inlet distance of 3.4 mm (d1), 6.4 mm (d2), 7.7 mm (d3), 10.5 mm (d4), and 12.8 mm (d5). Values reported in the parenthesis are the folded protein fractions. The electrospray solvent consisted of 10 mM aqueous ammonium acetate.

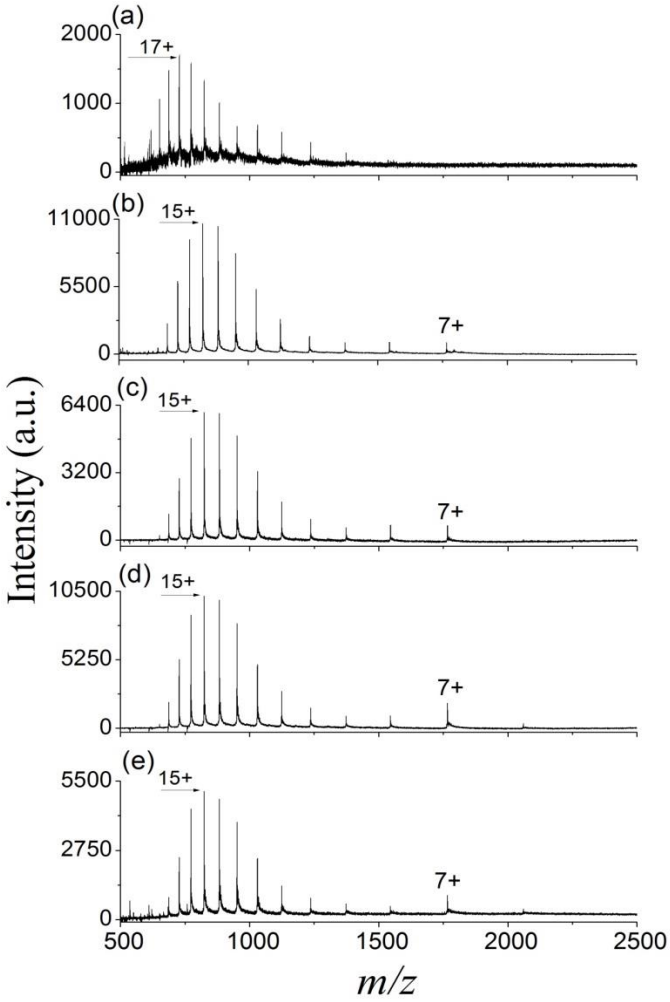

Figure 5.8. Representative nano-LEMS mass spectra resulting from laser induced vaporization of cytochrome c at pH 2.2 into the ES solvent consisting of 10 mM ammonium acetate. Protein was laser vaporized a) 2.4, b) 5.4, c) 6.7, d) 9.5, and e) 11.8 mm away from the MS inlet. The distance between the ES emitter and MS inlet (d1 to d5) was varied from 3.4 to 12.8 mm.

cytochrome c prepared in solution with pH 2.2 in aqueous ammonium acetate solution revealed a bimodal charge state distribution (CSD) centered at 7+ and 14+ (Fig 5.7 a), with an average charge state distribution (Z_{avg}) of 12.2±0.1 (reported in Table 5.2) for ES emitter to MS inlet distance of 3.4 mm. The presence of bimodal CSD indicates the presence of at least two conformations of the protein. The lower charge states ranging from 6+ to 8+ contain 12±3% of the cytochrome c ion intensity (Table 5.2), and indicate the folded states of cytochrome c. The charge states ranging from 9+ to 18+ indicate unfolded conformations. As distance between the ES to the MS inlet increases, the Z_{avg} of cytochrome c decreases, indicating to an increase in the fraction folded protein. This suggests that as the distance (between the ES to MS inlet) increases, laser vaporized protein is allowed to interact with ES droplets containing ammonium acetate for a longer time resulting in higher degree of protein folding. The fraction of folded protein increased from 12±5% when the ES emitter to MS inlet distance increased from 3.4 mm, corresponding to a droplet lifetime of 3.51±0.67 ms to 46±4% for a distance of 12.8 mm, corresponding to a droplet lifetime of 6.21±0.89 ms.

To further test the hypothesis that shorter droplet lifetime results in lower degree of protein folding, acid-denatured cytochrome c was laser vaporized into nanospray droplets containing ammonium acetate. The nano-LEMS measurement of cytochrome c prepared in solution with pH of 2.2 resulted in a monomodal distribution centered at 17+ (Figure 5.8 a), with an average charge state distribution (Z_{avg}) of 14.6±0.3 for spray emitter to MS inlet distance of 3.4 mm. The monomodal distribution indicates primarily

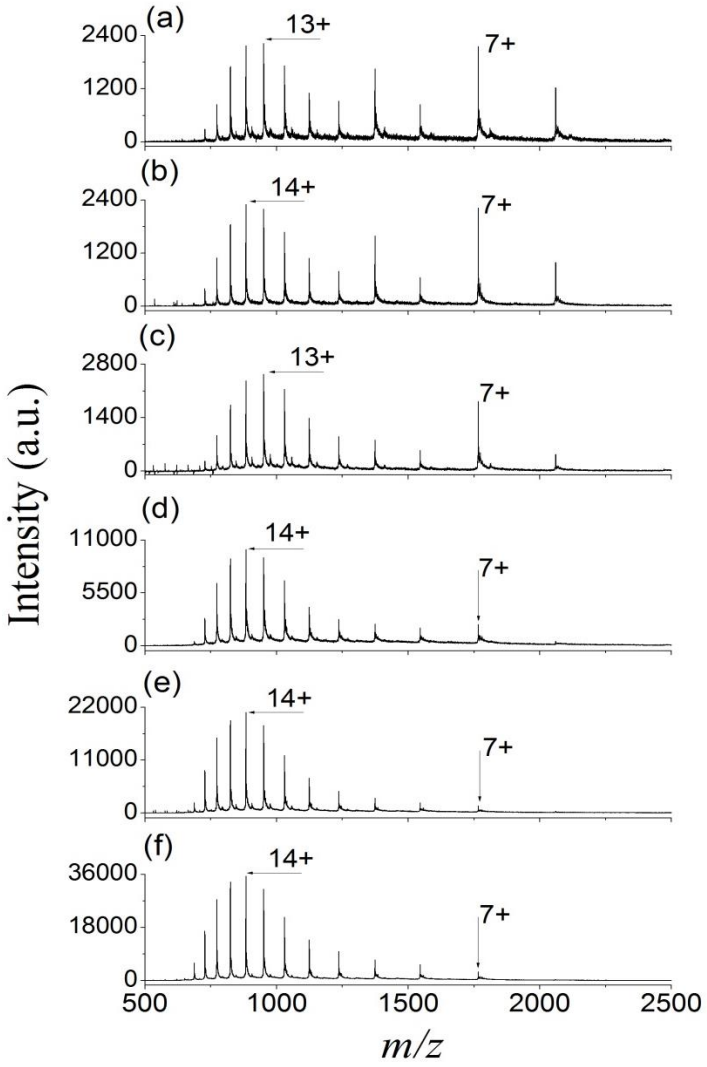

Figure 5.9. Representative LEMS mass spectra resulting from laser induced vaporization of cytochrome c at pH 2.2 into the electrospray solvent consisting of 10 mM ammonium acetate. The temperature of the drying gas (nitrogen) was maintained at a) 140, b) 180, c) 220, d) 260, e) 300 and f) 350 ^{o}C. The distance between the ES emitter and MS inlet was kept at 6.4 mm.

unfolded states of the protein, and is anticipated due to the short droplet lifetime (1.19±0.23 ms) measured at a distance of 3.4 mm for nano-LEMS experiment. As the distance between the nanospray emitter to the MS inlet increase the charge state distribution shifts to lower *m/z* ratio with the appearance of bimodal charge distribution centered at 7+ and 15+. The decrease in Z_{avg} with a corresponding increase in the fraction of folded protein for increased distance between the spray emitter and MS inlet (longer droplet lifetime, 1.86±0.32 ms) suggests that ~15% protein folds within the nanospray droplets. This provides a measure of protein folding time within the nano-spray droplets for the given solvent condition.

The effect of droplet lifetime on fraction of folded cytochrome c was further tested by increasing the temperature of the drying gas (nitrogen). It was observed that the droplet lifetime decreases with increasing drying gas temperature. The LEMS mass spectra of cytochrome c revealed a trimodal CSD centered at 7+, 9+, and 13+ (Figure 5.9 a and b), for drying gas temperature of 140 ^{o}C and 180 ^{o}C. The presence of trimodal CSD indicates the presence of at least three conformations of the protein. The lower charge states ranging from 6+ to 8+ containing ~30% of the cytochrome c ion intensity for the drying gas temperature of 140 and 180 ^{o}C indicates folded protein, while the higher charge states peaked around 12+ indicate the unfolded protein. The ion intensity of 9+ charge state is slightly higher than 8+ and 10+ for the drying gas temperature of 140 ^{o}C and 180 ^{o}C, suggesting the presence of an intermediate state of the protein. The detection of intermediate states in this experiment is consistent with the theta spray measurements(6). The increase in temperature to 220 ^{o}C results in a bimodal CSD

centered at 7+ and 13+ (Figure 5.9 c), while the further increase in temperature results in a monomodal CSD peaked at 14+. Both the increase in Z_{avg} and decrease in the fraction of folded protein suggest the presence of higher protein population in unfolded states for higher drying gas temperatures. This is in agreement with the hypothesis that a shorter droplet lifetime for higher drying gas temperature results in a decrease in fraction folded protein. The Z_{avg} values of cytochrome c for the drying gas temperature of 140, 180, 220, 260, 300, 350 ^{o}C are 10.1±0.1, 10.7±0.2, 11.1±0.2, 11.8±0.2, 12.7±0.3, and 12.8±0.1, respectively. The fraction folded protein (6 - 8+, charge states) for the drying gas temperature of 140, 180, 220, 260, 300, 350 ^{o}C are 31±1%, 30±2%, 25±3%, 17±1%, 9±2%, and 8±1%, respectively.

5.4.5.2 Analysis of Myoglobin

Myoglobin contains a heme group attached to the interior of the protein (holo-myoglobin), which is released to form apo-myoglobin at solution pH < 3(36, 37). The structure of apo-myoglobin is similar to that of holo-myoglobin for the solution pH of 5 and 7(38). The pH required to maintain the native structure of myoglobin is slightly higher in comparison with cytochrome c where the protein adopts native conformation between the pH of 3 and 7(39, 40). Here we seek to investigate whether variation in droplet lifetimes affects fraction of folded myoglobin under similar solvent condition used in cytochrome c study. The amount of folding of denatured apo-myoglobin was measured as a function of droplet lifetime by varying the distance from emitter to the MS inlet. The fraction folded protein and the Z_{avg} of apo-myoglobin were calculated by varying the distances between spray emitter to MS inlet. The LEMS measurement of apo-

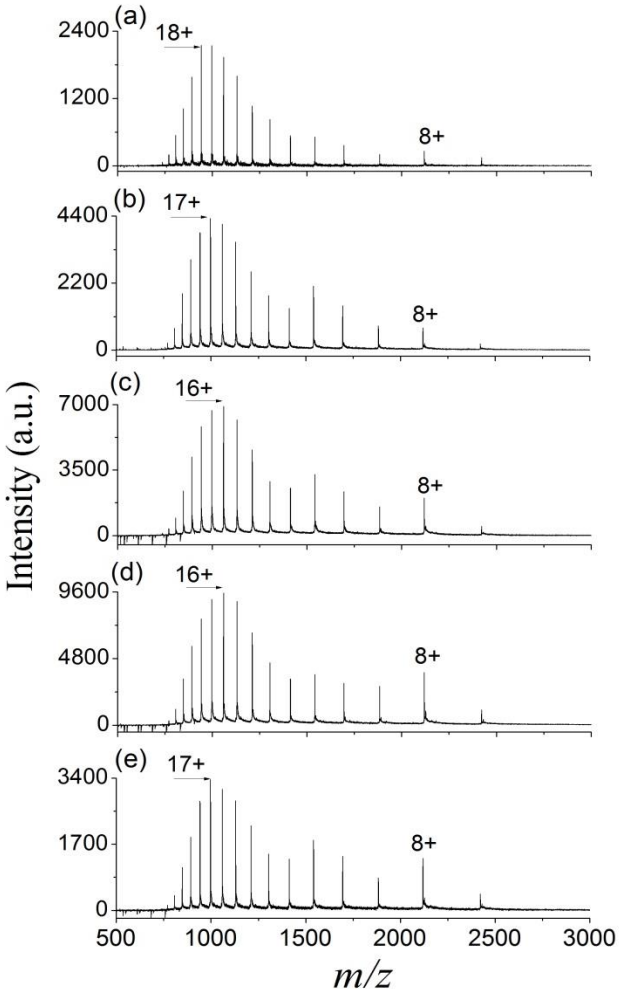

Figure 5.10. Representative LEMS mass spectra resulting from laser induced vaporization of myoglobin at pH 2.2 into the electrospray solvent consisting of 10 mM ammonium acetate. Protein was laser vaporized a) 2.4, b) 5.4, c) 6.7, d) 9.5, and e) 11.8 mm away from the MS inlet. The distance between the ES emitter and MS inlet (d1 to d5) was varied from 3.4 to 12.8 mm.

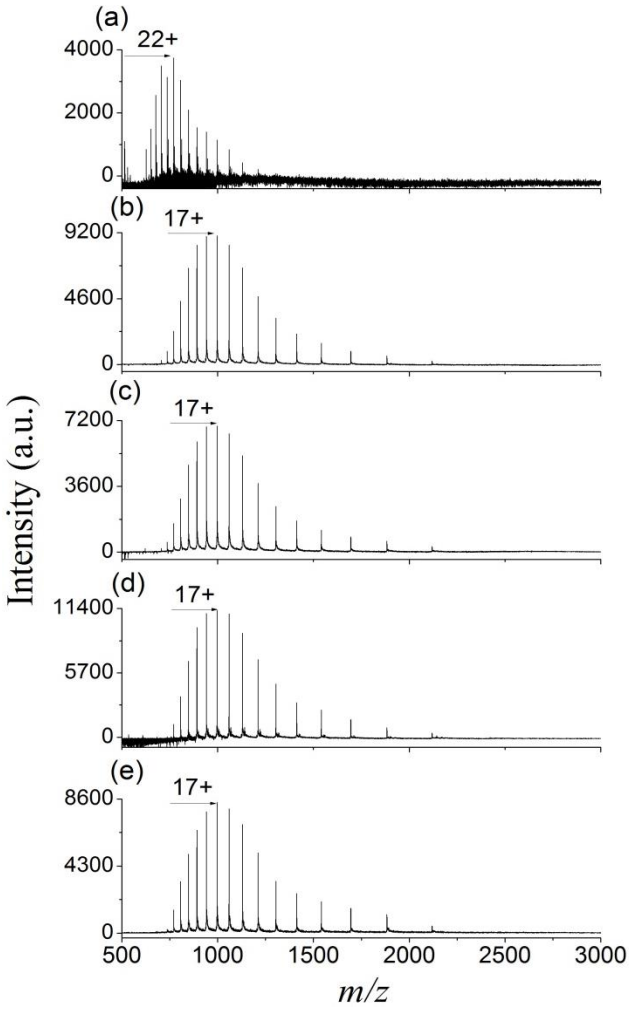

Figure 5.11. Representative nano-LEMS mass spectra resulting from laser induced vaporization of myoglobin at pH 2.2 into the electrospray solvent consisting of 10 mM ammonium acetate. Protein was laser vaporized a) 2.4, b) 5.4, c) 6.7, d) 9.5, and e) 11.8 mm away from the MS inlet. The distance between the ES emitter and MS inlet (d1 to d5) was varied from 3.4 to 12.8 mm.

myoglobin prepared in solution with pH 2.2 in aqueous ammonium acetate solution revealed a bimodal charge state distribution (CSD) centered at 8+ and 18+ (Figure 5.10 a), with an Z_{avg} of 15.9±0.2 for ES emitter to MS inlet distance of 3.4 mm. The bimodal CSD indicates the presence of at least two conformations of the protein. The lower charge states ranging from 7+ to 9+ contain 4±1% of the ion intensity (Table 5.2), indicating the folded states of myoglobin whereas the charge states ranging from 10+ to 22+, peaked at 18+ indicate the unfolded states. As the distance between the ES emitter to the MS inlet increases a trimodal CSD is observed peaked at 8+, 11+, and ~16+. The CSD centered around 11+ likely represents intermediate sates while the lower charge states ranging from 7+ to 9+, and higher charge states peaked around 16+ likely represents folded and unfolded protein, respectively. Both the decrease in Z_{avg} and fraction folded protein for the increased distance from electrospray emitter to the MS inlet suggests that increasing the droplet lifetime enables additional protein folding in LEMS measurements.

Similar measurements were performed using nano-LEMS measurements where the acid-denatured myoglobin was laser vaporized into nano-spray droplets containing ammonium acetate solution and the CSD was monitored as the function of distance between the nano-spray emitter and the MS inlet. The nano-LEMS measurement of apo-myoglobin in ammonium acetate for the emitter to MS inlet distance of 3.4 mm revealed a monomodal CSD peaked at 22+ (shown in Figure 5.11 a), with a Z_{avg} value of 21.8±0.4. As the distance between nano-spray emitter to MS inlet increases, the lower charge state 8+, and 9+ begin to appear however the fraction of folded protein is only about 2%

suggesting significantly unfolded protein. This is likely due to similar reasons as discussed for nano-LEMS measurement of cytochrome c. These measurements indicate that protein folding is governed by the time that the protein spends in the ammonium acetate solution and the effective pH of the ES solution after acid denatured protein interacts with the ES droplets containing ammonium acetate. In the case of myoglobin even though the time for protein folding is similar, the lower fraction of folded protein suggests that a slightly higher pH is required for apo-myoglobin to maintain its native conformation in comparison cytochrome c.

5.5 Conclusions

The lifetime of laser vaporized liquid droplets in LEMS and nano-LEMS measurements are found to depend on the initial size of the electrospray droplets. The decrease in initial diameter of the ES droplets when using a nanospray emitter with smaller inner diameter (30 μM) in comparison with the electrospray emitter (124 μM) resulted in shorter droplet lifetime. The increase in distance between spray emitter to laser vaporized spot also resulted in the decrease in droplet lifetime for both LEMS and nano-LEMS measurements. This suggests that the laser vaporized liquid droplet is interacting with smaller droplets as the distance between the spray emitter to laser vaporized spot increases. The increase in temperature of the drying gas also resulted in a shorter lifetime for laser vaporized liquid droplets for both LEMS and nano-LEMS measurements, which is likely due to efficient desolvation of the laser vaporized droplets upon interaction with electrospray droplets. If we assume that the reaction in rapidly desolvation electrospray droplets increase by ~ 1 to 3 orders of magnitude the shortest

lifetime for nano-LEMS measurement is between 19 μs and 190 ns for the drying gas temperature of 350^{o}C at the spray emitter to MS inlet distance of 6.4 mm.

Protein charge state distribution measured as a function of droplet lifetime showed higher folded protein fraction for acid-denatured cytochrome c and myoglobin in ammonium acetate solution for longer droplet lifetime. This suggests the possibility of detecting intermediate states during protein folding processes when schematically varying the experimental parameters for LEMS and nano-LEMS measurements coupled with ion-mobility measurements. Finally, these results indicate that LEMS and nano-LEMS setup can be used to obtain time resolved information from the given reaction system, and early events of protein folding/unfolding processes during electrospray ionization.

5.6 References

1. Kandori, H.; Sasabe, H.; Mimuro, M. Direct Determination of a Lifetime of the S2 State of. beta.-Carotene by Femtosecond Time-Resolved Fluorescence Spectroscopy. *J. Am. Chem. Soc.* **1994,** (116), 2671-2672.

2. Lian, T.; Bromberg, S. E.; Asplund, M. C.; Yang, H.; Harris, C. Femtosecond infrared studies of the dissociation and dynamics of transition metal carbonyls in solution. *J. Phys. Chem.* **1996,** (100), 11994-12001.

3. Johnson, K. A. Transient-State Kinetic Analysis of Enzyme Reaction Pathways. *Enzymes.* **1992,** (20), 1-61.

4. Bergt, M.; Brixner, T.; Dietl, C.; Kiefer, B.; Gerber, G. Time-resolved organometallic photochemistry: Femtosecond fragmentation and adaptive control of CpFe (CO) 2X (X= Cl, Br, I). *J. Organomet. Chem.* **2002,** (661), 199-209.

5. Cheng, S.; Wu, Q.; Xiao, H.; Chen, H. Online Monitoring of Enzymatic Reactions Using Time-Resolved Desorption Electrospray Ionization Mass Spectrometry. *Anal. Chem.* **2017,** (89), 2338-2344.

6. Mortensen, D. N.; Williams, E. R. Ultrafast (1 μs) mixing and fast protein folding in nanodrops monitored by mass spectrometry. *J. Am. Chem. Soc.* **2016,** (138), 3453-3460.

7. Sogbein, O. O.; Simmons, D. A.; Konermann, L. Effects of pH on the kinetic reaction mechanism of myoglobin unfolding studied by time-resolved electrospray ionization mass spectrometry. *J. Am. Soc. Mass Spectrom.* **2000,** (11), 312-319.

8. Zechel, D. L.; Konermann, L.; Withers, S. G.; Douglas, D. Pre-steady state kinetic analysis of an enzymatic reaction monitored by time-resolved electrospray ionization mass spectrometry. *Biochemistry.* **1998,** (37), 7664-7669.

9. Kolakowski, B. M.; Simmons, D. A.; Konermann, L. Stopped-flow electrospray ionization mass spectrometry: a new method for studying chemical reaction kinetics in solution. *Rapid Commun. Mass Spectrom.* **2000,** (14), 772-776.

10. Konermann, L.; Collings, B.; Douglas, D. Cytochrome c folding kinetics studied by time-resolved electrospray ionization mass spectrometry. *Biochemistry.* **1997,** (36), 5554-5559.

11. Carroll, B.; Hidrovo, C. Experimental investigation of inertial mixing in colliding droplets. *Heat Transfer Eng.* **2013,** (34), 120-130.

12. Perry, R. H.; Splendore, M.; Chien, A.; Davis, N. K.; Zare, R. N. Detecting reaction intermediates in liquids on the millisecond time scale using desorption electrospray ionization. *Angewandte Chemie.* **2011,** (123), 264-268.

13. Marquez, C. A.; Wang, H.; Fabbretti, F.; Metzger, J. r. O. Electron-transfer-catalyzed dimerization of trans-anethole: Detection of the distonic tetramethylene radical cation intermediate by extractive electrospray ionization mass spectrometry. *J. Am. Chem. Soc.* **2008,** (130), 17208-17209.

14. Lee, J. K.; Kim, S.; Nam, H. G.; Zare, R. N. Microdroplet fusion mass spectrometry for fast reaction kinetics. *Proc. Natl. Acad. Sci.* **2015,** (112), 3898-3903.

15. Mortensen, D. N.; Williams, E. R. Theta-glass capillaries in electrospray ionization: rapid mixing and short droplet lifetimes. *Anal. Chem.* **2014,** (86), 9315-9321.

16. Mark, L.; Gill, M.; Mahut, M.; Derrick, P. Dual nano-electrospray for probing solution interactions and fast reactions of complex biomolecules. *Eur. J. Mass Spectrom.* **2012,** (18), 439.

17. Juraschek, R.; Dülcks, T.; Karas, M. Nanoelectrospray—more than just a minimized-flow electrospray ionization source. *J. Am. Soc. Mass Spectrom.* **1999,** (10), 300-308.

18. Tang, K.; Gomez, A. Monodisperse electrosprays of low electric conductivity liquids in the cone-jet mode. *J. Colloid Interface Sci.* **1996,** (184), 500-511.

19. Li, Y.; Cole, R. B. Shifts in peptide and protein charge state distributions with varying spray tip orifice diameter in nanoelectrospray fourier transform ion cycltron resonance mass spectrometry. *Anal. Chem.* **2003,** (75), 5739-5746.

20. Gatlin, C. L.; Turecek, F. Acidity determination in droplets formed by electrospraying methanol-water solutions. *Anal. Chem.* **1994,** (66), 712-718.

21. Girod, M.; Dagany, X.; Antoine, R.; Dugourd, P. Relation between charge state distributions of peptide anions and pH changes in the electrospray plume. A mass spectrometry and optical spectroscopy investigation. *Int. J. Mass Spectrom.* **2011,** (308), 41-48.

22. Badu-Tawiah, A. K.; Campbell, D. I.; Cooks, R. G. Reactions of microsolvated organic compounds at ambient surfaces: droplet velocity, charge state, and solvent effects. *J. Am. Soc. Mass Spectrom.* **2012,** (23), 1077-1084.

23. Badu-Tawiah, A. K.; Campbell, D. I.; Cooks, R. G. Accelerated C–N bond formation in dropcast thin films on ambient surfaces. *J. Am. Soc. Mass Spectrom.* **2012,** (23), 1461-1468.

24. Badu-Tawiah, A. K.; Li, A.; Jjunju, F. P.; Cooks, R. G. Peptide cross-linking at ambient surfaces by reactions of nanosprayed molecular cations. *Angew. Chem. International Edition.* **2012,** (51), 9417-9421.

25. Girod, M.; Moyano, E.; Campbell, D. I.; Cooks, R. G. Accelerated bimolecular reactions in microdroplets studied by desorption electrospray ionization mass spectrometry. *Chemical Science.* **2011,** (2), 501-510.

26. Brady, J. J.; Judge, E. J.; Levis, R. J. Nonresonant femtosecond laser vaporization of aqueous protein preserves folded structure. *Proc. Natl. Acad. Sci.* **2011,** (108), 12217-12222.

27. Karki, S.; Flanigan, P. M.; Perez, J. J.; Archer, J. J.; Levis, R. J. Increasing protein charge state when using laser electrospray mass spectrometry. *J. Am. Soc. Mass Spectrom.* **2015,** (26), 706-715.

28. Karki, S.; Sistani, H.; Archer, J. J.; Shi, F.; Levis, R. J. Isolating Protein Charge State Reduction in Electrospray Droplets Using Femtosecond Laser Vaporization. *J. Am. Soc. Mass Spectrom.* **2017,** 1-9.

29. Perez, J. J.; Flanigan IV, P. M.; Karki, S.; Levis, R. J. Laser electrospray mass spectrometry minimizes ion suppression facilitating quantitative mass spectral response for multicomponent mixtures of proteins. *Anal. Chem.* **2013,** (85), 6667-6673.

30. Judge, E. J.; Brady, J. J.; Dalton, D.; Levis, R. J. Analysis of pharmaceutical compounds from glass, fabric, steel, and wood surfaces at atmospheric pressure using spatially resolved, nonresonant femtosecond laser vaporization electrospray mass spectrometry. *Anal. Chem.* **2010,** (82), 3231-3238.

31. Judge, E. J.; Brady, J. J.; Barbano, P. E.; Levis, R. J. Nonresonant femtosecond laser vaporization with electrospray postionization for ex vivo plant tissue typing using compressive linear classification. *Anal. Chem.* **2011,** (83), 2145-2151.

32. Shi, F.; Flanigan IV, P. M.; Archer, J. J.; Levis, R. J. Ambient Molecular Analysis of Biological Tissue Using Low-Energy, Femtosecond Laser Vaporization and Nanospray Postionization Mass Spectrometry. *J. Am. Soc. Mass Spectrom.* **2016,** (27), 542-551.

33. Flanigan IV, P. M.; Shi, F.; Archer, J. J.; Levis, R. J. Internal Energy Deposition for Low Energy, Femtosecond Laser Vaporization and Nanospray Post-ionization Mass Spectrometry using Thermometer Ions. *J. Am. Soc. Mass Spectrom.* **2015,** (26), 716-724.

34. Miao, Z.; Chen, H.; Liu, P.; Liu, Y. Development of submillisecond time-resolved mass spectrometry using desorption electrospray ionization. *Anal. Chem.* **2011,** (83), 3994-3997.

35. Karayannis, M. Comparative kinetic study for rate constant determination of the reaction of ascorbic acid with 2, 6-dichlorophenolindophenol. *Talanta.* **1976,** (23), 27-30.

36. Creighton, T. E., Proteins: structures and molecular properties, Macmillan, (1993).

37. Griko, Y. V.; Privalov, P.; Venyaminov, S. Y.; Kutyshenko, V. Thermodynamic study of the apomyoglobin structure. *J. Mol. Biol.* **1988,** (202), 127-138.

38. Goto, Y.; Fink, A. L. Phase diagram for acidic conformational states of apomyoglobin. *J. Mol. Biol.* **1990,** (214), 803-805.

39. Konno, T. Conformational diversity of acid-denatured cytochrome c studied by a matrix analysis of far-UV CD spectra. *Protein Sci.* **1998,** (7), 975-982.

40. Shastry, M. R.; Luck, S. D.; Roder, H. A continuous-flow capillary mixing method to monitor reactions on the microsecond time scale. *Biophys. J.* **1998,** (74), 2714-2721.

CHAPTER 6

SUMMARY AND OUTLOOK

The development of ambient mass spectrometric techniques capable of delivering non-volatile biological macromolecules intact into the gas phase is of growing interest for native mass spectrometry measurements. Previous studies using laser electrospray mass spectrometry (LEMS) have demonstrated the ability of femtosecond laser pulses to transfer intact protein into the electrospray droplets maintaining the solution phase structure. In this dissertation, electrospray solvents were doped with charge altering agents (supercharging regent and/or charge reducing additive) in order to manipulate protein charge state distribution after laser vaporized protein interacts with the electrospray droplets containing desired solution additive. Laser vaporization of condensed phase protein into electrospray droplets containing denaturing electrospray solution and supercharging reagent resulted in the increase in ion abundance of higher charge states making LEMS a suitable technique for Top-down protein sequencing experiments. Conversely, electrospray solution doped with additives varying in gas phase basicity resulted in charge state reduction for both native and acid denatured proteins. The ability of LEMS to decouple droplet processes from processes occurring in the bulk solution phase allows monitoring protein folding within the electrospray droplet.

The ability of LEMS to detect proteins from solution with high matrix effects was thoroughly examined by adding sodium chloride into protein solutions. LEMS was shown to be a better technique to detect protein molecules from solution with high salt

concentration in comparison with conventional electrospray. The detection of protonated protein feature as the dominating peak in the mass spectra for the salt concentration up to 250 mM NaCl was explained based on the difference in partitioning of laser vaporized protein and salt into the charged electrospray droplets. Using the forward rate constant for the reduction of 2, 6 –Dichloroindophenol by L-ascorbic acid in the bulk solution phase, electrospray and nano-spray droplet lifetimes were calculated for LEMS and nano-LEMS measurements, respectively.

These experiments contributed to a greater understanding of protein folding and unfolding processes within the electrospray droplet in a millisecond to microsecond timescale. The ability of LEMS to analyze molecules from solution with matrix interferences suggests that biomolecules that require higher salt concentrations to mimic the intracellular environment can be successfully analyzed without perturbing their structure. These measurements also have laid ground work for Top-down protein sequencing experiments, kinetics of protein folding and unfolding processes coupled with ion mobility mass spectrometer, direct analysis of marine samples and membrane proteins without the need of sample preprocessing.

BIBLIOGRAPHY

Aberth, W.; Straub, K. M.; Burlingame, A. Secondary ion mass spectrometry with cesium ion primary beam and liquid target matrix for analysis of bioorganic compounds. *Anal. Chem.* **1982,** (54), 2029-2034.

Arakawa, R.; Tachiashiki, S.; Matsuo, T. Detection of Reaction Intermediates: Photosubstitution of (Polypyridine) ruthenium (II) Complexes Using On-Line Electrospray Mass Spectrometry. Anal. Chem. **1995,** (67), 4133-4138.

Badu-Tawiah, A. K.; Campbell, D. I.; Cooks, R. G. Reactions of microsolvated organic compounds at ambient surfaces: droplet velocity, charge state, and solvent effects. *J. Am. Soc. Mass Spectrom.* **2012,** (23), 1077-1084.

Badu-Tawiah, A. K.; Campbell, D. I.; Cooks, R. G. Accelerated C–N bond formation in dropcast thin films on ambient surfaces. *J. Am. Soc. Mass Spectrom.* **2012,** (23), 1461-1468.

Badu-Tawiah, A. K.; Li, A.; Jjunju, F. P.; Cooks, R. G. Peptide cross-linking at ambient surfaces by reactions of nanosprayed molecular cations. *Angew. Chem. Int. Edit.* **2012,** (51), 9417-9421.

Ballew, R.; Sabelko, J.; Gruebele, M. Direct observation of fast protein folding: the initial collapse of apomyoglobin. *Proc. Natl. Acad. Sci. U.S.A.* **1996,** (93), 5759-5764.

Banerjee, S. Induction of protein conformational change inside the charged electrospray droplet. *J. Mass Spectrom.* **2013,** (48), 193-204.

Barber, M.; Bordoli, R. S.; Sedgwick, R. D.; Tyler, A. N. Fast atom bombardment of solids (FAB): A new ion source for mass spectrometry. *Journal of the Chemical Society, Chem. Commun.* **1981,** 325-327.

Bauer, K.-H.; Knepper, T. P.; Maes, A.; Schatz, V.; Voihsel, M. Analysis of polar organic micropollutants in water with ion chromatography–electrospray mass spectrometry. *J. Chromatogr. A.* **1999,** (837), 117-128.

Bergt, M.; Brixner, T.; Dietl, C.; Kiefer, B.; Gerber, G. Time-resolved organometallic photochemistry: Femtosecond fragmentation and adaptive control of CpFe (CO) 2X (X= Cl, Br, I). *J. Organomet. Chem.* **2002,** (661), 199-209.

Brady, J. J.; Judge, E. J.; Levis, R. J. Mass spectrometry of intact neutral macromolecules using intense non-resonant femtosecond laser vaporization with electrospray post-ionization. *Rapid Commun. Mass Spectrom.* **2009,** (23), 3151-3157.

Brady, J. J.; Judge, E. J.; Levis, R. J. Identification of explosives and explosive formulations using laser electrospray mass spectrometry. *Rapid Commun. Mass Spectrom.* **2010,** (24), 1659-1664.

Brady, J. J.; Judge, E. J.; Levis, R. J. Nonresonant femtosecond laser vaporization of aqueous protein preserves folded structure. *Proc. Natl. Acad. Sci. U.S.A.* **2011,** (108), 12217-12222.

Brady, J. J.; Judge, E. J.; Levis, R. J. Analysis of amphiphilic lipids and hydrophobic proteins using nonresonant femtosecond laser vaporization with electrospray post-ionization. *J. Am. Soc. Mass Spectrom.* **2011,** (22), 762-772.

Brady, J. J.; Judge, E. J.; Levis, R. J. Reply to Breuker et al.: How laser electrospray mass spectrometry (LEMS) measures condensed phase protein structure, not vacuum structure. *Proc. Natl. Acad. Sci. U.S.A.* **2012,** (109), E207-E207.

Bringer, M. R.; Gerdts, C. J.; Song, H.; Tice, J. D.; Ismagilov, R. F. Microfluidic systems for chemical kinetics that rely on chaotic mixing in droplets. *Philos. Trans. R. Soc. Lond. A.* **2004,** (362), 1087-1104.

Carroll, B.; Hidrovo, C. Experimental investigation of inertial mixing in colliding droplets. *Heat Transfer Eng.* **2013,** (34), 120-130.

Cassou, C. A.; Williams, E. R. Anions in electrothermal supercharging of proteins with electrospray ionization follow a reverse Hofmeister series. *Anal. Chem.* **2014,** (86), 1640-1647.

Catalina, M. I.; van den Heuvel, R. H.; van Duijn, E.; Heck, A. J. Decharging of globular proteins and protein complexes in electrospray. *Chem-Eur. J.* **2005,** (11), 960-968.

Cech, N. B.; Enke, C. G. Practical implications of some recent studies in electrospray ionization fundamentals. *Mass Spectrom. Rev.* **2001,** (20), 362-387.

Chang, D.-Y.; Lee, C.-C.; Shiea, J. Detecting large biomolecules from high-salt solutions by fused-droplet electrospray ionization mass spectrometry. *Anal. Chem.* **2002,** (74), 2465-2469.

Chen, H.; Talaty, N. N.; Takáts, Z.; Cooks, R. G. Desorption electrospray ionization mass spectrometry for high-throughput analysis of pharmaceutical samples in the ambient environment. *Anal. Chem.* **2005,** (77), 6915-6927.

Chen, H.; Touboul, D.; Jecklin, M. C.; Zheng, J.; Luo, M.; Zenobi, R. Manipulation of charge states of biopolymer ions by atmospheric pressure ion/molecule reactions implemented in an extractive electrospray ionization source. *Eur. J. Mass.* **2007,** (13), 273-280.

Chen, H.; Venter, A.; Cooks, R. G. Extractive electrospray ionization for direct analysis of undiluted urine, milk and other complex mixtures without sample preparation. *Chem. Commun.* **2006,** 2042-2044.

Cheng, S.; Wu, Q.; Xiao, H.; Chen, H. Online Monitoring of Enzymatic Reactions Using Time-Resolved Desorption Electrospray Ionization Mass Spectrometry. *Anal. Chem.* **2017,**

Chowdhury, S. K.; Katta, V.; Chait, B. T. Probing conformational changes in proteins by mass spectrometry. *J. Am. Chem. Soc.* **1990,** (112), 9012-9013.

Clemmer, D. E.; Hudgins, R. R.; Jarrold, M. F. Naked protein conformations: cytochrome c in the gas phase. *J. Am. Chem. Soc.* **1995,** (117), 10141-10142.

Cohen, S. L.; Ferré-D'Amaré, A. R.; Burley, S. K.; Chait, B. T. Probing the solution structure of the DNA-binding protein Max by a combination of proteolysis and mass spectrometry. *Protein Sci.* **1995,** (4), 1088.

Cole, R. B. Some tenets pertaining to electrospray ionization mass spectrometry. *J. Mass Spectrom.* **2000,** (35), 763-772.

Cook, K. D.; Todd, P. J.; Friar, D. H. Physical properties of matrices used for fast atom bombardment. *Biol. Mass Spectrom.* **1989,** (18), 492-497.

Coon, J. J.; Harrison, W. Laser desorption-atmospheric pressure chemical ionization mass spectrometry for the analysis of peptides from aqueous solutions. *Anal. Chem.* **2002,** (74), 5600-5605.

Coon, J. J.; McHale, K. J.; Harrison, W. Atmospheric pressure laser desorption/chemical ionization mass spectrometry: a new ionization method based on existing themes. *Rapid Commun. Mass Spectrom.* **2002,** (16), 681-685.

Cotte-Rodríguez, I.; Takáts, Z.; Talaty, N.; Chen, H.; Cooks, R. G. Desorption electrospray ionization of explosives on surfaces: sensitivity and selectivity enhancement by reactive desorption electrospray ionization. *Anal. Chem.* **2005,** (77), 6755-6764.

Creighton, T. E., Proteins: structures and molecular properties, W.H. Freeman & Co, New York (1993).

De La Mora, J. F. Electrospray ionization of large multiply charged species proceeds via Dole's charged residue mechanism. *Anal. Chim. Acta.* **2000,** (406), 93-104.

DeWitt, M. J.; Levis, R. J. Near-infrared femtosecond photoionization/dissociation of cyclic aromatic hydrocarbons. *J. Chem. Phys.* **1995,** (102), 8670-8673.

DeWitt, M. J.; Peters, D. W.; Levis, R. J. Photoionization/dissociation of alkyl substituted benzene molecules using intense near-infrared radiation. *Chem. Phys.* **1997,** (218), 211-223.

Dill, A. L.; Eberlin, L. S.; Zheng, C.; Costa, A. B.; Ifa, D. R.; Cheng, L.; Masterson, T. A.; Koch, M. O.; Vitek, O.; Cooks, R. G. Multivariate statistical differentiation of renal cell carcinomas based on lipidomic analysis by ambient ionization imaging mass spectrometry. *Anal. Bioanal. Chem.* **2010,** (398), 2969-2978.

Dixon, R. B.; Sampson, J. S.; Hawkridge, A. M.; Muddiman, D. C. Ambient aerodynamic ionization source for remote analyte sampling and mass spectrometric analysis. *Anal. Chem.* **2008,** (80), 5266-5271.

Dole, M.; Mack, L.; Hines, R.; Mobley, R.; Ferguson, L.; Alice, M. d. Molecular beams of macroions. *J. Chem. Phys.* **1968,** (49), 2240-2249.

Douglass, K. A.; Venter, A. R. Investigating the role of adducts in protein supercharging with sulfolane. *J. Am. Soc. Mass Spectrom.* **2012,** (23), 489-497.

Eberlin, L. S.; Dill, A. L.; Costa, A. B.; Ifa, D. R.; Cheng, L.; Masterson, T.; Koch, M.; Ratliff, T. L.; Cooks, R. G. Cholesterol sulfate imaging in human prostate cancer tissue by desorption electrospray ionization mass spectrometry. *Anal. Chem.* **2010,** (82), 3430-3434.

Fenn, J. B. Ion formation from charged droplets: roles of geometry, energy, and time. *J. Am. Soc. Mass Spectrom.* **1993,** (4), 524-535.

Fenn, J. B.; Mann, M.; Meng, C. K.; Wong, S. F.; Whitehouse, C. M. Electrospray ionization for mass spectrometry of large biomolecules. *Science.* **1989,** (246), 64-71.

Fidalgo, L. M.; Abell, C.; Huck, W. T. Surface-induced droplet fusion in microfluidic devices. *Lab Chip.* **2007,** (7), 984-986.

Fisher, C. M.; Kharlamova, A.; McLuckey, S. A. Affecting protein charge state distributions in nano-electrospray ionization via in-spray solution mixing using Theta capillaries. *Anal. Chem.* **2014,** (86), 4581-4588.

Flanigan IV, P. M.; Brady, J. J.; Judge, E. J.; Levis, R. J. Determination of inorganic improvised explosive device signatures using laser electrospray mass spectrometry detection with offline classification. *Anal. Chem.* **2011,** (83), 7115-7122.

Flanigan IV, P. M.; Perez, J. J.; Karki, S.; Levis, R. J. Quantitative measurements of small molecule mixtures using laser electrospray mass spectrometry. *Anal. Chem.* **2013,** (85), 3629-3637.

Flanigan IV, P. M.; Radell, L. L.; Brady, J. J.; Levis, R. J. Differentiation of eight phenotypes and discovery of potential biomarkers for a single plant organ class using laser electrospray mass spectrometry and multivariate statistical analysis. *Anal. Chem.* **2012,** (84), 6225-6232.

Flanigan IV, P. M.; Shi, F.; Archer, J. J.; Levis, R. J. Internal Energy Deposition for Low Energy, Femtosecond Laser Vaporization and Nanospray Post-ionization Mass Spectrometry using Thermometer Ions. *J. Am. Soc. Mass Spectrom.* **2015,** (26), 716-724.

Flanigan, P.; Levis, R. Ambient Femtosecond Laser Vaporization and Nanosecond Laser Desorption Electrospray Ionization Mass Spectrometry. *Annu. Rev. Anal. Chem.* **2014,** (7), 229-256.

Flanigan, P. M.; Shi, F.; Archer, J. J.; Levis, R. J. Internal energy deposition for low energy, femtosecond laser vaporization and nanospray post-ionization mass spectrometry using thermometer ions. *J. Am. Soc. Mass Spectrom.* **2015,** (26), 716-724.

Flanigan, P. M.; Shi, F.; Perez, J. J.; Karki, S.; Pfeiffer, C.; Schafmeister, C.; Levis, R. J. Determination of internal energy distributions of laser electrospray mass spectrometry using thermometer ions and other biomolecules. *J. Am. Soc. Mass Spectrom.* **2014,** (25), 1572-1582.

Flick, T. G.; Cassou, C. A.; Chang, T. M.; Williams, E. R. Solution additives that desalt protein ions in native mass spectrometry. *Anal. Chem.* **2012,** (84), 7511-7517.

Flick, T. G.; Merenbloom, S. I.; Williams, E. R. Anion effects on sodium ion and acid molecule adduction to protein ions in electrospray ionization mass spectrometry. *J. Am. Soc. Mass Spectrom.* **2011,** (22), 1968-1977.

Flick, T. G.; Williams, E. R. Supercharging with trivalent metal ions in native mass spectrometry. *J. Am. Soc. Mass Spectrom.* **2012,** (23), 1885-1895.

Fligge, T. A.; Kast, J.; Bruns, K.; Przybylski, M. Direct monitoring of protein–chemical reactions utilising nanoelectrospray mass spectrometry. *J. Am. Soc. Mass Spectrom.* **1999,** (10), 112-118.

Frederikse, H.; Lide, D. CRC handbook of chemistry and physics. *CRC, Boca Raton.* **1996.**

Frey, B. L.; Lin, Y.; Westphall, M. S.; Smith, L. M. Controlling gas-phase reactions for efficient charge reduction electrospray mass spectrometry of intact proteins. *J. Am. Soc. Mass Spectrom.* **2005,** (16), 1876-1887.

Gatlin, C. L.; Turecek, F. Acidity determination in droplets formed by electrospraying methanol-water solutions. *Anal. Chem.* **1994,** (66), 712-718.

Girod, M.; Dagany, X.; Antoine, R.; Dugourd, P. Relation between charge state distributions of peptide anions and pH changes in the electrospray plume. A mass spectrometry and optical spectroscopy investigation. *Int. J. Mass Spectrom.*. **2011,** (308), 41-48.

Girod, M.; Moyano, E.; Campbell, D. I.; Cooks, R. G. Accelerated bimolecular reactions in microdroplets studied by desorption electrospray ionization mass spectrometry. *Chem. Sci.* **2011,** (2), 501-510.

Girod, M.; Shi, Y.; Cheng, J.-X.; Cooks, R. G. Desorption electrospray ionization imaging mass spectrometry of lipids in rat spinal cord. *J. Am. Soc. Mass Spectrom.* **2010,** (21), 1177-1189.

Gobeli, D.; El-Sayed, M. Change in the mechanism of laser multiphoton ionization-dissociation in benzaldehyde by changing the laser pulse width. *J. Phys. Chem.* **1985,** (89), 3426-3429.

Good, D. M.; Wirtala, M.; McAlister, G. C.; Coon, J. J. Performance characteristics of electron transfer dissociation mass spectrometry. *Mol. Cell. Proteomics.* **2007,** (6), 1942-1951.

Goodman, J. M.; Kirby, P. D.; Haustedt, L. O. Some calculations for organic chemists: boiling point variation, Boltzmann factors and the Eyring equation. *Tetrahedron Lett.* **2000,** (41), 9879-9882.

Goto, Y.; Fink, A. L. Phase diagram for acidic conformational states of apomyoglobin. *J. Mol. Biol.* **1990,** (214), 803-805.

Grandori, R. Detecting equilibrium cytochrome c folding intermediates by electrospray ionisation mass spectrometry: Two partially folded forms populate the molten-globule state. *Protein Sci.* **2002,** (11), 453-458.

Grandori, R. Origin of the conformation dependence of protein charge-state distributions in electrospray ionization mass spectrometry. *J. Mass Spectrom.* **2003,** (38), 11-15.

Green, M. K.; Lebrilla, C. B. Ion-molecule reactions as probes of gas-phase structures of peptides and proteins. *Mass Spectrom. Rev.* **1997,** (16), 53-71.

Grey, A. C.; Chaurand, P.; Caprioli, R. M.; Schey, K. L. MALDI imaging mass spectrometry of integral membrane proteins from ocular lens and retinal tissue. *J. Proteome Res.* **2009,** (8), 3278-3283.

Griko, Y. V.; Privalov, P.; Venyaminov, S. Y.; Kutyshenko, V. Thermodynamic study of the apomyoglobin structure. *J. Mol. Biol.* **1988,** (202), 127-138.

Grimm, R. L.; Beauchamp, J. Evaporation and discharge dynamics of highly charged droplets of heptane, octane, and p-xylene generated by electrospray ionization. *Anal. Chem.* **2002,** (74), 6291-6297.

Hall, Z.; Robinson, C. V. Do charge state signatures guarantee protein conformations? *J. Am. Soc. Mass Spectrom.* **2012,** (23), 1161-1168.

Hedges, J. B.; Vahidi, S.; Yue, X.; Konermann, L. Effects of ammonium bicarbonate on the electrospray mass spectra of proteins: evidence for bubble-induced unfolding. *Anal. Chem.* **2013,** (85), 6469-6476.

Herron, W. J.; Goeringer, D. E.; McLuckey, S. A. Ion-ion reactions in the gas phase: Proton transfer reactions of protonated pyridine with multiply charged oligonucleotide anions. *J. Am. Soc. Mass Spectrom.* **1995,** (6), 529-532.

Hinsch, A.; Buchholz, M.; Odinga, S.; Borkowski, C.; Koop, C.; Izbicki, J. R.; Wurlitzer, M.; Krech, T.; Wilczak, W.; Steurer, S. MALDI imaging mass spectrometry reveals multiple clinically relevant masses in colorectal cancer using large-scale tissue microarrays. *J. Mass Spectrom.* **2017,** (52), 165-173.

Hogan Jr, C. J.; Carroll, J. A.; Rohrs, H. W.; Biswas, P.; Gross, M. L. Combined charged residue-field emission model of macromolecular electrospray ionization. *Anal. Chem.* **2008,** (81), 369-377.

Hogan Jr, C. J.; Loo, R. R. O.; Loo, J. A.; de la Mora, J. F. Ion mobility–mass spectrometry of phosphorylase B ions generated with supercharging reagents but in charge-reducing buffer. *Phys. Chem. Chem. Phys.* **2010,** (12), 13476-13483.

Horn, D. M.; Breuker, K.; Frank, A. J.; McLafferty, F. W. Kinetic intermediates in the folding of gaseous protein ions characterized by electron capture dissociation mass spectrometry. *J. Am. Chem. Soc.* **2001,** (123), 9792-9799.

Huber, C. G.; Buchmeiser, M. R. On-line cation exchange for suppression of adduct formation in negative-ion electrospray mass spectrometry of nucleic acids. *Anal. Chem.* **1998,** (70), 5288-5295.

Iavarone, A. T.; Jurchen, J. C.; Williams, E. R. Effects of solvent on the maximum charge state and charge state distribution of protein ions produced by electrospray ionization. *J. Am. Soc. Mass Spectrom.* **2000,** (11), 976-985.

Iavarone, A. T.; Jurchen, J. C.; Williams, E. R. Supercharged protein and peptide ions formed by electrospray ionization. *Anal. Chem.* **2001,** (73), 1455-1460.

Iavarone, A. T.; Udekwu, O. A.; Williams, E. R. Buffer loading for counteracting metal salt-induced signal suppression in electrospray ionization. *Anal. Chem.* **2004,** (76), 3944-3950.

Iavarone, A. T.; Williams, E. R. Mechanism of charging and supercharging molecules in electrospray ionization. *J. Am. Chem. Soc.* **2003,** (125), 2319-2327.

Ifa, D. R.; Wiseman, J. M.; Song, Q.; Cooks, R. G. Development of capabilities for imaging mass spectrometry under ambient conditions with desorption electrospray ionization (DESI). *Int. J. Mass Spectrom.*. **2007,** (259), 8-15.

Ikonomou, M. G.; Blades, A. T.; Kebarle, P. Electrospray-ion spray: a comparison of mechanisms and performance. *Anal. Chem.* **1991,** (63), 1989-1998.

Jackson, A. U.; Talaty, N.; Cooks, R. G.; Van Berkel, G. J. Salt tolerance of desorption electrospray ionization (DESI). *J. Am. Soc. Mass Spectrom.* **2007,** (18), 2218-2225.

Jasper, J. J.; Wedlick, H. L. Effect of Temperature on the Surface Tension and Density of Trifluoroacetic Acid. *J. Chem. Eng. Data*. **1964,** (9), 446-447.

Jiang, Y.; Hofstadler, S. A. A highly efficient and automated method of purifying and desalting PCR products for analysis by electrospray ionization mass spectrometry. *Anal. Biochem.* **2003,** (316), 50-57.

Johnson, K. A. 1 Transient-State Kinetic Analysis of Enzyme Reaction Pathways. *Enzymes.*. **1992,** (20), 1-61.

Judge, E. J.; Brady, J. J.; Barbano, P. E.; Levis, R. J. Nonresonant femtosecond laser vaporization with electrospray postionization for ex vivo plant tissue typing using compressive linear classification. *Anal. Chem.* **2011,** (83), 2145-2151.

Judge, E. J.; Brady, J. J.; Dalton, D.; Levis, R. J. Analysis of pharmaceutical compounds from glass, fabric, steel, and wood surfaces at atmospheric pressure using spatially resolved, nonresonant femtosecond laser vaporization electrospray mass spectrometry. *Anal. Chem.* **2010,** (82), 3231-3238.

Juraschek, R.; Dülcks, T.; Karas, M. Nanoelectrospray—more than just a minimized-flow electrospray ionization source. *J. Am. Soc. Mass Spectrom.* **1999,** (10), 300-308.

Kaltashov, I. A.; Abzalimov, R. R. Do ionic charges in ESI MS provide useful information on macromolecular structure? *J. Am. Soc. Mass Spectrom.* **2008,** (19), 1239-1246.

Kandori, H.; Sasabe, H.; Mimuro, M. Direct Determination of a Lifetime of the S2 State of. beta.-Carotene by Femtosecond Time-Resolved Fluorescence Spectroscopy. *J. Am. Chem. Soc.* **1994,** (116), 2671-2672.

Karas, M.; Bachmann, D.; Bahr, U. e.; Hillenkamp, F. Matrix-assisted ultraviolet laser desorption of non-volatile compounds. *Int. J. Mass Spectrom. and ion processes.* **1987,** (78), 53-68.

Karas, M.; Bachmann, D.; Hillenkamp, F. Influence of the wavelength in high-irradiance ultraviolet laser desorption mass spectrometry of organic molecules. *Anal. Chem.* **1985,** (57), 2935-2939.

Karayannis, M. Comparative kinetic study for rate constant determination of the reaction of ascorbic acid with 2, 6-dichlorophenolindophenol. *Talanta.* **1976,** (23), 27-30.

Karki, S.; Flanigan, P. M.; Perez, J. J.; Archer, J. J.; Levis, R. J. Increasing protein charge state when using laser electrospray mass spectrometry. *J. Am. Soc. Mass Spectrom.* **2015,** (26), 706-715.

Karki, S.; Levis, R. J. Measurement of lifetime for laser vaporized liquid droplets coupled with electrospray and nano-spray postionization mass spectrometry. *Manuscript in preparation.* **2017.**

Karki, S.; Shi, F.; Archer, J. J.; Sistani, H.; Levis, R. J. Direct analysis of proteins from solutions with high salt concentration using laser electrospray mass spectrometry. *Submitted to Analytical Chemistry.* **2017.**

Karki, S.; Sistani, H.; Archer, J. J.; Shi, F.; Levis, R. J. Isolating Protein Charge State Reduction in Electrospray Droplets Using Femtosecond Laser Vaporization. *J. Am. Soc. Mass Spectrom.* **2017,** (28) 470-478.

Kebarle, P.; Tang, L. From ions in solution to ions in the gas phase-the mechanism of electrospray mass spectrometry. *Anal. Chem.* **1993,** (65), 972A-986A.

Kharlamova, A.; DeMuth, J. C.; McLuckey, S. A. Vapor treatment of electrospray droplets: evidence for the folding of initially denatured proteins on the sub-millisecond time-scale. *J. Am. Soc. Mass Spectrom.* **2012,** (23), 88-101.

Kharlamova, A.; Prentice, B. M.; Huang, T.-Y.; McLuckey, S. A. Electrospray droplet exposure to gaseous acids for the manipulation of protein charge state distributions. *Anal. Chem.* **2010,** (82), 7422-7429.

Kolakowski, B. M.; Simmons, D. A.; Konermann, L. Stopped-flow electrospray ionization mass spectrometry: a new method for studying chemical reaction kinetics in solution. *Rapid Commun. Mass Spectrom.* **2000,** (14), 772-776.

Konermann, L.; Ahadi, E.; Rodriguez, A. D.; Vahidi, S. Unraveling the mechanism of electrospray ionization. *Anal. Chem.* **2012,** (85), 2-9.

Konermann, L.; Collings, B.; Douglas, D. Cytochrome c folding kinetics studied by time-resolved electrospray ionization mass spectrometry. *Biochemistry.* **1997,** (36), 5554-5559.

Konermann, L.; Douglas, D. Acid-induced unfolding of cytochrome c at different methanol concentrations: electrospray ionization mass spectrometry specifically monitors changes in the tertiary structure. *Biochemistry.* **1997,** (36), 12296-12302.

Konermann, L.; Douglas, D. Unfolding of proteins monitored by electrospray ionization mass spectrometry: a comparison of positive and negative ion modes. *J. Am. Soc. Mass Spectrom.* **1998,** (9), 1248-1254.

Konermann, L.; Rodriguez, A. D.; Liu, J. On the formation of highly charged gaseous ions from unfolded proteins by electrospray ionization. *Anal. Chem.* **2012,** (84), 6798-6804.

Konermann, L.; Silva, E. A.; Sogbein, O. F. Electrochemically induced pH changes resulting in protein unfolding in the ion source of an electrospray mass spectrometer. *Anal. Chem.* **2001,** (73), 4836-4844.

Konno, T. Conformational diversity of acid-denatured cytochrome c studied by a matrix analysis of far-UV CD spectra. *Protein Sci.* **1998,** (7), 975-982.

Laiko, V. V.; Baldwin, M. A.; Burlingame, A. L. Atmospheric pressure matrix-assisted laser desorption/ionization mass spectrometry. *Anal. Chem.* **2000,** (72), 652-657.

Lee, J. K.; Kim, S.; Nam, H. G.; Zare, R. N. Microdroplet fusion mass spectrometry for fast reaction kinetics. *Proc. Natl. Acad. Sci. U.S.A.***2015,** (112), 3898-3903.

Lemaire, D.; Marie, G.; Serani, L.; Laprévote, O. Stabilization of gas-phase noncovalent macromolecular complexes in electrospray mass spectrometry using aqueous triethylammonium bicarbonate buffer. *Anal. Chem.* **2001,** (73), 1699-1706.

Levis, R. J.; DeWitt, M. J. Photoexcitation, ionization, and dissociation of molecules using intense near-infrared radiation of femtosecond duration. *J. Phys. Chem A.* **1999,** (103), 6493-6507.

Levis, R. J.; Menkir, G. M.; Rabitz, H. Selective bond dissociation and rearrangement with optimally tailored, strong-field laser pulses. *Science.* **2001,** (292), 709-713.

Li, Y.; Cole, R. B. Shifts in peptide and protein charge state distributions with varying spray tip orifice diameter in nanoelectrospray fourier transform ion cycltron resonance mass spectrometry. *Anal. Chem.* **2003,** (75), 5739-5746.

Li, Y.; Shrestha, B.; Vertes, A. Atmospheric pressure infrared MALDI imaging mass spectrometry for plant metabolomics. *Anal. Chem.* **2008,** (80), 407-420.

Lian, T.; Bromberg, S. E.; Asplund, M. C.; Yang, H.; Harris, C. Femtosecond infrared studies of the dissociation and dynamics of transition metal carbonyls in solution. *J. Phys. Chem.* **1996,** (100), 11994-12001.

Liebl, H. Ion microprobe mass analyzer. *J. Appl. Phys.* **1967,** (38), 5277-5283.

Liu, C.; Hofstadler, S. A.; Bresson, J. A.; Udseth, H. R.; Tsukuda, T.; Smith, R. D.; Snyder, A. P. On-line dual microdialysis with ESI-MS for direct analysis of complex biological samples and microorganism lysates. *Anal. Chem.* **1998,** (70), 1797-1801.

Liu, J.; Konermann, L. Irreversible thermal denaturation of cytochrome C studied by electrospray mass spectrometry. *J. Am. Soc. Mass Spectrom.* **2009,** (20), 819-828.

Liu, J.; Konermann, L. Cation-induced stabilization of protein complexes in the gas phase: mechanistic insights from hemoglobin dissociation studies. *J. Am. Soc. Mass Spectrom.* **2014,** (25), 595-603.

Liu, J.; Qiu, B.; Luo, H. Fingerprinting of yogurt products by laser desorption spray post-ionization mass spectrometry. *Rapid Commun. Mass Spectrom.* **2010,** (24), 1365-1370.

Liu, X.; Cole, R. B. A new model for multiply charged adduct formation between peptides and anions in electrospray mass spectrometry. *J. Am. Soc. Mass Spectrom.* **2011,** (22), 2125-2136.

Lomeli, S. H.; Peng, I. X.; Yin, S.; Ogorzalek Loo, R. R.; Loo, J. A. New reagents for increasing ESI multiple charging of proteins and protein complexes. *J. Am. Soc. Mass Spectrom.* **2010,** (21), 127-131.

Lomeli, S. H.; Yin, S.; Ogorzalek Loo, R. R.; Loo, J. A. Increasing charge while preserving noncovalent protein complexes for ESI-MS. *J. Am. Soc. Mass Spectrom.* **2009,** (20), 593-596.

Loo, J. A.; Loo, R. R. O.; Udseth, H. R.; Edmonds, C. G.; Smith, R. D. Solvent-induced conformational changes of polypeptides probed by electrospray-ionization mass spectrometry. *Rapid Commun. Mass Spectrom.* **1991,** (5), 101-105.

Loo, J. A.; Udseth, H. R.; Smith, R. D. Peptide and protein analysis by electrospray ionization-mass spectrometry and capillary electrophoresis-mass spectrometry. *Anal. Biochem.* **1989,** (179), 404-412.

Loo, R. R. O.; Lakshmanan, R.; Loo, J. A. What protein charging (and supercharging) reveal about the mechanism of electrospray ionization. *J. Am. Soc. Mass Spectrom.* **2014,** (25), 1675-1693.

Loo, R. R. O.; Smith, R. D. Investigation of the gas-phase structure of electrosprayed proteins using ion-molecule reactions. *J. Am. Soc. Mass Spectrom.* **1994,** (5), 207-220.

Loo, R. R. O.; Winger, B. E.; Smith, R. D. Proton transfer reaction studies of multiply charged proteins in a high mass-to-charge ratio quadrupole mass spectrometer. *J. Am. Soc. Mass Spectrom.* **1994,** (5), 1064-1071.

Macfarlane, R.; Torgerson, D. Californium-252 plasma desorption mass spectroscopy. *Science.* **1976,** (191), 920-925.

Mandal, M. K.; Chen, L. C.; Hashimoto, Y.; Yu, Z.; Hiraoka, K. Detection of biomolecules from solutions with high concentration of salts using probe electrospray and nano-electrospray ionization mass spectrometry. *Anal. Methods.* **2010,** (2), 1905-1912.

Mark, L.; Gill, M.; Mahut, M.; Derrick, P. Dual nano-electrospray for probing solution interactions and fast reactions of complex biomolecules. *Eur. J. Mass.* **2012,** (18), 439.

Marquez, C. A.; Wang, H.; Fabbretti, F.; Metzger, J. r. O. Electron-transfer-catalyzed dimerization of trans-anethole: Detection of the distonic tetramethylene radical cation intermediate by extractive electrospray ionization mass spectrometry. *J. Am. Chem. Soc.* **2008,** (130), 17208-17209.

Marshall, A. G.; de Haseth, J. A.Fourier transform ion cyclotron resonance mass spectrometry.in: AIP Conference Proceedings, AIP, **1998**, 430,pp. 3-16.

McKay, A. R.; Ruotolo, B. T.; Ilag, L. L.; Robinson, C. V. Mass measurements of increased accuracy resolve heterogeneous populations of intact ribosomes. *J. Am. Chem. Soc.* **2006,** (128), 11433-11442.

McNeal, C. J.; Macfarlane, R. D. Observation of a fully protected oligonucleotide dimer at m/z 12637 by californium-252 plasma desorption mass spectrometry. *J. Am. Chem. Soc.* **1981,** (103), 1609-1610.

Mehmood, S.; Marcoux, J.; Hopper, J. T.; Allison, T. M.; Liko, I.; Borysik, A. J.; Robinson, C. V. Charge reduction stabilizes intact membrane protein complexes for mass spectrometry. *J. Am. Chem. Soc.* **2014,** (136), 17010-17012.

Metwally, H.; McAllister, R. G.; Konermann, L. Exploring the mechanism of salt-induced signal suppression in protein electrospray mass spectrometry using experiments and molecular dynamics simulations. *Anal. Chem.* **2015,** (87), 2434-2442.

Miao, Z.; Chen, H.; Liu, P.; Liu, Y. Development of submillisecond time-resolved mass spectrometry using desorption electrospray ionization. *Anal. Chem.* **2011,** (83), 3994-3997.

Miladinović, S. a. M.; Fornelli, L.; Lu, Y.; Piech, K. M.; Girault, H. H.; Tsybin, Y. O. In-spray supercharging of peptides and proteins in electrospray ionization mass spectrometry. *Anal. Chem.* **2012,** (84), 4647-4651.

Mirza, U. A.; Cohen, S. L.; Chait, B. T. Heat-induced conformational changes in proteins studied by electrospray ionization mass spectrometry. *Anal. Chem.* **1993,** (65), 1-6.

Mortensen, D. N.; Williams, E. R. Investigating Protein Folding and Unfolding in Electrospray Nanodrops Upon Rapid Mixing Using Theta-Glass Emitters. *Anal. Chem.* **2014,** (87), 1281-1287.

Mortensen, D. N.; Williams, E. R. Theta-glass capillaries in electrospray ionization: rapid mixing and short droplet lifetimes. *Anal. Chem.* **2014,** (86), 9315-9321.

Mortensen, D. N.; Williams, E. R. Ultrafast (1 μs) mixing and fast protein folding in nanodrops monitored by mass spectrometry. *J. Am. Chem. Soc.* **2016,** (138), 3453-3460.

Müller, T.; Badu-Tawiah, A.; Cooks, R. G. Accelerated Carbon□ Carbon Bond-Forming Reactions in Preparative Electrospray. *Angew. Chem. Int. Edit.* **2012,** (51), 11832-11835.

Myung, S.; Badman, E. R.; Lee, Y. J.; Clemmer, D. E. Structural transitions of electrosprayed ubiquitin ions stored in an ion trap over ~ 10 ms to 30 s. *J. Phys. Chem A.* **2002,** (106), 9976-9982.

Nagaraj, N.; Lu, A.; Mann, M.; Wiśniewski, J. R. Detergent-based but gel-free method allows identification of several hundred membrane proteins in single LC-MS runs. *J. Proteome Res.* **2008,** (7), 5028-5032.

Nemes, P.; Barton, A. A.; Li, Y.; Vertes, A. Ambient molecular imaging and depth profiling of live tissue by infrared laser ablation electrospray ionization mass spectrometry. *Anal. Chem.* **2008,** (80), 4575-4582.

Nemes, P.; Huang, H.; Vertes, A. Internal energy deposition and ion fragmentation in atmospheric-pressure mid-infrared laser ablation electrospray ionization. *Phys. Chem. Chem. Phys.* **2012,** (14), 2501-2507.

Nemes, P.; Vertes, A. Laser ablation electrospray ionization for atmospheric pressure, in vivo, and imaging mass spectrometry. *Anal. Chem.* **2007,** (79), 8098-8106.

Okur, H. I.; Kherb, J.; Cremer, P. S. Cations bind only weakly to amides in aqueous solutions. *J. Am. Chem. Soc.* **2013,** (135), 5062-5067.

Pace, C. N.; Trevino, S.; Prabhakaran, E.; Scholtz, J. M. Protein structure, stability and solubility in water and other solvents. *Phil. Trans. R. Soc. Lond., B, Biol. Sci.*. **2004,** (359), 1225-1235.

Page, J. S.; Kelly, R. T.; Tang, K.; Smith, R. D. Ionization and transmission efficiency in an electrospray ionization–mass spectrometry interface. *J. Am. Soc. Mass Spectrom.* **2007,** (18), 1582-1590.

Pan, P.; Gunawardena, H. P.; Xia, Y.; McLuckey, S. A. Nanoelectrospray Ionization of Protein Mixtures: Solution pH and Protein p I. *Anal. Chem.* **2004,** (76), 1165-1174.

Peng, I. X.; Ogorzalek Loo, R. R.; Shiea, J.; Loo, J. A. Reactive-electrospray-assisted laser desorption/ionization for characterization of peptides and proteins. *Anal. Chem.* **2008,** (80), 6995-7003.

Peng, I. X.; Shiea, J.; Loo, R. R. O.; Loo, J. A. Electrospray-assisted laser desorption/ionization and tandem mass spectrometry of peptides and proteins. *Rapid Commun. Mass Spectrom.* **2007,** (21), 2541-2546.

Perez, J. J.; Flanigan IV, P. M.; Brady, J. J.; Levis, R. J. Classification of smokeless powders using laser electrospray mass spectrometry and offline multivariate statistical analysis. *Anal. Chem.* **2012,** (85), 296-302.

Perez, J. J.; Flanigan, P. M.; Karki, S.; Levis, R. J. Laser Electrospray Mass Spectrometry Minimizes Ion Suppression Facilitating Quantitative Mass Spectral Response for Multi-Component Mixtures of Proteins. *Anal. Chem.* **2013,**

Perry, R. H.; Cahill, T. J.; Roizen, J. L.; Du Bois, J.; Zare, R. N. Capturing fleeting intermediates in a catalytic C–H amination reaction cycle. *Proc. Natl. Acad. Sci. U.S.A.***2012,** (109), 18295-18299.

Perry, R. H.; Splendore, M.; Chien, A.; Davis, N. K.; Zare, R. N. Detecting reaction intermediates in liquids on the millisecond time scale using desorption electrospray ionization. *Angewandte Chemie.* **2011,** (123), 264-268.

Pinho, S. P.; Macedo, E. A. Solubility of NaCl, NaBr, and KCl in water, methanol, ethanol, and their mixed solvents. *J. Chem. Eng. Data*. **2005,** (50), 29-32.

Popa, V.; Trecroce, D. A.; McAllister, R. G.; Konermann, L. Collision-induced dissociation of electrosprayed protein complexes: An all-atom molecular dynamics model with mobile protons. *J. Phys. Chem B.* **2016,** (120), 5114-5124.

Posthumus, M.; Kistemaker, P.; Meuzelaar, H.; Ten Noever de Brauw, M. Laser desorption-mass spectrometry of polar nonvolatile bio-organic molecules. *Anal. Chem.* **1978,** (50), 985-991.

Prentice, B. M.; Chumbley, C. W.; Caprioli, R. M. Absolute quantification of rifampicin by MALDI Imaging mass spectrometry using multiple TOF/TOF events in a single laser shot. *J. Am. Soc. Mass Spectrom.* **2017,** (28), 136-144.

Puolitaival, S. M.; Burnum, K. E.; Cornett, D. S.; Caprioli, R. M. Solvent-free matrix dry-coating for MALDI imaging of phospholipids. *J. Am. Soc. Mass Spectrom.* **2008,** (19), 882-886.

Rezenom, Y. H.; Dong, J.; Murray, K. K. Infrared laser-assisted desorption electrospray ionization mass spectrometry. *Analyst.* **2008,** (133), 226-232.

Riekert, L. Chemical Kinetics and Transport. von PC Jordan. Plenum Press, New York 1979. XVI, 368 S., geb. $25.80. *Angewandte Chemie.* **1979,** (91), 947-948.

Sampson, J. S.; Hawkridge, A. M.; Muddiman, D. C. Generation and detection of multiply-charged peptides and proteins by matrix-assisted laser desorption electrospray ionization (MALDESI) Fourier transform ion cyclotron resonance mass spectrometry. *J. Am. Soc. Mass Spectrom.* **2006,** (17), 1712-1716.

Sampson, J. S.; Hawkridge, A. M.; Muddiman, D. C. Construction of a versatile high precision ambient ionization source for direct analysis and imaging. *J. Am. Soc. Mass Spectrom.* **2008,** (19), 1527-1534.

Sampson, J. S.; Muddiman, D. C. Atmospheric pressure infrared (10.6 μm) laser desorption electrospray ionization (IR-LDESI) coupled to a LTQ Fourier transform ion cyclotron resonance mass spectrometer. *Rapid Commun. Mass Spectrom.* **2009,** (23), 1989-1992.

Scalf, M.; Westphall, M. S.; Krause, J.; Kaufman, S. L.; Smith, L. M. Controlling charge states of large ions. *Science.* **1999,** (283), 194-197.

Schachel, T. D.; Metwally, H.; Popa, V.; Konermann, L. Collision-Induced Dissociation of Electrosprayed NaCl Clusters: Using Molecular Dynamics Simulations to Visualize Reaction Cascades in the Gas Phase. *J. Am. Soc. Mass Spectrom.* **2016,** (27), 1846-1854.

Schmidt, A.; Karas, M.; Dülcks, T. Effect of different solution flow rates on analyte ion signals in nano-ESI MS, or: when does ESI turn into nano-ESI? *J. Am. Soc. Mass Spectrom.* **2003,** (14), 492-500.

Schnier, P. D.; Gross, D. S.; Williams, E. R. On the maximum charge state and proton transfer reactivity of peptide and protein ions formed by electrospray ionization. *J. Am. Soc. Mass Spectrom.* **1995,** (6), 1086-1097.

Shackman, J. G.; Watson, C. J.; Kennedy, R. T. High-throughput automated post-processing of separation data. *J. Chromatogr. A.* **2004,** (1040), 273-282.

Shastry, M. R.; Luck, S. D.; Roder, H. A continuous-flow capillary mixing method to monitor reactions on the microsecond time scale. *Biophys. J.* **1998,** (74), 2714-2721.

Shelimov, K. B.; Clemmer, D. E.; Hudgins, R. R.; Jarrold, M. F. Protein structure in vacuo: gas-phase conformations of BPTI and cytochrome c. *J. Am. Chem. Soc.* **1997,** (119), 2240-2248.

Shi, F.; Archer, J. J.; Levis, R. J. Nonresonant, femtosecond laser vaporization and electrospray post-ionization mass spectrometry as a tool for biological tissue imaging. *Methods.* **2016,** (104), 79-85.

Shi, F.; Flanigan IV, P. M.; Archer, J. J.; Levis, R. J. Direct Analysis of Intact Biological Macromolecules by Low-Energy, Fiber-Based Femtosecond Laser Vaporization at 1042 nm Wavelength with Nanospray Postionization Mass Spectrometry. *Anal. Chem.* **2015,** (87), 3187-3194.

Shi, F.; Flanigan IV, P. M.; Archer, J. J.; Levis, R. J. Ambient Molecular Analysis of Biological Tissue Using Low-Energy, Femtosecond Laser Vaporization and Nanospray Postionization Mass Spectrometry. *J. Am. Soc. Mass Spectrom.* **2016,** (27), 542-551.

Shiea, J.; Huang, M. Z.; HSu, H. J.; Lee, C. Y.; Yuan, C. H.; Beech, I.; Sunner, J. Electrospray-assisted laser desorption/ionization mass spectrometry for direct ambient analysis of solids. *Rapid Commun. Mass Spectrom.* **2005,** (19), 3701-3704.

Shiea, J.; Yuan, C.-H.; Huang, M.-Z.; Cheng, S.-C.; Ma, Y.-L.; Tseng, W.-L.; Chang, H.-C.; Hung, W.-C. Detection of native protein ions in aqueous solution under ambient conditions by electrospray laser desorption/ionization mass spectrometry. *Anal. Chem.* **2008,** (80), 4845-4852.

Shieh, I.-F.; Lee, C.-Y.; Shiea, J. Eliminating the interferences from TRIS buffer and SDS in protein analysis by fused-droplet electrospray ionization mass spectrometry. *J. Proteome Res.* **2005,** (4), 606-612.

Shrestha, B.; Vertes, A. In situ metabolic profiling of single cells by laser ablation electrospray ionization mass spectrometry. *Anal. Chem.* **2009,** (81), 8265-8271.

Shrivas, K.; Wu, H.-F. Modified silver nanoparticle as a hydrophobic affinity probe for analysis of peptides and proteins in biological samples by using liquid-liquid

microextraction coupled to AP-MALDI-ion trap and MALDI-TOF mass spectrometry. *Anal. Chem.* **2008,** (80), 2583-2589.

Simmons, D. A.; Konermann, L. Characterization of transient protein folding intermediates during myoglobin reconstitution by time-resolved electrospray mass spectrometry with on-line isotopic pulse labeling. *Biochemistry.* **2002,** (41), 1906-1914.

Smith, D. W. Ionic hydration enthalpies. *J. Chem. Educ.* **1977,** (54), 540.

Sogbein, O. O.; Simmons, D. A.; Konermann, L. Effects of pH on the kinetic reaction mechanism of myoglobin unfolding studied by time-resolved electrospray ionization mass spectrometry. *J. Am. Soc. Mass Spectrom.* **2000,** (11), 312-319.

Stephenson, J. L.; McLuckey, S. A. Ion/ion reactions in the gas phase: Proton transfer reactions involving multiply-charged proteins. *J. Am. Chem. Soc.* **1996,** (118), 7390-7397.

Sterling, H. J.; Batchelor, J. D.; Wemmer, D. E.; Williams, E. R. Effects of buffer loading for electrospray ionization mass spectrometry of a noncovalent protein complex that requires high concentrations of essential salts. *J. Am. Soc. Mass Spectrom.* **2010,** (21), 1045-1049.

Sterling, H. J.; Cassou, C. A.; Trnka, M. J.; Burlingame, A.; Krantz, B. A.; Williams, E. R. The role of conformational flexibility on protein supercharging in native electrospray ionization. *Phys. Chem. Chem. Phys.* **2011,** (13), 18288-18296.

Sterling, H. J.; Kintzer, A. F.; Feld, G. K.; Cassou, C. A.; Krantz, B. A.; Williams, E. R. Supercharging protein complexes from aqueous solution disrupts their native conformations. *J. Am. Soc. Mass Spectrom.* **2012,** (23), 191-200.

Sterling, H. J.; Prell, J. S.; Cassou, C. A.; Williams, E. R. Protein conformation and supercharging with DMSO from aqueous solution. *J. Am. Soc. Mass Spectrom.* **2011,** (22), 1178-1186.

Sterling, H. J.; Williams, E. R. Origin of supercharging in electrospray ionization of noncovalent complexes from aqueous solution. *J. Am. Soc. Mass Spectrom.* **2009,** (20), 1933-1943.

Takáts, Z.; Cotte-Rodriguez, I.; Talaty, N.; Chen, H.; Cooks, R. G. Direct, trace level detection of explosives on ambient surfaces by desorption electrospray ionization mass spectrometry. *Chem. Commun.* **2005,** 1950-1952.

Takats, Z.; Wiseman, J. M.; Cooks, R. G. Ambient mass spectrometry using desorption electrospray ionization (DESI): instrumentation, mechanisms and applications in forensics, chemistry, and biology. *J. Mass Spectrom.* **2005,** (40), 1261-1275.

Takats, Z.; Wiseman, J. M.; Gologan, B.; Cooks, R. G. Mass spectrometry sampling under ambient conditions with desorption electrospray ionization. *Science*. **2004,** (306), 471-473.

Talaty, N.; Takáts, Z.; Cooks, R. G. Rapid in situ detection of alkaloids in plant tissue under ambient conditions using desorption electrospray ionization. *Analyst.* **2005,** (130), 1624-1633.

Tanaka, K.; Waki, H.; Ido, Y.; Akita, S.; Yoshida, Y.; Yoshida, T.; Matsuo, T. Protein and polymer analyses up to m/z 100 000 by laser ionization time-of-flight mass spectrometry. *Rapid Commun. Mass Spectrom.* **1988,** (2), 151-153.

Tang, K.; Gomez, A. Monodisperse electrosprays of low electric conductivity liquids in the cone-jet mode. *J. Colloid Interface Sci.* **1996,** (184), 500-511.

Teo, C. A.; Donald, W. A. Solution additives for supercharging proteins beyond the theoretical maximum proton-transfer limit in electrospray ionization mass spectrometry. *Anal. Chem.* **2014,** (86), 4455-4462.

Thomson, J.Rays of Positive Electricity and their Application to Chemical Analysis. 1913.in, London: Longmans, Green and Co.

Touboul, D.; Jecklin, M. C.; Zenobi, R. Investigation of deprotonation reactions on globular and denatured proteins at atmospheric pressure by ESSI-MS. *J. Am. Soc. Mass Spectrom.* **2008,** (19), 455-466.

Trimpin, S.; Herath, T. N.; Inutan, E. D.; Cernat, S. A.; Miller, J. B.; Mackie, K.; Walker, J. M. Field-free transmission geometry atmospheric pressure matrix-assisted laser desorption/ionization for rapid analysis of unadulterated tissue samples. *Rapid Commun. Mass Spectrom.* **2009,** (23), 3023-3027.

Trimpin, S.; Inutan, E. D.; Herath, T. N.; McEwen, C. N. Matrix-assisted laser desorption/ionization mass spectrometry method for selectively producing either singly or multiply charged molecular ions. *Anal. Chem.* **2009,** (82), 11-15.

Tsybin, Y. O.; Fornelli, L.; Stoermer, C.; Luebeck, M.; Parra, J.; Nallet, S.; Wurm, F. M.; Hartmer, R. Structural analysis of intact monoclonal antibodies by electron transfer dissociation mass spectrometry. *Anal. Chem.* **2011,** (83), 8919-8927.

Valentine, S. J.; Clemmer, D. E. H/D exchange levels of shape-resolved cytochrome c conformers in the gas phase. *J. Am. Chem. Soc.* **1997,** (119), 3558-3566.

Verkerk, U. H.; Kebarle, P. Ion-ion and ion-molecule reactions at the surface of proteins produced by nanospray. Information on the number of acidic residues and control of the number of ionized acidic and basic residues. *J. Am. Soc. Mass Spectrom.* **2005,** (16), 1325-1341.

Verkerk, U. H.; Peschke, M.; Kebarle, P. Effect of buffer cations and of H3O+ on the charge states of native proteins. Significance to determinations of stability constants of protein complexes. *J. Mass Spectrom.* **2003,** (38), 618-631.

Vertes, A.; Nemes, P.; Shrestha, B.; Barton, A. A.; Chen, Z.; Li, Y. Molecular imaging by Mid-IR laser ablation mass spectrometry. *Applied Physics A.* **2008,** (93), 885-891.

Vickerman, J. C.; Briggs, D., ToF-SIMS: surface analysis by mass spectrometry, IM, (2001).

Vijay-Kumar, S.; Bugg, C. E.; Cook, W. J. Structure of ubiquitin refined at 1.8 Åresolution. *J. Mol. Biol.* **1987,** (194), 531-544.

Wang, G.; Cole, R. B. Mechanistic interpretation of the dependence of charge state distributions on analyte concentrations in electrospray ionization mass spectrometry. *Anal. Chem.* **1995,** (67), 2892-2900.

Weinkauf, R.; Aicher, P.; Wesley, G.; Grotemeyer, J.; Schlag, E. Femtosecond versus nanosecond multiphoton ionization and dissociation of large molecules. *J. Phys. Chem.* **1994,** (98), 8381-8391.

Williams, E. R. Proton transfer reactivity of large multiply charged ions. *Journal of mass spectrometry: JMS.* **1996,** (31), 831.

Wilson, D. J.; Konermann, L. A capillary mixer with adjustable reaction chamber volume for millisecond time-resolved studies by electrospray mass spectrometry. *Anal. Chem.* **2003,** (75), 6408-6414.

Wiseman, J. M.; Ifa, D. R.; Song, Q.; Cooks, R. G. Tissue imaging at atmospheric pressure using desorption electrospray ionization (DESI) mass spectrometry. *Angew. Chem. Int. Edit.* **2006,** (45), 7188-7192.

Wolfender, J. L.; Chu, F.; Ball, H.; Wolfender, F.; Fainzilber, M.; Baldwin, M. A.; Burlingame, A. L. Identification of tyrosine sulfation in Conus pennaceus conotoxins α-PnIA and α-PnIB: further investigation of labile sulfo-and

phosphopeptides by electrospray, matrix-assisted laser desorption/ionization (MALDI) and atmospheric pressure MALDI mass spectrometry. *J. Mass Spectrom.* **1999,** (34), 447-454.

Wyttenbach, T.; Bowers, M. T. Structural stability from solution to the gas phase: native solution structure of ubiquitin survives analysis in a solvent-free ion mobility–mass spectrometry environment. *J. Phys. Chem B.* **2011,** (115), 12266-12275.

Xu, B. J.; Caprioli, R. M.; Sanders, M. E.; Jensen, R. A. Direct analysis of laser capture microdissected cells by MALDI mass spectrometry. *J. Am. Soc. Mass Spectrom.* **2002,** (13), 1292-1297.

Yu, L.; Nassar, R.; Fang, J.; Kuila, D.; Varahramyan, K. Investigation of a novel microreactor for enhancing mixing and conversion. *Chem. Eng. Commun.*. **2008,** (195), 745-757.

Yue, X.; Vahidi, S.; Konermann, L. Insights into the mechanism of protein electrospray ionization from salt adduction measurements. *J. Am. Soc. Mass Spectrom.* **2014,** (25), 1322-1331.

Yuill, E. M.; Sa, N.; Ray, S. J.; Hieftje, G. M.; Baker, L. A. Electrospray Ionization from Nanopipette Emitters with Tip Diameters of Less than 100 nm. *Anal. Chem.* **2013,** (85), 8498-8502.

Zechel, D. L.; Konermann, L.; Withers, S. G.; Douglas, D. Pre-steady state kinetic analysis of an enzymatic reaction monitored by time-resolved electrospray ionization mass spectrometry. *Biochemistry.* **1998,** (37), 7664-7669.

Zou, J.; Talbot, F.; Tata, A.; Ermini, L.; Franjic, K.; Ventura, M.; Zheng, J.; Ginsberg, H.; Post, M.; Ifa, D. R. Ambient mass spectrometry imaging with picosecond infrared laser ablation electrospray ionization (PIR-LAESI). *Anal. Chem.* **2015,** (87), 12071-12079.

Zubarev, R. A.; Horn, D. M.; Fridriksson, E. K.; Kelleher, N. L.; Kruger, N. A.; Lewis, M. A.; Carpenter, B. K.; McLafferty, F. W. Electron capture dissociation for structural characterization of multiply charged protein cations. *Anal. Chem.* **2000,** (72), 563-573.

Zubarev, R. A.; Kelleher, N. L.; McLafferty, F. W. Electron capture dissociation of multiply charged protein cations. A nonergodic process. *J. Am. Chem. Soc.* **1998,** (120), 3265-3266.